Delezene, LK, Skinner, MM, Bailey, SE, Brophy, JK, Elliott, MC, Gurtov, A, Irish, JD, Moggi-Cecchi, J, de Ruiter, DJ, Hawks, J and Berger, LR

Descriptive catalog of Homo naledi dental remains from the 2013 to 2015 excavations of the Dinaledi Chamber, site U.W. 101, within the Rising Star cave system, South Africa

Descriptive catalogue of *Homo naledi* dental remains from the 2013–2015 excavations of the Dinaledi Chamber, Site U.W. 101, within the Rising Star cave system, South Africa

Lucas K. Delezene[a, b,*], Matthew M. Skinner[b, c, d], Shara Bailey[d, e], Juliet K. Brophy[b, f], Marina Elliott[b, g], Alia Gurtov[h], Joel D. Irish[b, i], Jacopo Moggi-Cecchi[j], Darryl J. de Ruiter[b, k], J. Hawks[b, l], Lee R. Berger[m, b]

[a] *Department of Anthropology, University of Arkansas, Fayetteville, AR 72701, USA*
[b] *Centre for the Exploration of the Deep Human Journey, University of the Witwatersrand, Private Bag 3, WITS 2050, South Africa*
[c] *School of Anthropology and Conservation, University of Kent, Marlowe Building, Canterbury, CT2 7NR, UK*
[d] *Department of Human Evolution, Max Planck Institute for Evolutionary Anthropology, Deutscher Platz 6, 04103 Leipzig, Germany*
[e] *Department of Anthropology, Center for the Study of Human Origins, New York University, New York, NY 10003, USA*
[f] *Department of Geography and Anthropology, Louisiana State University, Baton Rouge, LA 70803, USA*
[g] *Department of Archaeology, Simon Fraser University, 8888 University Drive, Burnaby, B.C. V5A 1S6, USA*
[h] *Stripe, Inc., 199 Water Street, 30th Floor, New York, NY 10038, USA.*
[i] *School of Biological and Environmental Sciences, Liverpool John Moores University, Liverpool L3 3AF, UK*
[j] *Laboratory of Anthropology, Department of Biology, University of Florence, Via del Proconsolo 12, Firenze 50122, Italy*
[k] *Department of Anthropology, Texas A&M University, College Station, TX 77843, USA*
[l] *Department of Anthropology, University of Wisconsin-Madison. Madison, WI 53706, USA*
[m] *National Geographic Society, 1145 17th Street NW, Washington DC 20036, USA.*

***Corresponding author.**
E-mail address: delezene@uark.edu (L.K. Delezene).

Descriptive catalogue of *Homo naledi* dental remains from the 2013–2015 excavations of the Dinaledi Chamber, Site U.W. 101, within the Rising Star cave system, South Africa

Abstract

More than 150 hominin teeth, dated to ~241–330 thousand years ago, were recovered during the 2013–2015 excavations of the Dinaledi Chamber of the Rising Star cave system, South Africa. These fossils comprise the first large single-site sample of hominin teeth from the Middle Pleistocene of Africa. Though scattered remains attributable to *Homo sapiens*, or their possible lineal ancestors, are known from older and younger sites across the continent, the distinctive morphological feature set of the Dinaledi teeth supports the recognition of a novel hominin species, *Homo naledi*. This material provides evidence of African *Homo* lineage diversity that lasts until at least the Middle Pleistocene. Here, a catalogue, anatomical descriptions, and details of preservation and taphonomic alteration are provided for the Dinaledi teeth. Where possible, provisional associations among teeth are also proposed. To facilitate future research, we also provide access to a catalogue of surface files of the Rising Star jaws and teeth.

Keywords: Middle Pleistocene; hominin; crown and root morphology; µCT

1. Introduction

For nearly a century, fossil discoveries in South Africa have shaped our understanding of hominin evolution (Dart, 1925). Nowhere is this more evident than in studies of Plio-Pleistocene dental morphology, for the caves of South Africa (e.g., Taung, Sterkfontein, Makapansgat, Kromdraai, Swartkrans, Gladysvale, Drimolen, Gondolin, and Malapa) have yielded hundreds of teeth of *Australopithecus* and *Paranthropus* (e.g., Robinson, 1956; Berger et al., 1993, 2010; Menter et al., 1999; Moggi-Cecchi et al., 2006, 2010; Martin et al., 2021; Rak et al., 2021). The pioneering work of Broom (1938) and Robinson (1954, 1956), which detailed and contrasted the morphology of *Australopithecus africanus* and *Paranthropus robustus*, influenced early hypotheses of dental and dietary evolution and set the stage for the recognition of dentally primitive species of *Homo* and other 'australopithecine' taxa in eastern and southern Africa (e.g., Broom and Robinson, 1949; Robinson, 1953; Leakey, 1959; Leakey et al., 1964; Tobias, 1965; Hughes and Tobias, 1977; Johanson et al., 1978; Berger et al., 2010; Irish et al., 2013).

Yet, amid a rich record of *Australopithecus* and *Paranthropus*, the dental evidence for extinct species of *Homo* in South Africa is comparatively sparse (e.g., Clarke, 1985; Grine et al., 1996, 2009; Moggi-Cecchi et al., 1998; Kuman and Clarke, 2000; Grine, 2005; Curnoe and Tobias, 2006). Broom and Robinson (1949) argued that the SK 15 mandible represents a species of nonrobust hominin contemporaneous with *P. robustus* in the Swartkrans deposits and erected the name *Telanthropus capensis* for that taxon. Robinson (1953) considered other Swartrkans specimens (e.g., SK 18, SK 45, SK 80) to also belong to *Telanthropus*. These individuals and a few others from Swartkrans

(Clarke, 1977a, 1977b; Grine et al., 2009), and a handful of jaws, teeth, and crania from Sterkfontein and Drimolen, are attributed to early *Homo* by some (Hughes and Tobias, 1977; Clarke, 1985; Moggi-Cecchi et al., 1998, 2010; Curnoe and Tobias, 2006; Kimbel, 2009; Herries et al., 2020). Despite this evidence, the taxonomic reality and identity of South African early *Homo* is debated. Various sources highlight affinities of some of the Swartkrans, Sterkfontein, and Drimolen *Homo* material with *Homo erectus* (*Homo ergaster* to some) and/or *Homo habilis* from eastern Africa or suggest that these fossils are phenotypically distinct from contemporary eastern African *Homo* (e.g., Grine et al., 1996, 2009; Kuman and Clarke, 2000; Grine, 2005; Davies et al., 2020; Herries et al., 2020). Whether specimens like Stw 53 and Stw 80 from Sterkfontein represent *Homo* or the same 'nonrobust' taxon sampled at Swartkrans and Drimolen is unclear (e.g., Smith and Grine, 2008; Davies et al., 2020). In fact, recent research casts doubts on the attribution of many of the Swartkans, Sterkfontein, Kromdraii, and Drimolen teeth to early *Homo*, including SK 15 and Stw 53, leaving very few dental specimens that are unequivocally early *Homo* in the South African fossil record (Zanolli et al., 2022).

The record of teeth from South Africa that bridges the temporal and phylogenetic gap from early *Homo* to *Homo sapiens* is also patchy, especially in comparison to similarly aged European (e.g., Martinón-Torres et al., 2012), northern African (e.g., Hublin et al., 2017), and Levantine (e.g., Vandermeersch, 1981) material, and the southern African specimens tend to be isolated and with poor chronological resolution (Berger et al., 2017). For example, an approximately one million-year-old M^1 from Cornelia-Uitzek, which is associated Acheulean tools, is argued to resemble South African early *Homo* specimens (Brink et al., 2012). Among southern African teeth argued

to derive from the Middle Pleistocene are those in the Cave of Hearths mandible (e.g., Davies et al., 2019b, 2020), which is likely associated with Late Acheulean artifacts (Curnoe, 2009; McNabb, 2009) and argued by Tobias (1971) to represent *Homo rhodesiensis* (*Homo heidelbergensis* or archaic *Homo sapiens* in other taxonomic schemes). From the Lincoln Cave of Sterkfontein, Stw 585 may be associated with Middle Stone Age stone tools and is referred to as "perhaps archaic *Homo sapiens*" (Reynolds et al., 2007: 267). Small samples of teeth from sites along the Eastern Cape coast (e.g., Grine and Klein, 1993; Berger and Parkington, 1995; Stynder et al., 2001) and an isolated third molar spatially associated with the Florisbad cranium could represent *H. rhodesiensis*, *Homo helmei*, or even early *H. sapiens* (Dreyer, 1935; Rightmire, 1978; Kuman and Clarke, 1986; Grün et al., 1996). The dental record from the Late Pleistocene is also sparse; yet, specimens attributable to *H. sapiens* are documented from sites that dot the South African coast (e.g., Die Kelders, Diepkloof, Pinnacle Point, Blombos, Klasies River Mouth, Ysterfontein) and from scattered inland sites (e.g., Equus Cave, Hofmeyr, Sibudu) that are argued to show an association between *H. sapiens* and the Middle Stone Age to Late Stone Age transition (e.g., Marean et al., 2004; Smith et al., 2006; Grine et al., 2007, 2017a, 2017b, 2021; Harvati et al., 2015; Grine, 2016; Riga et al., 2018; Will et al., 2019; Niespolo et al., 2021).

The ~241–330-thousand-year-old fossils from the Dinaledi Chamber of the Rising Star cave system provide the first assemblage of South African Middle Pleistocene-aged (Dirks et al., 2017; Robbins et al., 2021) *Homo* teeth that begins to approach the abundance of the older *P. robustus* and *A. africanus* samples from the region. The Dinaledi fossils are all attributed to *Homo naledi* (Berger et al., 2015). Given that the

89 previously known Middle Pleistocene southern African fossils could be argued to be *H.*
90 *sapiens* or their lineal ancestors (e.g., Rightmire, 2008; Bailey and Hublin, 2013; but see
91 Grün et al., 2020), it is perhaps surprising that the Dinaledi dental and skeletal material is
92 morphologically quite distinct from contemporaneous Eurasian and other African Middle
93 Pleistocene *Homo* samples. The short stature, small body mass, and absolute and relative
94 encephalization of *H. naledi* are on par with *Australopithecus* and *Paranthropus*;
95 additionally, its curved manual phalanges and an *Australopithecus*-like hip are out of step
96 with fossils attributed to *H. sapiens* and *H. neanderthalensis* (Harcourt-Smith et al., 2015;
97 Kivell et al., 2015; Feuerriegel et al., 2017; Garvin et al., 2017; Hawks et al., 2017;
98 Marchi et al., 2017; VanSickle et al., 2018). However, relative to *Australopithecus*, and
99 possibly early *Homo*, *H. naledi* is argued to share derived features with humans,
100 including aspects of endocast morphology (e.g., "extensive occipital petalial asymmetry";
101 Holloway et al., 2018: 5740), derived carpal shapes (e.g., "a boot-shaped trapezoid with
102 an expanded palmar non-articular surface; Kivell et al., 2015: 5), low magnitude sexual
103 size dimorphism, an elongated lower limb, and low relative limb joint size (Garvin et al.,
104 2017; Hawks et al., 2017; Prabhat et al., 2021). Thus, the emerging picture is that *H.*
105 *naledi* is not simply a relict species of 'early' *Homo* that survived into the Middle
106 Pleistocene, but, rather, a species with a distinct cluster of traits, some of which are
107 candidate autapomorphies (e.g., pillars on the superior aspect of the femoral neck, strong
108 distal attachment of the pes anserinus (Marchi et al., 2017), larger P_3 than P_4 (Davies et
109 al., 2020)). Thus, *H. naledi* cannot be slotted easily into a scenario whereby all Middle
110 Pleistocene African *Homo* populations were ancestral to extant humans; instead, the

111 unique trait pattern of *H. naledi* points toward a deep history of *Homo* lineage diversity in
112 the Pleistocene (Dembo et al., 2016; see also Grün et al., 2020).
113 Through 2015, the Dinaledi Chamber has yielded more than 190 catalogued
114 whole or fragmentary teeth, including those in situ in eight mandibles and one maxilla of
115 variable preservation (Table 1; Berger et al., 2015). The current Dinaledi dental
116 collection represents nearly all anatomical parts, as only the mandibular deciduous central
117 incisor is currently unrepresented. The sample captures individuals that range in age from
118 infant to older adult (Berger et al., 2015; Bolter et al., 2018). Already, the Dinaledi dental
119 collection has contributed to discussions of sample demography (Bolter et al., 2018), diet
120 and ecology (i.e., Towle et al., 2017; Berthaume et al., 2018; Ungar and Berger, 2018),
121 sexual dimorphism and sample-level variation (Garvin et al., 2017), growth and
122 development (Cofran and Walker, 2017; Guatelli-Steinberg et al., 2018; Skinner, 2019),
123 the status of *H. naledi* as a distinct species of *Homo* (e.g., Skinner et al., 2016; Irish et al.,
124 2018; Bailey et al., 2019; Davies et al., 2019a, 2019b, 2020; Kupczik et al., 2019; Brophy
125 et al., 2021), and the phylogenetic place of *H. naledi* (Dembo et al., 2016; Irish and
126 Grabowski, 2021).
127 Here, we provide a descriptive catalogue, with accompanying three-dimensional
128 surface models derived from micro-computerized tomographic scans, of the Dinaledi
129 dental assemblage as collected through 2015. We refrain from extensive interspecific
130 comparisons, as focused analyses of some aspects of dental morphology are provided in
131 Berthaume et al. (2018), Guatelli-Steinberg et al. (2018), Irish et al. (2018), Bailey et al.,
132 (2019), Davies et al. (2019a, 2019b, 2020), Kupzcik et al. (2019), Brophy et al. (2020),
133 and in forthcoming work. We do not systematically apply a standardized trait scoring

system, like the Arizona State University Dental Anthropology System (ASUDAS), to nonmetric variation. For interested researchers, ASUDAS summary data for this sample of *H. naledi* teeth can be found in Irish et al. (2018: Table 1; SOM Table S2). Individual trait expression should be discernable in the multiple high-resolution views provided of each tooth. Where appropriate to elucidate anatomical features, and when such comparisons could be made with the original material, we also examined the *H. naledi* fossils from the Lesedi Chamber, site U.W. 102 (e.g., Hawks et al., 2017).

This paper is intended to stand as the canonical catalogue of the U.W. 101 Dinaledi Chamber dental assemblage, to document the state of preservation for each element at the time of publication, and to stand as a reference for and to stimulate future research on the *H. naledi* teeth.

2. Materials and methods

2.1. Provenience

All specimens were collected from 2013 to 2015 from the Dinaledi Chamber (site U.W. 101) within the karstic Rising Star cave system. The site is in the Cradle of Humankind UNESCO World Heritage area in the Gauteng Province, South Africa, and is near other well-known hominin bearing sites (e.g., Swartkrans and Sterkfontein; Dirks et al., 2015, 2017; Kruger et al., 2016). The fossils were either collected from the surface of the chamber floor or retrieved from localized excavations (Berger et al., 2015). Details of the geology of the chamber and the methods of excavation are presented in Dirks et al. (2015). The fossils described are curated in the PalaeoSciences Building at the University of the Witwatersrand, Johannesburg, South Africa.

157

158 *2.2. Specimens*

159 With three exceptions, the teeth described here are those that comprise the
160 published paratype series of *H. naledi* from the Dinaledi Chamber that are iterated in
161 Berger et al. (2015: Supplementary File 1). Three paratype teeth, U.W. 101-020, U.W.
162 101-344, and U.W. 101-347, are not included in this monograph because they are from a
163 spatially discrete collection locus, the 'Hill Antechamber,' that is now considered to be
164 separate from the Dinaledi Chamber. The three Hill Antechamber teeth are being
165 examined as part of the material excavated after 2015 (e.g., Elliott et al., 2018). Where
166 differences occur, the specimen numbers and identification of the teeth herein supersede
167 that published in Berger et al. (2015).

168

169 *2.3. Assessment of visible anatomy and scanning procedures*

170 An inventory and description of the preserved visible anatomy is provided for all
171 accessioned dental specimens (Table 1). All teeth were examined with a low
172 magnification hand lens (10×). Where appropriate, micro-computerized tomographic
173 (µCT) scans were consulted to clarify anatomical detail and to assess structures obscured
174 by matrix or adhering bone. The teeth and jaws were scanned with a Nikon Metrology
175 XTH 225/320 µCT scanner housed in the PalaeoSciences Building at the University of
176 the Witwatersrand. Scanning parameters varied slightly by specimen but were 110–130
177 kV, 100–130 mA, 1500–2000 projections, 1–2 frame averaging, 1–2 mm Aluminium
178 filter. The isometric voxel size ranged between 0.027 and 0.036 mm^3. Crown lengths and
179 breadths were measured with fine-pointed digital calipers and root lengths and

interproximal facet sizes were measured with either calipers or digitally from three-dimensional models derived from µCT scans using the three-dimensional measuring tool in AvizoLite v. 9.1 (Thermo Fisher Scientific, Waltham). The extent of occlusal and incisal macrowear follows the delineations of stages outlined in Smith (1984).

In contrast to the common condition at other South African hominin-bearing sites, the Dinaledi tooth crowns are mostly complete, unbroken, and not deformed in shape postmortem. Microcracks are present in the enamel but have not altered crown shapes. Taphonomic modification, though minimal, is typically associated with the breakage of the roots and the abrasion of their external surfaces. Where such damage is present, it is noted. Many of the *H. naledi* crowns feature antemortem occlusal enamel chipping and such damage is identified in the descriptions. Towle et al. (2017) assessed chipping independently of this study and provide a summary of chipping frequency in their study.

2.4. Assessment of antimeres and metameres

The Dinaledi fossils are derived from a commingled assemblage (Dirks et al., 2015) and many of the teeth were excavated as isolated specimens in close spatial association. In some instances, isolated teeth belonging to a single individual (e.g., the U.W. 101-1126, U.W. 101-1131, U.W. 101-1132, and U.W. 101-1333 anterior mandibular teeth) were excavated in near-anatomical position. In most cases, though, spatial proximity is a poor guide as to whether specimens belong to the same individual. In addition, it is evident that there are duplicated teeth representing similarly aged individuals as judged by dental wear and crown developmental status (e.g., the U.W. 101-809 and U.W. 101-814 left M_1s), which complicates attempts to associate isolated, non-

203 articulating, and non-occluding teeth into biological individuals. Thus, a conservative
204 approach to assigning specimens to individuals is taken. Antimeres are proposed based
205 on morphological similarity. Metameric associations are proposed based on the
206 congruency of interproximal facets and consistencies in occlusal wear. In the case of
207 tooth germs, associations based on development status are proposed cautiously. By taking
208 such an approach, many teeth are likely left unlinked to others that could represent the
209 same individual. All proposed associations are provisional and will certainly require
210 revision with the recovery of additional teeth in future excavations.
211
212 *2.5. Abbreviations*
213 The following anatomical abbreviations are used throughout the text:
214 L = left
215 R = right
216 IC = incisocervically
217 OC = occlusocervically
218 MD = mesiodistal/ly
219 BL = buccolingual/ly
220 LaL = labiolingual/ly
221 Prd = Protoconid
222 Med = Metaconid
223 Hyd = Hypoconid
224 End = Entoconid
225 Hld = Hypoconulid

Pa = Paracone

Pr = Protocone

Me = Metacone

Hy = Hypocone

C5 = cusp five, maxillary molar

C6 = tuberculum sextum, mandibular molar

C7 = tuberculum intermedium, mandibular molar

Fa = anterior fovea

Fp = posterior fovea

MMR = mesial marginal ridge

DMR = distal marginal ridge

Mlg = median longitudinal groove

Co = crista obliqua/distal trigone crest

IPF = interproximal contact facet

EDJ = enamel-dentine junction

OES = outer enamel surface

3. Descriptions

As most of the Dinaledi teeth were recovered as isolated specimens, we describe the isolated specimens by tooth class and present them in ascending order according to their accession number. Where specimens with separate accession numbers have been physically refit to one another, they are described together as a single specimen. Teeth found in jaws are described together as a single specimen following the descriptions of

the isolated teeth. A companion database of images and viewable ply surface files derived from µCT scans is available at https://human-fossil-record.org/.

3.1. Deciduous maxillary central incisors

A single pair of proposed antimeric dI^1s is known from the Dinaledi Chamber deposits. Morphologically, the crowns are simple and lack prominent marginal ridges or features on the lingual face.

U.W. 101-544C: RdI^1 (Fig. 1A; Table 1) A narrow ribbon of dentine is exposed along the incisal surface (stage 3). A flat, teardrop shaped mesial IPF (2.5 mm IC by 1.5 mm LaL) sits near the incisal edge of the mesial shoulder. No distal IPF is present. The crown is short and wide with weak labial convexity at mid-crown but a more-or-less strait incisal edge. In mesial and distal views, the labial face exhibits only minor IC curvature. In lingual view, weak marginal ridges are visible on the incisal half of the crown. These become indistinct as they extend towards the mesially-displaced and bulbous basal eminence. There is also a faint median lingual ridge, accentuated by mesial and distal furrows. The mesial fossa is narrower and deeper than the distal fossa.

The LaL-flattened root is nearly complete, just missing the tip so that the root canal is exposed and is abraded externally. The maximum height preserved is 9.4 mm. In labial and lingual views, the root tilts slightly distally.

This specimen is proposed as the antimere of U.W. 101-1331. It shares a specimen number with U.W. 101-544A (RdP^4) and U.W. 101-544B (crown incomplete RC^1) because they were excavated in close spatial proximity. Though all represent sub-

adults, it is unlikely that they represent a single individual. Both U.W. 101-544B and U.W. 101-544C have proposed antimeres in the assemblage and are likely attributable to the nearly complete mixed dentition associated with the U.W. 101-1400 mandible and its associated antimeres and occluding teeth, which have erupted dP4s and nearly crown-complete M1s; this would preclude the developing RdP^4 germ, U.W. 101-544A, from belonging to the same individual as U.W. 101-544B and U.W. 101-544C. However, from a modern human perspective, the developmental status of U.W. 101-544A is not inconsistent with attribution to the same individual as U.W. 101-544B and U.W. 101-544C (AlQahtani et al., 2010). The possible association of U.W. 101-544B and U.W. 101-544C with U.W. 101-1400 are given a detailed treatment in the Discussion.

U.W. 101-1331: LdI^1 (Fig. 1B; Table 1) A narrow ribbon of dentine is exposed along the incisal surface (stage 3). It also exhibits a flat, teardrop shaped mesial IPF (1.5 mm LaL by 2.5 mm IC). No distal IPF is present. The crown is short and wide with weak labial convexity at mid-crown but a more-or-less strait incisal edge. In mesial and distal views, it exhibits only minor IC curvature. Lingually, weak marginal ridges are visible on the incisal half of the crown, accentuated by faint mesial and distal furrows, and become indistinct as they blend into the domed basal eminence.

The LaL-flattened root is nearly complete, just missing the tip so that the root canal is exposed. In labial view, the preserved root is 9.4 mm in height. The root is slightly abraded on its external surface.

This is likely the antimere of U.W. 101-544C, to which it is nearly identical in morphology and state of wear. These specimens are hypothesized to represent the same

individual as the U.W. 101-1400 mandible and other isolated deciduous and permanent teeth. These associations are given in more detail in the Discussion.

3.2. Deciduous maxillary lateral incisor

A single dI^2 is represented in the recovered Dinaledi Chamber material. Like the dI^1s, the dI^2 crown is simple and lacks prominent marginal ridges or features on the lingual face.

U.W. 101-1304: LdI^2 (Fig. 2; Table 1) Wear blunted the incisal edge and exposed a thin line of dentine and the DMR is worn along its surface (stage 1). No IPFs are present. In labial and lingual views, the crown is asymmetrical with an incisal edge that is strongly angled distally, resulting in lower distal and higher mesial aspects. The mesial corner is rounded, and the distal corner is more angular. The marginal ridges are apparent, especially so the mesial, which is much longer than the distal. There is a shallow groove adjacent to the MMR. The median lingual ridge is indistinct and blends into a dome-like basal eminence that occupies much of the lingual surface.

The root is nearly complete (8.0 mm in preserved height) but is broken before its apex. The root is obliquely oriented relative to the crown, with its major cross-sectional axis running mesiolabial to distolingual. The root is somewhat flattened LaL. A shallow groove runs along the length of the distal surface.

Based upon developmental status, including the absence of IPFs, this specimen is likely associated with the U.W. 101-1287A LdC^1.

3.3. Deciduous maxillary canines

Three dC^1s are known from the Dinaledi Chamber deposits. These include a pair of proposed antimeres, U.W. 101-728 and U.W. 101-1287A, and an isolated specimen, U.W. 101-595. The proposed antimeres are nearly identical, while U.W. 101-595 departs slightly from the morphology seen in the others. In all crowns, the shoulders are placed at approximately midcrown and the mesial and distal crests angle sharply from the shoulders to meet at a centrally placed apex. The lingual and distal faces lack notable features.

U.W. 101-595: LdC^1 (Fig. 3A; Table 1) The apex is slightly worn, exposing a dentine pit, as are the mesial and distal tubercles (stage 2). A small mesial IPF is visible, but one is not detectable distally. In occlusal view, the cervical outline is ovoid with the major axis MD and the minor axis LaL. In this view, the apex is more distally placed because of the longer mesial edge. The crown is moderately convex at mid-crown but has a straight occlusal edge. In mesial and distal views, the crown is only mildly convex with a swollen basal cingulum. In labial and lingual views, the crown is pentagonal, with a straight, if not slightly angled, cervical line, vertical mesial and distal shoulders, and angled mesial and distal edges that meet at a high apex, which sits very slightly mesial to the transverse axis. On the lingual aspect, there is a weak, slightly mesially offset, median ridge. The mesial and distal shoulders are quite prominent, forming distinct tubercles. They are delineated lingually by mesial and distal grooves and are associated with mesial and distal marginal ridges originating from the cingulum. The mesial tubercle is higher and larger than the distal tubercle. Labially, the mesial and distal tubercles are associated with

weak mesial and distal furrows, with the distal furrow slightly more prominent. The prominence of the tubercles departs from the condition in the other deciduous maxillary canines (i.e., U.W. 101-728 and U.W. 101-1287A) in the Dinaledi assemblage.

The root is slightly abraded and is preserved for approximately 9.6 mm in labial view, where it is broken just before the apex. The root extends straight from the crown. It is circular in cross section near the cervix and pinches near the apex, with its major axis MD and minor axis LaL.

U.W. 101-728: RdC^1 (Fig. 3B; Table 1) The apex is slightly blunted, exposing a pinpoint-sized dentine pit. Minor wear facets, with no dentine exposure, are also visible along the mesial and distal crests (stage 1). There is a teardrop shaped distal IPF (approximately 1.5 mm IC by 1.5 mm LaL) and no mesial IPF. In apical view, the crown is ovoid, longer MD than LaL, and the apex is more-or-less centrally placed. In labial and lingual views, the crown is pentagonal in outline with a straight cervical margin and angled mesial and distal crests. The mesial edge is slightly convex, while the distal edge is slightly concave. In lingual view, there is a slightly elevated, wide median ridge that merges with a weak, rounded basal cingulum. Weak mesial and barely perceptible distal fossae border the median lingual ridge. In labial view, there is a faint distal furrow associated with a slight projection of the distal shoulder.

The root is slightly abraded and missing its apex. In labial view, the root of the canine is preserved for approximately 10.2 mm where it is broken just before the apex. The root is ovoid in cross section and compressed LaL. It extends nearly directly above the crown with a slight distal tilt.

364 This is proposed as the antimere of U.W. 101-1287A. The specimens are nearly
365 identical in morphology and size. The only significant difference is that the small distal
366 IPF of U.W. 101-728 is lacking on U.W. 101-1287A. These teeth are also proposed to
367 belong to the nearly complete mixed dentition that includes the U.W. 101-1400
368 mandibular dentition and its antimeres.
369
370 U.W. 101-1287A: LdC^1 (Fig. 3C; Table 1) The tip of the apex is blunted by wear with a
371 small dentine pit exposed on its distal aspect. The wear facet continues along the distal
372 crest (stage 2). No IPFs are detectable. In occlusal view, the apex is offset to the mesial of
373 center and the crown is ovoid in profile, with the major axis MD and minor axis LaL. In
374 lingual and labial views, the crown is pentagonal, with vertical mesial and distal
375 shoulders and steeply angled mesial and distal edges. From the labial aspect, the crown
376 apex is slightly mesial of center. On the lingual aspect, the median ridge is slightly
377 swollen and set off by weak mesial and distal furrows. The mesial lingual fossa is a weak
378 groove adjacent to a faint MMR. The distal lingual fossa is barely perceptible and slightly
379 obscured by wear. Labially, a vertical mesial furrow is barely visible, while the distal
380 furrow, which associated with the distal shoulder, is wider and more distinct. Neither the
381 mesial and distal shoulders have distinct apices, as they do in U.W. 101-595, and they
382 lack sharp edges.
383 The root is broken near its apex and measures 11.6 mm as preserved. The exposed
384 root canal is filled with sediment. The root is ovoid in cross section and longer MD than
385 LaL.

This is proposed as the antimere of U.W. 101-728. The specimen is, however, slightly less worn than the RdC^1, lacking a distinct wear facet along the mesial crest, and it also lacks a distal IPF, which is present on the RdC^1. Based upon developmental status and the lack of adjoining IPFs on both teeth, this specimen is proposed to be associated with the U.W. 101-1304 LdI^2. Despite sharing an accession number based on the spatial proximity of their recovery, this specimen and U.W. 101-1287B (RM_1) cannot represent the same biological individual, as U.W. 101-1287B belongs to the mandibular dentition represented by U.W. 101-1142, which has a completely erupted and worn permanent dentition, while U.W. 101-1287A represents a young subadult with light wear on its deciduous canines.

3.4. Deciduous maxillary third premolars

A pair of proposed antimeric dP^3s, U.W. 101-823 and U.W. 101-1377, are known from the Dinaledi Chamber material. Both feature four well developed main cusps, a pentagonal occlusal outline, a beak-like mesial projection formed by the MMR, a continuous Co separating the hypocone from the trigone, a thick epicrista extending from the mesial crest of the Pa into the Fa, and a weakly-expressed Carabelli's feature.

U.W. 101-823: RdP^3 (Fig. 4A; Table 1) A small oval mesial IPF (1.5 mm BL by 1.0 mm OC) is located buccal to the midline. A distal IPF is absent. The crown is minimally worn with small facets present on the lingual face of the Pa and the apex and mesial crest of the Pr and small dentine pits are exposed over the Pr and Me (stage 2). The crown exhibits four well-developed cusps having the following size relationships: Pr > Pa ≥ Me > Hy.

The Hy is conical in shape and equal in height to the Me. In occlusal view, the crown is a squat pentagon in outline, reflecting the distolingually projecting Hy and well-developed, obliquely-angled mesiobuccal and mesiolingual aspects. The MMR is high and sharp. A thick epicrista, with a distinct tubercle and free apex, is separated from the MMR and the Pa essential ridge by distinct furrows. The well-developed MMR and epicrista form a mesiobuccal projection. An uninterrupted Co separates the Hy from the trigone. The DMR is thick, but is much lower than the MMR, and encloses a small, BL-oriented, groove-like Fp that is continuous with the groove separating the Hy and Me. There is a weak Carabelli's feature on the mesiolingual aspect of the Pr that takes the form of a v-shaped furrow and associated crest. The lingual groove is a narrow cleft near the occlusal margin and continues as a deep groove until it terminates at about mid-crown. The buccal groove is short and faint, extending about one-quarter of the crown height.

Three widely splayed roots are partially preserved. The remaining height of the distobuccal root is 6.7 mm, and that of the mesiobuccal is 4.8 mm. Both the mesiobuccal and distobuccal roots are longest BL and narrowest MD and rise nearly directly above the crown. The MD-elongated lingual root leans over the crown and 5.8 mm of its height remain in lingual view.

Based on similarities in morphology and wear status, this is the proposed antimere of U.W. 101-1377. Unlike U.W. 101-1377, however, this specimen possesses a mesial IPF.

U.W. 101-1377: LdP^3 (Fig. 4B; Table 1) An enamel chip sits at mesiobuccal aspect of the Pa at the intersection with the MMR. No IPFs are observed. The mesial cusps are lightly

worn, with a dentine pit exposed over the Pr and Pa and a wear facet visible on the mesial crest of the Pr (Stage 2). The crown is molariform, with four well-developed cusps arranged in size as Pr > Pa > Me > Hy. The Hy is large, conical in shape, and as high as the Me. In occlusal view, the crown is shaped like a pentagon, which reflects the large and distolingually projecting Hy and well-developed, obliquely angled mesiobuccal and distobuccal aspects. The MMR is high and well developed. Just distal to the MMR is a deep groove separating it from a thick epicrista that forms a distinct tubercle observed from the buccal aspect. The combination of the well-developed MMR and epicrista contributes to a mesiobuccal projection of the occlusal surface. A tall and uninterrupted Co extends between the Pr and Me. The DMR is thick and rounded, but is much lower than the Co, and bounds a small, groove-like and BL-oriented Fp that is continuous with the distal occlusal groove separating the Hy and Me. There is a weak Carabelli's feature on the mesiolingual aspect of the Pr that takes the form of a v-shaped furrow. The lingual groove is deep near the occlusal margin until it terminates at mid-crown. The buccal groove is a faint indentation that quickly fades below the occlusal surface.

Three widely splayed roots are partially preserved. The lingual root is completely broken away, the distal buccal root is broken at about half its height, and the mesial buccal root is broken near its apex. Both the mesiobuccal and distobuccal roots are longest LaL and narrowest MD. The preserved height of the distobuccal root is 5.4 mm in buccal view, and the mesiobuccal is 9.9 mm.

This specimen is proposed as the antimere of U.W. 101-823. Further, it is proposed to be associated with the U.W. 101-1376 LdP^4. Both specimens lack IPFs, which is consistent with this assignment, and were excavated within centimeters of each

other. Further, these teeth are proposed to be associated with the mixed dentition of U.W. 101-1400 and other isolated teeth.

3.5. Deciduous maxillary fourth premolars

Four dP^4s, representing a minimum of three individuals, are known from the Dinaledi Chamber deposits. Two of them are proposed as antimeres, U.W. 101-1376 and U.W. 101-1687, while the other two, U.W. 101-384 and U.W. 101-544A, must represent two additional individuals given differences in their crown developmental and macrowear statuses. The four teeth present a consistent morphological pattern featuring four well-developed cusps, a continuous Co, slightly rhomboidal occlusal profile with a Hy that projects distolingually, and weak Carabelli's expression.

U.W. 101-384: RdP^4 (Fig. 5A; Table 1) Enamel chipping to the occlusal edge of the MMR sits just above the mesial IPF and another chip is found on the buccal aspect of the Me. An oval mesial IPF (3.5 mm LaL by 1.5 mm OC) and a larger circular distal IPF (3.1 mm LaL by 3.7 mm OC) are present. Dentine patches are exposed on all cusps (stage 4). The dentine pool over the Pr is the largest, extending from the distal crest, broadening over the apex, continuing along its mesial crest, and curving buccally to include the region of the Fa. The four main cusps are well developed and have the following size relationships: Pr > Pa > Me > Hy. The occlusal outline is rhomboidal and mildly skewed, as the Hy projects distolingually. A trace of the groove separating the Pa and Me remains, as does a portion of the groove separating the Pa and Pr and a small portion of the groove delineating the Hy and terminating at the Fp remains as well. A short, shallow buccal

groove extends about half the distance of the crown. On the lingual surface, a small deep pit is all that remains of what was likely a deep lingual groove.

U.W. 101-544A: RdP^4 germ (Fig. 5B; Table 1) This is an unerupted crown with no trace of root formation. There is some post-depositional damage to the fragile cervix lingually and distally; though, the germ does not appear to be crown complete. The Hy broke away from the trigon postmortem and is refit to the crown. The break follows the contour of the lingual groove and parallels the Co onto the buccal side where the Me, a distal accessory ridge, and DMR meet. A deep crack remains and widens on the lingual aspect and, even though refit, the Hy is shifted slightly distally. The morphology is not affected by this damage, but the MD measurement is adjusted to account for this damage.

All four principal cusps are well developed and there is no hint of accessory cusps. In size, the cusp sizes are approximately Pr > Pa > Me > Hy. The Hy is large and conical in shape, nearly as high as the other three cusps, and projects distolingually, which gives the crown a rhomboidal occlusal outline. The mesial edge is slightly convex, while the buccal and lingual profiles are fairly straight with mild indentations for the lingual and buccal grooves. The essential ridges of the Pr, Me, and Hy are indistinct. The Pa has a narrow mesial accessory ridge, and the Pr has a short, but distinct, mesial accessory ridge that meets the mesial accessory ridge of the Pa at the central fovea. These accessory ridges define the distal extent of the Fa, which takes the form of a BL-oriented groove. The mesial aspect of the Fa is defined by a thick and rounded MMR that features two mesial accessory tubercles: the paraconule and mesial accessory tubercle (Scott and Turner, 1997; Scott and Irish, 2017). These tubercles extend into the Fa as short ridges.

501 The Fp is a small pit defined by an indistinct DMR. The Co is continuous. A small
502 Carabelli's feature is present and takes the form of a weak obliquely oriented ridge
503 associated with a small pit at its base. The buccal groove is shallow and extends
504 approximately one-quarter of the distance to the cervix. The lingual groove cannot be
505 accurately assessed due to the crown damage.
506 This specimen shares a specimen number with another deciduous tooth (U.W.
507 101-544C; RdI^1) and crown incomplete RC^1 (U.W. 101-544B) because they were
508 excavated in close spatial proximity. Though all represent sub-adults, it is unlikely that
509 they represent a single individual. For example, U.W. 101-544B and U.W. 101-544C
510 have proposed antimeres in the assemblage and are likely attributable to the nearly
511 complete mixed dentition associated with the U.W. 101-1400 mandible and its associated
512 antimeres and occluding teeth, which have erupted dP4s and nearly crown-complete M1s;
513 this would preclude the developing RdP^4 germ, U.W. 101-544A, from belonging to the
514 same individual as U.W. 101-544B and U.W. 101-544C. However, from a modern
515 human perspective, the developmental status of U.W. 101-544A is not inconsistent with
516 attribution to the same individual as U.W. 101-544B and U.W. 101-544C (AlQahtani et
517 al., 2010). The possible association of U.W. 101-544B and U.W. 101-544C with U.W.
518 101-1400 are given a detailed treatment in the Discussion.
519
520 U.W. 101-1376: LdP^4 (Fig. 5C; Table 1) The crown is unworn (stage 1) and no IPFs are
521 present. The crown possesses four well-developed cusps with the following size
522 relationships: Pr > Pa ≥ Me ≥ Hy. The Hy is relatively large and projects distolingually,
523 giving the crown a rhomboidal, mildly skewed outline. All cusps are high. The cusps

524 comprising the trigone are of equal height and the Hy only slightly lower. The cusps are
525 also widely spaced, and their tips are placed at the edge of the occlusal margin. The Pr
526 has a weakly-developed essential ridge and a larger mesial accessory ridge that forms a
527 protoconule with a free apex. The Pa has a weakly-developed essential ridge and a
528 narrower, sharper mesial accessory ridge. In addition to the protoconule, a second
529 marginal tubercle—the mesial accessory tubercle (Scott and Turner, 1997)—sits along
530 the MMR. Compared to the low, rather indistinct DMR, the MMR is high and prominent.
531 The Co is high, sharp, and continuous. It is separated from the trigone by a deep occlusal
532 groove that continues onto the lingual surface for about half the height of the crown. The
533 Hy has a faint essential ridge and a short distal accessory ridge. A Carabelli's feature,
534 consisting of a faint v-shaped ridge and groove, is limited to the mesiolingual corner. The
535 buccal groove is a shallow indentation at the occlusal surface that fades at mid-crown.
536 Portions of three widely splayed roots are preserved: two buccal and one lingual.
537 The mesiobuccal root is broken near the cervix, while the distobuccal and lingual roots
538 are broken at about half their length. The distobuccal root measures 4.8 mm from the
539 cervix, the mesial buccal root measures 2.5 mm, and the lingual root measures 3.3 mm.
540 The lingual root is BL compressed, while the two buccal roots are MD compressed.
541 The specimen is proposed to be associated with the U.W. 101-1377 LdP^3. Both
542 specimens lack IPFs, which is consistent with this assignment, and further, the teeth,
543 though isolated, were excavated within centimeters of each other. This specimen is
544 proposed as the antimere of the U.W. 101-1687 RdP^4. The other RdP^4 in the assemblage,
545 U.W. 101-544A, lacks any trace of root development and appears to be crown
546 incomplete. Thus, U.W. 101-1687 and U.W. 101-1376 represent a slightly older

individual. Further, it is proposed that U.W. 101-1376/1687 belong to the mixed dentition represented by U.W. 101-1400 and other isolated teeth.

U.W. 101-1687: RdP^4 (Fig. 5D; Table 1) Neither mesial nor distal IPFs are present and the crown is lightly worn (stage 1). The crown is rhomboidal in outline and only mildly skewed by the distolingual projection of the Hy. Four well-developed cusps are present with the following size relationship: Pr > Pa ≥ Me ≥ Hy. The cusp apices are high, with the cusps comprising the trigone equal in height and the Hy only slightly lower. The cusps are also widely spaced, and all cusp tips are oriented towards the edge of the occlusal margin. The Pr has a weakly-developed essential ridge and a pair of weak mesial accessory ridges. In addition to the Pa essential ridge, mesial and distal accessory ridges are present. The Me essential ridge merges with the distal margin of the Pr to form a high, sharp, and incompletely bisected Co. The Hy is separated from the trigone by a deep occlusal groove that continues as the lingual groove, which disappears at mid-crown. The buccal groove is a faint depression throughout. The MMR is thick and continuous. Two small tubercles (mesial marginal tubercle and the mesial Pa tubercle) rise from the MMR near the center of the crown. The low and indistinct DMR is separated from the occlusal basin by a thin groove-like Fp. A small Carabelli's feature presents as an obliquely angled swelling and groove on the mesiolingual corner.

Portions of three widely splayed roots, two buccal and one lingual, are preserved. All three roots are broken near the cervix and the mesiobuccal root canal is filled with sediment. Approximately 2.7 mm of the lingual root is preserved, 4.0 mm of the mesiobuccal root is preserved, and the distobuccal root is broken away at the cervix.

This is the proposed antimere of U.W. 101-1376. The configuration of the mesial portion of the Pr differs between the teeth, though. Along the mesial Pr crest of this specimen are small crests extending into the Fa, while in U.W. 101-1376 the crests are replaced by a more prominent protoconule. The configuration of the Carabelli's feature of this specimen differs from its proposed antimere, where the feature is more v-shaped. This tooth also likely belongs to a mixed dentition that includes U.W. 101-1400.

3.6. Deciduous mandibular lateral incisor

A single dI_2 is currently known from the Dinaledi Chamber deposits. The crown is simple in form, with weak marginal ridges and a featureless lingual fossa.

U.W. 101-1612: RdI_2 (Fig. 6; Table 1) An ovoid mesial IPF (0.9 mm LaL by 1.1 mm IC) is present, but no distal IPF is detectable. The crown is only minimally worn with a short, thin line of dentine exposed on the mid-section of the incisal edge (stage 1). The crown is tall and narrow. In labial view, the crown lacks prominent features and is slightly convex IC. It is asymmetrical in both labial and lingual views with a marked distal slope and curved distal corner. The mesial and incisal edges, on the other hand, are nearly perpendicular to each other. The incisal edge is straight, and the mid-crown is mildly convex. On the lingual surface, there are weak marginal ridges that gradually disappear as they reach cervically. The lingual fossa is featureless.

The root is missing its tip. In the labial view, its preserved height is 9.2 mm. The root is teardrop shaped in cross-section and is MD flattened. A shallow groove runs along the length of its distal aspect. The root tip deflects slightly mesially.

This specimen is proposed to be part of the group of teeth that also includes the U.W. 101-1400 mandible and associated specimens.

3.7. Deciduous mandibular canines

Three isolated dC_1s (U.W. 101-824, U.W. 101-1571, U.W. 101-1611) and a fourth found in the U.W. 101-1400 mandible are known from the Dinaledi Chamber deposits. Collectively, these teeth represent at least three individuals. The morphology of the dC_1 is best discerned from the two lightly worn proposed antimeres, U.W. 101-1400 and U.W. 101-1611, with the two more worn specimens consistent with the pattern. In labial view, the dC_1 crown is asymmetric in profile, with a short, convex mesial crest meeting a mesial shoulder that sits more apically than the distal shoulder. The distal crest is longer, nearly vertical, and terminates in a tubercle. The crown apex is slightly offset distally. The morphology of the deciduous canine mirrors that of the permanent canine.

U.W. 101-824: LdC_1 (Fig. 7A; Table 1) The apex of the crown is chipped labially. Despite the presence of occlusal wear, neither mesial nor distal IPFs are detectable. A large dentine pool is exposed at the crown apex and narrows along the distal crest (stage 3–4). The crown is asymmetrical in lingual and labial view: it has a high, mesially placed apex from which the occlusal edge slopes distally. The distal edge is notably longer than the mesial and terminates at a small tubercle delineated by labial and lingual furrows. On the lingual surface, the basal cingulum is rounded and weakly developed. The bulk of this prominence is distally placed in occlusal view.

615 The root is abraded on all sides and broken at its apex. The root is ovoid in cross
616 section and wider MD than LaL. The maximum preserved height, approximately 10.3
617 mm, exists distolabially.
618
619 U.W. 101-1571: LdC_1 (Fig. 7B; Table 1) A small IPF is present distally and a larger (1.5
620 mm LaL by 2.2 mm OC) teardrop shaped mesial IPF is present. Wear is evident, as the
621 apex is blunted and dentine is exposed here and slightly along the mesial crest (stage 4).
622 The distal tubercle is flattened by wear, but no dentine is exposed. The morphology of the
623 remaining crown resembles the other, better-preserved, mandibular deciduous canines.
624 The crown is asymmetrical and, based on the size of the occlusal dentine exposure, the
625 original cusp was likely high. The distal tubercle is intact and is circumscribed by weak
626 labial and lingual fossae. The cervical eminence is weak, and a broad lingual ridge
627 divides the crown into mesial and distal fossae. The preserved mesial fossa is small and
628 appears as a shallow depression. The distal fossa is also quite shallow and appears as a
629 small feature adjacent to the DMR and distal tubercle.
630 The root is broken at a sharply oblique lingual-to-labial angle. Along the buccal
631 face, approximately 4.7 mm of root remain. Sediment fills the pulp chamber.
632
633 U.W. 101-1611: RdC_1 (Fig. 7C; Table 1) The crown is minimally worn, with a small
634 facet on the apex and a longer facet running along the distal crest. Neither facet exposes
635 any dentine (stage 1). The crown is ovoid in occlusal view. In labial and lingual views,
636 the crown is asymmetrical with a short, high mesial shoulder and a long distal edge
637 terminating in a tubercle. The mesial crest is convex, while the distal is steeply angled

and slightly concave because of wear. The crown apex is slightly offset distally. In lingual view, the crown possesses a broad dull median lingual ridge that narrows as it approaches the apex. The mesial and distal fossae are both shallow, with the distal narrower and more groove-like. In labial view there is a weak distal fossa associated with the tubercle.

The root is broken at its apex. Approximately 9.3 mm of root remains in labial view. The root is ovoid in cross-section and somewhat flattened LaL.

The tooth is consistent in morphology with its proposed antimere in the U.W. 101-1400 mandible.

3.8. Deciduous mandibular third premolar

A proposed antimeric pair of dP_3s is currently known from the Dinaledi Chamber deposits. One is in situ in the U.W. 101-1400 mandible, while its antimere, U.W. 101-1685, is isolated. Morphologically, both present a molarized occlusal pattern, with five main cusps present. The crowns are elongated MD compared to the BL breadth and are slightly BL broader across the talonid than the trigonid. A strong mesial trigonid crest extends into the Fa, creating a narrow, groove-like, Fa that parallels the MMR and mesial crest of the Pr. Both lack a protostylid and accessory cusps. The mesial and distal roots are both plate-like.

U.W. 101-1685: RdP_3 (Fig. 8; Table 1) The RdP_3 is preserved in a small, mostly lingual, portion of the mandibular corpus, which retains a portion of the crypt of the P_3. There is an enamel chip distally along the DMR between the End and Hld. There is a small distal

IPF offset buccally, but no facet is detectable mesially. The crown shows light wear with a small facet visible on the buccal aspect of the Prd cusp tip, and small dentine pits are exposed on the End, Hyd, and Hld (stage 2). There is also a small facet, with no dentine exposed, on the distoocclusal portion of the Hld. The occlusal outline is rectangular, being MD elongated and BL narrow. The crown possesses five well-developed cusps with following size relationships: Prd > Hyd > Med > End > Hld. The talonid is wider than the trigonid and the trigonid cusp apices reach higher than those of the talonid. The Med cusp tip is higher than that of the Prd. The Prd cusp tip sits mesial to that of the Med and is internally placed close to the central groove. The MMR is thick and separated from the Prd and Med by shallow and deep grooves, respectively. Two cuspules, premetaconulid and mesioconulid, rise from the MMR and are delineated by weak grooves. The buccal segment of the MMR is thicker than the lingual and, where the two portions meet at an angle, their junction is marked by a groove. The thick MMR is continuous with the mesial Prd crest and passes mesially to a strong mesial trigonid crest emanating from the Prd; thus, the Fa exists as a narrow groove running between these crests. The midtrigonid crest is separated from the Med by a groove. Near the occlusal surface, the mesiobuccal groove is a deep narrow cleft and then it opens up at mid-crown. The deep mesiobuccal groove and associated v-shaped furrow contribute to the waisted appearance in occlusal view. There is a detectable distobuccal groove only at the occlusal surface. There is a minor mesiolingual groove that extends less than 1.5 mm cervically from the mesial Med crest. The distolingual groove is faint across its course. A faint groove adjacent to the MMR is visible in buccal view. The buccal face presents a slight cervical prominence, but the surface is smooth; no protostylid is present.

Plate-like mesial and distal roots are present. The apex of the mesial root is closed. The mesial root is preserved in its entirety and is 9.4 mm in height along its buccal edge. The distal root is also preserved in its entirety and is 9.3 mm in height. The roots are widely splayed, and with the adhering mandible, preserve a portion of the crypt of the P_3.

This is the antimere of the LdP_3 preserved in the U.W. 101-1400 mandible. Further, it articulates with U.W. 101-1686 (RdP_4).

3.9. Deciduous mandibular fourth premolar

A proposed antimeric pair of dP_4s is currently known from the Dinaledi Chamber deposits. One is in situ in the U.W. 101-1400 mandible, while the other, U.W. 101-1686, is isolated. Morphologically, both present a molarized occlusal pattern, with five main cusps present. In comparison to the associated dP_3s, the Hld is relatively larger and the BL breadth across the talonid is noticeably greater than the breadth across the trigonid. As with the dP_3, a strong midtrigonid crest is present; however, on the dP_4 it is continuous between the mesial crests of the Med and Prd and completely bounds the Fa distally. Both lack accessory cusps and have faint protostylids. The mesial and distal roots are both plate-like.

U.W. 101-1686: RdP_4 (Fig. 9; Table 1) The crown surface is lightly worn, with a small wear facet visible along the mesial Prd crest (stage 1). The occlusal outline is rectangular, being MD elongated and BL narrow. Five primary cusps are present and the talonid is wider than the trigonid. The cusps have the following size relationships: Med > Hyd >

Prd > End > Hld. The MMR is thick and three small cuspules (preprotoconulid, mesioconulid and premetaconulid) outlined by shallow occlusal and mesial grooves rise from the MMR. The Prd and Med each have prominent mesial crests, which meet to form a mesial trigonid crest separated from the MMR and essential ridges of the Prd and Med by deep grooves. The Med exhibits an incipient postmetaconulid. The essential ridge of the Hyd is bifurcated. The substantially larger mesial portion constricts slightly in the middle and then expands before terminating at the central groove. The End possesses a weak mesial accessory ridge. The components of the DMR originating from the Hld and End meet at an angle and delineate a narrow and weak Fp. The mesiolingual groove is short and shallow terminating about one-quarter the distance to the cervix. In addition, there are short and shallow lingual vertical furrows associated with the cuspules of the MMR and with the postmetaconulid. The mesiobuccal groove is deep, forms a wide v-shaped fovea near the occlusal edge, and terminates at approximately mid-crown. A deep distobuccal groove terminates approximately mid-crown. A short cingular swelling sits on the buccal face of the Hld and terminates at the distobuccal groove. A faint swelling mesiolingually may represent a weakly expressed protostylid.

The broken mesial root is refit to the crown (not evident in Fig. 9). The mesial root is damaged apically, and lingual and buccal root canals are exposed. As preserved, in the mesial view the buccal aspect of the root is 7.5 mm, the lingual aspect is 7.3 mm, and the maximum BL width is 9.8 mm. The lingual and buccal aspects of the root are rounded tubes with a MD thin section of root stretched between them. The distal root is broken so that only a 2.2 mm section remains distobuccally.

This specimen is morphologically very similar to its proposed antimere, the LdP_4 of U.W. 101-1400. However, the two teeth differ in the configuration of accessory ridges on the lingual face of the Hyd, with U.W. 101-1400 having three discernible crests and U.W. 101-1686 only two. Further, this specimen is associated with the U.W. 101-1685 RdP_3. Their reciprocal IPFs are a good match.

3.10. Permanent maxillary central incisors

Five isolated I^1s, representing at least four individuals, are known from the Dinaledi Chamber deposits. A fifth individual is represented by the I^1 found in situ in the U.W. 101-1277 maxilla. All known I^1s from the Dinaledi Chamber are worn across the incisal edge to such an extent that dentine is exposed. The I^1s present a consistent morphological pattern characterized by a featureless lingual fossa, weak basal eminence, and low marginal ridges.

U.W. 101-038: RI^1 (Fig. 10A; Table 1) There is a large teardrop shaped mesial IPF (3.0 mm along its major axis by 1.8 mm across its minor axis). A small vertical ovoid distal IPF, less than 1.0 mm in all dimensions, is also present. A thin line of dentine is exposed along most of the incisal edge, but it does not quite extend to the distal margin (stage 3–4). Labially, the crown is featureless and mildly convex at midcrown. Lingually, the crown exhibits mild basal swelling. Weak tuberculum dentale, expressed as finger-like extensions, emanate from the basal swelling, extend into the otherwise featureless lingual fossa, and terminate at or just before the incisal edge. Both the MMR and DMR are

751 weakly expressed, giving the tooth a mild shovel shape. The MMR is cut short by the
752 encroachment of the mesial IPF. The DMR is slightly more prominent than the MMR.
753 The apex of the root is broken away. In labial view, approximately 14.2 mm of
754 the root is preserved. The root is broader LaL than MD, has subtle depressions running
755 along both the mesial and distal faces, and, especially apparent apically in labial and
756 lingual views, tilts slightly distally.
757 This specimen and U.W. 101-039 were both found on a rock and had been
758 arranged by cavers prior to excavation (see area D in Dirks et al., 2015: Figure 6B).
759
760 U.W. 101-591: LI^1 (Fig. 10B; Table 1) Most of the mesial IPF has been removed by
761 wear; the remaining portion (3.0 mm LaL by 1.0 mm IC) merges with the incisal edge.
762 The distal IPF (2.8 mm by 1.2 mm) is obliquely oriented relative to the crown. A thick,
763 wide band of dentine is exposed along the entire incisal surface (stage 4) and there is a
764 steep lingual slope to the wear plane. An enamel chip is located incisal to the distal IPF.
765 The basal eminence is slight and bulbous and the median lingual ridge flat. These two
766 features occupy most of the remaining lingual face; though, shallow grooves delineating
767 the marginal ridges are visible near the incisal edge. Labially, the crown is minimally
768 convex at midcrown.
769 Especially distally and mesially, the root is abraded and cracked across its
770 exposed surface. Further, it is broken just before its apex (12.7 mm in preserved height),
771 exposing the canal. The root is ovoid in cross section with its major axis LaL and minor
772 axis MD.
773

U.W. 101-931: LI^1 (Fig. 10C; Table 1) There is a larger teardrop shaped mesial IPF (3.1 mm LaL by 4.1 mm IC) and a smaller distal IPF (1.8 mm by 3.6 mm). A thin strip of dentine, which does not extend to the mesial and distal edges, is exposed along the incisal surface (stage 3–4). The labial face is minimally convex MD and IC. On the lingual surface, a weak lingual basal eminence is slightly offset mesially. Faint finger-like ridges extend towards, and in some cases reach, the incisal edge. The crown is weakly shovel-shaped with low, rounded marginal ridges that become indistinct where they merge with the basal cingulum. The DMR is stronger than the MMR. Linear hypoplasias are observed in the cervical third of the crown (for a discussion of hypoplasias on this specimen, see also Skinner, 2019).

The root is abraded across most of its surface and its apex is missing, exposing the canal. Labially, 14.2 mm of the root are preserved. At the cervix, the root is rounded in profile and tapers towards its apex to become more compressed MD.

The mesial IPF fits well with the IPF of its proposed antimere, U.W. 101-1012, while the distal IPF is a reasonable match for that of the mesial facet of U.W. 101-932. As U.W. 101-932 has proposed antimere, U.W. 101-709, that also fits well with U.W. 101-1012, this tooth likely belongs to a complete set of maxillary incisors (U.W. 101-709, -931, -932, and -1012) and antimeric canines (U.W. 101-706 and U.W. 101-816). This attribution is consistent with the fit of their respective IPFs, incisal wear, and morphological status as antimeres.

U.W. 101-1012: RI^1 (Fig. 10D; Table 1) Two enamel chips are missing from the lingual aspect adjacent to the mesial IPF. There is a large teardrop shaped mesial IPF (4.1 mm

LaL by 3.1 mm IC) sitting at the incisal edge where it squares off the mesial corner. A smaller distal IPF (3.6 mm LaL by 1.8 mm IC) is also present. A thin strip of dentine is exposed along the incisal edge (stage 2). Labially, the crown is featureless, and the crown is minimally convex both IC and MD at midcrown. Lingually, faint finger-like projections reach into the lingual fossa and fade prior to the incisal edge. The crown is mildly shovel-shaped with weak marginal ridges. The DMR is more prominent than the MMR. Linear hypoplasias are visible in the cervical third of the crown (for a discussion of hypoplasias on this specimen, see also Skinner, 2019).

The root is abraded across most of its surface, and it is broken at its apex, exposing the root canal. On the labial aspect, 14.0 mm of root is preserved. Near the cervix, the root is rounded in cross section and tapers apically to become compressed MD. The apex of the root is distally inclined.

The mesial IPF is a good match with that of U.W. 101-931, its proposed antimere. The distal IPF is consistent in size and shape with that of U.W. 101-709. This tooth likely belongs to a complete set of maxillary incisors (U.W. 101-709, -931, -932, and -1012) and antimeric canines (U.W. 101-706 and U.W. 101-816). This attribution is consistent with the fit of their respective IPFs, incisal wear, and morphological status as antimeres.

U.W. 101-1558: RI^1 (Fig. 10E; Table 1) Neither mesial nor distal IPFs are preserved. The crown has a large dentine exposure and a complete enamel ring (stage 5). The incisal wear has a distolingual inclination. The preserved labial face is flat and featureless. No marginal ridges are preserved.

The root is broken just before its apex and the root canal is exposed. The maximum root height is 14.5 mm. Cementum is cracked and flaking off the external surface, especially labially. The root is ovoid, being compressed MD.

3.11. Permanent maxillary lateral incisors

Seven isolated I^2s are known from the Dinaledi Chamber deposits. Additionally, an I^2 is in situ in the U.W. 101-1277 maxilla. Collectively, these eight I^2s represent at least six individuals. They present a consistent morphological pattern characterized by a featureless lingual fossa, weak basal eminence, and low marginal ridges. The incisal edge is straight, but the crown is moderately MD convex at mid-crown and only slightly convex IC. In labial and lingual views, the I^2 crown flares incisally, with squared mesial and convex distal edges.

U.W. 101-073: RI^2 (Fig. 11A; Table 1) A small mesial IPF (approximately 1.5 mm IC by 1.0 mm LaL) is present; however, no distal IPF is detected. The crown is well preserved and exhibits minimal wear: the incisal surface is polished, but no dentine is exposed (stage 1). The incisal edge is minimally convex, but the tooth is moderately convex at mid-crown. A subtle notch is present in the center of the incisal margin. This divot resembles more pronounced notches seen on less worn maxillary (i.e., U.W. 101-1588) and mandibular (i.e., U.W. 101-1075, U.W. 101-1131, and U.W. 101-1400) lateral incisors. In both labial and lingual view, the mesial edge is perpendicular, while the distal edge is rounded. Lingually, there is a lingual fossa, but the marginal ridges are faint, merging into a slightly swollen basal cingulum that is more prominent than the marginal

ridges. Within the lingual fossa are trace ridges, with the ridge nearest the DMR being the most prominent among them.

The root is broken just before the apex and its surface is abraded. In labial view, the remaining root is 12.3 mm in height. The root is compressed MD, with a shallow invagination along the distal face. In lingual and labial views, the root tilts subtly distally.

This is a possible antimere of the U.W. 101-1588 LI^2. The teeth are similar morphologically, in their wear status, and in the presence of small mesial IPF and absence of a distal IPF.

U.W. 101-417: LI^2 (Fig. 11B; Table 1) The root broke from the crown near the cervical line and the two portions have been refit. The fit is mostly flush, except distally where the joint is not clean. A small mesial IPF (2.6 mm IC by 1.0 mm LaL) is adjacent to the MMR and continues to the incisal edge. No distal IPF is visible. A line of dentine extends along the incisal edge (stage 3). The wear facet angles distally so that the preserved crown height is shorter distally than mesially. In incisal view the crown is moderately convex, while in mesial or distal view the crown and root are only minimally convex. Labially, the crown is featureless except for minor linear hypoplastic defects in the cervical third. Lingually, the faint MMR and DMR converge at the base and circumscribe a shallow, featureless lingual fossa. There is a slight lingual basal eminence that is offset distally.

In addition to the damage near the cervix, the root is broken at the apex, which exposes the sediment-filled canal. From the labial cervix, the preserved root height is

16.8 mm. In cross section, the root is longer LaL than MD and has a subtle groove running along the distal face.

U.W. 101-709: RI^2 (Fig. 11C; Table 1) The mesial IPF (approximately 2.3 mm LaL by 3.3 mm IC) is larger than the distal IPF (2.7 mm by a maximum of 1.2 mm). The distal IPF is complex in shape and has two facets strongly angled relative to each other so that one facet is placed more incisally, having eaten into the DMR, and faces lingually, while the other is placed more cervically on the distal edge. The incisal edge itself is polished but no dentine is exposed (stage 1). The incisal edge is straight, but the tooth is moderately convex at mid-crown. It is only slightly convex IC. In labial and lingual views, the crown flares incisally with a squared mesial and convex distal edge. The labial face is featureless. Lingually, the crown exhibits weak shoveling and the marginal ridges circumscribe a shallow lingual fossa. There is a single, faint finger-like extension from the basal cingulum that ends at a distolingual wear facet. Though worn, a dip can be seen near the center of the incisal edge. This feature matches the morphology seen in less worn *H. naledi* I_2s (e.g., U.W.101-1131 and U.W. 101-1400) and I^2s (i.e., U.W. 101-1588).

The root is broken just before its apex, exposing the root canal. The preserved labial height is 11.2 mm. The root is elliptical in cross section, broader LaL than MD. The root tilts slightly distally, especially apically.

This specimen is proposed as the antimere of U.W. 101-932. They are similar in morphology, degree of occlusal wear, and even in the complex shape of their distal IPFs. Tentative associations are made with other anterior teeth. The mesial IPF possibly matches that of U.W. 101-1012 and the distal IPF is proposed to fit U.W. 101-816. If

these proposals are true, then this tooth belongs to a complete set of maxillary incisors (U.W. 101-709, -931, -932, and -1012) and a set of antimeric maxillary canines (U.W. 101-706 and U.W. 101-816).

U.W. 101-932: LI^2 (Fig. 11D; Table 1) The distal IPF is small and sits near just superior to the distal shoulder. The mesial IPF is larger (2.2 mm LaL by 3.3 mm IC). The incisal edge is lightly worn with no dentine exposure. The lingual face has moderate facets near the incisal edge, and there is a small facet on the distolingual near the distal IPF (stage 1). The mesial border is perpendicular to the incisal edge, and the distal border is convex in labial and lingual views. In occlusal view, the crown is straight at the incisal edge and moderately convex mid-crown. The labial face is featureless except for a faint distolabial depression near the incisal margin. The lingual face has a moderately elevated basal eminence and slight marginal ridges that are stronger as they approach the incisal edge. There are two faint finger-like extensions from the basal eminence that terminate at the lingual wear facets.

The root is missing its apex. What is preserved is abraded and deflects distally. The root is ovoid in cross section with its major axis LaL and minor axis MD. The preserved root measures 11.3 mm in height from the labial aspect.

The mesial IPF of this specimen is a good fit for U.W. 101-931 LI^1. Based on similarities in wear and morphology, this specimen is a reasonable antimere of U.W. 101-709. This tooth likely belongs to a complete set of maxillary incisors (U.W. 101-709, -931, -932, and -1012) and antimeric canines (U.W. 101-706 and U.W. 101-816). This

attribution is consistent with the fit of their respective IPFs, incisal wear, and morphological status as antimeres.

U.W. 101-952: LI^2 (Fig. 12A; Table 1) There is a large mesial IPF that reaches the worn incisal edge (2.1 mm LaL by 2.6 mm IC). Distally, a small IPF (approximately 0.7 mm LaL by 2.4 mm IC) is present along the DMR near the incisal edge. A distinct line of dentine is exposed across much of the incisal edge (stage 3). The labial face is featureless and moderately convex mid-crown. Lingually, there are weak marginal ridges that merge with the basal cingulum, forming a pit. The lingual fossa is shallow with trace fingerlike extensions arising from a weak basal eminence. Linear hypoplasias are observable in the cervical third (for a discussion of hypoplasias on this specimen, see also Skinner, 2019).

The root is broken and a fragment of root that fits neatly onto the fresh break is refit (not apparent in Fig. 12A or in the surface files). Other than the fracture, the root is well preserved, with some abrasion apparent near the apex of the root. The root is ovoid in cross section, with wide shallow depressions running along both mesial and distal faces. The preserved maximum height of the root is 19.0 mm in labial view.

U.W. 101-1588: LI^2 (Fig. 12B; Table 1) There is a small mesial IPF (1.2 mm LaL by 2.2 mm IC) that sits adjacent to the MMR and near the incisal edge. No distal IPF is detectable. The crown is lightly worn, with facets along the incisal edge and the lingual face, but no dentine is exposed (stage 1). Labially, the crown is featureless. It is moderately convex at mid-crown but has a straight incisal edge. Lingually, there are trace marginal ridges and a shallow lingual fossa. The lingual basal eminence is low and

rounded. As with some other *H. naledi* lateral incisors, maxillary and mandibular (e.g., U.W. 101-1075, U.W. 101-1400), a distinct notch sits in the center of the incisal edge. The mesial corner is nearly perpendicular, while that of the distal shoulder is gently curved.

The root is well preserved, with a break at the apex exposing the root canal. The root is MD compressed and ovoid in cross section. There is a shallow groove running along the distal face. The maximum preserved height is 14.9 mm.

This is the possible antimere of U.W. 101-073. The two teeth are similar in morphology and wear status, including the presence of small mesial IPF and absence of a distal IPF. The lingual wear facet is, however, more pronounced on U.W. 101-1588 and the incisal notch less pronounced on U.W. 101-073; though, the topography of the labial face suggests that a notch was present on U.W. 101-073 in the unworn state.

U.W. 101-1684: LI^2 (Fig. 12C; Table 1) The incisal edge is chipped mesially. Neither mesial IPFs is preserved at this level wear. A very small distal IPF remains. The crown is heavily worn and with a wide dentine exposure and complete enamel rim (stage 5). The labial face is featureless and flat. Lingually, what remains of the MMR and DMR is faint, and the lingual fossa is shallow. The basal eminence is low and rounded and offset mesially.

The root is broken obliquely so that the labial portion is longer than the lingual. The root is also abraded, especially mesially. In labial view, 11.7 mm of the root remains, while 5.1 mm remains along the lingual aspect. The root is MD compressed and ovoid in cross section. Its apex deflects distally.

The tiny distal IPF possibly matches an equally small IPF on the U.W. 101-1556 LC^1. Further, their degree of macrowear is consistent. Thus, tentatively, U.W. 101-1684 is proposed to belong to the associated left teeth U.W. 101-1556, -1560, and -1561.

3.12. Permanent maxillary canines

Eleven isolated maxillary canines are known from the Dinaledi Chamber deposits. Additionally, a C^1 is found in situ in the U.W. 101-1277 maxilla. Collectively, they represent at least eight individuals. The maxillary canines present a consistent morphological and macrowear pattern. The crown appears tall relative to its small base. In labial view, the crown is asymmetric because the mesial shoulder sits more apically than the distal shoulder and the mesial crest is shorter than the distal. In addition, the mesial shoulder is more angular than the rounded distal shoulder. The marginal ridges on the lingual face are weak and the lingual fossa is relatively featureless except for occasional faint ridging. At early stages of wear, the mesial crest of the crown is blunted, and the asymmetry of the labial crown profile is maintained. As wear progresses, the apex becomes blunted, and the wear surface becomes planar. At early stages of wear, a distinctive wear facet is frequently present on the distolingual face where it extends from the crown apex, runs parallel to the distal edge, and may extend onto the DMR near the distal shoulder.

U.W. 101-337: RC^1 (Fig. 13A; Table 1) No IPFs are visible mesially or distally. The apex of the tooth is chipped, and wear blunted the apex, exposing a small patch of dentine; further, a moderately sized facet has flattened the mesial crest (stage 1). A very

small wear facet is present on the lingual face adjacent to the distal crest at about its midpoint. The placement of the facet suggests that it represents the earliest phase of similar facets on *H. naledi* canines at more advanced stages of wear (i.e., U.W. 101-412, U.W. 101-501, U.W. 101-706, U.W. 101-908). The crown is tall relative to its narrow basal width (Table 1). The crown exhibits moderate labial convexity and is minimally convex in mesial and distal views. In labial view, the crown is asymmetric because the mesial shoulder sits more apically than the distal shoulder and the mesial crest is shorter than the distal. In addition, the mesial shoulder is more angular than the rounded distal shoulder. There are only faint mesial and distal vertical grooves; otherwise, the labial face is featureless. Lingually, the MMR is better defined, thicker and rounder than the DMR. A moderately-developed distal accessory ridge originates on the occlusal edge and merges with a thin and sharp ridge extending from the weak basal eminence. There is a weaker and more rounded mesial accessory lingual ridge that runs parallel to the MMR and becomes more topographically prominent near the occlusal edge. These accessory ridges divide the lingual face into a groove-like mesial lingual fossa and larger, more triangular distal and central fossae. Multiple linear hypoplasias are present along the cervical third of the lingual and labial faces (for a discussion of hypoplasias on this specimen, see also Skinner, 2019).

The root is mildly abraded on its external surface and is broken at about two-thirds of its maximum length, which exposes the sediment packed root canal. In labial view, 11.5 mm of root remain. The root is slightly dumbbell shaped in cross section with faint grooves running the length of the root distally and mesially. The mesial depression is slightly deeper. In labial view, the root tilts distally.

U.W. 101-412: LC^1 (Fig. 13B; Table 1) An enamel chip is present on the distal shoulder just above the distal IPF. The distal IPF (2.9 mm IC by 1.5 mm LaL) is adjacent to the DMR, below the apex of the shoulder. A tiny mesial IPF is present at the apex of the mesial shoulder where it is offset lingually. The cusp apex is worn exposing an oval patch of dentine. This occlusal facet extends onto the mesial aspect of the crown. In addition, there is a moderately-sized wear facet on the distolingual face that extends from the apex, running parallel to the distal edge and onto the DMR and extending slightly past the distal shoulder (stage 3–4). Although moderately worn, the original crown contour is largely preserved. The labial face is moderately convex MD at mid-crown and only slightly convex IC. As preserved, the apex is offset distal to the midpoint of the crown. The mesial and distal labial grooves are faint. Lingually, the MMR is wider and better developed than the DMR. Both are bordered by vertical grooves separating them from a swollen, but undefined, median lingual ridge. The basal lingual surface is flat. Linear hypoplasias are evident labially and lingually near the cervix (for a discussion of hypoplasias on this specimen, see also Skinner, 2019).

The distally curving root is broken just before its apex and measures 16.3 mm in height along its labial aspect. In cross section, the root is ovoid with shallow depression running along the mesial side of the root.

This is a possible antimere of U.W. 101-908. They are similar, but not identical, in morphology, size, and in the degree and pattern of wear. Both have wear facets on their lingual faces and dentine exposed at their apices. The specimens, however, differ in their lingual surface morphology, with U.W. 101-908 having a mesial accessory ridge.

Further, the mesial IPF on U.W. 101-908 is much larger than on U.W. 101-412 and U.W. 101-908 is slightly more heavily worn apically, which may point to it deriving from a slightly older individual.

U.W. 101-501: LC^1 (Fig. 13C; Table 1) Consistent with the early stages of apical wear, there are no IPFs visible mesially or distally. There is a tiny wear facet on the crown apex, and small facets are present on the distal accessory ridge and along the mesial occlusal crest (stage 1). The crown is tall relative to its narrow base (Table 1). The crown is asymmetric: the mesial shoulder sits more apically than the distal shoulder and the mesial edge is shorter and less steeply angled. The crown apex is placed near the MD midpoint. The crown has slight labial convexity at the occlusal edge and moderate convexity mid-crown. In mesial and distal views, it is mildly IC convex. The labial face presents faint mesial and distal vertical grooves. The lingual face also exhibits a moderate MMR and weaker DMR. There is no distinct median ridge but there are faint mesial and distal accessory ridges. These ridges converge in the middle of the lingual face, from which they angle vertically before fading into the basal portion of the crown. A narrow groove between these ridges maintains their independence, thus creating a tripartite lingual fossa. The mesial lingual fossa is a groove adjacent to the MMR, the central lingual fossa is shallow, and diamond shaped, and the distal lingual fossa is broader and shallow. Multiple mild hypoplastic defects in the cervical half of the labial crown face.

The root is broken just before its apex, about 11.5 mm in preserved height, and the exposed canal is packed with sediment. The root surface is abraded in patches. The root is elliptical in cross section with its major axis LaL, and minor axis MD. Subtle

grooves run along the mesial and distal faces of the root, with the mesial groove deeper than the distal. In labial view, the remaining root tilts distally.

U.W. 101- 544B: RC^1 germ (Fig. 13D; Table 1) This crown is about two-thirds complete. The mesial shoulder is complete and is associated with a shallow labial groove. Lingually, it is associated with a moderate marginal ridge and groove. The median lingual ridge is faint and bipartite, with central and mesial branches. The distal edge is nearly vertical and the distal shoulder (if present—see U.W. 101-1548, presumed antimere) is not yet developed.

This is the antimere of the crown U.W. 101-1548 canine germ. This specimen shares a specimen number with U.W. 101-544A (RdP^4) and U.W. 101-544C (RdI^1) because they were excavated in close spatial proximity. Though all represent sub-adults, it is unlikely that they represent a single individual. Both U.W. 101-544B and U.W. 101-544C have proposed antimeres in the assemblage and are likely attributable to the nearly complete mixed dentition associated with the U.W. 101-1400 mandible and its associated antimeres and occluding teeth, which have erupted dP4s and nearly crown-complete M1s; this would preclude the developing RdP^4 germ, U.W. 101-544A, from belonging to the same individual as U.W. 101-544B and U.W. 101-544C. However, from a modern human perspective, the developmental status of U.W. 101-544A is not inconsistent with attribution to the same individual as U.W. 101-544B and U.W. 101-544C (AlQahtani et al., 2010). The possible associations of U.W. 101-544B and U.W. 101-544C with U.W. 101-1400 are given detailed treatment in the Discussion.

U.W. 101-706: LC^1 (Fig. 14A; Table 1) The crown has a small mesial IPF (1.3 mm IC by 1.7 mm LaL). Distally, a small facet (2.0 mm along the DMR axis by <1.0 mm perpendicular to the DMR) is visible on the lingual face of the DMR at its most apical extent; this may represent an IPF. Wear blunted the mesial edge, but crown height is not affected (stage 1). As in other *H. naledi* maxillary canines (i.e., U.W. 101-337, U.W. 101-908, U.W. 101-412, and U.W. 101-510), a distinct wear facet is present on the lingual face distally near the occlusal margin. Here, the facet extends along the distal crest to slightly more than half its length. This facet resulted from contact with mesial protoconid crest of the P_3 and is independent of the small facet distally that may represent an IPF. In labial view, the crown appears tall relative to its narrow base (Table 1). The crown is asymmetric in profile, with the mesial shoulder placed more apically than the distal; correspondingly, the mesial crest is shorter than the distal. The apex is placed near the MD midpoint of the crown. The crown exhibits moderate mid-crown convexity in occlusal view and moderate IC convexity in mesial view. The labial surface features a weak vertical mesial groove and a shallow distal v-shaped furrow. The lingual surface features weak distal and mesial accessory ridges. These ridges, as well as the marginal ridges, merge into a basal swelling mid-crown. There are no distinct lingual fossae; rather, the marginal ridges are delineated by shallow grooves. There are two prominent hypoplastic defects located in the cervical third of the labial surface (for a discussion of hypoplasias on this specimen, see also Skinner, 2019).

The root is abraded across most of its surfaces and is also broken at about two-thirds its length, exposing the canal. In labial view, the maximum root height is 9.3 mm.

The root is a rounded ellipse in cross section, with a wide and shallow invagination along the mesial face.

The mesial IPF is a potential fit for U.W. 101-932. Further, this specimen is proposed as the antimere of U.W. 101-816. Their morphology and degree of wear are similar, as are the patterns of hypoplasias near the labial cervix. There is a conspicuous difference in their wear patterns though, with U.W. 101-706 having a wear facet on the lingual face that is lacking on U.W. 101-816. Thus, these canines either represent the same individual with asymmetric patterns of wear or are different individuals at approximately the same state of wear. This tooth could belong to a complete set of maxillary incisors (U.W. 101-709, -931, -932, and -1012) and a set of antimeric canines (U.W. 101-706 and U.W. 101-816). This attribution is consistent with the fit of their respective IPFs, incisal wear, and morphological status as antimeres.

U.W. 101-816: RC^1 (Fig. 14B; Table 1) There is a small IPF (1.8 mm by 1.0 mm) just below the mesial shoulder. There is no distal IPF. Additional wear facets are observed lingually along the DMR and the mesial crest (stage 1). Unlike other *H. naledi* maxillary canines at comparable occlusal wear, there is no wear facet on the lingual face adjacent to the distal crest. The crown is tall relative to its narrow base (Table 1). In occlusal view, the crown is strait at the occlusal edge but moderately convex mid-crown; it also has moderate IC convexity. The crown is asymmetric in lingual and labial profiles, with the mesial shoulder higher and the mesial crest shorter than the distal. There are shallow mesial and distal labial grooves. Lingually, the MMR and DMR emerge from a broad flat cervical region and increase in expression as they approach the mesial and distal edges.

Two weak finger-like projections extend into the lingual fossa. The mesial lingual ridge is truncated by the mesial edge wear. The distal lingual ridge ultimately intersects the distal crest. There are no distinct lingual fossae; rather, the mesial and distal marginal ridges are delineated by shallow grooves and the area between the lingual ridges is essentially flat. There are prominent linear hypoplasias in the cervical third of the crown (for a discussion of hypoplasias on this specimen, see also Skinner, 2019).

The root tilts distally. It is abraded across most of its surfaces and only about half its length is preserved. In labial view, the maximum height of the preserved root is 9.2 mm. In cross section, the root is ovoid with a shallow groove along the mesial face.

Based on similarities in crown morphology and size, as well as the number and position of hypoplastic defects, U.W. 101-706 is proposed as the antimere of this specimen. The canines do differ slightly in the pattern of wear, with U.W. 101-706 having a distolingual wear facet. Further, the mesial IPF of this specimen is a potential fit for the U.W. 101-709 I^2 distal facet. This tooth could belong to a complete set of maxillary incisors (U.W. 101-709, -931, -932, and -1012) and a set of antimeric canines (U.W. 101-706 and U.W. 101-816). This attribution is consistent with the fit of their respective IPFs, incisal wear, and morphological status as antimeres.

U.W. 101-908: RC^1 (Fig. 14C; Table 1) Enamel chips are present at the occlusal ends of both IPFs. The mesial IPF (2.7 mm by 1.7 mm) is teardrop shaped and placed at the apex of the shoulder. The distal IPF is larger and more elongated (3.5 mm by 1.9 mm) and placed very near the apex of the shoulder. As in other maxillary canines of similar occlusal wear stage, distinct mesial and distal wear planes meet so that the worn apex is

offset distally in labial view. In this manner, the wear planes reflect the contours of the unworn crown. The apex is flattened by wear and a small dentine pit is exposed (stage 2). Wear is more extensive along the mesial crest than along the distal and the mesial wear plane dips lingually as well. A wear facet is also present on the distolingual face, extending from the DMR to the distal lingual ridge. The maximum MD length of this facet is 3.3 mm, and its maximum IC height is 2.7 mm. Though worn, in labial view the crown appears tall relative to its narrow basal size. Curvature at midcrown is minimal. The mesial and distal labial grooves are quite faint; otherwise, the labial face is morphologically featureless. Lingually, the flat median lingual ridge and faint mesial accessory ridge create narrow grooves adjacent to the MMR and DMR and between the accessory ridge and median lingual ridge. Linear hypoplasias are evident along cervical third of the lingual and labial faces (for a discussion of hypoplasias on this specimen, see also Skinner, 2019).

The root is slightly abraded along its mesial surface and the apex of the root is broken, which exposes a bit of the root canal. Nearly the complete height (18.3 mm in labial view) of the distally tilting root is preserved. There is a slight depression along the mesial side of the root; otherwise, the root is a rounded ellipse in cross section, with the major axis LaL and the minor axis MD. The root is broadest labially and narrows lingually.

This specimen is the probable antimere of U.W. 101-412. They are similar, but not identical, in morphology, size, and the degree and pattern of wear. Differences are seen in their lingual surface morphology, with the mesial accessory ridge absent on U.W.

101-412, and the development of the IPF for the I^2 on U.W. 101-908 and its near absence on U.W. 101-412. Further, U.W. 101-908 is slightly more worn than U.W. 101-412.

U.W. 101-1403: RC^1 root (Fig. 14D; Table 1) This specimen was recovered near U.W. 101-1401 (RP^4) and U.W. 101-1402 (RP^3). It is a large root fragment missing its crown, which broke away. Its ovoid cross-sectional shape, size, and morphology match that of other maxillary canines and this attribution is consistent with its excavated position relative to U.W. 101-1401 and U.W. 101-1402. The root is damaged below the position of the missing crown. Damage is also evident on the labial face as a v-shaped missing section. Cracks are apparent in the cementum covering the root. Its maximum preserved height is 17.5 mm, its maximum LaL width is 9.2 mm, and its MD length is 6.0 mm.

This specimen is proposed to be associated with the U.W. 101-1401 and U.W. 101-1402 maxillary premolars. These premolars have proposed antimeres, U.W. 101-1560 and U.W. 101-1561, that articulate with a LC^1, U.W. 101-1556. Thus, U.W. 101-1403 and U.W. 101-1556 are tentatively proposed as antimeres. This proposal cannot be validated with comparisons of crown morphology, as U.W. 101-1403 lacks a crown, but is consistent with their root sizes and shapes and with the relative thickness of cementum covering their roots.

U.W. 101-1510: RC^1? (Fig. 15A; Table 1) This specimen preserves the remnant of a heavily worn crown and root that is ovoid in cross section. Remnants of an enamel ring remain labially and lingually, while none is preserved mesially and distally (stage 7). Assuming this is a right tooth, there is a strong distal angle to the occlusal wear and the

root has a distal inclination. The preserved LaL dimension approximates the maximum LaL dimension of the crown in the unworn state, but the MD dimension is reduced relative to the unworn state. The root is abraded across its surface and broken before the apex. The maximum height of the preserved root is 16.2 mm along the labial edge; this is, however, not the full length of the root, as the apex is broken.

The shape, size, and tilt of the root suggest that it is an upper right canine. The contour of the cervical line and the strong MD wear gradient is inconsistent with attribution to any incisor. In addition, the measured LaL breadth exceeds that of every incisor and mandibular canine in the assemblage and falls within the range of maxillary canines (range = 8.2–9.7 mm), supporting attribution to that class. The root height is also consistent with this attribution.

U.W. 101-1548: LC^1 germ (Fig. 15B; Table 1) Approximately two-thirds of this crown is complete. The mesial shoulder is complete and is associated with a shallow labial groove. Lingually, this feature is associated with a moderately-developed groove and marginal ridge. The median lingual ridge is moderately developed and bipartite, with central and mesial branches. The apex of the distal shoulder is developed, suggesting asymmetry seen in other *H. naledi* maxillary canines. This specimen is the antimere of U.W. 101-544B and attributable to the mixed dentition present in the mandible of U.W. 101-1400 mandible and the antimeres of those teeth.

U.W. 101-1556: LC^1 (Fig. 15C; Table 1) A large distal IPF (approximately 5.4 mm along the DMR by 2.1 mm LaL at the occlusal edge) extends along much of the length of the

distal aspect of the DMR; its OC height is reduced by apical wear. A tiny IPF is present mesially at the very apex of the preserved MMR. Wear has removed the crown to nearly the level of the mesial shoulder and dentine is exposed across the entirety of the occlusal surface (stage 5). There is a slight distolingual inclination to the wear plane and, in labial view, there are distinct mesial and distal occlusal wear planes that meet at a slight angle at mid-crown. A remnant of a shallow distal labial groove is present but no trace of a mesial labial groove is visible. Lingually, a remnant of the mesial fossa is visible as a small pit. There are linear hypoplasias near the cervix labially (for a discussion of hypoplasias on this specimen, see also Skinner, 2019).

The root surface is covered in extensively cracked cementum. There is minor abrasion on the root surface, especially distally. The apex of the root is broken. The maximum preserved root height is 15.6 mm. The root is ovoid in cross section and MD compressed. There are shallow invaginations running along the mesial and distal surfaces, with the mesial slightly deeper than the distal. The root deflects distally.

The root fits well in the preserved alveolus of the U.W. 101-859 maxillary fragment; however, we do not consider this a conclusive association. In addition, the distal IPF is a perfect match for the mesial IPF of the U.W. 101-1560 LP^3, which itself articulates distally with U.W. 101-1561, and the two teeth were removed from the same mass of sediment and fragments (block U.W. 101-1477) that was recovered *en bloc*. Thus, U.W. 101-1556, -1560, and -1561 belong to the same individual. The U.W. 101-1560 and -1561 premolars have proposed antimeres, U.W. 101-1401 and U.W. 101-1402, that are associated with a canine root, U.W. 101-1403. If these proposed associations are correct, then U.W. 101-1403 and U.W. 101-1556 are antimeres; though, there is no

morphological means to confirm this proposal given the absence of a crown for U.W. 101-1403. Both U.W. 101-1403 and U.W. 101-1556 come from individuals with advanced apical wear and both roots are covered in a thick layer of cementum. The tiny mesial IPF and state of macrowear match the tiny distal IPF and state of macrowear on the U.W. 101-1684 LI^2; a tentative association between them is proposed.

3.13. Permanent maxillary third premolars

Eight isolated P^3s and one preserved in situ in the U.W. 101-1277 maxilla are known from the Dinaledi Chamber. Collectively, they represent at least seven individuals. The *H. naledi* P^3s present a consistent morphological pattern. In occlusal view, the crown profile is slightly asymmetric, with the Pr marginally smaller than the Pa, especially along the MD axis. The lingual margin is more convex than the straighter buccal margin. The buccal grooves are both shallow and present only in the occlusal third of the crown height. In addition to a low essential crest, weak mesial and distal accessory ridges are present on the Pa, which creates a trilobate Pa face. Except for U.W. 101-786 and U.W. 101-1004, with a single canal, the other P^3s have three distinct root canals: two buccal and one lingual. The roots are individualized externally to varying degrees, showing greater separation in U.W. 101-037, U.W. 101-182, U.W. 101-729, and U.W. 101-1107 than in U.W. 101-1402 and U.W. 101-1560. Even the single rooted specimens show external clefts in the root mass that hint at the multirooted morphology seen in the other specimens.

U.W. 101-037: RP^3 (Fig. 16A; Table 1) Enamel chipping is present at the occlusal margin near the mesial IPF and another chip sits on the lingual side of the mesial Pr crest. A large IPF is present distally (4.2 mm BL by 2.8 mm OC) and a much smaller one sits mesially (3.2 mm BL by 2.1 mm OC) and is offset buccal to the center of the crown. The crown is moderately worn with small pits of dentine exposed over the Pa and Pr (stage 2). The morphological features have been smoothed over by wear, but the ridge and fissure pattern remain. The occlusal outline is a rounded rectangle, and the Pr is smaller than the Pa, especially in its MD length. An abbreviated distolingual corner contributes to the asymmetry of the occlusal profile. The lingual margin is more tightly convex, and the buccal margin is straighter, although indented by shallow mesiobuccal and distobuccal grooves. These vertical grooves delineate mesial and distal ridges on the buccal face, which become imperceptible at mid-crown. Though worn, subtle mesial and distal accessory ridges (sensu Scott and Irish, 2017) arise from either side of the Pa. Both ridges terminate at the Mlg. The essential ridge of the Pa is worn but appears to have been broad; thus, in combination with the accessory ridges, the Pa face is trilobate. The Mlg curves around the Pa mesially and distally. It is deeper mesially, suggesting the presence of a pit-like Fa. The lingual crown is featureless.

Two buccal roots and one lingual root are present. All roots are broken at their tips and the exposed surfaces are stained by adhering matrix. The buccal roots are both compressed with their major axis BL and minor axis MD. The lingual root is larger in cross sectional area with its major axis running from mesiolingual to distobuccal. The buccal roots are vertically oriented above the crown, and, in buccal view, their apices flare apart MD. The taller lingual root angles out lingually over the crown. The lingual

root canal is individuated from the buccal roots near the cervix, while the buccal root canals become separated at about one-third of their heights from the cervix. The mesial buccal root is 10.7 mm in preserved height, while the distal buccal root is 11.9 mm in preserved height, and 11.1 mm of the lingual root remains.

This isolated tooth is identified as a P^3, and not a P^4, by the combination of asymmetry in IPF size and orientation and the crown asymmetry in occlusal view.

U.W. 101-182: RP^3 (Fig. 16B; Table 1) The occlusal surface is lightly worn: small facets are visible on the ridges extending from the Pa. The apex of the Pr is also rounded by wear (stage 1–2). Neither mesial nor distal IPFs are visible. The Pa is slightly larger than the Pr and its apex sits distal to that of the Pr. The crown has an abbreviated distolingual corner, which yields an asymmetrical crown outline. The Pa has three distinct occlusal ridges. None of the ridges connects directly to the center of Pa apex; the relief of the ridges is slightly reduced by occlusal wear, and they are similarly prominent at this state of wear. All ridges terminate at the Mlg. The Pr does not have accessory ridges and the essential ridge is not well defined. The MMR is distinct but mostly limited to the region mesial to the Pr, where it bulges out mesially. A groove-like Fa is formed between the MMR and the mesial-most ridge of the Pa. It is continuous with the Mlg. The DMR is not well defined. The Mlg broadens at its distal-most extent where it terminates as a small pit. Subtle mesiobuccal and distobuccal grooves are present, with the mesial deeper than the distal. Both disappear before mid-crown. The lingual face is smooth and unremarkable.

Portions of three roots are preserved. Minor abrasion is present on the mesiolingual corner of the lingual root and on the mesial surface of the mesiobuccal root. There is single nearly circular lingual root, with its major axis mesiobuccal to distolingual, and two buccal roots that are compressed MD in cross section. The lingual root is nearly complete except for a small portion that has broken away near the apex. The remaining lingual root is 10.2 mm in height. The distobuccal root is broken at approximately half its height, about 3.9 mm from the cervix, while the mesiobuccal root is broken much nearer its apex, preserving 7.2 mm of its height. The lingual root tilts out over the crown, while the buccal roots, as preserved, extend nearly vertically from the crown.

This isolated tooth is likely a P^3. This identification is supported by the crown asymmetry in occlusal view and the mesial flare of the MMR, which tends to be flatter on inferred P^4s. However, the absence of IPFs makes this attribution less certain.

U.W. 101-729: RP^3 (Fig. 16C; Table 1) No IPFs are present. A tiny facet is present on the mesial aspect of the Pa (stage 1), which indicates that the crown was like erupting at death and had just begun occlusal contact. The crown profile is slightly asymmetric, with a more tightly convex lingual margin and Pr that is nearly equal in size and height to the Pa; the Pr apex is mesial to that of the Pa. The Pr essential crest is indistinct, and it lacks accessory ridges. As in other *H. naledi* maxillary premolars, the Pa possesses two ridges that originate on either side of the cusp apex and terminate at the Mlg. Another minor ridge is merged with the distal Pa ridge and could be considered the essential ridge, but it does not continue to the apex of the Pa either. The mesial ridge of the Pa is more

topographically prominent than the distal ridge. A third ridge arises from the junction of the distal Pa crest and DMR and encroaches on the space that would be occupied by the Fp. The MMR dips just buccal to the Mlg and blends into the undefined mesial ridge of the Pr. Viewed mesially, the MMR is v-shaped with the deepest point of the v set buccal to the midpoint of the crown. The Pa mesial accessory ridge is hypertrophied, delineated from the MMR by a groove-like Fa; the groove crosses onto the buccal face as a shallow vertical indentation. In mesial view, this lingual aspect of the MMR appears as a tubercle-like bulge. The Fp is undefined. The DMR is low and rounded and barely elevated on the occlusal surface and the FP is a poorly defined pit. Mesiobuccal and distobuccal grooves are each shallow and become imperceptible at mid-crown. The lingual face is featureless.

The tooth has three roots: two buccal roots and one lingual. The roots are cracked on their external surfaces. Slightly less than half the root mass is preserved, and the root canals are packed with sediment. The buccal roots run parallel to each other and are compressed and joined by a thin sheath of dentine. They are approximately the same size in cross sectional area. The larger lingual root is ovoid in cross section, with its major axis running mesiolingual-to-distobuccal. It flares out lingually. The preserved height of the lingual root is 5.9 mm, while that of the distobuccal root is 7.8 mm and that of the mesiobuccal root 5.5 mm.

U.W. 101-786: LP^3 (Fig. 16D; Table 1) Enamel chipping is observed on the occlusal surface just above an ovoid distal IPF (3.4 mm BL by 1.8 mm OC). There is no mesial IPF. There is light occlusal wear on the Pa and Pr apices, on the Pa mesial accessory ridge, and on the distal portion of tan accessory ridge extending from the junction of the

distal Pa crest and DMR (stage 1). The occlusal profile is slightly asymmetric, with a more tightly convex lingual profile and straighter buccal profile slightly indented by the buccal grooves. The crown is longer MD along the Pa than along the Pr. The cusps are sub-equal in height and the Pr apex is mesial to that of the Pa. The MMR is low and rounded and the buccal and lingual segments dip where they meet so that the MMR is v-shaped in mesial view with its low point buccal to the midpoint of the crown. The essential lobe of the Pr is poorly developed. Two ridges are present on the Pa face and neither connects directly to the apex of the crown. The mesial of the two ridges has a slight extension that crosses the Mlg and helps to define the Fa distally. The distal of the two Pa ridges terminates at the Mlg. Wide and shallow buccal grooves are associated with the mesial and distal Pa ridges; both fade at mid-crown. The lingual face is featureless.

Unlike some other *H. naledi* maxillary premolars, only a single root, with two distinct radicals, extends above the crown. It is abraded along most of its external surface and is broken before its apex, exposing the root canal. The preserved buccal root height is 10.2 mm. The root is compressed MD and longer BL with a wide and shallow groove running along the mesial face, a narrower and deeper groove running the length of the distal face and a narrower but shallow groove running along the buccal face.

The U.W. 101-1004 RP^3 is proposed as the antimere of this tooth. Their crown morphologies are similar as are their root morphologies; for example, some of the *H. naledi* P^3s show a splaying of the roots but U.W. 101-786 and U.W. 101-1004 do not.

U.W. 101-1004: RP^3 (Fig. 17A; Table 1) A distal IPF (5.1 mm BL by 2.1 mm OC) reaches the occlusal margin. A smaller mesial IPF (2.8 mm BL by 1.9 mm OC) is evident near midcrown extending nearly to the cervix. Occlusal wear is minimal, but the crown apices and occlusal ridges have been blunted (stage 1). In occlusal view, the crown is nearly symmetric, with the Pr only slightly shorter MD than the Pa and the two cusps are nearly equal in area. The essential ridges of both cusps are indistinct. A well-developed accessory ridge extends towards the Mlg from the intersection of the distal Pa crest and DMR. The groove-like Fa is continuous with the Mlg and passes mesial to the Pa. The MMR is a continuous rim and reaches most cervically just mesial to the Pa. In occlusal view, the MMR arcs from the Pr to reach its most mesial extent adjacent to the Pa. The Fp is scarcely more than a pit at the end of the Mlg bounded by a low and dull DMR and the distal accessory ridge of the Pa. The mesio- and distobuccal grooves are shallow, with the distobuccal groove slightly deeper; both fade away approximately mid-crown. No lingual grooves are present.

The single root is broken near its apex, exposing the root canal, and the root surface is abraded. The preserved root measures 11.9 mm along the buccal face. The root has a cleft running along the buccal aspect and subtle depressions evident along mesial and distal faces, giving it a slight figure-of-eight cross section.

The U.W. 101-786 LP^3 is proposed as the antimere of this tooth. Their crown morphologies are similar as are their root morphologies; for example, some of the *H. naledi* P^3s show a splaying of the roots but U.W. 101-786 and U.W. 101-1004 do not.

U.W. 101-1107: LP^3 (Fig. 17B; Table 1) An enamel chip is missing just mesial to the Pa apex. No IPFs are visible mesially or distally. The crown is minimally worn with wear facets visible on the Pr apex, as well as mesial and distal to it. A small facet is also visible on the DMR (stage 1). The Pr is slightly smaller in area and MD length than the Pa. The buccal profile is pinched in association with shallow mesiobuccal and distobuccal grooves, while the lingual profile is continuous and more tightly convex. The marginal ridges are restricted to the Pa and the DMR is slightly broader than the MMR. As in other inferred P^3s, the MMR flares as it passes mesial to the Pa. There is no essential ridge on the apex; instead, mesial and distal ridges arise on either side of the Pa apex. A fissure-like Fa is restricted to the Pa and is nearly continuous with the Mlg, separated by a slight crest connecting the MMR and mesial Pa accessory crest. Both buccal grooves are shallow and extend less than a third of the way down the buccal face before they become imperceptible.

Parts of three damaged roots are preserved. Significant abrasion is evident near the broken edges of the root apices and along the mesial side of lingual and mesiobuccal roots. Breaks expose the root canals. What remains of the distobuccal root is 6.4 mm, that of the mesiobuccal root is 6.3 mm, and that of the lingual root is 9.6 mm. The mesiobuccal and distobuccal roots are similar in cross-sectional area and are both MD compressed. The lingual root is ovoid in cross section and is larger than both buccal roots. The buccal roots extend vertically from the crown, while the lingual root deflects lingually. The buccal roots flare apart to a greater extent than other *H. naledi* maxillary premolars.

U.W. 101-1402: RP^3 (Fig. 17C; Table 1) Enamel chipping is visible along the mesial and distal margins. The chip in the distal IPF matches the chipping on the mesial IPF of the U.W. 101-1401 RP^4. The distal IPF is large (5.4 mm BL by 2.3 mm OC), while the mesial IPF is small (2.4 mm BL by 0.8 mm OC). Dentine is exposed over the Pa and Pr apices. The pool of dentine on the Pa extends distally, while that of the Pr extends mesially and is paired with a thin strip of dentine along the distal crest (stage 4–5). Trace remnants of the mesiobuccal and distobuccal grooves are palpable. They are more pronounced than on the U.W. 101-1401 RP^4 associated with this specimen. The occlusal morphology has been removed by wear and only a short, thin groove of the Fa remains mesial to the Pa.

A bit of the alveolus remains attached to the root mass distally. The roots are broken at their apices. Three roots are present: a single lingual root and two buccal roots. The roots are tightly compressed into a single external mass, much like U.W. 101-1401. The µCT scans show three distinct canals associated with lingual, mesiobuccal, and distobuccal roots. The lingual root has a slight distal inclination. The mesiobuccal root is also inclined distally. All roots are MD compressed, with the buccal roots more compressed than the lingual. The maximum height of the preserved lingual root is 11.1 mm. The maximum mesiobuccal root height is 12.4 mm, and the maximum distobuccal root height is 9.4 mm.

This specimen was near U.W. 101-1401 (RP^4) when excavated and has a good distal articulation with it. It is the proposed antimere of U.W. 101-1560; though, that determination is difficult to confirm given their advanced wear state. This specimen was also excavated near the U.W. 101-1403 RC^1, which lacks a crown, but is consistent with

attribution to a maxillary canine. We provisionally propose that U.W. 101-1401, -1402, and -1403 belong to the same individual.

U.W. 101-1560: LP^3 (Fig. 17D; Table 1) There is enamel chipping along the mesial and distal margins. There is a large obliquely oriented mesial IPF (5.7 mm along the long oblique axis by approximately 2.4 mm OC near the center of the IPF) and a smaller distal IPF (4.7 mm BL by 2.0 mm OC). The occlusal morphology has been obliterated by wear. The moderate-sized pool of dentine on the Pa extends along its distal crest, while that of the Pr occurs over the apex with an additional strip along the mesial crest (stage 4–5). The occlusal profile is fairly symmetric, and the Pr and Pa are nearly equal in area. As judged by the dentine exposures, the Pr apex was placed well mesial to that of the Pa. Remnants of the mesiobuccal and distobuccal grooves are preserved.

Three roots are present: a mesiobuccal, distobuccal, and lingual root. The roots are covered in cementum, which is flaking off, and their apices are all broken away; though, only the lingual root canal is exposed. The preserved height of the lingual root is 10.1 mm, that of mesiobuccal root is 10.6 mm, and that of the distobuccal root is 9.6 mm. The buccal roots are inclined distolingually, especially near their apices, while the lingual root is more vertically oriented. The buccal roots are ovoid in cross section, being MD compressed, while the lingual root is rounder. All three roots are tightly pressed together. The buccal roots are joined near the cervix, but a cleft develops between them towards their apices. The µCT scans indicate that the three roots share a common canal for about half their lengths before the common canal splits almost simultaneously into three separate canals.

The shape of the mesial IPF is a perfect fit for the distal IPF of the U.W. 101-1556 LC^1. This specimen also articulates distally with U.W.101-1561. Further, this is the proposed antimere of U.W. 101-1402. Given the advanced state of wear of both specimens, it is, however, difficult to confirm their status as antimeres; in fact, their wear patterns are not identical, with U.W. 101-1402 having a dentinal exposure along the distal Pr crest that is absent in U.W. 101-1560.

3.14. Permanent maxillary fourth premolars

Eight isolated P^4s and one in situ in the U.W. 101-1277 maxilla represent at least seven individuals in the Dinaledi Chamber deposits. The P^4s present a consistent morphological pattern. The crown is mildly asymmetric in occlusal outline, as the Pa slightly exceeds the Pr in area, and the lingual and buccal profiles are similar in their curvature. The buccal grooves are shallow and only present in the occlusal third of the crown height. The number and shape of the roots differs between individuals. Some specimens (e.g., U.W. 101-277, U.W. 101-1362) have three clearly distinct roots externally, while others (e.g., U.W. 101-1401, U.W. 101-1561) have multiple distinct root canals but show weak separation of the radicals externally. In all, there is a single canal in the cervical third of the root mass and the canals become distinct apically. In some (e.g., U.W. 101-334), the roots are broken near enough to the cervix that it is difficult to discern if the tooth would have been multirooted.

U.W. 101-277: LP^4 (Fig. 18A; Table 1) Occlusal enamel chipping is evident along the MMR and another chip is evident along the DMR. Large, BL-oblong semicircular IPFs

are visible mesially (6.0 mm BL by 3.0 mm OC) and distally (5.6 mm BL and 2.3 mm OC). Wear has polished the occlusal surface, flattening the cusp apices, but no dentine is exposed (stage 1–2). Despite the moderate wear, much of the occlusal morphology is preserved. In occlusal view, the crown is mildly asymmetric in outline, as the Pa slightly exceeds the Pr in area, and the lingual and buccal profiles are similar in the curvature. The buccal profile is somewhat lobate. The Pa possesses three occlusal ridges that are nearly equal in size: the essential ridge widens as it reaches the Pa apex. The mesial and distal accessory ridges are thinner. The mesial accessory ridge crosses the Mlg and merges with the essential ridge of the Pr. The Pa essential ridge and distal accessory ridge, on the other hand, terminate at the Mlg. The Pr also likely possessed mesial and distal accessory ridges based on the deep occlusal grooves that are preserved. A short, thin crest extends mesially from the Pr accessory ridge and connects to the MMR, while the distal accessory ridge terminates at the Mlg. The MMR expression is obscured by wear and chipping but an Fa, expressed as a narrow groove confined to the Pa with a short buccal segment preserved, is present. Distally, the Mlg merges with a BL-oriented groove that curves around the distal accessory ridge of the Pa. The DMR is dulled by wear but is thick and rounded. The mesial and distal Pa accessory crests are associated with mesiobuccal and distobuccal grooves, which are both palpable but shallow. The distal groove is deeper than the mesial groove. Both fade away about mid-crown, but the distal groove extends a bit farther along the crown.

Portions of three roots are present. Some abrasion is evident on the mesial and distal aspects of the lingual root, near the preserved apex of the mesial buccal root on its mesial face, and along the distal face of the distobuccal root. Both buccal roots are

broken, exposing their root canals. The lingual root, which leans over the lingual face and cants distally as well, is nearly circular in cross section, with its major axis mesiolingual to distobuccal. The two buccal roots are pressed together and do not splay apart apically as preserved. They extend nearly directly above the crown, are compressed in cross section, being broader BL than MD. The mesial buccal root is slightly broader BL than is the distal buccal root. The buccal roots share a common canal near the cervix; however, the canals are fully individualized before the break and the radicals themselves begin to differentiate just prior to the break. The lingual root is preserved completely and measures 15.8 mm in height lingually. The mesiobuccal and distobuccal roots are each broken at slightly more than half of their height. The preserved mesiobuccal root is 7.8 mm long and the preserved distobuccal root is 9.2 mm long.

This specimen is considered a P^4 based on its crown morphology, the placement and size of its IPFs, and because it likely articulates distally with the U.W. 101-1676 LM^1. The shapes and sizes of their IPFs are a good match. Additionally, if they are associated, both specimens have enamel chips occlusal to their congruent IPFs.

U.W. 101-333: LP^4 (Fig. 18B; Table 1) The crown is unworn, with neither occlusal nor interproximal wear present (stage 1). The occlusal profile is nearly symmetrical, with similarly sized cusps and the apex of the Pa offset slightly mesial to the Pr. Though both are dull, the MMR is narrower than the rounded DMR, which is associated with a slight distobuccal cuspule. Similar to other *H. naledi* P^4s, two ridges are visible on the face of the Pa and neither connects to the apex of the cusp. The mesial ridge is pinched in near its origin occlusally and becomes wider towards the Mlg. The Fp is a groove extending

buccally to the distal crest of the Pa and lingually past the Mlg as a small pit. The Fa is a groove adjacent to the mesial Pa ridge and contiguous with the Mlg. There is a faint cuspule at the distal terminus of the Mlg. On the buccal face, the mesiobuccal groove is barely detectable even at the occlusal margin, while the distobuccal groove is wider and deeper. It is associated with the distobuccal cuspule where it crosses the occlusal margin but becomes imperceptible at about mid-crown. The lingual face is unremarkable.

The root was still forming at the time of death and only a sliver is preserved around the cervix. The root canal is packed with sediment.

This is the probable antimere of U.W. 101-334. The two teeth are virtually identical morphologically and in their state of wear. The teeth were also excavated within centimeters of each other.

U.W. 101-334: RP^4 (Fig. 18C; Table 1) The crown is unworn, with neither occlusal nor interproximal wear (stage 1). The occlusal profile is nearly symmetrical, with similarly sized cusps and the apex of the Pa offset slightly mesial to the Pr. Though both are dull, the MMR is narrower than the DMR, which is wide and rounded. Like other *H. naledi* P^4s, the crown features two ridges on the face of the Pa and neither connects to the apex of the cusp. On the buccal face, the mesiobuccal groove is barely detectable even at the occlusal margin, while the distobuccal groove is wider and deeper. It is associated with a weak distobuccal cuspule where it crosses the occlusal margin but becomes imperceptible at about mid-crown. The lingual face is unremarkable.

The roots are abraded across their surfaces and broken apically. Though the roots are broken, this specimen is obviously multirooted, with a rounded lingual root separated

from the buccal roots. Buccally, a cleft is present in the center of the buccal root mass, which may indicate two distinct buccal root apices. In buccal view, the maximum height of the preserved root is 2.0 mm, while, in lingual view, the maximum root height is 4.0 mm.

This tooth is the proposed antimere of U.W. 101-333. They are virtually identical morphologically and in their state of wear.

U.W. 101-455: RP^4 (Fig. 18D; Table 1) Reflecting its relatively unworn state, no IPF is present mesially and a small one (approximately 2.5 mm LaL by 1.8 mm OC) sits distally next to the Pa. The crown is minimally worn with small facets near the tip of the Pr and along the essential ridge of the Pa (stage 1). The Pa is slightly larger in area and ML longer than the Pr, giving the crown an asymmetrical profile in occlusal view. Though continuous, the lingual and buccal segments of the MMR are lower than the Pr and Pa essential crests. The segments slope from their origins to meet at angle on the mesial surface so that the low point of the MMR is mesial to the Pa. A groove-like Fa is limited to the Pa and merges with the Mlg. It is bordered mesially by the MMR and distally by a hypertrophied ridge extending from the near the apex of the Pa. As with several *H. naledi* P^4s, there are two ridges extending from the Pa towards the Mlg and neither ridge precisely intersects the apex of the Pa. The distal of the two ridges is much narrower than the mesial ridge. A third ridge extends from near the junction of the distal crest of the Pa and the DMR and enters the space that might otherwise be occupied by the Fp, which is merely a pit at the distal end of the Mlg. The DMR is indistinct. The Pr essential ridge is wide, and it terminates at the Mlg. On the buccal face, the mesial groove is short and

faint. The distobuccal groove is more distinct and extends to about two-thirds the crown height. It crosses the occlusal margin, becoming a shallow occlusal groove delineating an accessory ridge described above. The lingual face is featureless.

In contrast to some other maxillary premolars in the assemblage, only a single root is present. The maximum preserved height of the broken and abraded root is approximately 7.0 mm in buccal view and 5.6 mm in lingual view. The root canal is exposed. On the buccal face, an invagination runs longitudinally along the root and subtle depressions run along the mesial and distal faces. The root is mostly compressed MD, with its major axis BL.

This specimen is proposed as the antimere of U.W. 101-808. They are similar in occlusal and root morphology and the state of occlusal wear; however, their crown outlines are slightly different with the distolingual corner less abbreviated in U.W. 101-808.

U.W. 101-808: LP^4 (Fig. 18E; Table 1) There is no mesial IPF and a small rounded distal IPF (2.7 mm BL by 1.8 mm OC). The crown is lightly worn with small facets on the Pa distal crest and on the mesial aspect of the Pr apex (stage 1). The Pr and Pa are sub-equal in height and the crown is only mildly asymmetric, with the lingual profile fairly straight and only slightly more tightly convex than the buccal. The apex of the Pr is mesial to that of the Pa. The MMR is low and rounded; and the buccal and lingual segments dip where they meet so that the MMR is v-shaped in mesial view. The Pr essential ridge is low and rounded and bordered mesially and distally by weak accessory ridges. The Pa is occlusally more complex: there is a distinct mesial ridge that starts narrow near the apex

but widens quickly, flaring mesially and distally as it reaches the Mlg. Distal to this ridge, there is a thin, sharp crest that that also widens about mid-crown (but less so) and merges with the mesial ridge at the Mlg. As is common with the *H. naledi* maxillary premolars, neither of these crests is associated directly with the Pa apex. A third crest rises from near the junction of the distal Pa crest and DMR and is associated with a distinct occlusal elevation and occlusal and buccal grooves. The hypertrophied mesial Pa ridge forms the distal boarder of a fissure-like Fa that is limited to Pa and bordered mesially by the MMR. The DMR is not well-defined. No Fp is observed. The mesiobuccal and distobuccal grooves are wide and shallow and they fade away about one-third the crown height. A small pit, possibly hypoplastic, is observed about mid-crown on the buccal aspect.

The root is abraded on all surfaces and broken irregularly so that the maximum preserved height is 7.0 mm buccally, while only 5.6 mm of the root remains lingually. In buccal view, a small cleft is visible running longitudinally along the root; however, given the state of preservation of the root, it is unclear if the apices would have diverged.

This specimen is proposed as the antimere of U.W. 101-455. Articulation with U.W. 101-708 distally is reasonable as their IPFs are similar in size and shape and appear congruent.

U.W. 101-1362: LP^4 (Fig. 19A; Table 1) Extensive chipping circumscribes the crown. Further damage is evident in the region of the mesial IPF, and recent damage removed a portion of the distal occlusal surface. Nearly the entire crown has been removed by wear and the pulp chamber is exposed. An enamel rim is primarily present buccally where it

extends around the distobuccal corner and preserves a portion of the distal IPF. Additionally, a thin sliver of enamel still lines the lingual cervix (stage 7). The wear surface has a strong lingual slope, such that approximately 4.7 mm of the crown's height remains buccally but only a sliver, less than 0.5 mm in OC height, remains lingually.

The tooth has two roots. The buccal root has moderate damage to its apex and the lingual root is nearly completely preserved. Both roots are covered in a thick layer of cementum. The lingual root is conical, longer, and more circular in cross section than the buccal root. The buccal root has two radicals separated by a moderate invagination running along its buccal surface. The µCT scans reveal two distinct buccal root canals for nearly half the length of the root. The buccal roots are more individualized than apparent now because of the thick layer of cementum that has accumulated along the roots. The preserved height of the buccal root is 10.3 mm, while the lingual root is 10.9 mm.

The distal IPF is a good fit for the mesial IPF of U.W. 101-796 (LM^1), which is argued to be associated with U.W. 101-528 (LM^2) and U.W. 101-527 (LM^3). If these proposed associations are correct, this would constitute a heavily worn set of maxillary postcanine teeth from a single individual. An association with the equally heavily worn teeth in the U.W. 101-361 mandible is also possible.

U.W. 101-1401: RP^4 (Fig. 19B; Table 1) Enamel chipping is visible along the mesial and distal margins. Large mesial (5.6 mm BL by 2.2 mm OC) and distal (6.7 mm BL by 2.3 mm OC) IPFs are present. The crown is worn, with a small dentine patch on the Pa apex and a larger pool at the Pr apex that extends to the mesial margin (stage 5). Very little surface topography remains beyond a remnant of the Mlg. The mesiobuccal and

distobuccal grooves are faint but detectable as shallow indentations. The lingual face is featureless.

A portion of the buccal root face is broken away near its apex, where a notch is removed. While some *H. naledi* maxillary premolars have three distinct roots, in this specimen there is a single external root mass. This appearance results in part from a thick layer of cementum that obscures the contours of the underlying dentine but it is clear that the roots did not splay from one another. An examination of the µCT scans show three distinct canals near the root apices with two tightly compressed buccal roots. Externally, two radicals are visible on the buccal face. The mesiobuccal root is BL broader than the distobuccal root. Both buccal roots are lingually inclined and, above the break, the mesiobuccal root deflects distally. The lingual root has a slight mesial inclination. All root components are separated by strong grooves. The nearly complete lingual root is 13.0 mm tall. The preserved height of the mesiobuccal root is 9.5 mm and the distobuccal root is 8.8 mm tall.

This specimen was excavated near U.W. 101-1402 (RP^3), with which it has a good mesial articulation. It also has a good distal articulation with U.W. 101-1396 (RM^1). The LP^4 U.W. 101-1561 is proposed as its antimere; though, U.W. 101-1401 is slightly less worn than U.W. 101-1561. Given the advanced state of wear of both specimens, it is difficult to confirm their status as antimeres.

U.W. 101-1561: LP^4 (Fig. 19C; Table 1) There is enamel chipping along the mesial and distal margins. Large horizontally oriented IPFs are present mesially (4.9 mm BL by 2.1 mm OC) and distally (7.6 mm BL by 2.6 mm OC). The occlusal surface is worn and

preserves little detail. The moderately-sized dentine pools on the Pa and Pr are connected mesially by a narrow strait (stage 5). Shallow remnants of the mesiobuccal and distobuccal grooves are preserved. The lingual face is featureless.

There are three distinct root components—two buccal and one lingual—with separate apices. They are tightly compressed into a single mass. The roots are abraded and the mesiobuccal and distobuccal roots are missing their apices, exposing the canals. The buccal roots are slightly distally inclined and run parallel to each other. They are more ovoid in cross section than the lingual root. The lingual root is also nearly vertical with a slight mesial inclination near its apex. The µCT scans show that the buccal components are associated with separate root canals for about half their length, while the lingual root canal separates closer to the cervix. The preserved height of the nearly complete lingual root is 12.2 mm. The maximum height of the mesiobuccal root is 9.6 mm and that of the distobuccal root is 7.5 mm.

This specimen articulates mesially with the U.W. 101-1560 LP^3. It also proposed as the antimere of U.W. 101-1401; though, their wear patterns are not identical.

3.15. Permanent maxillary first molars

Eleven isolated M^1s and one present in the U.W. 101-1277 maxilla represent at least seven individuals. The sample includes a developing antimeric pair, U.W. 101-1305 and U.W. 101-1688, which were nearing crown completion at death, through a range of wear stages, including a heavily worn specimen, U.W. 101-796, in which the steep bucco-lingual wear gradient had worn to the level of the pulp chamber. The specimens are all similar in morphology and size. Where detail can be assessed, all M^1s have four

principal cusps and no supernumerary cusps. The Hy is relatively large and projects distolingually, giving the crown a rhomboidal occlusal outline. Carabelli's feature is evident mesiolingually as a faint obliquely oriented crest or small groove in some specimens. The Co is continuous. Buccal grooving is shallow; the lingual groove is narrow at the occlusal margin and widens as it reaches cervically.

U.W. 101-445: LM^1 (Fig. 20A; Table 1) A large ovoid mesial IPF (4.2 mm LaL by 2.9 mm OC) is present. No distal IPF is detectable. Wear is present on all cusps, which removed details of occlusal ridging, and along the distal edge of the Co; however, no dentine is exposed (stage 1). There are four principal cusps and no supernumerary cusps. The Hy is relatively large and projects distolingually and the DMR—an extension of the Hy distal accessory lobe—is swollen, which rounds the distal profile and yields a rhomboidal occlusal outline. In size, the relative cusp sizes are Pr > Me ≥ Hy > Pa. The mesial IPF has obscured the MMR, but a trace of the Fa remains as a small pit. A pit-like Fp is present between the Hy and Me; its size is reduced by the presence of a small distal tubercle. The Co is continuous. The buccal groove is a shallow depression throughout its course to the cervix. The lingual groove is deep and narrow near the occlusal margin and widens at mid-crown, becoming shallow as it approaches the cervix. A Carabelli's feature is evident mesiolingually as a faint obliquely oriented crest.

Three roots, a mesiobuccal, distobuccal, and centrally placed lingual root, are evident. The lingual and mesiobuccal roots are broken near their apices, exposing their root canals, and are abraded along their outer surfaces. The distobuccal root broke away at the cervix (apparent in the µCT scans) but has been refit to the crown, which is evident

in Figure 20A. Approximately 11.0 mm of the distally tilting lingual root is preserved. The lingual root angles out over the lingual face; in cross section it is longest MD and compressed BL with a prominent groove running along its lingual surface and a subtler groove along its buccal surface. In buccal view, approximately 10.0 mm of the mesiobuccal root is preserved. The mesiobuccal root is longer BL and compressed MD in cross section, shallow depressions run along its mesial and distal faces, and it tilts slightly distally.

This specimen is a possible antimere of U.W. 101-583. The teeth are similar morphologically and in their state of occlusal and interproximal wear. The teeth do differ slightly distally where U.W. 101-583 has a slight crest on the distal face that is absent in this specimen.

U.W. 101-525+1574: RM^1 (Fig. 20B; Table 1) This tooth comprises two pieces that were recovered and catalogued separately. U.W. 101-525 is a crown with most of the mesiobuccal and lingual roots remaining attached. A portion of refitting distobuccal root is catalogued as U.W. 101-1574. For clarity, we describe them together here.

There are enamel chips missing along the mesiobuccal corner and just occlusal and buccal to the mesial IPF. Another chip is evident distobuccally. A large oval IPF (5.2 mm BL by 2.0 mm OC) reaches the occlusal margin. A larger distal IPF (5.2 mm BL by 3.6 mm OC) is also present and offset lingually. A large, mesially extended dentine pit is present on the Pr, and smaller dentine pits cover the apices of the Me and Hy (stage 3). In occlusal view, the crown outline is rhomboidal, with a mesiobuccally projecting Pa and a large, distolingually-projecting Hy. Interproximal wear creates a slightly concave mesial

profile. Although worn, there is no indication of a C5 at the outer enamel surface (there is no dentine horn at the EDJ for a C5 either). A remnant of Carabelli's trait can be observed as a small groove on the mesiolingual aspect of the Pr that spills onto the worn occlusal surface. Occlusal and interproximal wear have obliterated the Fa and MMR. Distally, the Fp remains as a moderately-sized pit between the Hy and Me and bordered mesially by their distal margins and distally by a low rounded DMR. The Co is worn but thick and continuous; a continuous Co is confirmed with examination of the EDJ. A shallow buccal groove remains. The occlusal portion of a deep lingual groove can still be observed near the occlusal margin. This groove widens and becomes shallow as it reaches the cervix.

Three roots are evident: a lingual root, a mesiobuccal root, and a distobuccal root. The roots are abraded, especially the mesial and distal aspects of the lingual root. The entire height (14.1 mm in lingual view) of the lingual root is preserved; however, the mesiobuccal root is broken off 8.8 mm from the cervix and the distobuccal root is broken off 4.1 mm from the cervix. A separate 8.4 mm fragment, catalogued as U.W. 101-1574 (not illustrated in Figure 20), is broken at its apex but refits to the distobuccal root of U.W. 101-525. The lingual root is wider MD than BL, with shallow invaginations running along both the buccal and lingual faces. The root angles strongly to the lingual side. The buccal roots are close together and are wider BL in cross section. The mesial buccal root is broader than the distal near the cervix. Grooves run along the mesial and distal sides of the mesial buccal root. A slight groove sits on the mesial side of the distal buccal root as well.

This specimen is a possible antimere of U.W. 101-1676. They are virtually identical in the occlusal wear pattern and in preserved morphology.

U.W. 101-583: RM^1 (Fig. 20C; Table 1) Enamel chips are missing along the buccal portion of the MMR and near the apex of the Me. There is a large ovoid mesial IPF (4.2 mm BL by 3.2 mm OC), but no distal IPF. All four cusps are flattened by wear but no dentine is exposed (stage 2). The crown is rhomboidal in occlusal outline due to the relatively large, distolingually projecting Hy. The relative cusp sizes are Pr > Hy > Me ≥ Pa. Part of the MMR has been removed by interproximal wear but what is preserved is thin and rounded. The Fa is a moderately-sized, buccolingually-, and slightly distally oriented groove bordered mesially by the MMR and distally by mesial extensions of the Pa and Pr. None of the cusps preserve accessory fissures or ridges. Though worn, the groove pattern suggests that the Co is continuous, which is confirmed by inspection of the EDJ. The buccal groove is very shallow and fades away mid-crown. The lingual groove is a deep fissure where is crosses the occlusal rim, then quickly becomes shallow and disappears at mid-crown. Carabelli's feature takes the form of a short obliquely oriented crest and associated pit restricted to the mesiolingual corner. The groove separating the Hy and Me opens into a small Fp that is formed by distal margins of the Me and Hy and a weak DMR. The distal face presents a v-shaped crest and groove just below the occlusal margin.

There are three roots, a mesiobuccal, distobuccal, and vertically oriented lingual root. The root surfaces are cracked. The lingual root is broken just before its apex and measures 10.8 mm in height. The distobuccal root is broken at the cervix, while the

mesiobuccal root is broken just before its apex. The distobuccal root is preserved as a separate fragment glued onto the fresh break (not apparent in the µCT scans but visible in Figure 20C). The mesiobuccal root measures 9.6 mm in height and the distobuccal root 9.4 mm. The lingual root has two distinct radicals and a complex cross-sectional shape. In apical view, it is L-shaped with a MD-oriented section along the lingual face and a LaL-oriented section along the distal face. The µCT scans shows that the two portions share a single canal for most of their length. The lingual root tilts over the lingual margin of the crown and slightly distally as well. The mesiobuccal and distobuccal roots are compressed with their long axes BL. The distal root is broader BL than the mesial root. The buccal roots are more vertically oriented than the lingual root.

This specimen is proposed as the antimere of U.W. 101-445. The teeth are similar morphologically and in their state of occlusal and interproximal wear. The U.W. 101-583 specimen does feature grooving on the distal face of the crown and has a more well-defined Fa than U.W. 101-445.

U.W. 101-708: LM^1 (Fig. 20D; Table 1) The crown exhibits a large ovoid mesial IPF (4.2 mm BL by 2.6 mm OC) and no distal IPF. Wear facets are present on all cusps; though, the occlusal topography is well preserved (stage 1). In occlusal outline, the crown is rhomboidal, with a strong distolingual projection of the Hy. The relative cusp sizes of the four cusps are Pr > Hy > Me ≥ Pa. Any accessory ridges that were present have been obscured by wear, and the essential ridges are rounded and wide. Though worn, the Co appears to be continuous at the OES (a continuous Co is present at the EDJ). The faint groove-like Fa is barely preserved. The small Fp is bounded by a weak DMR. The buccal

groove is shallow and becomes indistinct at mid-crown. The lingual groove is deep and forms a sharp cleft near the occlusal surface. This cleft becomes shallow about one-third the crown height and disappears at mid-crown. Carabelli's feature is expressed as a weak obliquely oriented crest confined to the mesiolingual corner of the Pr.

There are three roots, a mesiobuccal, distobuccal, and lingual root. All roots have damaged apices that expose their canals. In cross section, the mesiobuccal root is an elongated figure-of-eight shape, with prominent grooves along its mesial and distal faces. It is BL broader than the distobuccal root. The mesiobuccal root tilts slightly distally and buccally. The distobuccal root is smaller in cross sectional area than the mesial, is more ovoid in cross section, and shows a stronger buccal tilt. The buccal roots are pressed together in buccal view. In cross section, the major axis of the labial root is MD and depressions run along the lingual and buccal faces, with the lingual face more deeply indented than the buccal. In buccal view, the mesial buccal root height is 10.2 mm, the distal buccal root is 9.3 mm, and in lingual view, the lingual root measures 11.2 mm in height.

This specimen is a reasonable antimere of U.W. 101-999. The teeth are similar morphologically and in their state of occlusal and interproximal wear. An articulation mesially with U.W. 101-808 is reasonable.

U.W. 101-796: LM^1 (Fig. 20E; Table 1) Extensive wear and chipping have obliterated most of the crown. Enamel is preserved only on the buccal and distal aspects (stage 7–8). Both mesial and distal IPFs are present but not completely preserved, being reduced by occlusal wear. On the buccal aspect, about half the crown height is preserved. This

contrasts with the extensive lingual wear, which has completely removed the enamel and some of the root and exposed a large portion of the pulp chamber. The worn lingual surface must extend beyond the original cervix of the crown. In mesial and distal views, the wear angle is steep. A trace of the weak buccal groove is observable.

There are three roots: a mesiobuccal, distobuccal, and centrally placed lingual root. All roots are covered in a thick layer of cementum that has flaked off in places. Both buccal roots are missing their apices, though the root canals are not exposed. As measured from the buccal cervix, the mesiobuccal root is 10.1 mm tall and the distobuccal root is 10.0 mm tall. Each of the buccal roots is ovoid in cross section, with their major axes oriented BL. The major axis of the lingual root, in contrast, is oriented MD. The buccal roots project directly above the crown, while the lingual root splays lingually. The fully preserved lingual root measures 10.6 mm along its lingual face.

The preserved distal IPF is a good match for the mesial IPF of U.W. 101-528 (LM^2), which is also heavily worn. U.W. 101-528 is arguably associated with U.W. 101-527 (LM^3). The mesial IPF of this specimen is a good match for the preserved distal IPF of U.W. 101-1362 (LP^4). If these proposed associations are correct, this would constitute a heavily worn set of maxillary postcanine teeth from a single individual. An association with the heavily worn teeth in the U.W. 101-361 mandible is also possible.

U.W. 101-999: RM^1 (Fig. 21A; Table 1 There is minor enamel chipping along the mesial margin. A large, ovoid mesial IPF (approximately 4.8 mm by 2.9 mm) is present. No distal IPF is visible. The lingual cusps are flattened by wear, but no dentine is exposed, and the occlusal topography is well preserved (stage 1). Four cusps are present and

arranged in size as Pr > Me ≥ Hy > Pa. The occlusal outline is rhomboidal due to the distolingual projection of the relatively large Hy. The Fa is restricted to the Pa and is continuous with the central groove. Wear has thinned the MMR so that, as preserved, it is low and narrow. The Fp is bounded mesially by Me and Hy occlusal ridges and distally by the DMR. The DMR is low, dipping well below the height of the Me and Hy occlusal ridges. The Co is continuous. The lingual groove forms a deep, narrow cleft near the occlusal margin, fades at mid-crown, and appears as a pit just above the cervix. The buccal groove is shallow, extending from the occlusal margin to the cervix. A small Carabelli's feature, restricted to the mesiolingual aspect of the Pr, is expressed as an oblique crest.

All three roots are broken just prior to their apices and the root canals are exposed. The roots are abraded along their surfaces, especially the mesial and distal faces of the buccal roots and the lingual face of the lingual root. The lingual root is LaL compressed. It is an elongated figure-of-eight shaped in cross section as a result of buccal and lingual grooves running the length of the root. The lingual root deflects lingually and slightly distally. The two buccal roots are shorter than the lingual root and are more vertically oriented. The buccal roots are pressed together, but distinct, and run parallel to one another. Each buccal root is ovoid, being compressed MD. The mesiobuccal root is wider than the distobuccal root, has two distinct radicals, and is figure-of-eight in cross section. The narrower distobuccal root is ovoid in cross section. The lingual root is 11.2 mm in height along the lingual aspect. The mesiobuccal root is 9.8 mm in height and the distobuccal root is 10.1 mm tall.

This specimen is a possible antimere of U.W. 101-708. They are quite similar morphologically, in their wear status, in the size of their mesial IPFs, and lack of distal IPF.

U.W. 101-1305: LM^1 germ (Fig. 21B; Table 1) The nearly crown-complete germ shows no root development. The distal and mesiolingual cervical margins are slightly damaged. The crown outline is rhomboidal with a large distolingually projecting Hy. There are four cusps arranged in size as Pr > Me ≥ Pa > Hy. The Hy is tall and conical, with its apex subequal in height with those of the trigone. The essential ridges are well developed but not as well defined as the accessory ridges. The Pr and Pa have small, narrow mesial accessory ridges that meet, but do not join, at the central groove. These ridges form the distal border of a weak Fa. The Pr mesial accessory ridge presents as a small tubercle with a free apex (protoconule) and is adjacent to another small tubercle emanating from the MMR (mesial accessory tubercle). This ridge and tubercle pattern is unusual in the sample of maxillary molars. The Co is a continuous crest and composed of the distal accessory ridges of the Pr and Me. The wide Fp comprises a small pit and a BL-oriented groove mesial to the DMR. The DMR is low relative to the height of the Hy and Me and slopes cervically from its occlusal-most point adjacent to the Hy. The lingual groove is a deep, narrow cleft near the occlusal surface fading to a wider and shallower groove mid-crown and continuing to the cervix. The buccal groove is shallow throughout its course. Carabelli's feature is expressed as short horizontal shelf and associated pit restricted to the mesiolingual corner.

This specimen is proposed as the antimere of U.W. 101-1688. The teeth are nearly identical in morphology and their developmental status. These teeth likely belong to the same individual as the U.W. 101-1400 mandible and its associated antimeres and other isolated maxillary teeth. More details on these associations are provided in the Discussion.

U.W. 101-1396: RM^1 (Fig. 21C; Table 1) Enamel chipping is evident along the mesial and distal margins occlusal to the IPFs. There is a large oblong mesial IPF (6.7 mm BL by 2.1 mm OC) and a large bean shaped distal IPF (7.1 mm BL by 3.9 mm OC). Most of the surface morphology has been removed by wear. Two coalesced dentine pools connect over the Pr and Pa, while smaller dentine patches are evident over the Hy and Me (stage 5). The occlusal outline is a rounded, slightly tapered square that is slightly broader mesially than distally. The lingual groove is well preserved, especially its narrow and deep lingual and distal segments; it terminates distally in a moderate Fp. On the lingual aspect, it becomes shallow at mid-crown and continues to the cervix. The worn Co appears to be continuous; an examination of the µCT scans shows that the Co is continuous at the EDJ. A shallow buccal groove is visible as an indentation at the occlusal surface.

The three roots are missing their apices and are heavily abraded. The distobuccal root is broken near the crown cervix and refit to the crown. A notch of dentine is missing from the buccal side of the mesiobuccal root at about half its height. The buccal roots are ovoid in cross section, extend vertically from the crown, run parallel to each other, and are completely separated from one another. The mesiobuccal root is BL broader than the

distobuccal root. The lingual root has two radicals separated by a shallow groove, which results in a slight figure-of-eight shape in cross section. It is BL compressed and tilts lingually. The maximum height of the mesiobuccal root is 9.8 mm buccally, and the maximum height of the distobuccal root is 9.4 mm along the buccal aspect. The maximum height of the lingual root is 11.1 mm on its lingual aspect.

This specimen articulates mesially with U.W. 101-1401.

U.W. 101-1463: RM^1 (Fig. 21D; Table 1) Enamel chips are present along the mesial and distal margins. There is a large mesial IPF (5.4 mm BL by 2.0 mm OC) and a more circular distal IPF (4.8 mm BL by 3.5 mm OC). The crown is moderately worn, with small dentine patches exposed over the Pa and Hy and a larger dentine pool exposed over the Pr that extends mesially (stage 3). The crown has a rhomboidal occlusal outline due to a large, distolingually-projecting Hy. The relative cusp areas are Pr > Hy > Pa ≥ Me. Occlusal wear has obscured details of the mesial crown; only two small fissures, presumed to be associated with the Fa, remain. The deeper Fp is preserved as a small pit. A Co is present. Remnants of the lingual and buccal grooves are preserved at the occlusal edge, and both become shallow depressions on their respective faces. A Carabelli's feature is absent.

Two buccal roots and one lingual root are present, and a portion of the alveolar bone remains wedged between them. The buccal roots are both oval in cross section, being MD compressed. The mesial root is broader BL than the distal root. The buccal roots run parallel to each other and are pressed together, so that only a narrow, deep cleft separates them. Both roots are abraded and missing their apices. The maximum height of

the mesiobuccal root is 12.2 mm. The distobuccal root is also broken near its apex, exposing the canal. The break angles distally so that the maximum height of the distobuccal root preserved along its mesial margin is 10.2 mm. The lingual root is broken near its apex, exposing the canal. It is also oval in cross section; however, it is compressed MD, with grooves along both the lingual and buccal faces, which gives it a shallow figure-of-eight shape in cross section. The lingual root is much broader distally than lingually. The lingual root has a strong lingual inclination and is broken near its apex, exposing the canal. In lingual view, the preserved maximum height of the root is 12.4 mm.

This specimen is the probable antimere of the U.W. 101-1277 LM^1. Their patterns and wear status, and even the pattern of enamel chips, are very similar. However, the determination is complicated by the lack of detailed occlusal morphology preserved on either specimen.

U.W. 101-1676: LM^1 (Fig. 21E; Table 1) Enamel chipping is visible along the mesial and distal margins. There are large mesial (5.5 mm BL by 2.2 mm OC) and distal (5.4 mm BL by 3.5 mm OC) IPFs. Dentine patches are exposed on all four cusps. The largest is a pool over the Pr that extends mesially (stage 3–4). The crown is rhomboidal in occlusal outline, with a large, distolingually projecting Hy. Most of the occlusal morphology has been removed by wear but remnants of the occlusal grooves remain between the Pa and Pr and between the Hy and Me. The Co, though worn, appears continuous. A remnant of Carabelli's trait can be observed as a small groove on the mesiolingual aspect of the Pr that spills onto the worn occlusal surface. Occlusal and interproximal wear have

obliterated the Fa and MMR. Distally, a small remnant of the Fp remains. The preserved morphology does not suggest that accessory cusps were present. The buccal groove is shallow and the lingual groove is not well preserved.

The roots are broken away and sediment adheres to the surface of the pulp cavity. In buccal view, a maximum of 2.5 mm of root are preserved below the cervix. A trace of the cleft between the mesial and distal buccal roots is visible.

This specimen is proposed as the antimere of U.W. 101-525. It may articulate mesially with the U.W. 101-277 LP^4. This proposition is reasonable because their reciprocal IPFs are a good match, and they have similar patterns of enamel chipping in the adjoining regions. It may also articulate distally with U.W. 101-1522. Their respective IPFs fit well, and their wear statuses are similar.

U.W. 101-1688: RM^1 germ (Fig. 21F; Table 1) This is the nearly crown-complete germ of the RM^1 with no root development. There is minor damage to the cervix distobuccally. The four primary cusps are present, and the crown is rhomboidal in outline due to the distolingually projecting Hy. The relative cusp sizes are Pr > Me ≥ Pa > Hy. The essential ridges of the Pa and Me are developed but those of the Pr and Hy are not well defined. The Pr has a weak mesial accessory ridge, and the Pa has a stronger one. They meet at the central groove but do not form an epicrista. The Me essential ridge becomes a wide triangle towards the occlusal basin. The Fa is weakly defined by the Pr and Pa mesial accessory ridges and continuous with the central groove. The DMR is low and forms the distal border of a small Fp. The lingual groove forms a narrow and deep cleft near the occlusal surface that becomes a shallow groove mid-crown as it continues to the cervix.

The buccal groove is barely perceptible. Carabelli's feature takes the form of a faint, obliquely oriented ridge and associated pit that is restricted to the mesiolingual corner.

This is the antimere of U.W. 101-1305. They are nearly identical in morphology and their state of development. As a result, this tooth is part of the set of teeth assigned to the subadult specimen that includes the U.W. 101-1400 mandible.

3.16. Permanent maxillary second molars

Ten isolated M^2s and one present in the U.W. 101-1277 maxilla, representing at least seven individuals, are known from the Dinaledi Chamber deposits. The M^2 sample includes an antimeric pair, U.W. 101-1063 and U.W. 101-1135, which were nearing crown completion, as well as other crowns with a range of of wear stages. The sample includes a pair of heavily worn antimeres, U.W. 101-005 and U.W. 101-528, in which the steep bucco-lingual wear gradient had worn the crown to the level of the pulp chamber. The specimens are all similar in morphology and size. Where detail can be assessed, all M^2s have four principal cusps and, except for U.W. 101-867, no supernumerary cusps. The Hy is relatively large and projects distolingually, giving the crown a rhomboidal occlusal outline. Carabelli's feature is either absent or weak in expression. In contrast to the M^1, except in U.W. 101-1006, the Co is not continuous. Buccal grooving is shallow; the lingual groove is narrow at the occlusal margin and widens as it reaches cervically.

U.W. 101-005: RM^2 (Fig. 22A; Table 1) The entire circumference of the tooth has undergone modification through chipping, which is especially extensive along the lingual and mesial occlusal margins. Other occlusal chips are present mesiobuccally and

distobuccally. A portion of the mesial IPF remains, especially buccally, and it extends obliquely along the occlusal wear plane. Here, its maximum preserved dimension parallel to the occlusal surface is 4.2 mm and its maximum OC dimension is 1.5 mm. Occlusal wear obliterated the mesial IPF along its lingual extent. A large distal IPF (5.8 mm maximum BL breadth) is visible; though, occlusal wear and enamel chipping have reduced its lingual extent. The crown is severely worn and a large dentine pool spreads across all but a small portion of enamel between the Pa and Me and an enamel rim (<1.0 mm on the lingual aspect) surrounding the crown (stage 6). The worn surface shows a strong BL slope, with approximately half of the crown's height remaining buccally and very little of its height remaining lingually.

Three roots are present. Both buccal roots are broken and about two-thirds of their maximum height is preserved, while the lingual root is complete. The maximum preserved height of the mesiobuccal root is approximately 7.0 mm and the maximum preserved height of the distobuccal root is 8.2 mm. The height of the lingual root is 10.7 mm. The external root surfaces are covered in cementum and evince some abrasion. In cross section, the buccal roots each have their major axis BL and minor axis MD. In contrast, the major axis of the lingual root is MD and the minor axis BL. The lingual root is invaginated along both buccal and lingual faces. The buccal roots extend vertically above the crown, while the lingual root is more strongly splayed.

This tooth was recovered within centimeters of U.W. 101-006 (RM_3), another heavily worn molar. However, as U.W. 101-005 and -006 are from different arches, attribution to a single individual cannot be confirmed. The U.W. 101-528 LM^2 is a

candidate antimere but this proposal is difficult to evaluate since both express advanced occlusal wear that has removed most morphological detail.

U.W. 101-505: LM^2 germ (Fig. 22B; Table 1) This is a nearly crown-complete germ (stage 1). The occlusal outline is rhomboidal, with a relatively large, distolingually projecting, Hy. There are four principal cusps arranged in size as Pr > Hy > Me ≥ Pa. The essential lobes lack distinct occlusal ridges and the occlusal surface lacks complexity. There are small pits on the apices of all four cusps and a small groove and ridge complex on the Pr near the central fovea; otherwise, there are no accessory features. The MMR is indistinct and lacks accessory tubercles. The groove-like, shallow Fa is confined to the Pa and defined distally by a weak Pa mesial accessory ridge. The Fp is a pit at the distal termination of the central groove. The essential ridges of the Pr and Me are separated by a deep groove and no Co is present. Carabelli's feature is absent. A deep lingual groove separates the Pr and Hy. It is a narrow cleft near the occlusal surface but becomes imperceptible near mid-crown. The buccal groove is a shallow v-shaped fossa near the occlusal edge, becoming a shallow groove that travels towards the cervix. Just before reaching the cervix, it becomes a short deep invagination.

Given the ontogenetic status of this specimen, there was likely little-to-no root development on this crown. The surface of the pulp chamber is exposed and stained by sediment.

Based upon morphological similarity and lack of occlusal wear, this specimen is proposed as the antimere of U.W. 101-593. The right M^2 of the pair does evince minimal root development.

U.W. 101-528: LM^2 (Fig. 22C; Table 1) The enamel rim is missing in an arc that extends from the distolingual corner, along the lingual side, around the mesiolingual corner, and to a point about halfway along the mesial edge of the tooth. When originally observed in 2014, enamel extended to the middle of the lingual face, nearly to the groove between the Hy and Pa; the distolingual rim is missing as of 2015. Enamel chipping is present distally, especially along the lingual half, just above the IPF. Distally, a large centrally placed IPF (6.9 mm BL by 2.8 mm OC) is present. Mesially, the IPF (5.0 mm BL by 2.2 mm OC) is evident where enamel is preserved. The crown is heavily worn, with a large dentine pool covering the lingual surface (stage 5). The wear surface is not planar, with the lingual moiety scooped out and the wear plane reaching its deepest point mesially.

Three roots are present. The lingual root is damaged near its apex, especially along its mesial edge. Significant abrasion to the cementum covering the root is also evident lingually, especially concentrated near the cervix and extending to about half the root's length distally and lingually and across the entire mesial surface of the root. The cementum of the mesiobuccal root is abraded along its mesial and labial surfaces and the apex is broken away. The distobuccal root is also abraded along its distal surface and the apex damaged. Further, the apex of the distobuccal root is broken. The buccal roots extend directly above the crown, while the lingual root tilts over the crown. The mesiobuccal root is considerably broader than the distobuccal root; further, the mesiobuccal root is ovoid, while the distobuccal root is more circular in cross section. The lingual root is considerably larger in cross section than the buccal roots. A shallow groove runs along the lingual side and a deeper groove runs along the buccal side of the

lingual root. The height of the mesiobuccal root, as measured from the buccal cervix, is 10.3 mm; the distobuccal root is 9.3 mm in height from the buccal cervix; and the lingual root is 11.8 mm in height from the lingual cervix.

The distal IPF is a good fit for the mesial facet of the U.W. 101-527 LM^3. The mesial IPF is a reasonable match for the distal facet of the heavily worn U.W. 101-796 LM^1, which is in turn argued to be associated with U.W. 101-1362 (LP^4). Above, it was suggested that U.W. 101-527 may occlude with the M_3 in the U.W. 101-361 mandible. Thus, this specimen may occlude with the U.W. 101-361 as well. The U.W. 101-005 RM^2 is a candidate antimere but this proposal is difficult to evaluate since both express advanced occlusal wear that has removed most morphological detail.

U.W. 101-593: RM^2 (Fig. 22D; Table 1) The crown is unworn (stage 1) and lacks IPFs. The relative sizes of the four primary cusps are Pr > Hy > Me ≥ Pa. The distal lobe of the Hy is hypertrophied and it is bordered by shallow depressions on either side, but this is not a true C5 and no distinct dentine horn is present at the EDJ. In occlusal outline, the crown is roughly rhomboidal due to the mesiobuccal projection of the Pa and the slight distolingual projection of the Hy. The swollen Hy distal accessory ridge gives a rounded outline to the distal border. However, the Hy is less projecting than in some other *H. naledi* maxillary molars since the distal lobe fills in the crown outline distally. The essential ridges are not well defined, except on the Me and Pa, where they are associated with accessory fissures. There is no continuous Co. There is a small, possibly hypoplastic, pit on the apex of the Me, and the Pr exhibits an unusual a small groove and ridge at its base. A mesial accessory ridge on the Pa defines the distal border of the Fa,

which is a short mesiobuccal extension of the central groove. A thin MMR bounds the Fa mesially and is continuous from the mesial crests of the Pa and Pr. No Carabelli's feature is evident. The lingual groove is narrow and deep near the occlusal margin but fades away near mid-crown and reappears as a pit near the cervix. The buccal groove is very shallow throughout ending in a pit near the cervix.

Though the roots were developing at death, very little of them remains and sediment fills the exposed pulp chamber.

This tooth is the likely antimere of U.W. 101-505. They are nearly identical in morphology and developmental state.

U.W. 101-867: RM^2 (Fig. 22E; Table 1) A broad mesial IPF (approximately 6.0 mm BL by 3.4 mm OC) is centered near the occlusal margin, while the distal IPF is smaller (approximately 2.6 mm BL by 2.7 mm OC), offset lingually, and located at about half the crown height. Distinct wear facets are visible on the occlusal surface, but no dentine is exposed (stage 1). The occlusal outline is slightly rhomboidal due to the minor projection of the Hy distolingually and the stronger projection of the Pa mesiobuccally. Distally, the crown is worn, but the pattern of grooving suggests the presence of a small C5 or ridge extending from the DMR. In size, the cusps are approximately Pr > Hy > Pa ≥ Me. The region of the Fa and MMR is worn, but a remnant of the Fa is preserved as a slight groove mesial to the Pa. The Fp is preserved as pit adjacent to the C5. Though worn, the Co is not continuous on the outer enamel surface; this is confirmed at the enamel dentine junction as well. The buccal groove is quite shallow as it crosses the crown face; the lingual groove is a deep and narrow cleft in the occlusal half and then widens just below

mid-crown to continue as a shallow indentation. The Carabelli's feature is expressed as a small crest and associated groove mesiolingually.

A portion of alveolar bone remains wedged between the roots. The distobuccal (14.2 mm) and lingual (14.9 mm) roots are nearly complete; however, the mesiobuccal root (10.8 mm) is broken at about two-thirds its height. The buccal roots are pressed together and their mass tilts distally. The distobuccal root also leans over the crown face. In cross section, the buccal roots are both longer BL than they are MD, with the mesial root larger than the distal root in cross sectional area. The major axis of the lingual root is perpendicular to the buccal roots. There is a distinct invagination along its buccal face and a shallower depression along its lingual face, which gives it a shallow c-shape in cross section. The lingual root leans over the lingual face with a slight distal tilt, especially apically.

U.W. 101-1006: RM^2 (Fig. 23A; Table 1) The crown is unworn and lacks IPFs (stage 1). The crown has a slight distal taper, and the occlusal outline is rhomboidal due to the distolingual projection of the Hy. There are four principal cusps and a small distal cusp 5 defined by weak grooves. In size, the relative cusp sizes are Pr > Pa > Hy ≥ Me. The essential lobes of the main cusps are well broad but, apart from the Pa, not defined by distinct ridges. The Pa essential ridge is mesially offset and bifurcates near the apex into two thick ridges. The mesial-most ridge forms the distal border of the Fa. In addition, there are two faint distal accessory ridges on the Pa originating from the distal occlusal crest. The distal lobe of the Pr forms a crest that is constricted in the middle and then takes a mesial turn to merge with the mesial lobe of the Me to become the Co. The Me

essential ridge defects distally and meets the Hy essential ridge. There are small hypoplastic pits at the tips of the Hy and Me. The Fa is restricted to the Pa and is continuous with the central fovea. The MMR is lower than the essential Pr and Pa ridges and rounded. It slopes to its most cervical point mesial to the Pa. The DMR is low and rounded and includes a small cusp rising from it. A small bifurcation of the Fp extends buccally up the Me. The lingual groove is deep and narrow. It forms a cleft near the occlusal margin, disappears about mid-crown and then reappears as a pit just above the cervix. The buccal groove is broad and shallow. Mesiolingually, there is a very small pit-like Carabelli's feature associated with a small, nearly vertically oriented, mesial crest. The roots have broken away from the crown. Given the lack of occlusal wear and IPFs, the roots were incompletely developed at death.

This is a possible antimere of U.W. 101-1015. The two teeth are similar in morphology, wear status, absence of IPFs, and in size. Of note, U.W. 101-1015 does preserve a small portion of its roots. The two teeth differ in the morphology of the Carabelli's feature, which is absent on U.W. 101-1015 but present on U.W. 101-1006. They also differ in the morphology of the Co, which is discontinuous in U.W. 101-1015 but continuous in U.W. 101-1006, and in the morphology of the DMR, where a distinct cusp sits near the Me on U.W. 101-1006 but is absent on U.W. 101-1015.

U.W. 101-1015: LM^2 (Fig. 23B; Table 1) The crown is unworn (stage 1). The relative cusp sizes are Pr > Pa > Hy ≥ Me. The crown tapers distally and is rhomboidal in outline due to the distolingual projection of the Hy. The essential lobes of the four primary cusps are well developed but lack strong ridges. The Pa mesial accessory crest is hypertrophied

and forms the distal border of the Fa. The Pr has a distal accessory ridge that deflects mesially and terminates at the occlusal basin. There is no Co. The Fa is restricted to the Pa and is continuous with the central fovea. The rounded MMR is lower than the essential ridges of the Pr and Pa. The DMR is a low and rounded ridge bounding the pit-like Fp. The lingual groove is deep and narrow and forms a cleft near the occlusal margin, disappears about mid-crown, and then appears as a pit just above the cervix. The buccal groove is broad and shallow throughout its course. There is no Carabelli's feature visible.

Most of the roots are broken away from the crown. About 2.5 mm of root remains lingually adjacent to the Pr, a maximum of 3.2 mm remains mesially in an irregularly broken surface, and 3.0 mm remains buccally adjacent to the Pa. Given the absence of occlusal wear and IPFs, the roots were likely incomplete at death.

This specimen is a possible antimere of U.W. 101-1006. The two teeth differ in the morphology of the Carabelli's feature, which is absent on U.W. 101-1015 but present on U.W. 101-1006, in the morphology of the Co, which is discontinuous in U.W. 101-1015 but continuous in U.W. 101-1006, and in the morphology of the DMR, where a distinct swelling near the Me of U.W. 101-1006 is absent on U.W. 101-1015.

U.W. 101-1063: LM^2? (Fig. 23C; Table 1) This is a developing tooth germ. The poorly mineralized enamel is covered with cracks. Especially deep cracks extend longitudinally around the margins of the tooth and the delicate cervix is broken in many places, especially mesiobuccally and mesiolingually. This fragile specimen was complete when

it was first examined in 2014, scanned in 2015, and photographed in 2016. The specimen was broken some time in 2016 and is now repaired.

Only the four primary cusps are present. The crown tapers somewhat distally and is rhomboidal in outline due to the projecting Hy. The Fa is expressed as a BL-elongated fissure that bordered distally by a weak epicrista connecting the mesial accessory crests of the Pr and Pa. The shallow Fp is bordered mesially by the essential ridges of the Me and Hy. The distal lobe of the Pr is hypertrophied, widening towards, and then terminating at, the central groove. As in other *H. naledi* M^2s, but not M^1s, The Co is absent, which is confirmed by the examination of the EDJ morphology. The lingual groove is a narrow cleft, and the buccal groove is shallow. Crown damage precludes assessing Carabelli's trait expression.

This specimen is the proposed antimere of U.W. 101-1135. They are identical in developmental status and similar in morphology. It is also likely associated with U.W. 101-1002 based upon the similar degree of crown completeness.

U.W. 101-1135: RM^2? (Fig. 23D; Table 1) This is a developing tooth germ. The poorly mineralized enamel is covered with cracks. A large flake of enamel on the mesiolingual corner has been refit to the crown. There are four primary cusps and a small distal accessory cusp (C5) arising from the DMR. The accessory cusp is associated with a small dentine horn at the EDJ. The crown tapers somewhat distally and is rhomboidal in outline due to the slight projection of the Hy. The MMR slopes to its most cervical extent adjacent to the Pa. The Fa is expressed as a BL-elongated fissure bordered distally by a weak epicrista connecting the mesial accessory crests of the Pr and Pa. The shallow Fp is

bordered mesially by the essential ridges of the Me and Hy. The distal lobe of the Pr is hypertrophied, widening towards, and then terminating at, the central groove. As in other *H. naledi* M^2s, but not M^1s, a Co is absent. The lingual groove is a narrow cleft, and the buccal groove is shallow. Crown damage precludes assessing Carabelli's trait expression.

Based upon similarities in morphology and developmental status, this is the antimere of U.W. 101-1063. These antimeres are probably associated with the U.W. 101-1002 RM_2, which is at a similar state of crown development and mineralization.

U.W. 101-1522: LM^2 (Fig. 23E; Table 1) There is a large mesial IPF (4.9 mm BL by 3.5 mm OC) and a smaller distal IPF (2.1 mm BL by1.9 mm OC). Minor enamel chipping is present on the Me. Occlusal wear facets are present, but no dentine is exposed (stage 2). The occlusal outline is slightly rhomboidal. The relative cusp sizes of the four primary cusps are Pr > Me ≥ Pa ≥ Hy. The essential lobes are well developed but not associated with distinct crests. The MMR is only partially preserved. It forms the mesial border of a small Fa that is restricted to the Pa and is continuous with the central fovea. In mesial view, the MMR slopes from the Pr to reach its most cervical point mesial to the Pa. A small Fp is bordered mesially by Me and Hy occlusal crests. The Me has a doubled apex with a shallow groove separating each apex and continuing onto the buccal face. A Co is absent. There is a faint indentation associated with Carabelli's feature restricted to the mesiolingual aspect of the Pr. A shallow buccal groove terminates at the cervix. The lingual groove is a deep and narrow cleft near the occlusal margin that fades approximately mid-crown and then reappears as a pit above the cervix.

A portion of alveolar bone remains between the mesial and distal buccal roots. The lingual root is broken at the apex, exposing the root canal, while the buccal roots are completely preserved. The buccal roots are MD compressed and ovoid in cross section. In buccal view, these roots are pressed together and tilt distally. The mesiobuccal root has a stronger apical distal tilt than the distobuccal root. In distal view, the buccal and lingual roots splay out from one another. The mesiobuccal root is 15.5 mm in height and the distobuccal root is 14.6 mm in height. The lingual root is invaginated buccally, giving it a c-shape cross section. The lingual root also apparently tilts distally, but its apex is broken. The maximum height of the lingual root is 12.1 mm.

The distal IPF is very similar in size and shape to the mesial IPF of the U.W. 101-418C M^3. Further, an articulation mesially with the U.W. 101-1676 M^1 is also reasonable based upon the morphology of their respective IPFs.

3.17. Permanent maxillary third molars

Six isolalated M^3s represent at least four adults in the Dinaledi Chamber deposits. They present a consistent morphological pattern. While all M^3s are squarer than the M^1s and M^2s, the Hy still projects more distally than does the Me except in the specimens with the most pronounced C5s (i.e., U.W. 101-418C and U.W. 101-594). A supernumerary C5 is present on all specimens. In contrast to M^1s, no Co is present. Carabelli's feature is either weak or absent. Where preserved, the M^3s all present a distintive root morphology in comparison to the M^1s and M^2s in the assemblage. The M^3s possess three roots, of which the lingual root is the largest. The two buccal roots differ in size and orientation, with the larger and flatter mesial buccal root being vertically

oriented and the much small and more circular distal buccal root having a strong buccal and distal cant.

U.W. 101-418C: LM^3 (Fig. 24A; Table 1) A semicircular mesial IPF (3.3 mm BL by 2.8 mm OC) is evident and offset lingual to the midpoint of the crown. No distal IPF is detectable. The cusp apices are unworn but there are small facets on the Pr essential ridge, Pa mesial accessory ridge, and Me essential ridge (stage 1). The crown outline is square with more or less parallel sides and slightly convex mesial and distal margins. There are five cusps evident, including a centrally placed C5. The relative cusp sizes are Pr > Pa > Me > Hy > C5 and the cusps are widely spaced. The flat MMR, a small Hy, and prominent C5 square off the crown to yield a roughly rectangular outline with a slight distolingual projection of the Hy and C5. The Hy and C5 are similar in size: both are remarkable in that they project to nearly the same height as the other cusps. The Fa is a centrally placed pit with buccal and lingual extensions. It is bordered distally by mesial accessory ridges of the Pr and Pa, which merge to form a mesial trigone crest. The Mlg shallowly bisects this crest. The MMR forms a mesially extended shelf that features a small mesial accessory tubercle (sensu Scott and Irish, 2017). The essential ridge and distal accessory ridge of the Pr are well developed (the distal ridge more so than the essential ridge). The distal accessory ridge angles mesially as it reaches the Mlg and meets the essential ridge. In contrast, the Pa lacks essential and distal accessory ridges. The Me essential lobe is well developed. It is separated from a short but distinct distal accessory ridge by a deep groove. This ridge merges with the C5 near the central fovea. There is a short Fp between the Hy and C5. The Me and Pr are separated by a deep

groove; thus, no Co is present. The Carabelli's feature is evident as a very small pit and associated vertical groove. The lingual groove separating the Pr and Hy is deep and narrow, forming a cleft near the occlusal margin and then becoming a faint groove roughly one-third of the crown's height and disappearing as it reaches the cervix. The buccal groove is a shallow depression originating at the occlusal rim that becomes a short deep invagination near the cervix. The roots are broken off at the cervix and some sediment staining is evident in the pulp chamber.

This specimen is the proposed antimere of U.W. 101-594. The crowns are not, however, identical in morphology, with the C5 relatively larger on U.W. 101-418C. Moreover, U.W. 101-418C may articulate with U.W. 101-1522, as they both have similarly shaped and small interproximal facets. The U.W. 101-1522 M^2 may articulate mesially with U.W. 101-1676, completing the set of left molars.

U.W. 101-527: LM^3 (Fig. 24B; Table 1) Several enamel chips are missing from the mesiolingual and mesiobuccal corners, and around the buccal margin. A large mesial IPF (5.0 mm BL by 3.2 mm OC) is partially preserved on the Pa; the lingual extent is removed by occlusal wear. There is no distal IPF. Extensive wear has removed all occlusal features except for a portion of the groove between the Hy and Me, which indicates that a Co was not present. A large pool of dentine is exposed over the Pr (stage 3). There is a strong mesiobuccal wear gradient, with the Pa representing the current topographical high point. The crown outline is trapezoidal, being BL broadest across the mesial cusps and tapering distally. The Hy is large and projects farther distally than does the Me. The lingual and buccal grooves are both indistinct.

There are two buccal roots, one mesial and one distal, and a centrally placed lingual root. The lingual root is broken near its apex and its surface is abraded, especially mesially and to a lesser extent along the distal face. The preserved height of the lingual root is 10.9 mm. Both buccal roots are missing portions of their apices; though, the root canals are not exposed. The preserved height of the mesiobuccal root is 10.1 mm and the distobuccal is 7.7 mm. The major axis of the lingual root cross section is MD elongated with a shallow groove on its lingual side. The lingual root angles out over the crown face. The mesial buccal root is vertically oriented, and the distal buccal root has a stronger buccal and distal cant. The mesial buccal root is ovoid in cross section, while the distal buccal root is much smaller and more circular in cross section. Both buccal roots have their long axes BL. The strong asymmetry in size, shape, and orientation of the buccal roots is seen in other *H. naledi* M^3s (i.e., U.W. 101-594, U.W. 101-1398A, U.W. 101-1471, and U.W. 102-001).

The mesial IPF of this specimen articulates well with the distal facet of U.W. 101-528 (LM^2), which is in turn arguably associated with U.W. 101-796 (LM^1) and U.W. 101-1362 (LP^4). If these proposed associations are correct, this would constitute a heavily worn set of maxillary postcanine teeth from a single individual. Further, occlusion of this tooth with the in situ M_3 in the U.W. 101-361 mandible is reasonable. This specimen and the U.W. 101-361 M_3 also show occlusal chipping in their corresponding regions.

U.W. 101-594: RM^3 (Fig. 24C; Table 1) A large ovoid mesial IPF (5.2 mm BL by 5.3 mm OC) is centered on the mesial face. There is no distal IPF. Small wear facets are present on all cusps but no dentine is exposed (stage 1). The crown is square in occlusal

outline, owing to a large Me, a moderately sized, non-projecting Hy and a distinct C5. The relative cusp sizes are Pr > Pa > Me > Hy > C5. The essential ridges of the Pr and Hy are not well defined, whereas those on the Pa and Me are delineated on either side by distinct grooves. Accessory ridges are present on all four cusps. The Pa has well-developed mesial and distal accessory ridges; The Pr has a hypertrophied distal accessory ridge. The distal lobes of the Me and Hy are strong and that of the Hy forms a medium-sized C5. There is no Co. The Fa is BL-oriented groove that is expressed predominantly on the Pa and to a lesser extent on the Pr. The MMR is lower than the accessory ridges of the Pa and Pr and gently slopes from the Pr to reach its lowest point mesial to the Pa. The Carabelli's feature is a very small pit and vertically oriented furrow. The lingual groove is narrow and deep and fades at mid-crown where it intersects a weak horizontal shelf extending onto the Hy. The buccal groove is shallow throughout its course until it becomes a deep short fissure near the cervix.

Portions of three roots are preserved: a lingual root, a distobuccal root, and a mesiobuccal root. A small bit of alveolar bone remains wedged between them. The lingual root is abraded mesially, buccally, and distally. The mesiobuccal root is also abraded mesially. The lingual and distobuccal roots are broken at half or more of their lengths, and the mesiobuccal root is broken at about a third of its length. All breaks expose the root canals, which are packed with sediment. In lingual view, the lingual root is 9.0 mm in height and, in buccal view, the mesiobuccal root is 8.8 mm in height along its distal margin and the distobuccal root is 9.0 mm in height. In cross section, the major axis of the lingual root is MD, and a prominent groove runs along its buccal face. As preserved, the lingual root begins to tilt distally and lingually just before the break. The

distal tilt is especially evident when tracing the contour of the mesial edge of the root. The mesiobuccal root is very narrow MD and much broader BL. The distobuccal root is more circular in cross section than the mesiobuccal root. Both buccal roots tilt distally, with the distobuccal root more strongly inclined. The distobuccal root also angles strongly buccally. The asymmetry in the size, cross-sectional shape, and tilt seen in the buccal roots is consistent with the morphology of other *H. naledi* M^3s (i.e., U.W. 101-527, U.W. 101-1398A, U.W. 101-1471, and U.W. 102-1) that preserve their roots.

This is the proposed antimere of U.W. 101-418C. They are nearly identical in occlusal morphology, in the state of occlusal wear, and the development of the mesial IPFs.

U.W. 101-1269: LM^3 (Fig. 24D; Table 1) An oval mesial IPF (4.7 mm BL by 2.4 mm OC) is present. No distal IPF is present. Each cusp is lightly polished by wear, but no dentine is exposed (stage 1). The crown outline is less rhomboidal than some maxillary molars in the sample and is rounded square, with the moderately sized Hy. The crown is BL broadest across the mesial cusps and tapers distally. In addition to the four principal cusps, the crown possesses a small C5. The relative cusp sizes are Pr > Pa > Hy ≥ Me > C5. The MMR is well developed, with the lingual and buccal components of the MMR sloping to meet at an angle with a faint groove at their junction in the midline. The fissure-like Fa is wide and continuous with the central groove. Its buccal branch is slightly shorter than its lingual segment. The Fa is bordered distally by a thin, discontinuous epicrista joining the mesial aspects of the Pr and Pa. The Co is interrupted

by the central groove. A small pit-like Carabelli's feature sits on the mesiolingual aspect of the Pr.

The tooth is three rooted; however, the distobuccal root broke off a few millimeters from the cervix. The mesiobuccal root is MD compressed with a depression separating two radicals along its distal face. Its apex curves distally. On the buccal aspect, the mesiobuccal root is 11.3 mm tall. The lingual root is robust, and MD compressed. It is c-shaped in cross section, especially apically, due to a strong invagination along the buccal face. The lingual root angles lingually and deflects distally. Its tip is broken just before its apex, exposing a small portion of the root canal. On the lingual aspect, the preserved height of the root is 11.3 mm.

The mesial IPF of this specimen is proposed to match the distal IPF of the M^2 in the U.W. 101-1277 maxilla.

U.W. 101-1398A: RM^3 (Fig. 24E; Table 1) An enamel chip is present along the distal margin. The crown has a very large, oval mesial IPF (6.9 mm BL by 4.2 mm OC), which reaches the occlusal surface and has no distal IPF. The occlusal surface is polished by wear but no dentine is exposed (stage 1–2). The occlusal outline is a rounded square with a convex distal margin. A cingular shelf crossing the lingual groove affects the lingual contour. There are four primary cusps. There was likely a C5; wear precludes its assessment at the outer enamel surface but a distinct dentine horn for it is present at the EDJ. The distal lobe of the Me is hypertrophied and divided from the essential lobe by a fissure. The expression of the MMR cannot be assessed due to IP wear. The Fa is preserved as a short groove still visible on the Pr. It appears to be divided from the central

fovea by an epicrista joining the Pr and Pa (an epicrista is present at the enamel-dentine junction). Carabelli's feature is expressed as a v-shaped groove and associated weak shelf. The buccal groove is shallow.

The crown has three roots: two buccal and one lingual. The distobuccal root is broken about mid-length and the mesiobuccal root is missing its apical third. The root surfaces are abraded. The lingual root is MD wide and comprises two components separated by a buccal invagination, which gives it a c-shape in cross section. The lingual root is distally inclined, especially along its mesial margin. The mesiobuccal root is MD compressed. At the cervix, the distobuccal root is more circular and smaller in cross section than the mesiobuccal root. It takes a strong buccal turn and slight distal inclination, which is quite different from the vertical orientation of the mesiobuccal root. The maximum height of the lingual root is 10.6 mm along its lingual aspect. The maximum height of the mesiobuccal root is 11.5 mm along its buccal aspect and the maximum height of the distobuccal root is 5.9 mm.

This specimen is proposed as the antimere of U.W. 101-1471. Both specimens are likely M^3s. Their diagnosis as M^3s is based in part upon the morphology of their roots, which are better preserved on U.W. 101-1471 than U.W. 101-1398A. The distobuccal roots of these specimens are much smaller and more circular than the mesiobuccal roots and show a strong, and unusual, buccal and distal tilt. A similar heteromorphic root morphology is present in the U.W. 102-1 M^3s (Hawks et al., 2017; L.D., personal observation), in contrast to the U.W. 102 M^2s. Further, there is no distal interproximal facet present on either specimen. For comparison, the U.W. 101-1277 M^2, which is at a

similar state of occlusal wear, has a distinct distal facet. In addition, the occlusal outline, which features a rounded Hy and divided Me, is matched in other proposed M^3s.

U.W. 101-1471: LM^3 (Fig. 24F; Table 1) There is an enamel chip on the Me apex. There is a large semicircular mesial IPF (5.8 mm BL by 3.4 mm OC) and no distal IPF. The cusps are flattened by occlusal wear, but no dentine is exposed (stage 2). The crown is somewhat rhomboidal in occlusal outline due to the distolingual projection of the relatively large Hy and a reduced Me. The four primary cusps have the following relationship: Pr > Hy ≥ Pa > Me. In addition, there is a small cuspule distal to the Me. The expression of the MMR and Fa is obscured by wear; however, it appears that the Fa is preserved as a small pit that was separated from the central fovea by a continuous epicrista connecting the Pr and Me. The lingual groove is a deep cleft at the occlusal margin but becomes shallow and broad below the occlusal surface. A small pit associated with Carabelli's feature is present on the mesiolingual aspect of the Pr. No crest extends distally from the Carabelli's feature; though, a subtle swelling of the cingulum is evident distal to the lingual groove. There is no buccal groove.

The crown has two buccal roots and one lingual root. The lingual root apex is broken, exposing the root canal. The mesiobuccal root is also broken, exposing a tiny pinhole of the canal. The lingual root is large and angles distally. A prominent groove runs along its buccal face, giving it a c-shape in cross section. The mesiobuccal root is a MD-compressed oval. It is more plate-like than the distobuccal root, which is smaller and more circular in cross section. The mesiobuccal root angles slightly distally, while the

distobuccal root angles distobuccally. The maximum height of the lingual root is 11.8 mm. The mesiobuccal root is 11.0 mm tall and the distobuccal root is 8.5 mm tall.

This specimen is proposed as the antimere of U.W. 101-1398A. The assessment of this tooth as an M^3, and not M^2, is based on several features. The buccal roots of this specimen are strongly heteromorphic in cross sectional size, shape, and orientation. Such root asymmetry is not seen, for example, in the U.W. 101-1277 M^2, which is in situ in the maxilla. Further, *H. naledi* specimen U.W. 102-001, from the Lesedi chamber (Hawks et al., 2017), preserves all three maxillary molars bilaterally. The 102-001 M^3s share with U.W. 101-1471 the distinctive buccal root heteromorphy (L.D., personal observation). The absence of a distal IPF is consistent with the identification of this tooth as an M^3. Further, the occlusal outline, which features rounded Hy and reduced Me are matched in other proposed M^3s.

3.18. Permanent mandibular central incisors

Six isolated I_1s and those in the U.W. 101-1261 mandible represent at least four individuals. Morphologically, the teeth are simple in form. In labial and lingual views, the crown flares towards the incisal edge; the labial face is featureless and minimally convex at mid-crown; lingually, the marginal ridges are faint and bound a featureless lingual fossa.

U.W. 101-039: RI_1 (Fig. 25A; Table 1) Minor damage is evident to the labial and lingual cervical lines and enamel chipping is evident near the lingual margin of the mesial IPF. The mesial IPF (2.5 mm along its major axis) is teardrop shaped and located near the

incisal edge. A much smaller distal IPF runs along the DMR below the incisal edge. The crown is worn with dentine exposed along the incisal edge and lingually along the mesial shoulder (stage 4). In labial and lingual views, the crown flares towards the incisal edge. The labial face is featureless and minimally convex at mid-crown. Lingually, the MMR and DMR are barely perceptible and defined by faint lingual grooves. The DMR is more visible than the MMR, which is obscured by incisal wear. The DMR is also stronger towards the incisal edge. There is no basal swelling.

The root is abraded across its surface and slightly damaged just below the lingual cervix. The root is broken apically at an angle so that more of the labial height (9.4 mm) is preserved than the lingual. In cross section, the long axis of the root runs LaL. There is a wide and shallow depression running along the distal root face.

This is the proposed antimere of the U.W. 101-601 LI_1. They are morphologically homogenous, their occlusal wear is similar, and their IPFs match.

This specimen and U.W. 101-038 were both found on a rock and had been arranged by cavers prior to excavation (see area D in Figure 6B of Dirks et al., 2015).

U.W. 101-601: LI_1 (Fig. 25B; Table 1) The tooth is fragmented. One portion contains most of the crown, while the other contains the lingual cervix and root. The rejoined surfaces are not flush. Enamel chipping is evident in the region of the small mesial IPF, which is located very near the incisal edge. A larger distal IPF (2.3 mm IC by 1.3 mm LaL) is located at the incisal edge. Dentine is exposed along the incisal edge and the incisal aspect of the MMR (stage 3). The labial face is featureless and minimally convex at midcrown. Lingually, the MMR and DMR are barely defined by faint grooves that

separate them from a featureless lingual fossa. The marginal ridges increase in topographical prominence as they approach the incisal edge; both are, however, worn on their lingual aspects near the incisal edge. Further, the MMR is truncated by the encroaching mesial IPF.

The root is minimally abraded on its mesial side and the exposed root canal is packed with sediment. Labially, the preserved height of the root is approximately 9.3 mm, accounting for the refit. In cross section, the root is broader LaL than MD and there is a subtle depression running along the distal side.

This is proposed as the antimere of U.W. 101-039. Their wear is similar and their adjoining IPFs match in shape and the placement of enamel chipping.

U.W. 101-1005A: LI_1 (Fig. 25C; Table 1) An enamel chip is missing from the lingual margin of the distal IPF near the incisal edge. A large distal IPF (1.7 mm LaL by 3.2 mm IC) intersects the incisal edge. The similarly sized mesial IPF (1.7 mm LaL by 3.1 mm IC) also runs up to the incisal edge. A thin strip of dentine is exposed along most of the incisal edge (stage 2). The crown flares MD as it reaches the incisal edge; though, its maximum MD length is reduced by incisal and interproximal wear. The labial surface is featureless and minimally convex. The lingual surface is flat with faint marginal ridges.

The root is abraded and broken just before the apex. In labial view, 11.4 mm of root is preserved. The root is MD compressed and deflects distally near its apex.

Incisors U.W. 101-1005A (LI_1), U.W. 101-1005B (RI_1), and U.W. 101-1005C (RI_2) were excavated in contact with one another and are assigned a single accession number. Their morphology and interproximal facets are consistent with their attribution

to a single individual. This is the antimere of U.W. 101-1005B to which its interproximal facet clearly articulates. It also articulates well with the U.W. 101-998 LI_2, which is also chipped along the adjoining IPF. This tooth is proposed to belong to the same individual as the U.W. 101-377/1014 mandibular specimens and their associated antimeres.

U.W. 101-1005B: RI_1 (Fig. 25D; Table 1) An enamel chip is missing from the lingual margin of the distal IPF near the incisal edge. A large distal IPF (2.6 mm LaL by 1.3 mm IC) intersects the incisal edge. The larger mesial IPF (1.7 mm LaL by 3.2 mm IC) also runs up to the incisal edge. A thin strip of dentine is exposed along the incisal edge (stage 2). The crown flares as it reaches the incisal edge; though, its maximum MD length is reduced by wear. The labial surface is featureless and minimally convex. The lingual surface is flat with faint marginal ridges.

The root is abraded and broken near the apex so that the root canal is exposed. In labial view, 10.3 mm of the root height is preserved. The root is MD compressed and deflects distally at its apex.

This is the antimere of U.W. 101-1005A to which its interproximal facet clearly articulates. Incisors U.W. 101-1005A (LI_1), U.W. 101-1005B (RI_1), and U.W. 101-1005C (RI_2) were excavated in contact with one another and are assigned a single accession number. Their morphology and interproximal facets are consistent with their attribution to a single individual. This tooth is proposed to belong to the same individual as the U.W. 101-377/1014 mandibular specimens and their associated antimeres.

U.W. 101-1132: LI_1 (Fig. 25E; Table 1) There is a small (0.9 mm LaL by 1.9 mm IC), slightly lingually offset, mesial IPF and no distal IPF. A thin strip of dentine is exposed in the central half of the incisal edge (stage 1). The incisal edge is straight and the mid-crown is minimally convex. The labial face is featureless. Lingually, there are trace marginal ridges that are primarily expressed near the incisal edge and quickly fade towards the cervix. The weak basal eminence is slightly offset mesially in incisal view. Linear hypoplasias are visible on the cervical quarter of the crown (for a discussion of hypoplasias on this specimen, see also Skinner, 2019).

The root is abraded on all surfaces. Further, it is broken at about two-thirds of its height (8.8 mm in height in labial view), exposing the root canal. In cross section, the root is MD compressed.

This tooth is the antimere of U.W. 101-1133. Both were excavated in anatomical contact and are identical in morphology and wear status. Further, the specimen articulates distally with U.W. 101-1131.

U.W. 101-1133: RI_1 (Fig. 25F; Table 1) There is an enamel chip along the incisal edge distally. A small mesial (1.1 mm by 1.9 mm) IPF is present, but one appears to be absent distally. A thin line of dentine is exposed in the center of the incisal surface edge (stage 1). The labial face is featureless. It is minimally convex mid-crown with a straight incisal edge. Lingually, the weak basal eminence is offset mesially. There are faint marginal ridges that are expressed primarily near the incisal edge. Linear hypoplasias are visible on the cervical quarter of the crown (for a discussion of hypoplasias on this specimen, see also Skinner, 2019).

The root is broken above its apex and abraded. The preserved length of the root is 10.0 mm along the labial aspect. In cross section, the root is compressed MD.

This is the antimere of U.W. 101-1132. The teeth were excavated in anatomical contact, they are identical in morphology, and their degree and pattern of wear matches. Further, the specimen articulates distally with U.W. 101-1075.

3.19. Permanent mandibular lateral incisors

Five isolated I_2s are known from the Dinaledi Chamber deposits. A developing I_2 was recovered from its exposed crypt in the U.W. 101-1400 mandible and the U.W. 101-1261 mandible preserves both I_2s in situ. Collectively, the I_2s represent at least five individuals. The incisal edge is straight, but the crown has moderate labial convexity at mid-crown. In labial view, the mesial corner sits slightly higher than the distal; the mesial shouler is more perpendicular than the rouded distal shoulder. Weak marginal ridges bound a featureless lingual fossa. A developmental notch is present in the center of the incisal edge in those specimens that are unworn or relatively unworn.

U.W. 101-335: RI_2 (Fig. 26A; Table 1) The distal IPF (approximately 1.3 mm LaL by 2.5 mm IC) is vertically oriented, while the mesial IPF (approximately 1.0 mm LaL by 1.5 mm IC) is much smaller and placed very near the incisal edge. Dentine is exposed as a tiny speck in the center of the incisal edge and wear facets flatten the mesial and distal marginal ridges on the lingual face (stage 2). The incisal edge is straight, but the tooth has moderate labial convexity at mid-crown. The crown and root are also moderately convex in mesial and distal views. In labial view, the incisal margin is rounded with the mesial

corner slightly higher and somewhat more perpendicular than the distal. Weak mesial and distal marginal ridges bound a shallow and featureless lingual fossa. The labial face is morphologically featureless, although there are several linear hypoplasias present in the cervical third (for a discussion of hypoplasias on this specimen, see also Skinner, 2019).

The root surface is abraded along all faces and broken at the apex, which exposes the root canal. Its preserved labial height is 11.8 mm. The root is compressed MD and broader LaL in cross section. There are faint grooves on the mesial and distal aspects running the length of the root. The distal groove is deeper than the mesial.

This specimen and U.W. 101-339 (RC_1) were recovered within centimeters of each other and their respective facets are potential matches.

U.W. 101-998: LI_2 (Fig. 26B; Table 1) Enamel chipping is present along the lingual margin of the mesial IPF. The mesial IPF (1.9 mm LaL by 3.0 mm IC) is teardrop shaped and located near the incisal edge. The distal IPF (2.0 mm LaL by 2.9 mm IC) is ovoid, concave, and located near the incisal edge. A thin strip of dentine is exposed in the center of the incisal edge (stage 2). Labially, the crown is minimally convex at midcrown. The labial face is featureless except for a minor distolabial depression. The marginal ridges are both low and rounded; as preserved, the DMR is stronger than the MMR. The lingual face is flat. Multiple linear hypoplasias are visible in the cervical third of the crown (for a discussion of hypoplasias on this specimen, see also Skinner, 2019).

The root is missing its apex and is broken into two pieces that easily refit and are rejoined as of June 2018 (not evident in Figure 26B or scans). The root is abraded along most of its surface. When repaired, the root is 14.9 mm in height along the labial margin.

The root is ovoid in cross section, being compressed MD. A wide, shallow depression runs along its distal aspect.

This is the antimere of the U.W. 101-1005C RI_2. In addition, the mesial IPF is a good match for the distal IPF of the U.W. 101-1005A LI_1, which also evinces minor enamel chipping along its incisolabial aspect. Finally, the contact with the mesial IPF of the U.W. 101-1076 LC_1 is reasonable. If these associations are correct, then this specimen belongs to a nearly complete set of mandibular teeth that includes the U.W. 101-377 mandible and other associated postcanine teeth.

U.W. 101-1005C: RI_2 (Fig. 26C; Table 1) The mesial IPF is close to the incisal edge (1.6 mm LaL by 2.5 mm IC). The distal IPF is smaller (1.8 mm LaL by 3.8 mm IC), lingually oriented and comprised of two distinct planes. The incisal edge is minimally worn with a hairline strip of dentine exposed (stage 2). Incisal wear spills over onto the lingual surface. The crown flares towards the incisal edge, which is moderately convex. In incisal view, the labial face is minimally convex. It possesses a shallow vertical distal depression but is otherwise featureless. The lingual face is flat with faint marginal ridges. The DMR is associated with a slight distal projection that can be observed in both lingual and labial views. Multiple linear hypoplasias are visible in the cervical third of the crown (for a discussion of hypoplasias on this specimen, see also Skinner, 2019).

The root is missing its apex and is abraded along most of its external surface. In labial view, the preserved height is 10.3 mm. The root is compressed MD, with a shallow depression running the length of the distal face.

Incisors U.W. 101-1005A (LI_1), U.W. 101-1005B (RI_1), and U.W. 101-1005C (RI_2) were excavated in contact with one another and are assigned a single accession number. Their morphology and interproximal facets are consistent with their attribution to a single individual. The complexly shaped distal IPF of U.W. 101-1005C fits well with that of the mesial IPF of the U.W. 101-1014 RC_1; thus, this specimen is proposed to link these associated anterior teeth with those in situ in the U.W. 101-377 mandible and their associated antimeres.

U.W. 101-1075: RI_2 (Fig. 27A; Table 1) Labially, damage is evident to the distal portion of the cervical line. The crown evinces light incisal wear (stage 1). No IPFs are visible mesially or distally. Like other lightly or unworn *H. naledi* I_2s (e.g., U.W.101-1131 and U.W. 101-1400) and I^2s (i.e., U.W. 101-1588), a distinct developmental notch is present in the center of the incisal edge. In labial and lingual views, the mesial profile is vertical and the distal profile flares out with a rounded distal corner. The crown exhibits minimal labial convexity, with a straight incisal edge and a gently curved mid-crown. The labial face is featureless. Lingually, there is trace shoveling. The MMR and DMR are low and rounded, becoming stronger towards the incisal margin. There are multiple linear hypoplasias in the cervical third of the crown (for a discussion of hypoplasias on this specimen, see also Skinner, 2019).

The root is abraded on all its external surfaces and is broken just before the apex. The preserved height of the root is 11.7 mm labially. The root is MD compressed with a shallow depression running the length of the distal facet.

Based on shared morphology, size, and wear status, this is the proposed antimere of U.W. 101-1131. If this association is correct, then U.W. 101-1075 is also associated with the U.W. 101-886 RC_1, which is the antimere of the U.W. 101-1126 LC_1 and was excavated in anatomical contact with U.W. 101-1131. The association of U.W. 101-1075 and U.W. 101-886 cannot be directly confirmed, however, because both specimens lack IPFs.

U.W. 101-1131: LI_2 (Fig. 27B; Table 1) The crown is lightly worn (stage 1) and no IPFs are present. The incisal edge is straight, and the mid-crown is minimally convex. The labial face is featureless. The lingual face presents trace marginal ridge development, primarily visible close to incisal edge and then fading quickly towards the cervix. The incisal edge is notched, similar to the lateral incisors in the maxilla (i.e., U.W. 101-1588) and mandible (i.e., U.W. 101-1075, and U.W. 101-1400). Faint linear hypoplasias are visible on the cervical third of the crown (for a discussion of hypoplasias on this specimen, see also Skinner, 2019).

The root is broken, and its surface is abraded. Its preserved is 10.8 mm along the labial aspect. In cross section, the root is compressed MD, with a shallow depression running the length of the distal aspect.

Based upon similarities in size, morphology, and wear status, this is proposed as the antimere of U.W. 101-1075. This specimen was excavated in anatomical position with the U.W. 101-1126 (LC_1), U.W. 101-1132 (LI_1), and U.W. 101-1133 (RI_1).

U.W. 101-1400: LI_2 germ (Fig. 27C) This is an incompletely formed crown recovered from the exposed crypt of the U.W. 101-1400 mandible. Few morphological details are evident, but faint marginal ridges are visible. As in unworn and lightly worn I_2s (i.e., U.W. 101-1075 and U.W. 101-1131), a notch is present along the incisal edge.

3.20. Permanent mandibular canines

Eight isolated mandibular canines have been recovered from the Dinaledi Chamber. Canines are also present in the U.W. 101-010, U.W. 101-377, and U.W. 101-1261 mandibles, and a developing C_1 is visible in its exposed crypt in the U.W. 101-1400 mandible. Collectively, these canines represent a minimum of nine individuals if U.W. 101-010 and U.W. 101-359 are antimeres. The *H. naledi* mandibular canines present a consistent suite of features. These include an asymmetrical crown in labial and lingual views, a mesially oriented apex, a high mesial shoulder, and a strongly sloping distal crest that ends in a low tubercle. The distal tubercle and adjacent lingual furrow are well defined. The crowns appear relatively tall compared to their small basal dimensions.

U.W. 101-245: RC_1 (Fig. 28A; Table 1) The crown is heavily damaged. Enamel from the labial face is almost entirely missing, leaving enamel distally and along the lingual face. Additionally, the cervical line is damaged across its preserved course. The crown is moderately worn. The apex is missing, leaving an elongated circular dentine patch and a wear facet that extends along the distal crest and onto the apex of the distal tubercle (stage 4). Despite the marked apical wear, there is no distal IPF. The original crown was asymmetrical with a mesially oriented apex, a high mesial shoulder, and a strongly

sloping distal occlusal edge. The distal edge ends in a low distal tubercle. The distal tubercle and adjacent lingual furrow are well defined, as is common in all other *H. naledi* mandibular canines. The most cervical extent of the mesial lingual fossa is also preserved adjacent to the MMR, but its superior extent is removed by the break that detached the enamel from the crown. A trace of the distal labial groove defining the labial extent of the distal tubercle is also present. The lingual basal aspect is flat and the median lingual ridge, as preserved, is indistinct, flat, and broad.

The root is broken near its apex, exposing the root canal. Additionally, abrasion is evident across the surface of the root. Measured from the inferred location of the labial cervix, the preserved root measures 14.1 mm in height. A subtle invagination runs along the mesial face.

U.W. 101-339: RC_1 (Fig. 28B; Table 1) There is a small and faint mesial IPF (1.2 mm LaL by 2.5 mm IC) near the apex of the mesial shoulder and along its lingual crest. No distal IPF is present. The crown apex is blunted by wear and the distal occlusal crest exhibits a shallow concave (J-shaped in labial view) facet that runs onto the apex of the distal tubercle. No dentine is exposed (stage 1). The crown is tall relative to its narrow base (Table 1). The occlusal edge is straight, but the mid-crown is moderately convex. The crown is minimally convex in mesial and distal views. In labial view, the crown is asymmetrical with an apex that is slightly offset distal to the MD midpoint. The mesial occlusal crest is short, convex, and situated more apically than the distal. The distal crest is longer and more vertically oriented and terminates at a distal tubercle. There are faint mesial and distal vertical grooves on the labial face. The distal labial groove is better

defined than the mesial, but it is rather indistinct compared to the deep distal groove on the lingual face. Adjacent to the distolingual groove is a shallow triangular-shaped fossa bounded mesially by a weak median lingual ridge. There is a shallow mesiolingual fossa between the median lingual ridge and a moderately-developed MMR. The median lingual ridge bifurcates as it travels apically, with one branch extending towards the apex and the other towards the mesial occlusal crest. A pair of linear hypoplasias is observed on the cervical third of the labial face and fainter hypoplasias are also evident lingually.

The root is abraded externally and broken at approximately half of its height, exposing the sediment packed root canal. In cross section, the root is broader LaL than MD. There is a faint invagination running along the root mesially. The preserved height of the root is 7.1 mm labially and 9.4 mm lingually.

This tooth is the potential antimere of U.W. 101-985. They are similar in size and morphology, and both have a pair of prominent linear hypoplasias in their cervical regions. They do differ in the degree of occlusal wear. A wear facet runs along the distal crest of U.W. 101-339 but is absent on U.W. 101-985. There is also a small mesial IPF on U.W. 101-339 that is not apparent on U.W. 101-985. This could indicate a more advanced eruption status for U.W. 101-339 than U.W. 101-985. This specimen and U.W. 101-335 (RI_2) were recovered within centimeters of each other and their respective facets are potential matches.

U.W. 101-359: LC_1 (Fig. 28C; Table 1) Occlusal wear is extensive, having removed all but a thin sliver of enamel (approximately 4.3 mm in length and 1.4 mm in height) mesiolabially (stage 7). The dentinal surface was functional given its polished

appearance. The pulp chamber is exposed occlusally, and the margins are polished and rounded. The root is covered in cementum, which is extensively cracked. The maximum dimensions as preserved at the occlusal surface are 6.8 mm by 7.2 mm and the maximum length of the remaining root, which is damaged at the root apex, and crown is 16.6 mm.

Specimens U.W. 101-357 to U.W. 101-359 were recovered from fragments and sediments associated with the U.W.101-361 mandible and are consistent with belonging to a single individual. This specimen evinces comparablewear to that of the U.W. 101-010 RC_1; that said, the absence of detailed crown morphology limits the inference that they represent antimeres.

U.W. 101-886: RC_1 (Fig. 28D; Table 1) The crown is unworn (stage 1). The labial crown face is minimally convex at midcrown. In labial and lingual views, it is tall relative to its narrow base (Table 1) and asymmetrical, with the apex situated distal to the MD midpoint. The convex mesial edge is shorter and higher than the longer, straighter and more vertically oriented distal edge. The distal edge terminates in a tubercle, which is associated with a short, faint distal groove on the labial face and a deeper fossa on the lingual face. A shallow and faint mesial labial groove runs nearly the entire crown height. The median lingual ridge is weakly developed. It is wide and flat near the base of the lingual fossa and becomes thinner, but more distinct, near the apex. The DMR is bordered by a groove and weak fossa. Linear hypoplasias are present in the cervical third of the crown (for a discussion of hypoplasias on this specimen, see also Skinner, 2019).

The root is abraded and broken with only 4.8 mm remaining labially and 3.0 mm lingually. A shallow broad furrow is present on the mesial side of the root, and, in cross section, it is ovoid and slightly broader LaL than MD.

Given the absence of occlusal or interproximal wear, but the presence of some root development, this tooth was likely unerupted at death and the root incompletely formed. Based upon shared morphology, its unworn state, and similarities in placement and presence of hypoplastic defects, U.W. 101-1126 and U.W. 101-886 are probable antimeres. The developmental defects are, however, more prominent on the lingual surface of U.W. 101-886 than on U.W. 101-1126. As U.W. 101-1126 was excavated in near anatomical contact with the U.W. 101-1131, U.W. 101-1132, and U.W. 101-1133 mandibular incisors, then, if their status as antimeres is correct, U.W. 101-886, along with U.W. 101-1075, would form a complete set of anterior mandibular teeth.

U.W. 101-985: LC_1 (Fig. 29A; Table 1) Apart from minor damage to the cervical region distolabially, the crown is complete. Neither mesial nor distal IPFs are present. A very small facet blunted the apex (stage 1). In labial and lingual views, the crown is tall relative to its narrow base (Table 1), and is asymmetrical, with the apex situated distal to the MD midpoint. The mesial edge is short and convex, while the distal edge is longer, straighter, and more vertically oriented. The mesial shoulder is high, while the distal shoulder, which comprises a small tubercle, is much lower. This tubercle is associated with a subtle distal labial groove and a deeper lingual groove. A faint mesiolabial groove runs the length of the crown. The labial face is moderately convex at mid-crown; though, the occlusal edge is straight. The crown and root are moderately convex. A weak median

lingual ridge extends to the crown apex and is bordered on either side by shallow mesial and distal fossae. A faint accessory ridge runs parallel to the MMR. Multiple linear hypoplasias are present on the cervical third of the labial face (for a discussion of hypoplasias on this specimen, see also Skinner, 2019).

The root is broken in a radial manner so that more of the root is preserved lingually and mesially than labially and distally. Lingually, the maximum remaining height is 10.0 mm, while labially the preserved root height is 2.5 mm. The root is ovoid in cross section, being MD compressed.

This is a potential antimere of U.W. 101-339. They are similar in size and morphology, and both have a pair of prominent linear hypoplasias in their cervical regions. They do differ in the degree of occlusal wear. A wear facet runs along the distal crest of U.W. 101-339, while one is absent on U.W. 101-985. Further, there is a small mesial IPF on U.W. 101-339, while one is not apparent on U.W. 101-985. This could indicate a more advanced eruption status for U.W. 101-339 than U.W. 101-985 regardless of their status as antimeres.

U.W. 101-1076: LC_1 (Fig. 29B; Table 1) A large mesial IPF (2.1 mm LaL by 2.5 mm OC) sits high on the mesial shoulder and a small distal IPF (1.8 mm LaL by 1.6 mm OC) is placed at the apex of the tubercle. There is a long concave wear facet along the distal crest and a smaller facet dulls the mesial crest as well (stage 1). The crown is tall relative to its narrow base. In labial and lingual views, the apex sits slightly distal to the MD midpoint. The mesial crest is short and convex, and the mesial shoulder sits high on the crown, while the distal crest is more vertically oriented and terminates at a distinct

tubercle that sits low on the crown. A wide but shallow distal labial groove and shallow mesial groove are associated with the distal tubercle. The faint median lingual ridge that fades at mid-crown and reappears just below the crown apex. There is a shallow mesiolingual fossa between the median lingual ridge and the MMR and a well-developed fossa between the distal tubercle and the median lingual ridge that widens and becomes shallower towards the distal margin. A linear hypoplasia crosses the lingual crown near the cervix, while labially there are several linear and pit hypoplastic defects visible in the cervical third of the crown (for a discussion of hypoplasias on this specimen, see also Skinner, 2019).

The root is broken and abraded across most of its preserved surface. It measures 7.8 mm labially. The root is ovoid in cross section and MD compressed.

This is the probable antimere of the canine in the U.W. 101-377+1014 mandible. The crowns are similar in morphology and wear status. Further, this specimen articulates well with the U.W. 101-998 LI_2 and with the U.W. 101-889 LP_3. As such, this specimen is proposed to be associated with a nearly complete set of mandibular teeth that also features those in situ in the U.W. 101-377/1014 mandible.

U.W. 101-1126: LC_1 (Fig. 29C; Table 1) The crown is unworn (stage 1); further, IPFs are not detectable mesially or distally. In labial and lingual views, the crown is tall relative to its narrow base (Table 1) and asymmetrical, with the apex situated distal to the MD midpoint. The convex mesial crest is shorter and higher than the longer, straighter and more vertically oriented distal crest. The distal crest terminates in a tubercle that is associated with a short, faint distal groove on the labial face. A shallow and faint mesial

labial groove runs nearly the entire crown height. The median lingual ridge is faint, except near the apex, where it is low and dull. The adjacent mesial and distal fossae are each broad and shallow. The distal tubercle is bordered lingually by a deep groove and weak fossa. Multiple hypoplastic defects are visible on the labial and lingual faces. Pit-like defects are also evident in the cervical third of the labial face as well (for a discussion of hypoplasias on this specimen, see also Skinner, 2019).

The root surface is abraded and broken so that only 4.6 mm remains below the cervix labially. The preserved root is ovoid in cross section, being more MD compressed.

This is the proposed antimere of U.W. 101-886. Both are similar in morphology and wear status. Their pattern of hypoplastic defects is also similar; although, the lingual hypoplasias are more prominent on the left canine. This specimen was excavated in anatomical contact with U.W. 101-1131 (LI_2), U.W. 101-1132 (LI_1), and U.W. 101-1133 (RI_1). As an antimere of U.W. 101-1131, this set of anterior teeth would also include U.W. 101-1075 (RI_2).

U.W. 101-1610: RC_1 germ (Fig. 29D; Table 1) The crown is developing. The mesial shoulder is visible and high on the crown. The distal margin is nearly vertical, and no distal shoulder is apparent, giving the crown an asymmetric shape. The mesial crest is convex, while the distal crest is nearly vertical. There is a shallow mesiolabial and no distolabial groove. Lingually, the median ridge is wide and low. There is a weak mesial fossa between the median ridge and MMR that becomes a groove adjacent to the ridge. The distal fossa is barely perceptible.

This specimen is proposed as the antimere of the U.W. 101-1400 LC_1 germ that is still in its crypt and is associated with the U.W. 101-544B and U.W. 101-1548 maxillary canine germs. Each is at approximately the same developmental status.

3.21. Permanent mandibular third premolars

Seven isolated P_3s have been recovered from the Dinaledi Chamber deposits. Other P_3s are found in situ in the U.W. 101-001, U.W. 101-010, U.W. 101-377, and U.W. 101-1261 mandibles. Collectively, these teeth represent at least eight individuals. The *H. naledi* P_3s are 'molarized'; they are fully bicuspid, with the Med and Prd separated by a longitudinal groove, and have a broad talonid. The MMR is continuous between the mesial crests of the Med and Prd. The buccal grooves are shallow and fade at midcrown. Two roots are present, with the distal root BL-broader than the smaller and more circular mesiobuccal root. The roots share a common canal at the cervix but separate apically.

U.W. 101-144: LP_3 (Fig. 30A; Table 1) Distally, a circular IPF (2.8 mm LaL by 3.0 mm OC) is present and slightly offset buccally. No mesial IPF is evident. The crown is minimally worn: there are small wear facets, but no dentine visible on the mesial Prd crest extending to the apex of the Prd, along the Prd distal accessory crest, and along the talonid (stage 1). The crown possesses two well developed cusps and a broad talonid. The Med is high with a free apex. It stands directly across from the Prd and is separated from it by a well-defined Mlg. The Med is smaller in area and slightly lower in height than the Prd but occupies a significant portion of the mesial crown area. The essential ridges of the Prd and Med are low and rounded. The Prd also has a narrow mesial accessory ridge

that extends towards the Mlg and defines the distal border of the Fa. A thin MMR forms the mesial border of the Fa and takes the form of a continuous rim connecting the Med and Prd; it is low relative to the cusp apices. The Fa is a narrow BL-oriented groove continuous with the Mlg. The buccal branch of the Fa is longer than the lingual branch. The Mlg bifurcates distally into a transverse groove that separates the Prd and Med from a well-developed talonid. This fissure spills onto the buccal face to form a shallow distobuccal groove, which fades out before mid-crown, and onto the lingual aspect to form a weak furrow. A weak mesiobuccal groove is also present; like the distobuccal groove, it fades out before mid-crown. Distally, the polished talonid slopes up from the transverse groove to the distal border of the crown where the worn DMR is not detectable as a topographically distinct feature.

Two roots are present, and a small fragment of alveolar bone remains wedged between them. Both roots are abraded on their exposed surfaces and the canals are packed with sediment. The distal root is larger and BL-broader than the mesiobuccal root. Their configuration conforms to the 2R: D+MB pattern of Wood et al. (1988). The roots share a common canal at the cervix but become individualized just above where they are broken. Buccally, the maximum preserved height of the mesiobuccal root is 7.7 mm and that of the distal root is 7.9 mm.

Based upon similarities in morphology, the state of occlusal wear (i.e., presence of a small wear facet on the buccal aspect of the mesial Prd crest), and the presence of a distal IPF, but lack of a mesial IPF, this specimen is proposed as the antimere of U.W. 101-506. They do differ slightly in the morphology of the Fa, with U.W. 101-506 lacking the accessory ridge defining the Fa distally; they are otherwise similar.

U.W. 101-298: RP_3 (Fig. 30B; Table 1) IPFs are absent. The crown is nearly unworn, with only a small wear facet visible on the buccal aspect of the mesial Prd crest near the cusp apex (stage 1). Two principal cusps are evident and separated by a well-defined Mlg. The Med is slightly smaller than the Prd in area but nearly equal to it in height and their cusp apices are aligned transversely. The MMR is not well defined; rather than being a continuous horizontally oriented structure, the buccal and lingual segments are short and thin and separated by a narrow groove. The two segments of the MMR dip towards the cervix to form a v-shaped contour when viewed mesially. The Fa is a pit contiguous with the Mlg and defined distally by subtle accessory ridges extending from the mesial crests of the Prd and Med. The talonid slopes up from the transverse groove, which extends completely between the distal Prd and Med crests without evident bifurcation. A small distolingual cusplet and larger distobuccal cusplet are present, with the distobuccal cusplet the more topographically prominent. A distinct DMR hardly exists as a crest discrete from the planar surface of the talonid. Instead, in distal view, the occlusal extent of the distal talonid slopes from the distobuccal cusplet to reach its most cervical extent lingually. The mesiobuccal groove is absent and the distobuccal groove is faint; the distobuccal groove extends about a third of the way down the buccal face before it fades away. No lingual grooves are present. The root(s), which were likely developing at the time of death, are broken away at the cervix and sediment fills in the exposed pulp cavity.

U.W. 101-298 is morphologically similar to U.W. 101-1565, which may suggest that they are antimeres. However, U.W. 101-1565 has a distal IPF, which is lacking in

U.W. 101-298, and more advanced occlusal wear. Such wear asymmetry is not unexpected for an individual, but it is possible that U.W. 101-298 represents a slightly younger individual.

U.W. 101-358: LP_3 (Fig. 30C; Table 1) Distally, a portion of the IPF (approximately 4.0 mm LaL) is preserved and offset to the lingual side. Mesially, a small portion of an IPF is also preserved on the lingual side. The occlusal enamel is worn away, leaving only a thin rim. The rim is incomplete mesially and mesiolingually where two large antemortem enamel chips have been removed (stage 6+). The exposed dentine is polished from wear. The wear surface dips cervically from lingual to buccal and the outline of the pulp chamber is visible.

A larger plate-like root sits distally and a smaller, more elliptical, root is situated mesiobuccally. The roots are covered in a thick layer of cementum and abrasions are evident on many surfaces of the roots. An examination of the µCT scans shows that the thick layer of cementum partially fills in the space between the mesial and distal roots, which are more clearly individuated when only the dentine is considered. The apex of the distal root is broken away and at least half of the height of the mesiobuccal root is missing. In buccal view, the maximum preserved height of the mesial root is 5.5 mm, and the distal root is 9.7 mm.

Given the advanced occlusal wear, the tooth's assignment as an LP_3 is based on the morphology of its roots. All well-preserved Dinaledi P_4s in the assemblage with two roots have roots that are similar in cross sectional area. Only unequivocal P_3s express two

roots, one plate-like and distal and one rounded and mesiobuccal, which is the pattern observed in this specimen.

Along with U.W. 101-357 (LP_4) and U.W. 101-359 (LC_1), this specimen was recovered from fragments and sediments associated with the U.W.101-361 mandible and its in situ left molars. These spatially associated specimens express advanced occlusal wear, are from the left side, and are consistent with belonging to a single biological individual.

U.W. 101-506: RP_3 (Fig. 30D; Table 1) The distal IPF (2.9 mm by 2.3 mm) is offset buccally with its major axis obliquely oriented. No mesial IPF is evident. The crown is minimally worn, with only small facets present on the mesial and distal Prd crests (stage 1). There are two principal cusps separated by a well-developed Mlg. The Med is smaller in area and slightly lower than the Prd. The cusp apices are nearly aligned transversely. The MMR sits low on the occlusal surface and is continuous between the mesial crests of the Med and Prd. These crests and the MMR enclose a small basin-like Fa that extends from the Mlg. Faint accessory ridges emanate from the mesial Med crest and extend into the Fa. A deep transverse groove separates the trigonid and talonid portions of the crown. This fissure bifurcates before its lingual termination. The DMR is not an entity distinct from the sloping surface of the talonid. The buccal face possesses a weak mesiobuccal groove and a deeper distobuccal groove, which extends about a third of the way down the buccal face before becoming imperceptible. The distobuccal groove crosses the occlusal rim as a weak indentation that defines a small distobuccal cuspule. There are no lingual grooves.

Portions of two broken roots, with exposed canals, are preserved. A plate-like distal root sits below the talonid, while a smaller elliptical root is placed beneath the mesiobuccal corner, thus conforming to the 2R: D+MB pattern of Wood et al. (1988). In buccal view, the preserved height of the mesiobuccal root is 8.2 mm, while the maximum preserved height of the distal root is 6.0 mm. The mesiobuccal root is abraded along its mesial and lingual faces and the distal root has patches of abrasion along its distal face.

This is a possible antimere of U.W. 101-144. They differ slightly in the morphology of the Fa, with U.W. 101-144 having a mesial accessory Prd ridge extending into the Fa but are otherwise similar in crown and root morphology. They are similar in wear status, as both have distal IPFs and no mesial IPF, and both have only small wear facets on the buccal aspect of the MPC. However, U.W. 101-144 also exhibits polishing on the talonid.

U.W. 101-800: RP_3 (Fig. 31A; Table 1) Minor chipping is present along the occlusal surface of the distal margin. There is a large ovoid distal IPF (4.4 mm BL by 2.2 mm OC); however, despite the advanced wear, no mesial IPF is evident. Details of the occlusal morphology have been removed by wear and moderate dentine patches are exposed over the cusp apices (stage 4–5). The Prd dentine patch is larger than that of the Med. A trace of the Fa is present as a small pit distal to the worn MMR, which is set low on the occlusal surface. Additionally, a short lingual portion of the transverse groove remains. Only trace expression of the mesiobuccal and distobuccal grooves are present, while the lingual face is featureless.

Two roots are completely preserved, with a portion of alveolar bone remaining between them, and are covered in a cracked layer of cementum. There is a wide distal root and a smaller mesiobuccal root, which conforms to the 2R: D+MB configuration (Wood et al., 1988). In cross section, both roots are broader BL and compressed MD. Wide and shallow grooves run along the mesial face of the mesiobuccal root and along the distal face of the distal root. The roots are more widely spaced lingually than buccally. In buccal view, the mesiobuccal root is 14.5 mm tall and the distal root is 14.9 mm tall.

U.W. 101-889: LP_3 (Fig. 31B; Table 1) Enamel chips are evident in the occlusal surface just above the distal IPF. Mesially, a small IPF (approximately 1.7 mm BL by 1.6 mm OC) is present in the center of the crown's height. The distal IPF is larger (approximately 3.5 mm BL by 2.2 mm OC) and centered BL. The crown is minimally worn, with wear facets evident along the mesial and distal Prd crests and along the buccal portion of the talonid (stage 1). The crown is fully bicuspid with the Prd and Med separated by a well-defined Mlg and the Med only slightly smaller in area than the Prd. The Med is less worn than the Prd and its preserved height nearly equals that of the Prd. The MMR is continuous, and the Fa parallels it to run from mesiobuccal to distolingual. The branch of the Fa lingual to the Mlg is broader than the portion buccal to the Mlg. The deepest point of the Fa is also offset lingual to the Mlg. A minor accessory ridge originating from the mesial Prd crest helps to define the distal extent of the Fa. The essential ridges are nearly nonexistent. The talonid is flat and, though the area is worn, the DMR is not elevated as a crest distinct from the planar surface of the talonid. A local topographic high

distobuccally suggests the presence of a cusplet. The mesiobuccal and distobuccal grooves are faint and both become imperceptible at mid-crown. The lingual face lacks grooves.

The preserved roots are abraded on their external surfaces and broken at about half their maximum height. In lingual view, the mesial root is 6.8 mm in height and the distal root is 7.7 mm in height. Though broken, the configuration of the preserved roots suggests a smaller mesiobuccal root and a larger, broader distal root that are separated for at least part of their lengths, especially lingually. At the height where broken, the mesial and distal roots are joined into a single canal but likely would have separated nearer their apices. In buccal view, a cleft is apparent running longitudinally; here, the portion mesial to the cleft is broader than the section distal to it. In lingual view, the roots are more clearly separated. The preserved distal root is clearly compressed MD and broader BL. And, in mesial view, a buccal cant to the mesiobuccal root is evident.

Based upon morphological similarities of the crown and root, this is the proposed antimere of the P_3 in the U.W. 101-1014/377 mandible. If they are antimeres, wear asymmetry is evident. A wear facet along the U.W. 101-889 mesial Prd crest is absent on U.W. 101-377. Further, this specimen articulates reasonably well with the U.W. 101-1076 mandibular canine, which is consistent with the hypothesis that these isolated teeth belong to the same biological individual as U.W. 101-377/1014.

U.W. 101-1565: LP_3 (Fig. 31C; Table 1) There is a moderately-size distal IPF (3.1 mm BL by 3.2 mm OC) and no mesial IPF. Wear facets are visible on the Prd near the apex and along the Prd crests, especially along the buccal aspect of the mesial Prd crest (stage

1). The crown is fully bicuspid and a deep Mlg separates the smaller and slightly shorter Med from the broader and taller Prd. The Med sits only slightly mesial to the Prd. The MMR is low and narrow, set low on the occlusal surface, continuous from the mesial crests of the Med and Prd, and encloses a small Fa that appears as a narrow BL-oriented groove paralleling the MMR and bounded distally by mesial accessory ridges extending from the cusps. The essential ridges are not well defined. The talonid is planar and slopes up to the DMR, which is not detectable as a distinct feature, except for a short segment distolingually near the distal Med crest. The talonid is delineated from the trigonid by a deep transverse groove, which extends buccally to define a small distobuccal cuspule. This cuspule is associated with a short, shallow distobuccal groove that fades before mid-crown. The mesiobuccal groove is faint and only visible close to the occlusal rim. The distal buccal groove is shallow and extends about halfway down the buccal face before it becomes imperceptible. The lingual face is featureless.

The root(s) is broken near the cervix and sediment fills in the exposed canal. The maximum preserved root height, 3.6 mm, is preserved distolingually.

This specimen is morphologically similar to U.W. 101-298 and is proposed as its antimere. However, U.W. 101-298 lacks the distal IPF that is evident on U.W. 101-1565. Though such asymmetry in eruption is not unexpected, alternatively, U.W. 101-1565 may represent a slightly more ontogenetically advanced individual.

3.22. Permanent mandibular fourth premolars

Three isolated P_4s and those found in situ in the U.W. 101-001, U.W. 101-377, and U.W. 101-1261 mandibles collectively represent at least four indviduals in the

Dinaledi Chamber deposits. The P_4s are all similar and subtly differ from the P_3s in crown and root morphology. Like the P_3s, the P_4 crowns are bicuspid, with the two cusps separated by a longitudinal groove, and the talonid is relatively broad. In constrast to the P_3s, the P_4s tend to be MD shorter and more rounded in occlusal profile. The morphology of the roots is not well represented in the isolated specimens but, where preserved, they tend to depart from the P_3s. The U.W. 101-887 P_4 is single rooted, while U.W. 101-383 is multirooted, with a mesial root that is more plate-like than observed in the P_3s.

U.W. 101-184: LP_4 (Fig. 32A; Table 1) The crown is unworn and no IPFs are detectable (stage 1). The crown is noticeably BL broadest across the cusp apices and its rounded profile tapers distally. The Prd and Med are separated by a well-defined Mlg. The Med is smaller in area than, but equal in height to, the Prd. The cusp apices are nearly aligned transversely, with the Med set slightly mesial to the Prd. The MMR is limited to a small area just mesial to a pit-like Fa; the buccal and lingual MMR segments are separated by a narrow groove. The Prd possesses three occlusal ridges that are very similar in expression, with the essential ridge the narrowest and sharpest of the three. The distal accessory ridge is thicker, and rounder and it terminates at the Mlg. The essential ridge of the Med is not well delineated from the rest of the cusp. The Med has a thin distal accessory crest that originates mid-cusp and terminates at the Mlg. The Mlg is deep and runs from the mesial border to the transverse groove that separates the Prd and Med from the talonid. The transverse groove extends the width of the crown spilling over to the buccal and lingual faces. Both buccally and lingually, this groove bifurcates to form small distobuccal and distolingual cusplets. The distobuccal cusplet is larger and better

defined by deeper grooves than is the distolingual cusplet and it is separated from the mass of the Prd by the extension of the transverse groove. The surface of the talonid slopes up distally from the transverse groove but the DMR is indistinct. There is no mesiobuccal groove and the distobuccal groove is shallow and becomes imperceptible at mid-crown. There is no mesiolingual groove but a small and shallow distolingual groove is evident adjacent to the distolingual cusplet.

Given the absence of occlusal and interproximal wear, the crown was likely erupting at the time of death and the roots were incompletely developed. As preserved, the root(s) are broken just inferior to the cervix so that a maximum of 4.3 mm of root extends below the crown mesially and 3.2 mm extends below the cervix buccally. Sediment fills the exposed root canal. A single root canal is exposed, but clefts are present along the buccal and lingual faces of the root mass.

This specimen is a reasonable antimere of U.W. 101-383. They are morphologically similar, and both lack occlusal and interproximal wear. This specimen does bear some similarities to P_3s in the assemblage but differs in the relative height of the Med, the placement of the Med mesial to the Prd, and in the presence of a discernible distobuccal cusp, which is absent in the unequivocal P_3s. It also differs from P_3s in the absence of a mesiobuccal groove, and in the crown outline, which is rounded and tapers distally.

U.W. 101-383: RP_4 (Fig. 32B; Table 1) The crown is unworn, but the Prd apex is damaged, reducing its height (stage 1). The bulk of the Med, and its apex, are situated slightly mesial to the Prd. The Prd is larger in area, but the Med is slightly higher as

preserved. The Fa is a pit extending to a short BL-oriented groove situated between the MMR and the Prd mesial accessory ridge. Its deepest point is in the crown center at the intersection with Mlg. The MMR is low and rounded, with its buccal and lingual segments meeting at an angle at the center of the crown. In mesial view, the MMR is lower than the mesial accessory ridges. The Med lacks a distinct essential ridge, while the essential ridge of the Prd is equal in width to, but slightly lower in relief than, the mesial and distal accessory ridges. The Med also has a distal accessory ridge, but it is shorter and thinner than that of the Prd. The talonid is separated from the trigonid by a deep transverse groove that is divided into lingual, distal, and buccal components. The buccal component comprises a small distobuccal cusplet bounded mesially and distally by occlusal grooves that extend over onto the buccal face. The mesial groove becomes the distobuccal groove, which fades about half the distance to the cervix. The distal groove terminates shortly after crossing the occlusal rim. The distal portion of the talonid is not well defined, but it does possess a ridge and associated furrows that terminate at the transverse groove. The lingual portion of the talonid takes the form of a small, but palpable, distolingual cusplet that is not defined by occlusal grooves. There is no distinct DMR. The lingual face is featureless. In addition to the distobuccal groove, a shallower mesiobuccal groove is also visible on the buccal face but it does not cross the occlusal rim.

From photos taken shortly after excavation when still covered in the sediment, the roots were more complete and it appears that this specimen is multi-rooted, with plate-like mesial and distal roots. As it exists at the time of description, the root is almost entirely broken away at the cervix, with the largest remaining portions present mesially

and buccally. From the mesial cervix, the maximum preserved root height is approximately 5.0 mm and from the buccal cervix the maximum height is 4.2 mm. An associated, but detached, 5.4 mm root fragment fits cleanly onto the distal side. Additional undescribed root fragments are also associated with this specimen.

This specimen is a reasonable antimere of U.W. 101-184. They are similar in crown morphology and in their absence of occlusal and interproximal wear.

U.W. 101-887: LP_4 (Fig. 32C; Table 1) IPFs are centered mesially (3.5 mm BL by 2.3 mm OC) and offset lingually (3.8 mm BL by 2.1 mm OC) on the distal face. Occlusal wear is minimal, with a small wear facet visible along the buccal aspect of the mesial Prd crest (stage 1). The Med is smaller in area but nearly equal in height to the Prd. The apex of the Med is placed slightly mesial to that of the Prd and a well-defined Mlg separates the cusps. The MMR is low, but continuous, between the mesial crests of the Med and Prd and encloses a small Fa. The Fa appears as a groove situated mostly mesiobuccally, with a fainter extension lingually, and its deepest point is in the center of the crown's BL axis. A rounded accessory ridge running from the mesial Prd crest is matched by a swelling on the mesial aspect of the Med and these ridges bound the Fa distally. The Med and Prd have weakly expressed essential ridges. The talonid is broad, with shallow grooves radiating up the DMR, which is only slightly topographically distinct from the sloping surface of the talonid. A faint distobuccal cusplet pokes up from the DMR. The mesiobuccal groove is shallow and becomes imperceptible approximately one third of the way down the crown face. The distobuccal groove is also shallow, though deeper than the

mesial, and becomes indistinct about a third of the way down the crown face. The lingual face is featureless.

The root is abraded across its external surface and broken so that approximately 8.4 mm of its height is preserved buccally. Though broken, the root was apparently singular and is MD longer along the lingual margin than along its buccal margin, which gives the root a rounded triangular shape in cross section.

The mesial facet of U.W. 101-887 is reasonably congruent with the distal IPF of U.W. 101-889. Further, the RP_4 of U.W. 101-377 is proposed as the antimere of this specimen. The teeth are nearly identical in occlusal morphology, their state of occlusal wear, and in the morphology of their roots. The hypothesis that U.W. 101-887 and U.W. 101-889 belong to the same individual is also reasonable, as both are proposed to have antimeres in the U.W. 101-377 mandible.

3.23. Permanent mandibular first molars

Eight isolated M_1s are known from the Dinaledi Chamber. Additionallly, a developing M_1 crown was recovered from its exposed crypt in the U.W. 101-1400 mandible and the U.W. 101-001, U.W. 101-377, and U.W. 101-1261 mandibles retain M_1s. Collectively, these teeth represent a minimum of eight individuals. The M_1s present a consistent morphology. The five principal cusps are present, the Fa is not bounded distally by a midtrigonid crest, supernumerary cusps are absent, the mesial buccal groove is a cleft at the occlusal margin, and the distal buccal groove is shallow. The protostylid is either absent or a faint crest restricted to the mesiolingual corner of the crown. The two roots are plate-like.

U.W. 101-285: RM_1 (Fig. 33A; Table 1) Mesially, a large bean shaped IPF (3.0 mm OC by approximately 5.0 mm BL) is present. Distally, no IPF is detectable. Wear facets are visible on all five cusps and most occlusal ridging has been removed through wear; though, dentine is only exposed as a small pinpoint at the tip of the Prd (stage 2). The crown is a rounded rectangle with the talonid and trigonid nearly equal in breadth. The large mesial IPF has made the mesial margin concave, while the lingual profile is nearly straight, and the buccal profile is bilobed as the result of a deep mesiobuccal groove. The large Hld forms a rounded distobuccal contour. Only the five primary cusps are present, and their relative sizes are Hyd > Prd > Med > Hld ≥ End. The crown has a Y-5 fissure pattern, with the Med and Hyd in contact. The central groove is contiguous with the Fa, which is manifest only as a short groove limited to the Med. The apparent size of the MMR is reduced by the encroachment of the large mesial IPF. The distal aspects of the Hyd and Hld form a continuous crest that borders a fovea-like cleft on the distobuccal aspect of the crown. The DMR is short and worn on its buccal extent. A faint protostylid is restricted to the mesiobuccal corner where it is angled obliquely and distally and then turns towards the cervix disappearing at approximately mid-crown well before intersecting the mesiobuccal groove. The mesiobuccal groove is deep and narrow near the occlusal surface and at mid-crown becomes wider and shallower while continuing to the cervix. A shallow distobuccal groove terminates nearer the occlusal surface. The distolingual groove is only a faint depression occlusally, while the mesiolingual groove, which is placed slightly distal to the mesiobuccal groove, is a broad shallow depression near the occlusal margin.

The roots are broken so that a maximum of 2.0 mm remains on the mesiobuccal side. Sediment stains the broken surface and fills in the exposed pulp chamber.

This specimen is proposed as the antimere of U.W. 101-582 to which it is comparable in size, morphology, and its stage of occlusal and interproximal wear. The two crowns due differ slightly in the configuration of the distobuccal groove, which terminates at a pit in U.W. 101-582 but continues as a shallow groove in U.W. 101-285.

U.W. 101-297: RM_1 (Fig. 33B; Table 1) Enamel chipping is evident along the DMR above the distal IPF and on the buccal side of the Hyd. IPFs are present mesially (5.0 mm BL by 2.8 mm OC) and distally (5.2 mm BL by 3.2 mm OC). Moderate sized patches of dentine are exposed over each of the five principal cusps (stage 4). The talonid is slightly wider than the trigonid and the crown outline is roughly rectangular. Significant interproximal wear resulted in concave mesial and straight distal profiles. The crown has a Y-5 fissure pattern, with a substantial portion of the Med and Hyd in contact and a well-developed Hld; there is no evidence from the preserved topography or the pattern of grooves to suggest the presence of a C6 and a C7 is absent. Much of the occlusal topography is removed by wear, but a faint remnant of the Fa remains as pit mesiobuccal to the Med and just distal to the worn MMR. A weakly expressed protostylid presents as a shallow depression and indistinct crest limited to the mesiobuccal aspect of the Prd. The crest likely had its origin at the MMR, from which it is angled distocervically. The mesiobuccal groove is deep and cleft-like near the occlusal margin; it becomes wider and shallower as it extends to the cervix. The distobuccal groove is shallower and disappears approximately one third of the way down the crown face. The lingual grove is situated

slightly distal to the mesiobuccal groove; it is shallow and becomes imperceptible at mid-crown.

The mesial root is nearly completely preserved except for the apex of the buccal radical. The distal root is broken away at the cervix so that less than 1.0 mm of its height remains. The exposed break is stained by matrix. The mesial root measures 14.3 mm in height buccally and 15.8 mm lingually. Its maximum BL breadth, approximately at mid-root, is 11.1 mm. In mesial view, the mesial root is vertically oriented, while in buccal and lingual view it has a subtle distal tilt, especially apically. The circular buccal and lingual canals of the mesial root are joined by a thin isthmus for about two-thirds of their length until the isthmus closes and the root canals become individuated, giving the root a dumbbell shape in cross section. Externally, broad gutters extend the length of the mesial and distal faces.

This specimen is similar morphologically and in its state of wear to its proposed antimere, U.W. 101-905.

U.W. 101-582: LM_1 (Fig. 33C; Table 1) A large mesial IPF (5.7 mm BL by 3.5 mm OC) extends to the occlusal margin. There is no distal IPF. Wear facets are evident on all five cusps and has removed most of the detail of occlusal ridging (stage 2) and the mesial face is concave as a result of interproximal wear. In occlusal view, the crown is roughly rectangular in outline, with the centrally placed Hld forming the rounded distal contour. The talonid and trigonid are nearly equally broad BL. The crown has a Y-5 fissure pattern, with a substantial portion of the Med and Hyd in contact and a well-developed Hld. The relative cusp sizes are Hyd > Prd > Med > Hld ≥ End. The deep central groove

is contiguous with the Fa as it curves around mesial to the Med. There is no evidence of a buccal branch of the Fa. The mesial IPF has mostly removed the MMR. The partially preserved DMR is low and rounded. The protostylid takes the form of a faint but palpable obliquely oriented ridge that is restricted to the mesiolingual corner of the Prd. It ends at approximately mid-crown and is independent of the mesiobuccal groove. The mesiobuccal groove is a deep, narrow cleft that widens at mid-crown and then deepens again near the cervix. The distobuccal groove is broader than the mesiobuccal groove and is restricted to the occlusal third of the crown where it terminates in a pit created by a short cingular crest passing between the End and Hld. The mesiolingual groove, which is placed slightly distal to the mesiobuccal groove, is a faint depression near the occlusal margin. The distolingual groove is a faint depression near the occlusal rim.

Plate-like mesial and distal roots are present. The vertically oriented mesial root is broken at the apices of the lingual and buccal radicals. A broad central gutter runs along the mesial root. As preserved, the lingual side of the mesial root is 12.1 mm in height, while the buccal side is 9.9 mm in height. The maximum breadth of the mesial root is 11.4 mm. The buccally angled distal root is a broad oval and with a single canal exposed by a break near its apex. As preserved, the buccal side of the distal root is 10.0 mm in height and the lingual side is 10.6 mm. The maximum breadth of the distal root is approximately 9.0 mm. Further details of root morphology are provided by the µCT-based analysis of Kupczik et al. (2019).

Based upon similarities in morphology and the state of occlusal and interproximal wear, this is a proposed as the antimere of U.W. 101-285. The two crowns do differ subtly in the configuration of their distobuccal grooves.

U.W. 101-809: LM_1 (Fig. 33D; Table 1) Enamel chipping is evident along the mesial and distal margins and on the Hyd near the cusp apex. There is a large, deeply excavated, mesial IPF (5.0 mm BL by 3.5 mm OC) that extends to the occlusal surface and a faint distal IPF. Wear facets are evident on all principal cusps and a small dentine pit is exposed on the Prd apex (stage 2). The lingual crown is not indented by a lingual groove, the trigonid and talonid are nearly equally broad BL so that the crown does not taper until it reaches the distally rounded Hld. Five principal cusps are oriented in a Y-5 fissure pattern, with a substantial portion of the Med and Hyd in contact. The relative cusp sizes are Hyd > Prd > Med > Hld > End. Wear has flattened the essential ridges and removed any accessory ridges that may have been present. However, a Med distal accessory ridge can be inferred from a weak occlusal groove. This accessory ridge is likely not associated with a C7 as a similar configuration is evident in the unerupted U.W. 101-1400 and U.W. 101-1689 M_1s (Figs. 34C and 34D) where the ridge rises to meet a postmetaconulid along the distal metaconid crest. Wear precludes assessment of the MMR, but the lingual extent of a fissure-like Fa remains and is contiguous with the deep central groove. A small Fp is formed between the DMR and the End distal lobe. The protostylid is a moderate oblique crest limited to the mesiobuccal crown face that disappears before reaching the mesiobuccal groove. The mesiobuccal groove crosses the occlusal edge as a deep and narrow cleft, becomes shallow about mid-crown, and then deepens again just above the cervix. The distobuccal groove is also deep and narrow near the occlusal edge but disappears at mid-crown. The mesiolingual groove is distal to the mesiobuccal groove. It

crosses the occlusal margin as a narrow and shallow groove, fading at mid-crown. The distal lingual groove is a wide, shallow indentation restricted to the occlusal margin.

The crown has plate-like mesial and distal roots with a small portion of alveolar bone wedged between them. The roots are abraded and broken near the apices. In buccal view, the preserved mesial root height is 10.5 mm, while in buccal view the maximum preserved height of the distal root is 9.1 mm. In mesial view, the maximum breadth of the mesial root is 10.5 mm and in distal view the maximum breadth of the distal root is 8.2 mm. Both roots have a slight distal deflection. The mesial root is dumbbell shaped in cross section with wide shallow depressions running along the mesial and distal faces. The distal root is a broad oval in cross section and is narrower than the mesial root. The distal root is offset slightly buccal to the crown.

Based on similarities in morphology and the state of occlusal wear, this is a reasonable antimere of the RM_1 preserved in the U.W. 101-377/1014 mandible. The small distal IPF of this specimen is also congruent with the mesial facet of U.W. 101-789. This mesial IPF of this specimen also fits well with the distal IPF of U.W. 101-887. The association of U.W. 101-789, -809, and -887 is also reasonable because each is hypothesized to have an antimere in the U.W. 101-377 mandible. This specimen and U.W. 101-814, both LM_1s, are nearly identical in their degree of occlusal wear, with U.W. 101-809 possessing a distal IPF, which is lacking in U.W. 101-814. These specimens, of similar ontogenetic status, illustrate the difficulty in associating isolated teeth based on expected patterns of occlusal wear.

U.W. 101-814: LM_1 (Fig. 33E; Table 1) Chipping is present on the End apex and along the mesial margin. There is a large, convex mesial IPF (5.5 mm BL by 3.3 mm OC) that extends to the occlusal surface. There is no distal IPF. Wear facets are evident on all cusps and a small dentine pit is exposed on the Prd apex (stage 2). The crown outline has a straight lingual profile, a bi-lobed buccal profile, and a concave mesial margin. The large Hld sits just buccal to the center of the tooth's axis and forms the rounded distal profile. The crown has five well developed cusps arranged in a Y-5 fissure pattern, with a substantial portion of the Med and Hyd in contact. The relative cusp sizes are Hyd > Prd ≥ Med > End ≥ Hld. The talonid is wider than the trigonid. Wear has flattened the essential ridges and removed any accessory ridges that may have been present. Wear precludes assessment of the MMR, but the lingual extent of a fissure-like Fa remains and is contiguous with the deep central groove and limited to the mesial Med. It is bordered distally by Prd and Med ridges. The Fp is partially obscured by wear, but is a short fissure bordered distally by a broad and rounded DMR that sits low on the crown. There is no indication of a protostylid. The mesiobuccal groove crosses the occlusal edge as a deep and narrow cleft, becomes shallow about mid-crown and then deepens again just above the cervix. The distobuccal groove is also a deep cleft near the occlusal surface; however, it terminates as a pit and small shelf about one third of the way down the crown face. The mesiolingual groove is distal to the mesiobuccal groove. It is narrow and shallow before it fades away about mid-crown. The distolingual groove is a faint depression near the occlusal margin.

The crown has plate-like mesial and distal roots with a small portion of alveolar bone wedged between. Both roots are broken near their apices; additionally, there is

significant abrasion on all but the mesial root surfaces. In buccal view, the preserved mesial root measures 10.1 mm and the distal root 9.2 mm in height. The maximum breadth of the mesial root is 9.4 mm, and the maximum breadth of the distal root is just below the cervix and is 7.9 mm. The mesial root is vertically oriented, and dumbbell shaped in cross section, with wide, shallow depressions running along the mesial and distal faces. The distal root is more figure-of-eight shaped in cross section because it does not pinch in as extensively as the mesial root does. The distal root angles slightly buccally relative to the mesial root.

U.W. 101-905 + U.W. 101-294: LM_1 crown and associated root (Fig. 34A; Table 1)

Enamel chipping lines the crown distally. Another, especially large chip is present on the occlusal margin distolingually, where it extends onto the crown face. Occlusally, a crack runs from the mesiolingual corner and passes through the dentinal exposures at the Med, Prd, Hyd, and Hld to terminate at the large distolingual enamel chip. The crack does not displace enamel or distort the morphology of the crown. Interproximal wear excavated deeply into the mesial margin, creating a concave facet, and the distal contour is also squared off by interproximal wear. Pools of uncoalesced dentine are exposed over the Prd, Med, and Hyd, and a very small pit is present on the Hld (stage 4). The preserved occlusal profile is roughly rectangular, with the Hld centrally placed in the crown's axis. The crown is slightly broader BL across the distal cusps than across the mesial. The crown has a Y-5 fissure pattern, with a substantial portion of the Med and Hyd in contact, and a well-developed Hld. The Fa and Fp are mostly obliterated by wear, with only the slightest remnant of the Fa remaining mesiobuccal to the Med apex. A weak protostylid

is evident mesiobuccally as a faint crest. A remnant of the cleft of the mesiobuccal groove sits near the occlusal margin and then it opens up immediately and continues to the cervix as a broader indentation. The distobuccal groove is also deep at the preserved occlusal margin; though, it terminates at mid-crown. The lingual groove is set slightly distal to the mesiobuccal groove and is a shallow indentation across its entire preserved course.

The roots are broken away near the cervix. The associated mesial root, recovered separately and catalogued as U.W. 101-294, is preserved as a detached fragment (not figured). The root has distinct rounded canals buccally and lingually that are connected by a narrow chamber stretching between them. A broad gutter is present along the mesial surface of the root. When refit, in buccal view the preserved root is 12.7 mm in height. The maximum breadth of the root is approximately 10.9 mm.

Based upon similarities in crown morphology and wear state, this is a reasonable antimere for U.W. 101-297.

U.W. 101-1287B: RM_1 (Fig. 34B; Table 1) Enamel chipping is evident along the mesial and distal margins. The mesial IPF is large and concave (6.0 mm LaL by 2.7 mm OC), while the distal IPF is larger (7.3 mm LaL by 3.8 mm OC) and flattened the distolingual face. Both IPFs reach the occlusal edges. Large pools of dentine are exposed over each of the five principal cusps, with some coalescence between those of the Med and Prd (stage 4). The crown has a rectangular profile modified by interproximal wear. The buccal profile is bilobed while the lingual profile is smooth. The talonid is wider than the trigonid. Very little occlusal morphology remains. The mesiobuccal groove is preserved

as a deep, narrow cleft at the occlusal margin that becomes wider and slightly shallower as it reaches the cervix. The distobuccal and lingual grooves remain as shallow features near the occlusal margin.

A portion of alveolus remains between the mesial and distal roots. The roots are complete, but their surfaces are abraded. The mesial root is wide and plate-like with two distinct radicals that bifurcate into separate apices. A shallow and broad depression runs between the rounded buccal and lingual root margins. The distal root also has two radicals, although they are less distinct. It is a broad oval in cross section. The mesial and distal roots deflect distally, running parallel to each other. In buccal view, the maximum height of the mesial root is 13.8 mm and that of the distal root measured buccally is 12.0 mm.

This tooth fits into the M_1 alveolus preserved in the U.W. 101-1142 mandible. Further, the distal IPF of U.W. 101-1287B perfectly matches the mesial IPF of the U.W. 101-1142 M_2. This specimen is incorrectly published as U.W. 101-1304 in Berger et al. (2015: Supplemental File 1) and in the analysis of Odes et al. (2018). Despite sharing an accession number based on the spatial proximity of their recovery, this specimen and U.W. 101-1287A (LdC^1) cannot represent the same biological individual, as U.W. 101-1287B belongs to an individual with a completely erupted and worn permanent dentition, while U.W. 101-1287A represents a young subadult with light wear on its deciduous canines.

U.W. 101-1400: LM_1 germ (Fig. 34C; Table 1): This is a nearly complete crown with no trace of root development. The crown was in situ in its exposed crypt in the U.W. 101-

1400 mandible at the time of excavation. In occlusal view, the crown is roughly pentagonal, with a straight lingual profile and bi-lobed buccal profile. The talonid is slightly wider than the trigonid. The crown has a Y-5 fissure pattern, with a substantial portion of the Med and Hyd in contact, and a well-developed Hld. The relative cusp sizes are Med > Hyd > Prd > End > Hld. The Hld is placed near the center of the crown's BL axis and forms the rounded distal contour. The essential lobes are well-developed but not associated with well-defined ridges. The Hy essential ridge widens mid-cusp, expanding into a triangular feature before it terminates. The End essential ridge bifurcates before reaching the occlusal basin. The distal accessory ridge of the Med is well developed, resulting in an incipient postmetaconulid. The MMR is lower than the essential ridges of the Pr and Med and its buccal and lingual components form a v-shape where they meet mesial to the Med. A small Fa is bordered mesially by the MMR and distally by weak mesial accessory ridges of the Prd and Med. The accessory ridges meet at the Mlg but do not form a mesial trigonid crest. A moderately sized Fp is bordered distally by the DMR and mesially by the occlusal ridges on the Hld and End. The protostylid is a faint, obliquely oriented crest on the mesiobuccal aspect of the Prd that terminates well before the mesiobuccal groove. The mesiobuccal groove is a narrow and deep cleft at the occlusal margin that becomes shallow at mid-crown and then deepens again just above the cervix. The distobuccal groove is deep and narrow and slightly shorter than the mesiobuccal groove. The lingual groove is situated distal to the mesiobuccal groove. It is very shallow and fades away at mid-crown.

Based on shared morphology and developmental status, this is the antimere of U.W. 101-1689.

U.W. 101-1689: RM_1 germ (Fig. 34D; Table 1) The crown is nearly complete and there is no trace of root development. There is minor damage to the cervix distolingually. In occlusal view, the crown is roughly pentagonal with a straight lingual profile and bi-lobed buccal profile. The crown has a Y-5 fissure pattern, with a substantial portion of the Med and Hyd in contact, and a well-developed Hld, which is offset slightly buccal to mid-crown. The relative cusp sizes are Med > Prd = Hyd > End > Hld. The MMR is low and comprises a small cuspule that is delineated by shallow mesial grooves. It forms the mesial border of a short, groove-like Fa, which is bound distally by weak Prd and Med mesial accessory ridges. The Prd also has a distal accessory ridge. The Med essential crest is well defined near the apex and widens into a triangular feature towards the occlusal basin. The distal lobe of the Med is well developed. The Hyd terminates in a tubercle-like ridge at the occlusal basin. The essential ridge of the End is moderately developed. The groove-like Fp is bounded distally by a bipartite DMR and mesially by the Hld and End occlusal ridges. The protostylid is a faint oblique ridge confined to the mesiobuccal aspect of the Prd. Both the mesiobuccal and distobuccal grooves are deep and narrow clefts near the occlusal margin. The distobuccal groove fades at mid-crown, while the mesiobuccal groove continues to the cervix as a shallow groove. The lingual groove is deep and narrow at the occlusal margin but quickly becomes shallow on the lingual face. It is distal to the mesiobuccal groove. This is the antimere of the LM_1 preserved in its crypt in the U.W. 101-1400 mandible.

3.24. Permanent mandibular second molars

Six isolated M_2s and those present in the U.W. 101-001, U.W. 101-361, U.W. 101-377, U.W. 101-1142, and U.W. 101-1261 mandibles represent at least nine individuals. The M_2 crown is rectangular in occlusal outline, with straight mesial and lingual margins, mildly bi-lobed buccal profile, and a rounded distal profile with a large Hld offset slightly buccal to the center of crown. The five principal cusps are present with a Y-5 fissure pattern. The occlusal surface is simple: supernumerary cusps are absent, essential ridges are not well defined, and the protostylid is either absent or a weak crest restricted to the mesiobuccal corner of the crown.

U.W. 101-145: LM_2 (Fig. 35A; Table 1) No wear facets are visible on the occlusal surface (stage 1) and IPFs are not present mesially and distally. Thus, it is likely unerupted, or at least not in functional occlusion, at the time of death. There are small developmental pits at the Hyd and End apices. Aside from minor damage at the cervical line lingually and distobuccally, the crown is complete. The crown is roughly rectangular in occlusal profile, with straight mesial and lingual margins, mildly bi-lobed buccal profile, and a rounded distal profile with a large Hld offset slightly buccal to the center of crown. Only the five principal cusps are present, and the crown has a Y-5 fissure pattern. A substantial portion of the Med and Hyd are in contact and the Hld is relatively large. The relative cusp proportions are Med > Prd ≥ Hyd > End > Hld. The essential ridges are not well defined, being thick and rounded. Those of the Prd and Med do not join to form any type of trigonid crest. The Prd and End each have a faint mesial accessory ridge. On the Prd, this ridge is separated from the essential ridge by a groove. The Med and Hyd each have a faint distal accessory ridge. The MMR is low and rounded and bordered

distally by a small Fa that is continuous with the Mlg. The Fa is short and BL-oriented and positioned between the Prd mesial accessory ridge and the bulbous Med essential ridge, with a slight topographical divide separating the shorter buccal arm from the longer lingual arm. The buccal groove forms a deep v-shaped cleft occlusally that becomes shallow at mid-crown as it continues to the cervix. The distobuccal groove is a distinct, yet shallower, groove rather than a cleft; it becomes imperceptible at mid-crown. There is only a faint suggestion of the protostylid, and it is limited to the mesiolingual aspect. It begins as a barely perceptible vertically oriented swelling that then curves distally to become indistinct under the Prd apex. The lingual groove sits slightly distal to the buccal groove, is shallow across its course, and fades at mid-crown. The developing roots are broken off so that only a small sliver remains buccally.

Based on shared morphology and degree of occlusal wear, this is proposed as the antimere of U.W. 101-507.

U.W. 101-284: LM_2 (Fig. 35B; Table 1) Enamel chips are present along the marginal ridges and at the apex of the End. A large mesial IPF (5.5 mm BL by 3.4 mm OC) is centered on the crown and extends to the occlusal margin. The distal IPF (4.0 mm BL by 3.2 mm OC) is distobuccally oriented and does not extend to the occlusal margin. Wear facets are visible on the occlusal surface, but no dentine is exposed (stage 1). In occlusal view, the width of the talonid and trigonid are approximately equal. The profile is a rounded rectangle, with a nearly straight lingual profile and bilobed buccal profile. The mesial margin is concave as the result of interproximal wear and distal interproximal wear squared off the once projecting Hld. The crown has a Y-5 fissure pattern, with a

substantial portion of the Med and Hyd in contact and a well-developed Hld. No accessory cusps are observed. In relative size, the cusps are Hyd > Prd > Med > End > Hld. The MMR is set low, and its apparent size has been reduced by the mesial IPF and occlusal wear. The essential ridges, and nearly all accessory ridges that may have been present, have been removed by occlusal wear. The exception is the Prd mesial accessory ridge, which defines the distal border of a short branch of the Fa, and its associated groove. The Fa is not well defined and is mostly manifest as an extension of the central groove as it curves around the Med. A deep central groove separates the Prd and Med and no middle-trigonid crest was present. The protostylid is limited to the mesiolingual aspect of the Prd. It appears as a faint, but palpable, swelling that begins near the MMR as a vertically oriented crest and then traverses obliquely to become indistinct under the Prd apex. The mesiobuccal groove is deep at the occlusal surface and then becomes shallow at mid-crown as it travels to the cervix. The distobuccal groove is much shallower and fades at mid-crown. The lingual groove is set slightly distal to the mesiobuccal groove and is a shallow indentation at the occlusal surface.

The roots are broken away near the cervix. The break is angled so that almost nothing of the roots remains below the lingual side, but approximately 3.3 mm of the mesial root and 3.2 mm of the distal root are preserved buccally. The broken surface is stained by matrix, suggesting that the break was ancient.

U.W. 101-507: RM_2 (Fig. 35C; Table 1) This is an unworn crown (stage 1). In occlusal view, the crown is roughly rectangular in profile with trigonid and talonid equal in width and a rounded distal profile formed by the projecting Hld. The crown has a Y-5 fissure

pattern, with a substantial portion of the Med and Hyd in contact and a well-developed Hld. The relative cusp sizes are Med > Prd ≥ Hyd > End > Hld. The mesial occlusal ridges of the Prd and Med join to form a thick rounded MMR that defines the mesial border of a groove-like Fa. The Fa is mostly limited to the Prd but extends a short distance lingually onto the Med. The Med essential ridge deflects sharply distally to form a deflecting wrinkle, but it does contact the End. The Med has a faint distal accessory ridge and the End presents a thin, short mesial accessory ridge. Otherwise, the occlusal surface is relatively simple. The DMR is a poorly defined, short crest that bounds a small groove-like Fp. A very faint, but palpable, vertical mesial groove is present on the mesiolingual corner of the Prd. The mesiobuccal groove is deep and narrow; it becomes shallower at mid-crown and then deeper again as it reaches the cervix. The distobuccal groove is shallower and becomes imperceptible about one-third of the crown height. The lingual groove is much shallower than the buccal grooves and is located slightly distal to the mesiobuccal groove. It fades at mid-crown.

The roots are mostly broken away at the cervix and the pulp chamber is filled with sediment. The tooth was likely unerupted at death and the roots minimally developed. What remains of the roots are small extensions below the buccal cusps.

This is the proposed antimere of U.W. 101-145. Their morphology is virtually identical, as is their developmental status, lack of IPFs, and lack of occlusal wear.

U.W. 101-655: $RM_{?}$ germ, likely RM_{2} (Fig. 35D; Table 1) The occlusal surface is complete but only about one-third of the crown height has been attained. In occlusal view, the crown is a rounded rectangle with the talonid wider than the trigonid and the

Hld offset buccal to the midline. The crown has five primary cusps arranged in a Y-5 fissure pattern, with a substantial portion of the Med and Hyd in contact, and a well-developed Hld. The protostylid is evident on the mesiolingual aspect of the Prd as a small depression and associated oblique shelf. The developing MMR is much lower than the essential crests of the Prd and Med, and lowest just mesial to the Prd. It projects as a shelf with accessory tubercles. This shelf is associated with a v-shaped cleft on the mesiolingual aspect of the Med. The Fa is manifest as a BL-oriented groove that extends buccally and lingually from the central groove. On the Prd portion, a faint mesial accessory ridge borders it distally. The essential lobes of all cusps are well developed, although sharp ridges do not define them. A weak middle-trigonid crest, which is bisected by the central groove, joins the Prd and Med. The portion of the mesiobuccal groove that is preserved forms a shallow cleft and wide weak groove. The distobuccal groove is shallow but lacks the cleft. No lingual grooves are observed.

The identification of the tooth as a permanent molar is based on the crown dimensions. It is likely an M_2 given the morphology of the Fa. Often in *H. naledi* M_1s, the Fa is restricted to the region mesial to the Med, while on M_2s the Fa passes mesial to the Prd as well. Further, in *H. naledi* M_1s, the Hld tends to be more centrally placed, while in M_2s it is placed more buccally. This is unlikely to be an M_3, which tends to taper distally with a wider trigonid and narrower talonid.

U.W. 101-789: LM_2 (Fig. 35E; Table 1) An IPF (approximately 3.0 mm by 2.4 mm OC) is found mesially, but no IPF is detectable distally. Occlusal wear facets are limited to the Prd and Med on or close to their cusp apices (stage 1). In occlusal view, the crown has a

straight lingual profile, straight mesial profile, bi-lobed buccal profile, and convex distal profile related to a large, Hld. The talonid is slightly wider than the trigonid. There are five well-developed primary cusps arranged in a Y-5 fissure pattern, with a substantial portion of the Med and Hyd in contact, and the relative cusp sizes are Med > Prd > End ≥ Hyd > Hld. The essential lobes are not defined by sharp ridges. Accessory ridges can be observed on the Hyd (distal) and End (mesial). A deflecting wrinkle is present on the Med. The MMR is lower than the essential crests of the Prd and Med, with its lingual portion lower than the buccal portion. A fissure-like Fa is positioned mesial to the Med and is contiguous with the central groove. Buccally, a topographically discrete section of the Fa is bounded by a small accessory tubercle extending from the MMR and the essential ridge of the Pr. A shallow, but wide, Fp is bordered distally by a low and rounded DMR. A deep mesiobuccal groove forms a cleft between the Prd and Hyd; it becomes shallow at mid-crown and deepens again just above to the cervix. The distobuccal groove is wider and shallower, fading away about mid-crown. The lingual groove is distal to the mesiobuccal groove and does not cross onto the lingual face. The protostylid is a faint, obliquely oriented swelling limited to the mesiolingual aspect of the Prd.

The roots are fragmented and some of the larger fragments have been refit to the crown. Many of the smaller fragments are pressed into the pulp chamber where they remain. The surfaces of the roots are abraded. A maximum of 6.1 mm of root remains mesially, 4.3 mm remains distolingually, 5.3 mm remains mesiolingually, and the roots are entirely broken away buccally.

This specimen is proposed as the antimere of the RM_2 in situ in the U.W. 101-377/1014 mandible. They are virtually identical in morphology and their state of eruption. Both have a small IPF mesially and lack one distally. The mesial IPF of this specimen is also a possible match for the small distal IPF of the U.W. 101-809 LM_1.

U.W. 101-1002: RM_2? germ (Fig. 35F; Table 1) The crown is incompletely formed and poorly mineralized. The occlusal surface is covered in cracks that developed post-depositionally. In occlusal view, the lingual profile is straight, the buccal profile slightly bi-lobed, and the distal profile has a buccal projection. The crown has a Y-5 fissure pattern, with a substantial portion of the Med and Hyd in contact, and a well-developed Hld. There is no evidence of supernumerary cusps. The MMR is low and indistinct. The weak, fissure-like Fa is primarily expressed on the Med but extends slightly onto the Prd. The wide Fp is bordered mesially by occlusal ridges of the Hld and End and distally by the DMR. The protostylid is limited to the mesiolingual aspect of the Prd. It is a faint oblique swelling that terminates mid-way to the buccal groove. The mesiobuccal groove is a deep and narrow cleft near the occlusal surface that continues to mid-crown where crown development ended. The distobuccal groove is much shallower.

The identification as an M_2 is based on the morphology of the Fa, which extends buccally onto the Prd and on the position of the Hld, which is offset buccally. In most of the Dinaledi M_1s, the Fa does not extend buccally to the Prd. The state of development of this specimen matches that of a pair of proposed antimeric maxillary molars, U.W. 101-1063 and U.W. 101-1135, and they are suggested to represent the same individual as U.W. 101-1002.

3.25. Permanent mandibular third molars

Two isolated M_3s and those present in the U.W. 101-001, U.W. 101-361, U.W. 101-1142, and U.W. 101-1261 mandibles collectively represent at least five individuals in the Dinaledi Chamber sample. The M_3 crown has five principal cusps arranged in a Y-5 pattern and the Hld is relatively large. Supernumerary cusps are absent and, with the notable exception of U.W. 101-1261, the protostylid is faint. The crown is BL broadest across the trigonid and tapers across the talonid. The M_3 roots present a consistent pattern as well. The mesial root is plate-like, while the distal root is more elliptical in cross section. The distal root tapers strongly along the lingual side, especially apically, which gives the root a buccal tilt in distal view. The mesial root has two distinct apices separated by a notch. The tapering of the distal root and the indentation between the mesial root radicals would have accommodated the passage of the mandibular canal.

U.W. 101-006: RM_3 (Fig. 36A; Table 1) A large enamel chip is evident along the occlusal margin mesiobuccally and other small chips dot the occlusal surface at the lingual margin, distally adjacent to the End, and in the area between the End and Hld. A large IPF is evident mesially with its full height preserved lingually (2.6 mm maximum OC by 6.6 mm maximum BL breadth); though, occlusal wear eliminated a portion of its buccal portion. A large dentine pool covers the buccal crown, and all but the distobuccal portion of the distal margin and the mesiobuccal portion of the mesial margin are worn away (stage 5). The wear plane is strongly angled distobuccally such that none of the crown is preserved above the distobuccal root.

Very little morphological information can be gleaned from this worn crown. The crown is flattened mesially by interproximal wear, has a mildly convex lingual profile, and a convex distal profile with the distal-most point offset buccally, suggesting the presence of an expansive Hld. The crown is broadest across the mesial cusps and tapers distally. The buccal crown profile is substantially altered by occlusal wear and enamel chipping. Although no dentine is exposed on the Med and End, neither cusp retains any morphological information. However, the preserved Med is much higher than the End. The occlusal surface, though worn, preserves a hint of the groove separating the Med and End, together with a small pit just mesial to it. There is a slight suggestion of another fissure separating the Hld from the End.

A portion of the mandibular alveolus remains wedged between the mesial and distal roots. The roots are minimally abraded, with only the tip of the mesiobuccal radical broken, and the exposed surfaces are covered with cementum. The mesial root is plate-like, while the distal root is more elliptical in cross section. The distal root has a fairly straight buccal profile but tapers strongly along the lingual side, especially in the apical quarter of its height, which, in distal view, gives the root a buccal tilt. The mesial root has two distinct apices, with the buccal one slightly shorter than the lingual. The tapering of the distal root and the separation of the mesial root radicals would have accommodated the passage of the mandibular canal. The maximum height of the mesial root buccally is 11.6 mm, while along the lingual radical it is 13.9 mm. The distal root is 11.8 mm in height. All root measurements approximate their full heights.

This tooth was recovered within centimeters of U.W. 101-005 (RM^2), another heavily worn molar. However, as U.W. 101-005 and -006 are from different arches, attribution to a single individual cannot be confirmed.

U.W. 101-516: LM_3 (Fig. 36B; Table 1) There are chips of enamel missing from the mesiobuccal corner just occlusal to the mesial IPF, along the occlusal extent of the mesial IPF, and along the occlusal rim on either side of the lingual groove. The large mesial IPF (5.9 mm BL by 2.7 mm OC) extends to the occlusal surface. There is no distal IPF. Wear flattened much of the occlusal topography and small round dentine pits are exposed on the Prd and Hyd (stage 3). In occlusal view, the crown is rectangular with a worn concave mesial profile, mildly bi-lobed buccal profile, straight lingual profile, and convex distal profile related to a large, buccally offset Hld. The crown is BL broadest across the trigonid and slightly tapers across the talonid. The mesial IPF and occlusal wear have obscured expression of the Fa and MMR. Although worn, the Y-5 groove pattern can still be identified. Judging from this preserved groove pattern, C6 and C7 are absent (an examination of the EDJ confirms the absence of dentine horns for C6 and C7). The mesiobuccal groove is a deep v-shaped cleft where it crosses the occlusal surface. It becomes shallower on the buccal surface about mid-crown and then deepens near the cervix. The distobuccal groove is faint, fading away before mid-crown. The lingual groove is offset distal to the mesiobuccal groove. It is a slight indentation at the occlusal surface and becomes a faint groove on the buccal face extending to the cervix.

A portion of alveolar bone remains wedged between the roots. The tips of the roots are damaged. The distal, lingual, and buccal surfaces of the distal root are abraded,

as are the labial and lingual surfaces of the lingual root. The mesial root is plate-like, with two distinct buccal and lingual radicals that become independent root apices. In buccal view, the mesial root is 11.8 mm in height and the distal root is 11.5 mm. The distal root is more circular in cross section, notably tapers in its cervical half, is strongly canted buccally, and has a slight notch near the apex of its lingual margin. The tapering, notch, and cant of the distal root, along with the bifurcation of the mesial root apices, would have permitted passage of the mandibular canal (Kupczik et al., 2019).

Based upon the morphology and occlusal wear similarity, this is proposed as the antimere of the M_3 preserved in the U.W. 101-001 mandible (for comparisons of the root morphology of these proposed antimeres, see also Kupczik et al., 2019).

3.26. Crown and root fragments

U.W. 101-293: C_1? (Fig. 37A; Table 1) This is the root of an anterior tooth lacking a crown. The preserved occlusal surface is polished, and the pulp canal is exposed. No enamel remains around the circumference of the crown (stage 8). The advanced wear, combined with the heavy accumulation of cementum along the root and tertiary dentine in the pulp canal, indicates that this tooth is from an ontogenetically advanced individual (it is of comparable, or more advanced wear, to the U.W. 101-010 mandibular canine, for example). The contours of the root throughout are hard to discern because the root is covered in a thick layer of cementum that has flaked away in some places. The root is roughly circular in cross section and somewhat flattened along what is inferred to be the distal side. The apex of the root is damaged, where a large cementum flake is missing, and the maximum length of root along the inferred mesial edge is 15.0 mm. The circular

cross-sectional shape of the root is inconsistent with incisors in the Dinaledi sample and is most like those of mandibular canine roots.

U.W. 101-357: mesial root of LM_1 or LP_4? (not figured; Table 1) This plate-like root preserves a thin sliver of enamel on either its mesial or distal side. The preserved occlusal surface was a functional surface with polished dentine. A broad shallow depression is present on one side. Minor damage occurs just below the occlusal surface on the grooved side. The maximum height of the preserved root is 13.5 mm, and its maximum BL width is 10.3 mm just below the preserved occlusal surface.

Specimens U.W. 101-357, U.W. 101-358, and U.W. 101-359 were recovered from fragments and sediments associated with the U.W.101-361 mandible and are consistent with belonging to a single individual.

U.W. 101-388: Root fragment (Fig. 37B; Table 1) This broken root fragment, 13.6 mm in length, is circular in cross section and curved along its longitudinal axis. The root is broken near the cervix and is also damaged near its apex. This root is from an older individual. A thick layer of cementum covers the root, and it is flaked off the external surface. Further, the µCT scans reveal that the root canal is nearly filled in with tertiary dentine. The shape, size, and the curvature of the root do not match canines, which are larger, or incisors, which are much more elliptical. This is possibly a root from a maxillary molar. If so, the closest matches in the Dinaledi assemblage are distobuccal roots of maxillary molars.

U.W. 101-589: $M_?$ root (Fig. 37C; Table 1) This is a heavily worn molar crown fragment and root. Based on the relative degree of occlusal wear and comparison with the U.W. 101-602 RM_1, this specimen is possibly an RM_1. The tooth is preserved in two fragments that poorly rejoin. The larger fragment preserves what is interpreted as the mesial root with a small piece of enamel remaining occlusally. An enamel chip is evident on the preserved occlusal surface. The root is covered throughout in a thick layer of cementum. The second fragment includes a piece of enamel, a portion of dentine from the occlusal surface, and a small bit of the root. Approximately one half of an IPF that extends to the occlusal surface is present on this fragment. The smaller fragment refits poorly with the larger. When they are refit, it is evident that the IPF continues onto the enamel fragment that remains attached to the root. The break between the fragments appears recent.

The mesial face of the root is flat, while a slight invagination runs along the distal face. The buccal apex of the root is shorter than the lingual apex. Such asymmetry is present in other mandibular molar roots. The maximum height of the root is 12.4 mm, and the maximum breadth is 9.3 mm.

U.W. 101-602: $RM_?$? (Fig. 37D; Table 1) This is a portion of heavily worn crown and associated root. The root appears to be the mesial root of a mandibular molar, which would make this a fragment of a right molar and the associated lingual rim. Occlusally, there is a portion of enamel along the inferred mesiolingual corner; the occlusal surface here features several antemortem chips. The remaining occlusal surface is polished dentine (stage 7–8) that shows a steep wear gradient with no enamel remaining mesially or buccally and approximately 3.4 mm of enamel remaining lingually. In fact, the wear

surface buccally is likely well below the original cervix of the crown. Enamel chipping is evident on the preserved occlusal surface.

The root is plate-like and damaged along the apex of its inferred mesial and lingual surfaces. The root is coated in a thick layer of cracked cementum. In mesial view, from the center of the BL axis of the tooth, the remaining root height is 11.9 mm and, below the preserved enamel rim it is 12.7 mm, and its maximum BL breadth is 10.5 mm. The inferred buccal profile of the root is nearly vertical, while the lingual profile is curved, and matches the profile of mesial roots of mandibular molars.

U.W. 101-652: Developing cusp (Fig. 38; Table 1) This specimen is a single cusp of a postcanine tooth germ. Crests extend mesially and distally, while the developing essential ridge is faint. What is interpreted as the mesial crest is longer than the preserved section of distal occlusal rim. A faint swelling can be seen on the longer crest. Whether this represents a permanent or deciduous tooth is undetermined; however, in preserved occlusal detail (i.e., faint essential ridge, longer mesial than distal crest, faint swelling on mesial crest) this specimen resembles the developing End on U.W. 101-655. Both specimens have similarly thin enamel as well.

U.W. 101-653: Incisor root? (Fig. 39A; Table 1) This is a single conical root that is ovoid in cross section. Its cross-sectional size and shape are consistent with attribution to an incisor. The thick cementum covering the root is flaking off. The occlusal surface is heavily worn, and all enamel has been removed except for the tiniest portion lingually (stage 7). The preserved maximum root height is 15.6 mm. Though the crown is likely

worn past the contours of the original cervix, the preserved maximum LaL width of the root near the cervix is 5.6 mm and the maximum MD length is 4.5 mm.

U.W. 101-654: LM? root (Fig. 39B; Table 1) This specimen is a single plate-like root with functional wear surface that slopes steeply downward toward the inferred buccal side. No enamel is preserved. Given the extent of exposed dentine, the thick layer of cementum evident along the external surface of the root, and the buildup of tertiary dentine in the root canals, which is evident on the μCT scans, this specimen must belong to an individual of advanced age (stage 8). There is moderate abrasion to the root surface near its apex. The maximum preserved height of the root in inferred buccal view is 11.9 mm and its breadth just below the deepest extent of the worn surface is 8.4 mm. The shape and size of the root are consistent with mesial roots of mandibular molars.

In the degree of occlusal wear and the profile of the root, it bears a strong resemblance to U.W. 101-589. There is no other evidence, however, to link these specimens.

U.W. 101-680: Lingual root of maxillary molar? (not figured) A single root with an invagination on one side. It resembles the lingual root of a maxillary molar.

U.W. 101-686: anterior tooth root? (Fig. 39C; Table 1) This specimen is an unidentified anterior tooth root lacking enamel and with a polished functional surface. The preserved root is short and circular in cross section. The root is damaged near the occlusal edge, where a portion of the root is flaked off. Additionally, opposite that damage, a linear

portion of the root is missing along nearly the entire length of the root. The apex of the root is preserved, which gives a maximum height of 13.4 mm and a maximum diameter near the surface of 6.0 mm.

U.W. 101-864: crown and root fragment (Fig. 39D; Table 1) This is a tooth fragment preserving a small ring of enamel and a portion of a root. Polished dentine and the lack of occlusal enamel indicate that this is a heavily worn tooth. The total height of the fragment from occlusal surface to the tip of the broken root is approximately 15.4 mm. The thick layer of cementum covering the external root surface further indicates the advanced age of the individual.

U.W. 101-1398B: I^2? root (Not figured; Table 1) This is a heavily worn root. It is covered in cementum, which is cracked and pitted over the entire surface. The root apex is broken away. The enamel is completely worn away, and the dentine exposed on the surface is polished by wear, suggesting the tooth was functional at death. The pulp chamber is exposed by wear and damaged postmortem. The root strongly curves just before its apex; the apparent curvature is accentuated by a thick layer of cementum. The root is elliptical in cross section and not as rounded in roots of the canines; thus, this most likely comes from an incisor. The maximum preserved height of the root is 16.2 mm, which is much longer than the measurable distobuccal roots of maxillary molars, which precludes this specimen from belonging to a postcanine tooth.

U.W. 101-1605: $LM_?$? (Not figured; Table 1) A developing tooth germ in fragments, in which the enamel surface is fractured.

3.27. Maxilla with teeth

U.W. 101-1277: LI^1–LM^2 (Fig. 40; Table 1) This set of teeth is associated with the U.W. 101-1261 mandibular dentition.

LI^1: Damage to the alveolus is evident labially, exposing approximately 6.0 mm of the root. The incisal wear plane slopes lingually, with a greater portion of dentine exposed along the MMR than along the DMR (stage 4–5). The labial face is featureless. Lingually, incisal wear removed most of the marginal ridges so that what remains are subtle swellings at the incisal edge. There is no hint of a median lingual ridge.

LI^2: Damage to the alveolus exposes approximately 3.1 mm of the root labially. The incisal wear plane slopes lingually and exposes more dentine along the MMR than along the DMR (stage 4). The remaining labial face is minimally convex. On the labial face, there is a circular depression of unknown etiology at approximately mid-crown. Linear hypoplasias are evident in the cervical third of the crown. Although worn, the MMR and DMR are still evident and were likely moderate in expression. As preserved, the DMR is broader than the MMR. The weak lingual basal eminence is offset mesially. The lingual fossa is moderately convex with a pit near the basal eminence.

LC^1: There is some damage to the labial alveolus that exposes 2.7 mm of the root. The crown is worn, with a large dentine patch exposed over the apex (stage 3). There is a large, lingually angled facet along the distal crest. At this stage of wear, it appears that the wear facet along the distal crest is like that typically seen on the lingual face of the *H.*

naledi maxillary canines (i.e., U.W. 101-337, U.W. 101-412, U.W. 101-501, U.W. 101-706, and U.W. 101-908). The occlusal and distal facets meet at an angle just distal to the crown apex. Labially, there are faint mesial and distal grooves running along the crown. Lingually, there is a broad median lingual ridge between a narrow mesial lingual groove and a broader and shallower distal fossa. The MMR is strong near the occlusal edge and then blends into the basal of the crown. Linear hypoplastic defects cross the labial face near the cervix.

LP^3: There is minor damage to the alveolus lingually. Enamel chips are present on the mesiolingual and buccolingual corners of the Pr. The occlusal topography is flattened by wear and a small dentine patch is exposed over the Pr apex (stage 2–3). The crown profile is slightly asymmetric in occlusal view with a more tightly convex lingual than buccal margin. The Mlg deflects buccally to form a short fissure-like Fa. The mesiobuccal and distobuccal grooves are shallow and disappear at mid-crown. The lingual face is featureless.

The external topography of the alveolar bone suggests the presence of multiple buccal roots, which is confirmed by examination of the µCT scans. Three roots are present: two buccal and one lingual. The three roots have separate canals for much of their lengths; though, the buccal roots are not widely splayed apart.

LP^4: The occlusal surface is polished by wear and there is a tiny dentine pit exposed over the Pr (stage 2). The crown is ovoid in occlusal view with the cusps approximately equal in size. The Pa is slightly MD longer than the Pr. Though worn, the Pa retains two occlusal ridges, each likely emanating from either side of the apex, as in less worn *H. naledi* P^{4}s. The Fa is a short groove confined to the Pa. The Fp is a

bifurcation of the Mlg with a short lingual branch and longer buccal branch. It is associated with a shallow distal buccal groove. A shallow mesiobuccal groove is also evident. They are more prominent than on the P^3 of this individual. The lingual crown is featureless.

The µCT scans were investigated to compare the root morphologies of the in situ P^3 and P^4. Like the P^3, the P^4 is three rooted, with two buccal roots and one lingual root. The root canals are separated for most of their lengths and the radicals of the buccal roots are also completely separated for most of their lengths.

LM^1: The alveolus surrounding the buccal roots is mostly missing and no alveolar bone remains distally or superiorly. Lingually, alveolar bone covering the root exists as a separate fragment refit to the maxilla. The cervical portion of the roots remains exposed. Enamel chipping exists along the mesial margin above the IPF. Dentine is exposed over the Pr, Hy, and Pa. The dentine pool over the Pr is large and deep (stage 3–4). Details of the occlusal morphology are obscured by wear, but the four principal cusps and most of the fissure pattern are preserved. The occlusal outline is rhomboidal due to the distolingual projection of the Hy. The expression of the MMR and Fa cannot be assessed. A remnant of the Fp remains as a pit between the Me and Hy. The Co was probably continuous, based on what is preserved, and the DMR retains its distinction. Portions of the buccal and lingual grooves are preserved, with the lingual deeper than the buccal. Wear precludes assessment of Carabelli's feature.

The two buccal roots are separated by a deep invagination, especially lingually. They are pressed together and run parallel to each other and perpendicular to the crown. The mesiobuccal root measures 10.7 mm and distobuccal root 10.5 mm. The buccal roots

are MD compressed and ovoid in cross section. The lingual root is the largest in cross sectional area. It is MD elongated with clefts running along its buccal and lingual faces, which gives the root a figure-of-eight shape in cross section. The lingual root has a sharp lingual inclination.

The U.W. 101-1463 RM^1 is a possible antimere to this tooth. They are very similar in their preserved morphology, wear status, and even the pattern of enamel chipping. However, given their lack of occlusal detail, this hypothesis is difficult to evaluate.

LM^2: Enamel chipping is evident along the worn mesial margin. The mesial IPF is obscured by the M^1. Distally, an IPF (4.9 mm by 2.4 mm) is present in the cervical half. The occlusal surface is smoothed by wear, but no dentine is exposed (stage 1). The four primary cusps are well developed, and a possible C5 may be present (wear precludes being certain) along the DMR. In occlusal view, the crown is rhomboidal with a distolingually projecting Hy. The relative cusp sizes are Pr > Hy > Pa > Me. The MMR and Fa cannot be assessed. Though worn, the Co appears to have been continuous. The Fp remains as a small, but deep pit between the Me and Hy. The lingual groove is deep and narrow at the occlusal margin, becoming shallow mid-crown and reappearing as a pit near the cervix. The buccal groove is wider and shallower, and it extends to the cervix. There is no indication of Carabelli's feature.

A portion of alveolar bone remains wedged between the roots. There are three roots: two buccal and one lingual. The buccal roots run parallel to each other but are more widely spaced, longer, and larger in cross sectional area than those of the adjacent M^1. Both roots are distally inclined, but the mesiobuccal root apex has a strong distal

deflection, while that of the distobuccal root deflects buccally. The mesiobuccal root is slightly taller (13.2 mm) than the distobuccal root (11.6 mm) along their buccal faces. The mesiobuccal root has a bifurcated apex and is more elliptical in cross section than the distobuccal root. The lingual root is the tallest of the three (13.0 mm). It possesses two distinct radicals separated by a shallow groove, giving it a figure-of-eight shape in cross section. It has a strong lingual and a slight distal inclination. The distobuccal and lingual roots are broken at their apices.

This tooth likely articulates with U.W. 101-1269 (LM^3) distally.

3.28. Teeth in mandibles

U.W. 101-001+U.W. 101-850: RP_3–M_3 (Fig. 41; Table 1) The U.W. 101-001 partial corpus contains RP_4–RM_3 in situ. An RP_3 with a portion of adhering mandibular corpus surrounding its roots, recovered separately and catalogued as U.W. 101-850, is now refit to the mandible. The morphology and preservation of the mandible are described in Laird et al. (2017).

RP_3: Part of the lateral portion of the inferior mandibular corpus, approximately 10.0 mm in height, remains attached to the RP_3 roots. The mandibular fragment extends superiorly along the mesial root of the P_3 and exposes the RC_1 alveolus mesially. Here, the maximum height of the alveolar fragment is approximately 15.7 mm. Lingually, alveolar bone surrounds only the mesial root, leaving the distal root free from adhering bone.

Enamel chipping is present along the occlusal surface of the DMR and adjacent to similar damage on the P_4. Occlusal to the mesial IPF, chipping is also evident along the

MMR. Mesially, a large IPF (approximately 4.4 mm BL by 2.0 mm OC) is evident. Both the Prd and Med are blunted by wear and dentine is exposed at the Prd apex (stage 4). A trace of the Mlg remains evident, indicating that the crown is fully bicuspid and that the Med is topographically distinct from the Prd; though, as is evident in less worn *H. naledi* P_3s, it would have been slightly smaller than the Prd in area. Much of the topography of the mesial crown is flattened by wear; however, a small centrally placed BL-oriented groove remains as evidence of the Fa. Though much of its extent is worn away, the transverse groove curves around a worn Med distal accessory ridge, with only a short segment of the groove remaining buccal to the Mlg. The distal occlusal surface is worn to such an extent that a DMR is not detectable as a feature rising above the talonid. No trace of a mesiobuccal groove remains and only a hint of a shallow distobuccal groove is evident at the occlusal rim. No grooves are visible on the lingual face.

Two roots are largely visible and preserved in their entireties. Buccally, approximately 10.5 mm of the mesial root is exposed, mesially about 5.6 mm of the root is exposed, and lingually about 4.8 mm of the root is exposed. In buccal view, about 9.1 mm of the distal root is exposed, while 13.4 mm is exposed in lingual view. Cementum has flaked off the exposed root surfaces. An examination of the µCT scans shows that the roots become individualized with separate canals at approximately one-third of their distance below the cervix. The distal root itself has two identifiable canals, one buccal and one lingual, throughout much of its length. The distal root is BL-broader and larger in cross sectional area than the mesiobuccal, which conforms to the 2R: D+MB pattern of Wood et al. (1988).

RP_4: Along the MMR and occlusal to the mesial IPF, several enamel chips are present and another chip is visible in the mesiolingual corner adjacent to the Med. Distally, especially distobuccally, smaller enamel chips are evident along the DMR as well. A large interproximal carious lesion, largely confined to the root but extending superiorly onto the distal crown, runs parallel to the cervix. This lesion also affects the mesial aspect of the adjacent M_1 and is visible in the lateral and buccal views of the specimen in Figure 41. Examination of µCT scans shows significant demineralization of the enamel and adjacent dentine, with sediment filling in the demineralized hollow (see Towle et al. (2021) for a systematic assessment of caries in *H. naledi*). Very little occlusal detail remains, as a large dentine pool obliterates most of the buccal crown moiety, leaving a buccal rim of enamel less than 2.0 mm in breadth. The dentine pool widens distally and reaches its greatest BL breadth along the distal margin. A small dentine pit is evident at the Med apex as well (stage 5). Occlusally, the only morphology that remains is a small remnant of the lingual arm of the transverse groove. Yet, it is clear that the Med was high — likely subequal in height to the Prd. No trace of the mesiobuccal and distobuccal grooves remains and the lingual face is featureless..

The bone delimiting the alveolar margin is preserved with minimal damage: approximately 2.9 mm of the RP_4 root is visible buccally and less than 1.5 mm of the root is visible lingually. Buccally, a shallow groove is evident along the root; however, separate radicals are not visible at this level. The µCT scans show deep lingual and buccal invaginations and that the mesial and distal root canals separate at about half the roots' heights and bifurcate into separate external mesial and distal radicals near the root apices.

RM_1: A large carious lesion is present on the mesial aspect of the root and crown. The lesion runs the width of the root and affects the mesial margin of the Prd. Mesially, demineralization associated with the caries is evident to the naked eye and is easily seen in Figure 41. Examination of the µCT scans shows that demineralization extends down the face of the mesial root (see Towle et al. (2021) for a systematic assessment of caries in *H. naledi*). Buccally, the crown is damaged just above the distal root. Here, a notch of enamel extending nearly to the cervix has broken from the crown. Distobuccally, enamel chipping is evident occlusally. Additional chipping is present in the mesiolingual corner and mesiobuccally. Further, the enamel rim is incomplete from near the center of the mesial IPF towards the buccal margin where the crown begins to turn distally. The preserved break is sharp and the adjacent dentine is recently damaged, suggesting that it may be postmortem; however, the missing enamel is in the region of an interproximal caries that likely weakened the enamel and contributed to the break. The crown is heavily worn: the buccal cusps are obliterated, and tertiary dentine fills in the pulp canals at the occlusal surface. Only a thin rim of enamel is preserved along the buccal and distal aspects. Wear flattened the lingual cusps and large dentine pits cover the Med and End as well (stage 5). The occlusal wear along the buccal half of the crown is not planar, having excavated nearly to the pulp chamber near the center of the occlusal surface.

Although the occlusal fissures are all but obliterated by wear, it is evident from the crown shape and cusp orientations that at least five cusps were originally present. Lingually, the Med is higher than the End; though, the extent of their dentine exposure is similar. Occlusally, the only remnant of surface morphology preserved is a weak groove separating the Med and End. This groove extends onto the lingual surface. A remnant of

a deep buccal groove is evident; though, the buccal crown is worn nearly down to the cervical line.

The alveolus of the mandible is broken away irregularly around the roots, exposing more of the roots buccally than lingually. Buccally, approximately 7.0 mm of the mesial root and 7.5 mm of the distal root are exposed. Lingually, the alveolus is largely undamaged, and less than 2.0 mm of the mesial root is visible. The buccal surfaces of both roots are covered with cementum and are abraded. The lingual root surfaces are less abraded than apparent on the buccal side. The broader mesial root is oriented vertically below the crown, while the smaller distal root cants buccally. Further details of root and pulp chamber morphology are presented in Kupzcik et al. (2019).

RM_2: Buccally, a large enamel chip is evident at the occlusal margin of the mesiobuccal groove, essentially on the face of the Hyd and reaching nearly to the cervix, and a smaller chip is present distobuccally adjacent to the Hld. Smaller enamel chips line the occlusal margins of both IPFs and sit lingually adjacent to End. The chip at the buccal groove is the largest and reaches nearly to the cervix, while the others are confined to the occlusal surface. The buccal contour has been altered by a large enamel chip at the occlusal surface. Enamel chipping has also altered the morphology of the mesiobuccal and distobuccal grooves. The crown is moderately worn, with large uncoalesced dentine patches over each buccal cusp and a tiny dentine pit on the End apex (stage 4). The Med is the highest of the preserved cusps, with a steep wear plane sloping buccally. Occlusal wear has removed most of the surface morphology, but remnants of the occlusal fissures remain. The crown has a Y-5 fissure pattern, with a substantial portion of the Med and Hyd in contact, and a well-developed Hld. The central groove is deep, while the

4005 remaining grooves separating Prd from Hyd, Med from End, and End from Hld are
4006 weaker. Although somewhat obscured by the large enamel chip at the buccal groove, in
4007 occlusal view the buccal profile was mildly bi-lobed, while the lingual profile is
4008 straighter. No trace of a protostylid is detectable. Though interproximal wear reduced the
4009 MD length of all the molars, the M_2 is larger in area than the M_1.
4010 Alveolar bone is broken irregularly along the buccal side, exposing small portions
4011 of the mesial and distal roots. Damage to the alveolar bone is greatest along the distal
4012 root, where approximately 2.0 mm of the root is exposed. Along the mesial root,
4013 approximately 2.0 mm of the root is exposed. The root surfaces are well preserved, with
4014 only minor abrasion evident. Further details of root and pulp morphology are presented in
4015 Kupzcik et al. (2019).
4016 RM_3: There are two small enamel chips along the DMR and others at the apices
4017 of the End and Med. Interproximal wear excavated into the mesial margin of the crown.
4018 The crown is mildly worn and much of the cuspal relief has been reduced. Only small
4019 dentine pits are exposed on the Prd and Hyd and the principal fissure pattern is preserved
4020 (stage 2). The Med apex represents the high point of the occlusal surface. The five
4021 principal cusps are present and oriented in a Y-fissure pattern. Cusp 7 is absent and there
4022 is no suggestion of a C6 from the preserved occlusal fissure pattern. In size, the cusps are
4023 ordered as Med = Prd > Hyd > Hld > End. The crown is BL-broadest across the mesial
4024 cusps and tapers distally so that the Hld is placed just buccal to the center of the crown.
4025 The Hld itself projects quite far distally. The central groove separating the Prd and Med is
4026 deep and curves around the mesial aspect of the Med to form a small Fa. The MMR and
4027 DMR are each worn away as distinct topographical features. The mesiolingual face is

smooth, but a faint indentation represents a weakly expressed protostylid. The mesiobuccal groove is deep and forms a cleft near the occlusal margin. It is oriented somewhat mesially. The distobuccal groove is barely perceptible and fades away at mid-crown. The lingual groove is faint but continues to the cervix. The M_3 is the largest molar in the sequence. The alveolar bone is undamaged, and the roots are not exposed either buccally or lingually; details of root and pulp morphology are presented in Kupzcik et al. (2019).

U.W. 101-010: RC_1–RP_3 (Fig. 42; Table 1) A portion of the right mandibular corpus holds the heavily worn crowns and roots of the canine and P_3. The morphology of the mandible is described in Laird et al. (2017).

RC_1: Nearly the entire crown has been removed by wear, with only a thin rim of enamel remaining distolabially (stage 7), and the pulp cavity is exposed at the surface. What is likely postmortem chipping is present mesially and labially; though, it seems that enamel would not have remained in that area. Polishing on the dentinal surface indicates that the tooth was in use at the time of death. The wear surface dips strongly towards the cervix mesially and lingually.

The surface of the exposed root is covered in cementum, which is extensively cracked. The root is roughly circular in cross section, with its LaL breadth slightly exceeding its MD length. Labially, 15.6 mm of root are exposed below the worn occlusal surface and the apex of the root is hidden in the alveolus.

This specimen is of comparable wear to that of the U.W. 101-359 LC_1; though, the absence of any remaining detailed crown morphology limits the inference that these specimens represent antimeres.

RP_3: Enamel chipping is evident along the occlusal margin above the buccal aspect of the distal IPF (5.4 mm BL by 2.1 mm OC). A mesial IPF is also evident, but its shape is obscured by contact with the distal surface of the canine. The crown is significantly worn; only an enamel ring circumscribes the crown and a small amount of enamel remains on the distolingual corner (stage 6–7). As a result of the extensive wear, little occlusal detail remains. A short segment of the lingual arm of the transverse groove remains distal to the metaconid. The distance from that remaining groove to the distal crown, combined with the profile of the crown, suggests an expanded talonid comparable to less worn Dinaledi P_3s. Abrasion to the alveolar bone exposes two roots: approximately 6.5 mm of the mesial root and 3.0 mm of the distal root are visible. The presence of two roots is confirmed through inspection of the µCT scans. The mesiobuccal root is the smaller of the two, with the distal root BL-expanded. The roots share a common canal at the cervix but are individuated for more than half their heights. The distal root itself has two distinct canals throughout much of its course. Thus, the roots correspond to the 2R: MB +D configuration of Wood et al. (1988).

U.W. 101-361: root fragment, LM_2–LM_3 (Fig. 43; Table 1) This specimen preserves much of a left mandibular corpus with LM_2 and LM_3 in place. The mandible is broken lateral to the symphysis and along the alveoli of the postcanine dentition. The break plane slopes inferiorly from the posterior molars. Thus, the M_3 alveolus is preserved intact and

the distal root of the M_2 sits in its alveolus, while the mesial root of the M_2 is exposed. Lingually, the mandible is damaged along the M_2 alveolar margin, exposing both the mesial and distal roots. The morphology of the mandible is described in Laird et al. (2017). As elaborated upon in the Discussion, a mandibular condyle, U.W. 101-196, is refit to the corpus and articulates with the DH3 cranium (Berger et al., 2015).

Specimens U.W. 101-357 to U.W. 101-359 were recovered from fragments and sediments associated with this specimen. These specimens express advanced occlusal wear and are from the left side and likely belong to a single biological individual.

Associated Root: LP_4? (not figured): This is a single ovoid root with a groove running along one side and a small piece of enamel adhering to the surface. The preserved occlusal surface was a functional surface with polished dentine. There is some abrasion apparent on the root near the enamel remnant and there is substantial damage to the side of the root opposite the enamel. The maximum height of the root is 13.9 mm and its maximum width is 7.1 mm.

LM_2: A prominent BL crack at mid-crown, effectively in the space between the mesial and distal roots, splits the tooth into mesial and distal portions. The entire enamel cap is removed by wear (stage 8). Much of the exposed dentine is polished, and the center of the occlusal basin is extensively scooped out by wear. The high point of the occlusal surface is the mesiolingual corner, while the wear plane dips so that the low points are the mesiobuccal and distobuccal corners.

The mesial root is exposed, while the distal root is obscured from view by alveolar bone. The exposed mesial root is covered in a thick layer of cementum. On the

mesiolingual corner of the mesial root, a notch is apparent near the occlusal margin. The contours of the notch are rounded, and it appears that it formed after the enamel cap was removed during life and the occlusal surface contour continued to wear into the exposed dentine. The maximum breadth of the mesial root in is 10.9 mm. Further details on the morphology of the in-situ roots are found in Kupczik et al. (2019).

LM_3: There is a large, wide mesial IPF present; its OC height has been reduced buccally by extensive occlusal wear. The crown is extensively chipped around the occlusal margin. A flake is missing in the lingual groove, another is evident extending mesially from the mesiobuccal groove, and multiple chips are present in the mesiolingual corner. A deep dentine pool extends from the Hyd to the Prd. The pool is narrowest distally and broadens over the Prd. The entire Prd, nearly down to the cervix, has been removed by wear. The Hyd has a large but shallower pool of dentine over its apex. Small pits of dentine are also exposed over the Hld and Med (stage 5). Little occlusal detail is preserved. The crown is broadest across the mesial cusps and tapers distally. The buccal margin of the tooth is straighter than the lingual margin, so that the most distal point is just buccal to the midpoint of the crown. The roots are not visible externally; however, their morphology is described in Kupczik et al. (2019).

U.W. 101-377+U.W. 101-1014: RC_1–RM_2 (Fig. 44; Table 1) U.W. 101-377 is a partial mandibular corpus of a sub-adult that contains RP_3–RM_2. The mandible is described in Laird et al. (2017). Details on root formation and dental eruption sequence are in Cofran and Walker (2017). The mandibular fragment also includes the distal portion of the right canine alveolus. An isolated RC_1, recovered separately and catalogued as U.W. 101-

1014, is now refit to the U.W. 101-377 mandible. The canine is described here with the remainder of the U.W. 101-377 dentition.

The teeth found in the mandible all have proposed antimeres. Further, a complete set of incisors (U.W. 101-998, -1005A, -1005B, and -1005C) likely belongs to this individual as well. If these proposed associations are correct, they represent one of the most complete mandibular dentitions of *H. naledi*.

RC_1: A large oblong IPF (2.5 mm IC by 2.3 mm LaL) is situated high on the mesial shoulder. A distal IPF is also evident, though its true extent is obscured by the P_3. Wear blunted the mesial crest near the apex, while wear along the distal crest is more extensive and created a J-shaped contour in labial view (stage 1). The crown appears tall in height relative to its narrow basal size (Table 1). The crown is asymmetric, with the apex placed distal to the MD midpoint. The mesial crest is short and convex, while the distal crest, which is partially obscured by contact with the mesial face of the P_3, is longer and more vertically oriented. The distal crest terminates at a tubercle that sits more cervically than the mesial shoulder. The labial grooves are both shallow and indistinct. Lingually, a few minor ridges run from a flat and indistinct median lingual ridge towards the mesial crest; otherwise, the lingual fossa is featureless. The MMR is low and rounded and the DMR is barely present, in part because the distal IPF eats into the DMR. Linear hypoplasias are evident in the lower third of the labial crown and near the lingual cervix.

The mandibular corpus in the region of the canine alveolus is broken labially and lingually, exposing a portion of the root in these regions. The root is entirely exposed in mesial view, where it measures 13.8 mm in height from the tip of the embrasure at the cervix. Abrasions are evident to the mesial, labial, and lingual sides of the root and the

distal side is now obscured from view by refitting. As judged from µCT scans, the apex of the root is open (see also Cofran and Walker, 2017).

This specimen is the probable antimere of U.W. 101-1076. The two canines are similar morphologically, in wear, in the position, size, and shape of the IPF, and in the position and type of hypoplasias on their labial faces. Further, this specimen reasonably articulates with the U.W. 101-1005C RI_2.

RP_3: The crown is lightly worn, with an elongated facet along the distal Prd crest that runs onto the buccal aspect of a distobuccal cuspule (stage 1). The Prd and Med are well developed and separated by a well-defined, uninterrupted Mlg. The Med area is slightly smaller than the Prd and its cusp apex is sub-equal in height. The Fa is a BL-oriented groove with extensions both lingual and buccal to the Mlg. It is bounded distally by mesial accessory ridges of the Prd and Med. The Prd mesial accessory ridge is more prominent than the one extending from the Med. The MMR forms a continuous rim extending from the Med to the Prd. In mesial view, it dips slightly at the Mlg and is lower than the mesial Prd and Med accessory crests. The Prd and Med essential ridges are strongly developed, although not sharply defined. The talonid is polished; however, a small cusplet, defined by buccal and occlusal grooves and a less distinct, but well developed, distolingual portion, is palpable distobuccally. Though wear removed some relief in the distal aspect of the talonid, the DMR is not detectable topographically as a feature distinct from the planar surface of the talonid. The mesiobuccal groove is faint and does not continue onto the occlusal rim, whereas the distobuccal groove is deeper at the occlusal rim. Both become imperceptible about a third of the way down the buccal face. Faint linear hypoplastic defects are apparent near the cervix on the buccal face. In

lingual view, the trigonid portion of the crown is much higher than the talonid portion. The lingual face is featureless.

The crown and roots are in situ in the mandible, with approximately 2.4 mm of the root mass exposed in buccal view. Examination of the µCT scans shows that two roots are present and conform to the 2R: MB + D pattern of Wood et al. (1988). In contrast to some other *H. naledi* P_3s, the mesiobuccal and distal roots do not become completely individualized until near their apices; in fact, their root canals are connected by an isthmus throughout most of their lengths.

Based upon similarities in morphology and the state of occlusal wear, this tooth is the antimere of the U.W. 101-889 LP_3.

RP_4: Wear is minimal, with a minor facet on the Prd apex and no dentine exposure (stage 1). The Med and Prd are separated by a well-defined Mlg. The Med is slightly smaller in area than the Prd, but equal in height. The apex of the Med sits well mesial to that of the Prd. The MMR is low and continuous and encloses a shallow Fa, which is a short and shallow groove with its deepest point where it meets the Mlg. It is bordered distally by the mesial accessory crests of the Prd and Med. The Med mesial accessory crest is rounded and originates from the cusp apex, while the Prd mesial accessory crest is better defined and originates as an extension of the mesial lobe. The essential ridges of the Prd and Med are well developed, rather broad, and not very distinct. The talonid is defined mesially by a deep transverse groove. Mesial to this groove, the Prd and Med possess distinct distal accessory ridges. Shallow indentations radiate distally from the transverse groove and the DMR is not distinct from the talonid. The buccal face is indented by shallow mesial and distal grooves, with the distal groove

4187 better defined than the mesial. Both extend about a third of the way down the face before
4188 becoming indistinct. There is no mesiolingual groove and but a faint and shallow
4189 distolingual indentation near the occlusal margin.
4190 Very little of the root is visible; though, an inspection of the µCT scans shows
4191 that this specimen has a single root that is round in cross section.
4192 Based upon similarities in occlusal and root morphology and occlusal wear state,
4193 this is the proposed antimere of U.W. 101-887.
4194 RM_1: Wear facets are evident on all cusps and a very small dentine pit is present
4195 on the Prd apex (stage 2). In occlusal view, the crown is nearly equally BL-broad across
4196 the trigonid and the talonid and the crown outline is roughly rectangular. The large Hld
4197 projects distally, forming the rounded distobuccal profile, and the buccal profile is deeply
4198 indented by the buccal grooves. Substantial interproximal wear resulted in a concave
4199 mesial contour. The crown has a Y-5 fissure pattern, with a substantial portion of the
4200 Med and Hyd in contact. The relative cusp sizes are Hyd > Prd > Med > Hld > End. Most
4201 of the MMR has been removed by interstitial wear; what remains is low and thin. The
4202 remnant of a small, pit-like Fa remains visible with a portion of it extending lingually
4203 onto the Med. The Fp is little more than a pit at the termination of the central groove and
4204 bordered mesially by weak distal accessory ridges of the End and Hld. The protostylid is
4205 limited to the mesiobuccal portion of the Prd and takes the form of a faint, but palpable,
4206 oblique crest that terminates mesial to the mesiobuccal groove. This groove is deep,
4207 forming a narrow cleft near the occlusal margin and broadening at mid-crown into a
4208 shallower groove that continues to the cervix. The distobuccal groove is partially
4209 obscured by matrix, but it was evidently shallower and shorter than the mesiobuccal

groove, fading away shortly after crossing the occlusal margin. The main lingual groove is placed slightly distal to the mesiobuccal groove. While deep at the occlusal margin it quickly becomes shallower and disappears at mid-crown. The distolingual groove is little more than an indentation near the occlusal margin.

Approximately 4.5 mm of the mesial buccal root is exposed by a break in the alveolar margin; though, little can be discerned of its morphology. Details of its morphology are provided by Kupczik et al. (2019) based upon an analysis of µCT based data.

Based upon similarities in morphology and wear state, this is a reasonable antimere of the U.W. 101-809 LM_1.

RM_2: A mesial IPF is present but, consistent with the developmental status of the individual, there is no distal IPF. The tooth was erupting at death (Cofran and Walker, 2017); however, a small wear facet is visible on the mesial to the Prd apex (stage 1). In occlusal view, the crown is roughly rectangular in profile, with a slightly wider talonid than trigonid. The lingual and mesial profiles are more-or-less straight, the buccal profile mildly bi-lobed, and distal profile convex because of a large Hld placed slightly buccal of center. The crown has a Y-5 fissure pattern, with a substantial portion of the Med and Hyd in contact. The relative cusp sizes are Med > Prd > End ≥ Hyd > Hld. The cusps do not possess well-defined essential ridges. The weak Med essential ridge travels towards the Mlg and then deflects distally to meet the Hyd (deflecting wrinkle). It also possesses a thin, but well-defined distal accessory ridge that takes the form of a small cuspule in lingual view. Although not a 'true' cusp 7 as defined by the ASUDAS, Skinner et al (2008: 179) have referred to this as "Metaconulid-type on the distal shoulder of the

Med." The End has a mesial accessory ridge that is independent of the cusp apex and meets the essential lobe near the occlusal basin. The MMR is not well defined and is lower than the essential lobes of the Prd and Med in mesial view. The majority of the groove-like Fa is situated mesial to the Med with a slight buccal extension onto the Prd (this is slightly different than the configuration seen on its proposed antimere). A moderate but shallow Fp is formed by grooves separating the End and Hld essential lobes from their distal accessory lobes, which comprise an indistinct DMR. The mesiobuccal groove is quite deep and narrow occlusally and becomes shallower and wider as it continues to the cervix. The distobuccal groove is much wider but shallower occlusally and is imperceptible by mid-crown. The mesiolingual groove is absent and the distolingual groove is a shallow triangular depression near the occlusal margin. The protostylid is evident as the faintest of swellings confined to the mesiobuccal aspect of the Prd. It begins as a vertically oriented crest that curves around distally to become indistinct half the distance to the mesiobuccal groove.

Matrix adheres to the crown mesially, along the buccal grooves, distally, and around the base lingually. The distal root is exposed in lingual and distal views. The distal root appears to be broken apically. In distal view, approximately 3.2 mm of root are exposed. Examination of the µCT scans indicates that the mesial root, which is preserved fully in situ, was open at death (see also Cofran and Walker, 2017).

Although not identical (the configuration of the Fa is slightly different), based upon morphological similarities and shared ontogenetic status, this is proposed as the antimere of U.W. 101-789.

U.W. 101-1142: RM_2–RM_3 (Fig. 45; Table 1) A fragment of mandibular corpus and ramus preserves M_2 and M_3 in situ. Portions of the alveoli for the M_1 mesial and distal roots are also present. An isolated RM_1, U.W. 101-1287B, fits into the preserved alveoli and its distal IPF is a match for the mesial IPF of the U.W. 101-1142 RM_2. The morphology of the mandible is described in Laird et al. (2017) and its neoplastic pathology is discussed in Odes et al. (2018).

RM_2: Enamel chips are present along the mesial and distal margins, above the respective IPFs. A large mesial IPF (7.4 mm BL by 3.5 mm OC) extends to the occlusal margin. The entire crown is smoothed by wear and small dentine pits are exposed on the Pr, Hy, and Hld (stage 2). Although worn, the crown retains its Y-5 fissure pattern, with a substantial portion of the Med and Hyd in contact. The occlusal topography of the crown is worn down; though, the Hyd appears relatively large. In fact, an investigation of the EDJ shows that two distinct, and nearly equally large, dentine horns are present distobuccally. Thus, this specimen likely would have expressed a C6 that is nearly the same size as the Hyd. No other M_2 in the current sample has a similar configuration distobuccally; however, a similar configuration is present at the EDJ of the M_3 of this individual. In occlusal view, the crown is roughly rectangular and with a slightly broader talonid than trigonid. The lingual profile is straight, while the buccal profile is mildly bi-lobed. The MMR and Fa are flattened by occlusal wear and obscured by interproximal wear. Mesiobuccally, trace expression of the protostylid is visible. The mesiobuccal groove is narrow and deep near where it crosses the occlusal margin; it fades at mid-crown and then appears again just above the cervix. The distobuccal groove is shallow at

the occlusal surface. Buccally, the alveolus is damaged, exposing approximately 3.5 mm of the mesial and distal roots. The lingual alveolar margin is undamaged.

RM_3: Enamel chipping is present along the mesial margin above the IPF, along the distolingual margin, and on the End apex. The crown is polished by wear, but no dentine is exposed (stage 1). The M_3 is larger in area than the M_2. In occlusal view, the lingual profile is mildly convex, the buccal profile is slightly bi-lobed, and the distal contour is convex with its distal-most point slightly buccal to midline. The talonid is wider than the trigonid and the crown is broadest at mid-crown before tapering distally. The crown has a Y-5 fissure pattern, with a substantial portion of the Med and Hyd in contact, and a well-developed Hld. The relative cusp sizes are Prd > Hyd > Med > Hld ≥ End. Some definition of the Prd essential ridge remains. Lingually, there are swellings on the mesial End crest, distal End crest, and distal Med crest. None are associated with grooving on the lingual face that suggests distinct, individualized cusps in the unworn state. The apparent area of the of Hld is quite large. Though the presence of a C6 is not evident at the outer enamel surface due to occlusal wear, an investigation of the EDJ surface show that two distinct dentine horns are present distobuccally, which indicates the likely presence of C6 that is nearly equal in size to the Hld. Another dentine horn is present distolingually; above that dentine horn at the outer enamel surface is an enamel chip that obscures the occlusal topography of the region. The expression of the MMR is obscured by wear, but a hint of the Fa groove can be seen passing mesial to the Med. The Fp remains as a small pit at the termination of the groove between the End and Hld. A weak protostylid is expressed as an oblique crest restricted to the mesiolingual corner of the Prd. The buccal grooves are both broad and shallow. Though the mesiobuccal groove

is more distinct than the distal, both lack the narrow cleft at the occlusal surface observed in many other *H. naledi* molars. There is no detectable lingual groove.

U.W. 101-1261: complete mandibular dentition (Fig. 46; Table 1) The specimen was recovered in numerous fragments that were initially assigned separate accession numbers (Laird et al., 2017: Table 2); upon refitting, a single accession number, U.W. 101-1261, is now assigned to the mandible and all the teeth. Damage to the alveolar bone is minor, but present throughout: the LM_1 alveolus is damaged, exposing a portion of the LM_1 distal root; the LP_3 alveolus is damaged, exposing most of the mesial root and a portion of the distal root; the area around the left canine is damaged, exposing a portion of its root; the labial alveolus across the incisal region is damaged; a portion of the right canine root is exposed; there is a clean break between RM_1 and RM_2 that exposes the distal root of the RM_1 and the mesial root of the RM_2; damage is evident to the lingual and distal alveolar margin near the LM_3; and the mesial root of the LM_1 is exposed. The morphology of the mandible is described in Laird et al. (2017). The U.W. 101-1261 dentition is associated with the U.W. 101-1277 partial maxillary dentition, its possible antimere RM^1 U.W. 101-1463, and the U.W. 101-1269 LM^3.

Left and Right I_1: Both I_1 roots are exposed labially for approximately 7.0 mm. At the point of exposure, the roots and crowns of the incisors broke cleanly from the mandible and have been refit.

The central incisors are worn, with wide dentine exposure along their incisal edges and enamel rims intact (stage 4–5). The incisal wear plane angles lingually, slightly more so distally than mesially. On both crowns, the labial face is featureless and more-or-

less flat. The lingual surface is flat, and the base is offset mesially. Marginal ridges were probably present, but wear precludes assessing their expression. There is no median lingual ridge.

Left and Right I_2: The RI_2 and LI_2 alveoli are damaged on the labial side. The LI_2 broke away with the central incisors. The RI_2 is apparently unbroken but became dislodged from its alveolus when the break to the incisors occurred. Lingually, the alveoli are also slightly damaged.

The crowns are worn, with wide dentine exposure across their incisal edges and intact enamel rim (stage 4–5). The wear plane is angled lingually, more so along the MMR than along the DMR. Labially, the crowns are featureless, with hypoplastic defects evident in the cervical third. Lingually, the mesial margin of the tooth is straighter than the distal, which is convex near the incisal edge. The lingual surface is flat and marginal ridge development has been mostly removed by wear.

Left and Right C_1: There is damage to both the left and right canine alveoli that exposes approximately 6.2 mm of the left root and approximately 2.6 mm of the right root. There is less damage to the lingual alveoli.

Both crowns are similarly worn. Exposed dentine extends from the mesial crest, across the apex, and terminates at or before the distal tubercle (stage 4). The wear surface is not planar, and, in labial view, there are distinct mesial to the distal wear facets that meet at the apex. Wear obscures some of the crown contours; however, it is apparent that the teeth show the typical *H. naledi* canine feature set. For example, the mesial shoulder sits higher than the distal shoulder and a faint distal labial groove is detectable adjacent to a small distal tubercle. Lingually, the MMR is strongest near the occlusal edge, while the

DMR, if present, is worn away. The wide median lingual ridge barely rises above the lingual fossa. There is a very narrow groove adjacent to the MMR and a deeper, but narrow, groove adjacent to the DMR. Multiple linearhypoplasias are evident in the lower third of the crown.

Left and Right P_3: The alveolus of the RP_3 is mostly undamaged but that of the LP_3 is heavily damaged, exposing most of both roots in buccal view and large portion of the distal root in lingual view.

For both crowns, enamel chips are present along the distal margin above the IPF. Occlusal wear is slightly more advanced on the LP_3 than the RP_3. For the LP_3, dentine is exposed over the Prd apex, and a smaller pit is exposed over the Med apex (stage 2). The RP_3 only has dentine exposed on the Prd; as a result, its Med retains more topographical relief than that of the LP_3. The P_3s are fully bicuspid and much of the course of the Mlg can be detected on the RP_3. Most of the detail of the Fa is worn away; though, in each case, the groove appears to curve slightly to the lingual side around the Med. Details of talonid morphology are better preserved on the RP_3; for both, the transverse fissure bifurcates slightly at its lingual end. Both P_3s possess faint mesiobuccal and distobuccal grooves. The mesiobuccal groove is shallower than the distal and does not extend as far down the crown. For the more worn LP_3, only the faintest trace of the distobuccal groove remains. The lingual face is featureless.

The root morphology can be determined from the more exposed LP_3 roots. On the buccal aspect, there is a clear separation between the mesial and distal root canals. On the lingual aspect, the distal root appears broader than the mesial, which is offset buccally relative to the distal root. Examination of µCT confirms that both P_3s are two rooted and

4370 that the mesial and distal roots are completely individualized just below the crown and
4371 conform to the 2R: D+MB pattern (Wood et al., 1988) seen in the other *H. naledi* P_3s.
4372 Left and Right P_4: The alveolus is nearly complete for the LP_4, while that of the
4373 RP_4 is minimally damaged along the lingual edge. Both crowns exhibit enamel chipping
4374 on the distal margin. The damage is more apparent for the RP_4, where a large enamel chip
4375 is missing just above the distal IPF. Minor enamel chipping is also evident above the
4376 mesial IPF. For the LP_4, a smaller chip is missing from the distal margin just above the
4377 IPF, and a second, smaller, chip is evident buccally. Small dentine patches are exposed
4378 over the Prd of both P_4s (stage 3). The RP_4 occlusal topography is better preserved than
4379 the LP_4. Both crowns are fully bicuspid with a well-defined Mlg. A thin, high crest
4380 interrupts the Mlg and connects the mesial aspects of the Prd and Med, defining the Fa
4381 distally. The Med is smaller in area than and its apex sits slightly mesial to that of the
4382 Prd. For both crowns, the MMR is worn, and the Fa is preserved as a small pit at the
4383 mesial termination of the Mlg. For the LP_4, very little is preserved of the buccal or lingual
4384 extensions of the transverse groove. For the RP_4, the fissure has a small lingual
4385 bifurcation; additionally, there a small deflection evident distobuccally where the groove
4386 and Mlg meet, which probably reflects an accessory ridge extending from the Prd as is
4387 common on other *H. naledi* premolars. For both P_4s, the mesiobuccal and distobuccal
4388 grooves are faint. The lingual aspects of both crowns are featureless.
4389 Examination of the µCT scans of the roots embedded in the mandible show that
4390 left and right teeth differ slightly in their root configuration. Both have distinct mesial
4391 and distal root canals for most of the roots' courses. However, the mesial and distal roots
4392 of the RP_4 are externally connected for much of their length with a very deep invagination

evident buccally and a shallower one lingually. For the LP_4, the mesial and distal roots are completely individualized for nearly half of their lengths. For the RP_4, the distal root is MD compressed, while the mesial root is obliquely oriented and runs from mesiobuccal to distolingual. For the LP_4, the major axes of both roots are parallel and approximately BL-oriented with the mesial root offset more to the buccal side than the more centrally placed distal root.

Left and Right M_1: The alveolus of the left tooth is undamaged. In contrast, damage is extensive to the alveolus of the right tooth where an ancient break cleanly separated the mandibular corpus between the first and second molars. As preserved, about 2.0 mm of the mesial RM_1 root is exposed buccally and approximately 10.3 mm of its distal root is exposed buccally. Additionally, a portion of the distal face of the distal root is also visible in the region of damage.

Both M_1s exhibit chipping to the distal margin above the IPF. On both crowns, concave dentine pools are exposed over the Prd, Hyd and Hld apices (stage 4). The LM_1 is slightly more worn than the RM_1. Both crowns are a rounded rectangle in occlusal view, with a concavely worn mesial margin and a flattened distal margin. The lingual margin is more-or-less straight, and the buccal margin is gently bi-lobed. Both crowns have five primary cusps and no accessory cusps. Although worn, the crowns retain a Y-5 fissure pattern, with a substantial portion of the Med and Hyd in contact and a well-developed Hld. The talonid is slightly wider than the trigonid in both crowns. For each, the Fa and MMR are worn, but a trace of the Fa is preserved as a short lingually-deflected extension of the central groove. A remnant of the mesiobuccal groove is preserved as a narrow and deep cleft near the occlusal margin that becomes shallow at mid-crown and

deepens again just above the cervix. The distobuccal and lingual grooves are shallow at the occlusal margin and fade away mid-crown. There is no indication of a protostylid preserved.

Left and Right M_2: The RM_2 has enamel chipping along the mesial margin of the Med and just above the IPF. The LM_2 is only obviously chipped along the MMR. Both crowns have moderate occlusal wear, which has flattened the cusps but no dentine is exposed (stage 2). The M_2s are larger than the M_1s in area but smaller than the M_3s. The crown is pentagonal in occlusal profile, with straight mesial and lingual profiles, mildly bi-lobed buccal profile, and relatively large Hld rounding the distal profile. In both M_2s, the talonid is wider than the trigonid. Both crowns have five principal cusps arranged in a Y-5 fissure pattern, with a substantial portion of the Med and Hyd in contact, and a well-developed Hld. The relative cusp areas are Hyd > Med ≥ End ≥ Prd > Hld. The pattern of grooves is better preserved on the right crown; though, there are no traces of supernumerary cusps for either. For each crown, the Fa is small and primarily a slight buccal extension of the central groove. Most of the MMR is obliterated by interproximal wear so that its expression cannot be assessed. The mesiobuccal groove is a narrow and deep cleft near the occlusal margin that becomes shallow at mid-crown. The distobuccal groove and lingual groove are both faint indentations in the crown face that disappear at mid-crown. Neither tooth presents any indication of a protostylid.

Left and Right M_3: There is slight damage to the lingual and distobuccal alveolus of the LM_3. The distobuccal damage represents a clean break between the corpus and the ramus of the mandible. The apices of the Prd, Hyd and Hld are blunted by occlusal wear and a wear facet is visible along the mesial aspect of the Med, but no dentine is exposed.

The lingual cusps remain mostly unworn (stage 1). The crown has five primary cusps arranged in a Y-5 fissure pattern, with a substantial portion of the Med and Hyd in contact, and a well-developed Hld. There are no accessory cusps. Relative cusp sizes are Med > Prd > Hyd > End > Hld (a large protostylid is included in the relative Prd area). The trigonid is wider than the talonid and the crown tapers distally. The wide and rounded MMR is lower than the essential crests of the Prd and Med. The fissure-like Fa appears as a lingual extension of the central groove, with a separate buccal section bounded distally by a small accessory Prd crest. The essential ridges of the primary cusps are not well defined. There are accessory ridges visible, especially on the RM_3 distally on the Med and mesially on the End. The End accessory ridge is slightly more prominent than the Med. The Fp is a slight distolingual extension of the central groove and is better expressed on the RM_3 than the LM_3. The mesiobuccal groove is a deep, narrow cleft near the occlusal margin that becomes shallow at mid-crown, and the distobuccal groove is a faint indentation that disappears mid-crown. The lingual grooves are faint indentations. Both crowns have a large protostylid; they are, in fact, the most prominent in the current Dinaledi sample. The LM_3 protostylid is more pronounced than that on the RM_3. For the both, the protostylid begins as a mesiolingual crest and becomes a distinct shelf that angles sharply towards the mesiobuccal groove. On the RM_3, the crest merges with the crown just prior to the mesiobuccal groove, while on the LM_3 the crest stops just at the mesiobuccal groove and does not cross it. The LM_3 protostylid has a free apex, while the RM_3 lacks such an occlusal-ward projection.

U.W. 101-1400: LdC_1–LM_1 (Table 1) This subadult left hemimandible holds the crowns of the dC_1, dP_3, and dP_4. The germs of the developing LI_2 and LM_1 were recovered from their damaged crypts and are described above with the isolated teeth. The LC_1 germ is visible in its crypt, where it remains. Several isolated teeth are attributed to this individual as well (for details on dental development and eruption sequences, see also Cofran and Walker, 2017) and are iterated in the descriptions and in the Discussion.

LdC_1 (Fig. 47): Alveolar bone is primarily preserved distally. The tooth is glued onto the U.W. 101-1400 mandible. No mesial IPF is visible. Dentine is exposed at its apex (stage 1). In occlusal view, the crown is ovoid. In labial and lingual views, the crown is asymmetrical, with a short, high mesial shoulder and a long distal edge that terminates in a low distinct tubercle. The mesial border is moderately angled and convex, while the distal border is more steeply angled and slightly concave. The crown apex is slightly offset distally. On the lingual surface, there is a shallow mesial groove and a slightly deeper distal groove and ridge associated with a distal tubercle. A shallow furrow delineates the distal tubercle labially. The labial aspect is otherwise unremarkable. On the lingual aspect, a broad median ridge is bordered by a weak groove-like mesial fossa and a wider and deeper distal fossa. From the occlusal aspect, the slightly swollen basal eminence is distally oriented.

The root is broken at is apex and approximately 8.0 mm of root remains visible labially. The root is nearly circular in cross-section and only slightly narrower BL than LaL. There is a shallow mesial groove running along its length.

This tooth is proposed as the antimere of U.W. 101-1611.

LdP_3 (Fig. 47): The crown exhibits minor wear on the mesial Prd crest, the buccal face of the End, the apex of the Hyd, and the apex of the Hld (stage 2). Enamel chipping is evident along the DMR. The occlusal outline is rectangular, being elongated MD and narrow BL. The crown is wider BL across the talonid than across the trigonid. The crown has a Y-5 fissure pattern, with a substantial portion of the Med and Hyd in contact, and a well-developed Hld; in size, they are arranged as Prd > Hyd > Med > End > Hld. The tip of the Prd is markedly mesial to that of the Med and it is internally placed, so much so that it lies nearly along the midline of the tooth. The groove-like Fa is bounded by a thick MMR mesially and a prominent mesial trigonid crest distally that is incompletely bisected by the central groove. Two cuspules (mesioconulid and premetaconulid) are evident along the MMR. Each cuspule, though worn, appears to have a free apex. The mesiobuccal groove is a narrow v-shaped furrow occlusally, which gives the crown a pinched in or 'waisted' appearance in occlusal profile. The crown lacks a distinct DMR and Fp; though, occlusal wear reduced the crown's height distally. On the buccal aspect of the crown, a faint vertical furrow is associated with the mesiolingual cuspule of the MMR.

Damage to the alveolar bone exposes its mesial root along the entire labial extent. 9.1 mm of the mesial root are evident, which is approximately the full height of the root.

This is proposed as the antimere of U.W. 101-1685.

LdP_4 (Fig. 47): The occlusal surface is lightly worn, with a small wear facet visible along the mesial Prd crest (stage 1). The occlusal outline is rectangular, being MD elongated and BL narrow, and broader across the talonid than the trigonid. Five cusps are present and have the following size relationships: Hyd > Med ≥ Prd > End > Hld. The MMR is

thick and comprises three small tubercles (premetaconulid, mesioconulid and preprotoconulid) defined by shallow grooves on both the occlusal and mesial surfaces. The Prd and Med each have prominent mesial accessory crests, which meet to form a thick mesial trigonid crest that divides the Fa into two transverse grooves. Occlusal complexity is present as a triplet of small ridges on the Hyd and an incipient post-metaconulid associated with a shallow vertical furrow mesial to the buccal groove. Very faint accessory ridges are present on the End and Hyd. The components of the DMR originating from the Hld and End meet at an angle and delineate a groove-like Fp. The mesiobuccal groove is deep, forms a wide v-shaped fovea near the occlusal edge, and terminates at approximately mid-crown.

This specimen is the antimere of U.W. 101-1686.

LC_1 germ (not figured): The developing crown is visible in its crypt within the mandible. The description is based upon the morphology evident in the μCT images. Labially, the apex is offset distal to the MD midpoint. The mesial margin is convex and terminates at the mesial shoulder. A slight mesial labial groove runs adjacent to the mesial crest. The distal crest is vertically oriented. A distal shoulder is not yet formed; thus, this specimen would have had an asymmetric placement of the shoulders as seen in other *H. naledi* mandibular canines. Lingually, the median lingual ridge is offset distally relative to MD midpoint. It is indistinct and rounded and reaches its greatest relief near the apex. The mesial and distal lingual fossae are each broad and shallow, with the mesial fossa deepening and narrowing adjacent to the MMR. The mesial fossa is broader than the distal fossa.

This germ is the proposed antimere of U.W. 101-1610.

4. Discussion

4.1. Significant associations

There are several sets of antimeres and metameres that are proposed for the known Dinaledi Chamber teeth and enumerated above. Correctly associating isolated teeth has implications for reconstructing the taphonomic history of the fossils in the Dinaledi chamber and will inform assessments of the demography of the sample. As well, associating isolated teeth will permit a fuller evaluation of dental proportions, dental development, and metameric variation. Though a cautious approach is taken in proposing such associations, there are nine associations for which many isolated teeth and/or teeth in jaws can be associated. The justifications for associating these specimens are discussed in more detail and listed in Table 2. Not all antimeres identified in the main text are repeated below; we restrict the following discussion to those cases where multiple teeth can be associated with some certainty. We refer to each set of teeth as Association 1 – Association 9; however, we do not intend to imply that each set of teeth represents a distinct biological individual. Further research may reveal that some associations (e.g., Associations 3 and 4) represent the same individual. We arrange the associations below in ontogenetic order from youngest to oldest.

<u>Association 1 (infant)</u> The U.W. 101-1400 mandible holds the crowns of the Ld_c, LdP_3, and LdP_4 and the germs of the developing LI_2 and LM_1 were recovered from their damaged crypts. Further, the developing crown of the permanent left canine is visible on

4552 the μCT scans. The LM_1 is nearly crown complete, while the permanent canine is only
4553 approximately half crown complete.
4554 Based upon morphological similarity, the proposed right antimeres of the U.W.
4555 101-1400 teeth are: U.W. 101-1611 (Rd_c), U.W. 101-1685 (RdP_3), U.W. 101-1686
4556 (RdP_4), U.W. 101-1610 (RC_1 germ), and U.W. 101-1689 (RM_1 germ). These antimeres
4557 were all recovered from a single excavation block, block 1477, that also contains
4558 undescribed subadult cranial fragments (J.H., personal observation). Specimen U.W. 101-
4559 1612 (RdI_2) was also found in block 1477 and is provisionally associated with this
4560 individual. Consistent with that attribution is the lack of a distal IPF on U.W. 101-1612
4561 and a mesial IPF on U.W. 101-1611.
4562 Associating isolated maxillary and mandibular teeth must be approached with
4563 caution in a commingled assemblage; however, a reasonable case can be made that
4564 several isolated maxillary teeth are associated with this individual. Also recovered from
4565 block 1477 are an RdP^4, U.W. 101-1687, and an RM^1 germ, U.W. 101-1688. The RM^1
4566 germ is nearly crown-complete and matches the developmental status of the U.W. 101-
4567 1400 and U.W. 101-1689 mandibular molars. An isolated LM^1 germ, U.W. 101-1305, is
4568 the proposed antimere of U.W. 101-1688. These M^1s are nearly identical in morphology
4569 and developmental status. Assigning the U.W. 101-1687 RdP^4 to the same biological
4570 individual cannot be certain, but its spatial association with the subadult material and the
4571 degree of its macrowear are consistent with that observed in the U.W. 101-1400
4572 mandibular deciduous molars. The antimere of the RdP^4 is proposed to be U.W. 101-
4573 1376, which was excavated within centimeters of an LdP^3, U.W. 101-1377. Both U.W.
4574 101-1376 and U.W. 101-1377 lack adjoining IPFs, which is consistent with their

attribution to the same individual. Further, a pair of maxillary deciduous canines (U.W. 101-728 and U.W. 101-1287A) is provisionally assigned to this individual. Their status as antimeres is proposed on morphological grounds. Their association with the other maxillary teeth assigned to this individual is consistent with the absence of IPFs between adjacent teeth and the degree of macrowear on the deciduous mandibular canine in the U.W. 101-1400 mandible and its antimere. Rounding out the deciduous teeth assigned to this individual are a pair of antimeric dI^1s (U.W. 101-544C and U.W. 101-1331), an LdI^2 (U.W. 101-1304), and a pair of permanent maxillary canine germs (U.W. 101-544B and U.W. 101-1548). The status of the dI^1s as antimeres is proposed on morphological grounds and the congruency of their mesial IPF. The status of the permanent maxillary canine germs, U.W. 101-544B and U.W. 101-1548, as antimeres is based on their morphology and developmental stages. Their developmental status matches that of the canine germ found in its crypt in the U.W. 101-1400 mandible. Finally, two developing antimeric M^2s, U.W. 101-1063 and U.W. 101-1135, and a developing M_2, U.W. 101-1002, may belong to this individual as well. Their association is tentative but consistent with their developmental status.

If these proposed associations are correct, then all deciduous tooth classes, except for the mandibular deciduous central incisor, are represented for this individual. Further, all four nearly crown-complete M1s are represented and so are all four permanent canine germs, which are approximately half crown complete.

Association 2 (sub-adult) The U.W. 101-377 mandible contains the crowns of RP_3–RM_2 in their alveoli and an isolated canine, U.W. 101-1014, is refit to this specimen. The roots

of the canine and M_2 are open, indicating that these teeth were erupting at the time of death (Cofran et al., 2017). The U.W. 101-377 mandible is described as a 'late juvenile' in Bolter et al. (2020). Based on morphological details and stage of occlusal wear, each of the U.W. 101-377/1014 teeth have proposed antimeres on the left side. From mesial to distal, these are U.W. 101-1076 (LC_1), U.W. 101-889 (LP_3), U.W. 101-887 (LP_4), U.W. 101-809 (LM_1), and U.W. 101-789 (LM_2). The assignment of the isolated left teeth to the same individual is consistent with the shapes and sizes of their IPFs. An RI_2, U.W. 101-998, has a complexly shaped distal IPF that is perfectly congruent with the mesial IPF of the U.W. 101-1014 RC_1 and likely belongs to this individual as well. Importantly, U.W. 101-998 has a proposed antimere, U.W. 101-1005C, which is part of a set of spatially associated mandibular incisors (U.W. 101-1005A, U.W. 101-1005B, and U.W. 101-1005C). The assignment of these anterior teeth to this individual completes the left and right dental arcades (to the M_2) for an individual that died while the M_2s and C_1s were erupting. There are only two isolated M_3s in the current Dinaledi assemblage (i.e., U.W. 101-006 and U.W. 101-516) and both have mesial IPFs and occlusal wear, which indicates that neither belong to this individual.

Association 3 (sub-adult/young adult): As indicated by their morphological similarity and the shapes of their adjoining IPFs, a complete set of lightly worn maxillary incisors and canines from a single individual may be formed by U.W. 101-706 (LC^1), U.W. 101-932 (LI^2), U.W. 101-931 (LI^1), U.W. 101-1012 (RI^1), U.W. 101-709 (RI^2), and U.W. 101-816 (RC^1). Relating these specimens to postcanine teeth cannot be certain because the canines lack distal IPFs and there are several lightly worn P^3s in the assemblage that lack mesial

IPFs (i.e., U.W. 101-182, U.W. 101-729, U.W.101-786, and U.W.101-1107). There are clearly several individuals of similar late sub-adult/young adult ontogenetic status in the assemblage.

Association 4 (subadult/young adult) An associated set of lightly worn mandibular anterior teeth, U.W. 101-1126 (LC_1), U.W. 101-1131 (LI_2), U.W. 101-1132 (LI_1), U.W. 101-1133 (RI_1), U.W. 101-1075 (RI_2), and U.W. 101-886 (RC_1) is suggested to belong to a single individual. This proposal is based on morphological grounds and the congruency of IPFs. Four of the teeth, U.W. 101-1126, U.W. 101-1131, U.W. 101-1132, and U.W. 101-1333 were excavated in anatomical contact, making their association certain. Both canines attributed to this individual lack distal IPFs, which complicates attempts to link this set of teeth to the postcanine dentition. There are two sets of proposed antimeric P_3s (U.W. 101-298/1565 and U.W. 101-144/506), which are both lightly worn and lack mesial IPFs. As with the lightly worn maxillary teeth in Association 3 discussed above, there are clearly several individuals of comparable late sub-adult/young adult ontogenetic status in the assemblage.

Association 5 (adult) A set of maxillary left postcanine teeth extending from LP^4–LM^3 for a single individual is arguably formed by U.W. 101-277 (LP^4), U.W. 101-1676 (LM^1), U.W. 101-1522 (LM^2), and U.W. 101-418C (LM^3). These associations are tentative and supported by the shapes and sizes of the respective IPFs. Though not confirmatory, especially given the high frequency of enamel chipping in the assemblage, patterns of interproximal enamel chipping are consistent with these attributions. Based on

morphological similarity, U.W. 101-525 (RM^1) and U.W. 101-594 (RM^3) may be antimeres of U.W. 101-1676 (LM^1) and U.W. 101-418C (LM^3), respectively.

Association 6 (adult) A set of moderately worn adult maxillary teeth formed by U.W. 101-1403 (RC^1), U.W. 101-1402 (RP^3), U.W. 101-1401 (RP^4), and U.W. 101-1396 (RM^1) are proposed to be associated. Supporting this inference, the RC^1 through RP^4 were excavated in anatomical contact. A comparably worn set of left teeth, U.W. 101-1556 (LC^1), U.W. 101-1560 (LP^3), and U.W. 101-1561 (LP^4) are also derived from a single individual. An LI^2, U.W. 101-1684, is arguably associated with U.W. 101-1556 based upon the shape and size of their adjoing IPFs and their degree of macrowear. The IPFs of the left canine through P^4 are perfectly congruent with one another. Given their stage of wear, it is difficult to confirm that the left and right teeth are antimeres, but their size, premolar root morphology, and patterns of macrowear are consistent with this assessment. Unfortunately, U.W. 101-1403 lacks a crown, which complicates attempts to confirm that it is the antimere of U.W. 101-1556.

Association 7 (adult) A complete mandibular dentition, U.W. 101-1261, is associated with a left maxilla, U.W. 101-1277, that contains the crowns of LI^1–LM^2 in their alveoli. The maxillary and mandibular teeth occlude perfectly. The mesial IPF of an isolated LM^3, U.W. 101-1269, is congruent with the distal IPF of the U.W. 101-1277 M^2. Further, an isolated RM^1, U.W. 101-1463, is provisionally assigned to this individual. Its inclusion is not certain but its status as an antimere of the U.W. 101-1277 M^1 is

consistent with its morphology and state of macrowear. These teeth belong to the holotype (DH1) of *H. naledi* (Berger et al., 2015).

Association 8 (older adult) Specimens U.W. 101-357 (mesial root of LM_1), U.W. 101-358 (LP_3), U.W. 101-359 (LC_1), and U.W. 101-361 (LP_4–LM_3 in situ) were recovered in close spatial proximity. These left teeth all express advanced occlusal wear. A fragment of mandibular condyle (U.W. 101-196) is refit to the U.W. 101-361 mandible and articulates with the mandibular fossa of the DH3 partial cranium (Berger et al., 2015). There are many other heavily worn mandibular teeth in the assemblage (e.g., U.W. 101-010 and U.W. 101-006) that are candidates to belong to this individual; however, there are currently no conclusive grounds to argue for their association.

Association 9 (older adult) The U.W. 101-1362 (LP^4), U.W. 101-796 (LM^1), U.W. 101-528 (LM^2), and U.W. 101-527 (LM^3) teeth form a metameric series from an adult showing advanced dental wear. Though it is difficult to evaluate given their wear stage, U.W. 101-005 (RM^2) is a possible antimere of U.W. 101-528. The degree of occlusal wear on this set of teeth is comparable to that of the U.W.101-361 (i.e., DH3) individual described above. While it is tempting to link these two sets of teeth together in a single individual, there is currently no confirmatory evidence to do so.

4.2. The Dinaledi dental feature set

Tooth size and relative size: In size, the Dinaledi incisors and canines are smaller on average (Table 1) than those of species of *Australopithecus* and *Paranthropus*, and only

overlap with the smallest-toothed specimens of early *Homo* (e.g., the I^2 MD for KNM-ER 1813 and OH 39); however, few early *Homo* specimens, except KNM-WT 60000 (Leakey et al., 2012), match the exceptionally small Dinaledi incisor breadths (Berger et al., 2015; Hawks et al., 2018). The *H. naledi* C_1 MD length also falls below species of *Australopithecus*, *H. habilis*, and early *H. erectus* (Hawks et al., 2018). The Dinaledi postcanine teeth are smaller than species of *Australopithecus* and *Paranthropus* and fall toward the lower end of the size range of early *Homo* species (Berger et al., 2015; Hawks et al., 2018). For *H. rudolfensis*, only the Koobi Fora specimens KNM-ER 60000 and KNM-ER 62000, which are among the smallest teeth of that species yet discovered (Leakey et al., 2012), are similar in size, and they lie either above the *H. naledi* range or just within its upper limits (Berger et al., 2015; Hawks et al., 2018). While not well represented, the postcanine teeth of the South African teeth previously attributed to early *Homo* (e.g., SK 15, SK 18a, SK 27, SKX 257/258, SKW 3114, DNH 39, DNH 62, DNH 67, DNH 70, Stw 19, Stw 53, Stw 80, SE 255, SE 1508) are also typically larger; though, the status of most of these teeth as *Homo* has been challenged (Zanolli et al., 2022), leaving few definitive South African early *Homo* specimens with which to compare *H. naledi* tooth size. Like the crowns, *H. naledi* mandibular molar roots are also smaller than those of species of *Paranthropus*, *Australopithecus*, and most early *Homo* specimens (Kupczik et al., 2019). *Homo naledi* is likely derived relative to species of *Australopithecus* and early *Homo*, and possibly convergent with species of *Paranthropus*, in having small anterior teeth. It is also likely derived relative to species of *Australopithecus*, *Paranthropus*, and early *Homo* in having smaller postcanine crowns and roots.

Three Dinaledi mandibles (U.W. 101-001, U.W. 101-1142 + 1287B, and U.W. 101-1261) preserve M_1–M_3, making their dental associations definitive (Figs. 41, 45, and 46); two others (U.W. 101-361, U.W. 101-377) preserve partial sequences (Figs. 43 and 44). In all cases, the molar size gradient is $M_3 > M_2 > M_1$. This gradient is typical of species of *Australopithecus* and *Paranthropus* and observed for some *H. habilis* (e.g., OH 13), but not all (e.g., OH 16), for *H. rudolfensis* (e.g., KNM-ER 60000), and for some early *H. erectus* (e.g., KNM-ER 992, KNM-BK 8518), but not others (e.g., KNM-BK 67; Wood and Abbott, 1983; Wood and van Noten, 1986; Wood, 1991). The gradient is variable among Dmanisi *H. erectus*, with some having reduced M_3s and an $M_1 > M_2 > M_3$ pattern, while D2600 evinces an $M_3 > M_2 > M_1$ gradient (Martinón-Torres et al., 2008). Among relevant South African specimens, molar proportions can only be judged directly for SK 15; its M_3 and M_2 are nearly the same MD length but the M_3 is narrower BL (Robinson, 1956), yielding an $M_2 > M_3 > M_1$ gradient. The SK 45 M_2 is larger than the M_1 and, based on the size of the M_3 alveolus, Robinson (1956) argued that, like SK 15, the M_3 would have been smaller than the M_2. Unfortunately, molar size cannot be determined accurately for Stw 80; though, its M_2 is clearly larger than its M_1. For LD 350-1, the most ancient fossil of *Homo*, the M_3 is slightly smaller than the M_2 (Villmoare et al., 2015). Middle and Late Pleistocene *Homo* tend to have reduced M_3s and a derived $M_1 > M_2 > M_3$ or $M_2 > M_3 > M_1$ size gradient. *Homo naledi* relative molar size may be plesiomorphic for genus *Homo*, but LD-350 hints that M_3 reduction was already present in some *Homo* specimens near the base of the genus; therefore, the relatively large M_3 could be a feature evolved convergently with species of *Australopithecus* and *Paranthropus*.

Mandibular canine morphology Despite their small size, the *H. naledi* C_1s share much of their crown shape and cingular morphology with species of *Australopithecus* and most specimens of early *Homo*. From the crown apex, the mesial crest is short and convex, while the distal is tall and vertical and terminates at a distal cuspule (Figs. 28 and 29). Robinson (1956: 46) described the distal cuspule on the canines of *A. africanus* when he wrote: "on the distal side of the crown there is a distinct small cusplet approximately half-way down the crown. This is formed by the remnants of the cingulum." Martinón-Torres et al. (2008) noted the presence of this feature on the C_1s of Dmanisi *H. erectus*, where they referred to it as an 'accessory distal cuspule.' Our inspection of original fossils show that is present on KNM-ER 992, KNM-ER 60000, and KNM-ER 3734 (the crown of this specimen is worn in the region of interest, but the remaining lingual and labial topography suggest its presence; L.D., personal observation). Among early *H. erectus* specimens, the cingulum of KNM-WT 15000 is weakly developed and departs from this general condition. Among fossils purported to represent South African early *Homo*, a distal cuspule is present on Stw 80 (Kuman and Clarke, 2000). In contrast, in Middle and Late Pleistocene *Homo* the C_1 cingulum may be prominent (e.g., *Homo antecessor*, *Homo heidelbergensis*, Zhoukoudian *H. erectus*; Bermudez de Castro et al., 1999; Carbonelli et al., 2005; see Weidenreich, 1937: plate VI and Weidenreich, 1943: Figure 282), but it rarely forms a topographically distinct prominence. Our examination of Krapina *Homo neanderthalensis* and extant *Homo sapiens* reveal little in the way of a cingulum and no trace of a distal tubercle. Thus, we consider the presence of the distal

4757 tubercle on the *H. naledi* C_1s to be a symplesiomorphy shared with species of
4758 *Australopithecus* and most specimens of early *Homo*.
4759
4760 Morphology of the permanent and deciduous premolars Both the Dinaledi dP^3 and dP_3
4761 are molariform. For the dP^3 (Fig. 4), there is no hint of distal cusp reduction seen in
4762 Neandertals and *H. sapiens* (Bailey et al., 2019). For the dP_3 (Fig. 8), all five principal
4763 cusps are well developed, the talonid is BL broader than the trigonid, and the Fa is
4764 enclosed by the MMR (Bailey et al., 2019; Brophy et al., 2021). In general terms, the dP_3
4765 of early species of *Australopithecus* (i.e., *Australopithecus anamensis* and
4766 *Australopithecus afarensis*) is comparatively primitive and the crown is dominated by the
4767 Prd without a prominent MMR (e.g., Leakey et al., 1998; Kimbel and Delezene, 2009). A
4768 five-cusped dP_3 with enclosed Fa is observed in *A. africanus* and in species of
4769 *Paranthropus*, but the MMR is reduced in mid-Pleistocene and younger species of *Homo*
4770 and the distal cusps are relatively small (Bailey et al., 2019). In species of early *Homo*,
4771 dP_3s are not well documented. Two that have been attributed to *Homo erectus*, KNM-ER
4772 1507 and KNM-ER 820, have only three cusps and a relatively large Prd (Wood, 1991).
4773 Thus, if *A. africanus* and species of *Paranthropus* capture the expected primitive states
4774 for genus *Homo*, then *H. naledi* retains a plesiomorphic configuration of the dP_3; the
4775 other alternative is that *H. naledi* is convergent with the morphology seen in those taxa.
4776 The *H. naledi* P_3s are also molarized in crown form: the mesiolingual corner of
4777 the crown is filled out, the crown is symmetric in occlusal view, the Med is large and
4778 fully separated from the Prd by a longitudinal groove, the Med is nearly the same height
4779 as the Prd, and the talonid is relatively large (Fig. 8). In general terms, these features can

be matched in species of *Australopithecus* and *Paranthropus*; though, at larger crown sizes. Early *Homo* specimens show a wide range of variation in P_3 crown morphology. At one extreme, KNM-ER 1802, which may represent *H. rudolfensis* (but see Leakey et al., 2012), is fully bicuspid and symmetrical about the mesiodistal axis in occlusal view (Wood, 1991). Though broken buccally, a similar configuration can be inferred for the isolated *Homo* sp. P_3 KNM-ER 2599. In contrast, in paradigmatic examples of *H. habilis* from Olduvai (i.e., OH 7, OH 13) and *H. erectus* (e.g., KNM-ER 820, KNM-ER 992), the Med tends to be smaller in height and area than the Prd (Wood, 1991; L.D., personal observation). The same is true of KNM-ER 62004, where the Med is barely topographically distinct from the Tc and probably true of the more worn KNM-ER 62000 (L.D., personal observation), where dentine is exposed on the Prd, but the Tc and Med remain covered in enamel at the same topographic wear plane. In Olduvai *H. habilis* (e.g., OH 7) and some early *H. erectus* (e.g., KNM-ER 992, KNM-WT 15000), the Med is not a topographically distinct cusp at all; it is instead linked to the Prd by a continuous and elevated Tc (a 'prominent triangular ridge' to Brown and Walker, 1993) not divided from the Prd by a longitudinal groove. In some *H. habilis* (e.g., KNM-ER 1507) and likely *H. erectus* (e.g., SKX 21204), a longitudinal groove is present, but the Med is subequal in height and projected area to the Prd. In *H. habilis* and early *H. erectus*, the mesiolingual corner of the P_3 is often abbreviated, giving the crown an asymmetric shape (e.g., D211, KNM-ER 820, KNM-ER 992, OH 7; Wood, 1991). In these regards, the specimens of *H. erectus* and *H. habilis* presage the reduced Med of Middle and Late Pleistocene forms. Thus, the *H. naledi* P_3 crown lacks the occlusal simplification, relative to *A. africanus* and species of *Paranthropus*, seen in some early *Homo* specimens; KNM-

ER 1802 and KNM-ER 2599 are exceptions. Despite these general resemblances, the KNM-ER 1802 P_3 enamel-dentine junction (EDJ) shape is not similar to *H. naledi*. In fact, P_3 EDJ shape clearly distinguishes *H. naledi* from all other hominin taxa (Davies et al., 2020). Further, Davies et al. (2020) noted that *H. naledi* is the only hominin to have a P_3 that is larger than the P_4 in centroid size; a notable exception is Stw 80, which is discussed above. Thus, if *A. africanus* and early *Homo* specimens KNM-ER 1802 and KNM-ER 2599 reflect the plesiomorphic condition for genus *Homo*, then *H. naledi* may retain a generally primitive P_3. Alternatively, its molarized morphology would be convergent with that of early *Homo* specimens like KNM-ER 1802.

The Dinaledi P_3s are all multirooted (2R: MB + D; Wood et al., 1988; Figs. 30 and 31). Some early *Homo* specimens express simple P_3 roots, with either a Tomes' or single root noted for most *H. erectus* and *H. habilis* specimens. The few multirooted examples are commonly attributed to *H. rudolfensis* (though not all have complex roots; Wood, 1991). Additionally, multirooted P_3s are seen in the enigmatic KNM-ER 1805, which may represent *H. habilis*, UR 501, and at least the D2600 specimen of Dmanisi *H. erectus* (Wood et al., 1988; Wood, 1991; Martinón-Torres et al., 2008; Lordkipanidze et al., 2013: Table S3B). In the small sample of South African P_3s from Swartkrans and Sterkfontein that have been attributed to early *Homo* (e.g., Robinson, 1953; Kuman and Clarke, 2000; Grine, 2005), none matches the morphology of *H. naledi*. Our inspection of the alveoli or exposed roots of SK 15, SK 18a, and Stw 80 show that they are all Tomes' in form. Zanolli et al. (2022) argue that SK 15 is not *Homo*, while the taxonomic status of Stw 80 is more ambiguous. Thus, there are very few southern African specimens of early *Homo* with which to compare *H. naledi*. *Homo naledi* P_3 roots, like the crown, are

distinct relative to the condition typically observed in small-toothed *Homo* specimens of eastern and southern Africa. As with crown form, if the multirooted early *Homo* specimens represent the plesiomorphic condition for the genus, then *H. naledi* retains a primitive root morphology.

Homo naledi P^3s and P^4s are occasionally three rooted, with two tightly compressed buccal roots paired with a lingual root (Figs. 16–19). Most early *Homo* P^3s are two-rooted, with buccal and lingual roots (e.g., OH 65, A.L. 666-1, KNM-ER 1470, KNM-ER 1805, KNM-ER 1813, OH 13), though there are some examples of three-rooted (e.g., OH 24) and one-rooted individuals (e.g., OH 16; e.g., Kimbel et al., 1997; Clarke, 2012; Lordkipanidze et al., 2013: Table S3B). Most early *Homo* P^4s are two- or three-rooted (e.g., Kimbel et al., 1997; Lordkipanidze et al., 2013: Table S3B). Thus, multirooted maxillary premolars in *H. naledi* are another candidate plesiomorphy shared with early *Homo* species; however, detailed comparisons of *H. naledi* premolar root form have yet to be conducted.

Nonmetric traits of the molars The consistent absence of mass additive traits, like prominent cingular features, distinguishes the Dinaledi molars from *Australopithecus*, *Paranthropus*, and many early *Homo* specimens. For example, all Dinaledi M^1s and M^2s have weakly expressed (or absent) Carabelli's features that are isolated on the mesiolingual corner of the crown and not in contact with the lingual groove (Figs. 20–23). In species of *Australopithecus* and *Paranthropus*, more prominent expression states are observed (either a large depression or pit, a cusp, or a crest-like feature), and the Carabelli's feature may wrap around the lingual surface of the crown to contact, or cross,

4849 the lingual groove (Van Reenen and Reid, 1995). Swartkrans specimen SKX 3114, a
4850 possible early *Homo* tooth, exhibits a large prominent feature with two deep vertical
4851 furrows on the mesiolingual corner of the crown. SKX 268 and SE 255 (both argued not
4852 to be *Homo* by Zanolli et al., 2022) have distinct Carabelli's (Grine, 1989; L.D., personal
4853 observation). From eastern Africa, *H. rudolfensis* can exhibit complex Carabelli's
4854 morphology (e.g., KNM-ER 1590 M^2; Wood, 1991;), while *H. habilis* and *H. erectus* can
4855 exhibit minimal or no expression at all (e.g., KNM-ER 1813, KNM-ER 3733; Wood,
4856 1991). For the mandibular molars, the Dinaledi protostylids are small, restricted to the
4857 mesiobuccal corner, and do not intersect or cross the buccal groove (Fig. 4). A wide
4858 range of molar protostylid expression is observed in fossil hominins. Hlusko (2004), for
4859 example, identified six forms on *Australopithecus* and *Paranthropus* molars and noted
4860 that in *Australopithecus* and *Paranthropus* the "protostylid is more centrally located on
4861 the buccal side of the crown with a stronger relationship to the buccal groove" (Hlusko,
4862 2004: 582). Importantly, the figured example in Hlusko (2004) of no protostylid
4863 expression (STW 309a) does possess a diagonal crest on the mesiolingual corner;
4864 however, she does not consider it to be part of the protostylid trait. The very faint sub-
4865 vertical depression on the mesiolingual corner of the Dinaledi Prd resembles this
4866 condition; Skinner et al. (2008, 2009) have argued that such features should be
4867 considered part of the protostylid complex. Many early *Homo* molars from eastern Africa
4868 and Dmanisi express the protostylid form where it is adjacent to or crosses the mesial
4869 buccal groove. The small Carabelli's feature and protostylid that are mesially restricted in
4870 the Dinaledi sample would appear to be derived relative to species of *Australopithecus*,
4871 *Paranthropus*, and most early *Homo* specimens.

Homo naledi mandibular molars lack crenulation, secondary fissures, and defined supernumerary cusps, which are frequently observed on molars of species of *Australopithecus*, *Paranthropus*, and early *Homo*; thus, *H. naledi* mandibular molars appear occlusally simple in comparison. All Dinaledi M_1s lack a C6, and only one M_2, U.W. 101-1142, expresses a C6 (Fig. 45). A C6 is common in species of *Paranthropus* (Wood and Abbott, 1983; Wood, 1991) and noted in *A. afarensis* and *A. africanus* as well (Guatelli-Steinberg and Irish, 2005; Bailey and Wood, 2007). Large C7s are not observed in the Dinaledi M_1 and M_2 sample (Irish et al., 2018). Some Dinaledi M_1s do express a small postmetaconulid (Figs. 33 and 34). Though not ubiquitous, examples of individualized C7s can be found on M_1s and M_2s attributed to all early *Homo* species (e.g., KNM-ER 1802, KNM-ER 1507, KNM-WT 15000, KNM-ER 60000, D211, OH 7, LD 350; Wood and Abbott, 1983; Wood, 1991; Leakey et al, 2012; Villmoare et al., 2015), among the Omo and Turkana 'nonrobust' assemblage (e.g., KNM-ER 5431, Omo 75-14) that may also represent early members of the genus (Wood, 1991; Suwa et al., 1996; Villmoare et al., 2015), and on DNH 67, a suggested early *Homo* M_1 from Drimolen (Moggi-Cecchi et al., 2009; but see Zanolli et al., 2022). The absence of a C7 appears to be derived in *H. naledi* relative to species of early *Homo*; the absence of a C6 is shared with most species of *Homo*.

Molar shape Dinaledi molar cuspal proportions are distinct from most Middle and Late Pleistocene *Homo* samples but resemble those in species of early *Homo*. For the Dinaledi sample, the M^1 and M^2 have a relatively large Hy and a 'rhomboidal' outline (e.g., Kimbel et al., 1997). For the Dinaledi M_1, the distal cusps (End and Hld) are relatively

large, and not reduced as is common in Middle and Late Pleistocene *Homo* (Zanolli, 2013). Thus, the rhomboidal shape of the maxillary molars and the relative cuspal size the maxillary and mandibular molars would be plesiomorphies shared with basal species of the genus *Homo*; however, analyses the M_1 and M_2 EDJ shape easily distinguish *H. naledi* from all other hominin taxa (Skinner et al., 2016).

Morphological summary The Dinaledi fossils capture a dental feature set that is distinct from all other hominins. The Dinaledi canines are small, but express features typical of basal members of the genus. The permanent and deciduous P_3s have molarized crowns that are reminiscent of *A. africanus* and species of *Paranthropus*, but at a much smaller size. Many features of the *H. naledi* dentition are candidate plesiomorphies shared with basal species of the genus *Homo* (e.g., distally increasing mandibular molar size gradient, molarized dP_3 and P_3, multirooted maxillary and mandibular premolars, rhomboidal maxillary molar outline, distal cuspule on C_1). Other traits are candidate apomorphies of *H. naledi* relative to basal members of the genus (e.g., anterior tooth size reduction, postcanine tooth size reduction, C7 absence on mandibular molars, configuration of the protostylid, postcanine EDJ shape). Though much comparative work remains to be done, the morphology of the Dinaledi teeth provides strong support for the taxonomic diagnosis of *H. naledi*.

5. Conclusion

Hominin fossils from the Dinaledi Chamber provide the first large single-site sample of Middle Pleistocene-aged dental remains from Africa. Though comparative

analyses are just beginning, their abundance, excellent state of preservation, and completeness provide a detailed picture of the *H. naledi* dental feature set. The teeth are commingled and often found in isolation, but it is clear that numerous individuals, from infants to older adults, are represented in the dental assemblage. In fact, several significant associations are proposed, including two subadults that will provide insight into the life history and dental development of *H. naledi*. The Dinaledi teeth hold a wealth of information that is only beginning to be prospected for their potential. We expect that this sample will provide valuable insights into the paleobiology of *H. naledi* for years to come.

Acknowledgements

We are indebted to Bernhard Zipfel and Sifelani Jirah for access to and assistance with the hominin collections at the Evolutionary Studies Institute at the University of the Witwatersrand. We also express our thanks to the staff of the Evolutionary Studies Institute, especially Wilma Lawrence and Sonia Sequeira, for help in organizing research trips. We are grateful to Kudakwashe Jakata for his assistance with tomographic scanning. The discovery, recovery and preparation of the material was funded by a Grant from the National Geographic Society and the Lyda Hill Foundation. Research was also supported by a workshop grant from the National Research Foundation of South Africa. We are grateful for a workshop grant (to L.K.D. and M.M.S.) from the Wenner-Gren Foundation that funded participation for many coauthors. L.K.D. thanks the Office of Research and Development at the University of Arkansas and the Connor Family Faculty Foundation for providing funding. J.K.B. thanks the LSU Council of Research Summer

Stipend Grant for funding research on the material. Participation of M.M.S. supported by European Research Council (grant agreement No. 819960). We thank Tom Davies and William Plummer for helpful discussions and comparative images of tooth crown morphology and Mykolas Imbrasas for assistance with figure revision. We also thank the Editor-in-Chief, Clément Zanolli, the Associate Editor, and the reviewers of the manuscript for their thoughtful and thorough edits and, especially, for their patience.

References

AlQahtani, S.J., Hector, M.P., Liversidge, H.M., 2010. Brief communication: The London atlas of human tooth development and eruption. American Journal of Physical Anthropology 142, 481–490.

Bailey, S.E., Brophy, J.K., Moggi-Cecchi, J., Delezene, L.K., 2019. The deciduous dentition of *Homo naledi*. Journal of Human Evolution 136, 102655.

Bailey, S.E., Hublin, J.J., 2013. What does it mean to be dentally "modern"?. In: Scott, G. R., Irish, J.D. (Eds.), Anthropological Perspectives on Tooth Morphology: Genetics, Evolution, Variation. Cambridge University Press, Cambridge, pp. 222–249.

Bailey, S. E., Wood, B. A., 2007. Trends in postcanine occlusal morphology within the hominin clade: the case of *Paranthropus*. In: Bailey, S.E., Hublin, J.-J. (Eds.), Dental Perspectives on Human Evolution: State of the Art Research in Dental Anthropology. Springer, Dordecht, pp. 33–52.

Berger, L.R., De Ruiter, D.J., Churchill, S.E., Schmid, P., Carlson, K.J., Dirks, P.H., Kibii, J.M., 2010. *Australopithecus sediba*: A new species of *Homo*-like australopith from South Africa. Science 328, 195–204.

Berger, L.R., Hawks, J., de Ruiter, D.J., Churchill, S.E., Schmid, P., Delezene, L.K., Kivell, T.L., Garvin, H.M., Williams, S.A., DeSilva, J.M., Skinner, M.M., Musiba, C.M., Cameron, N., Holliday, T.W., Harcourt-Smith, W., Ackermann, R.R., Bastir, M., Bogin, B., Bolter, D., Brophy, J., Cofran, Z.D., Congdon, K.A., Deane, A.S., Dembo, M., Drapeau, M., Elliott, M.C., Feuerriegel, E.M., Garcia-Martinez, D., Green, D.J., Gurtov, A., Irish, J.D., Kruger, A., Laird, M.F., Marchi, D., Meyer, M.R., Nalla, S., Negash, E.W., Orr, C.M., Radovcic, D., Schroeder, L., Scott, J.E., Throckmorton, Z., Tocheri, M.W., VanSickle, C., Walker, C.S., Wei, P., Zipfel, B., 2015. *Homo naledi*, a new species of the genus *Homo* from the Dinaledi Chamber, South Africa. eLife 4, e09560.

Berger, L.R., Hawks, J., Dirks, P.H., Elliott, M., Roberts, E.M., 2017. *Homo naledi* and Pleistocene hominin evolution in subequatorial Africa. eLife 6, e24234.

Berger, L.R., Keyser, A.W., Tobias, P.V., 1993. Gladysvale: First early hominid site discovered in South Africa since 1948. American Journal of Physical Anthropology 92, 107–111.

Berger, L.R., Parkington, J.E., 1995. A new Pleistocene hominid-bearing locality at Hoedjiespunt, South Africa. American Journal of Physical Anthropology 98, 601–609.

Bermúdez de Castro, J. M., Rosas A., Nicolás, M. E., 1999. Dental remains from Atapuerca–TD6 (Gran Dolina site, Burgos, Spain). Journal of Human Evolution 37, 523–566.

Berthaume, M.A., Delezene, L.K., Kupczik, K., 2018. Dental topography and the diet of *Homo naledi*. Journal of Human Evolution 118, 14–26.

Bolter, D.R., Elliott, M.C., Hawks, J., Berger, LR., 2020. Immature remains and the first partial skeleton of a juvenile *Homo naledi*, a late Middle Pleistocene hominin from South Africa. PloS One 15, e0230440.

Bolter, D. R., Hawks, J., Bogin, B., Cameron, N., 2018. Palaeodemographics of individuals in Dinaledi Chamber using dental remains. South African Journal of Science 114, 1–6.

Brink, J.S., Herries, A., Moggi-Cecchi, J., Gowlett, J., Bousman, C.B., Hancox, J.P., Grün, R., Eisenmann, V., Adams, J.W., Rossouw, L., 2012. First hominine remains from a ~1.0 million year old bone bed at Cornelia-Uitzoek, Free State Province, South Africa. Journal of Human Evolution 63, 527–535.

Broom, R., 1938. The Pleistocene anthropoid apes of South Africa. Nature 142, 377–379.

Broom, R., Robinson J.T., 1949. A new type of fossil man. Nature 164, 322–323.

Brophy, J.K., Moggi-Cecchi, J., Matthews, G.J., Bailey, S.E., 2021. Comparative morphometric analyses of the deciduous molars of *Homo naledi* from the Dinaledi Chamber, South Africa. American Journal of Physical Anthropology 174, 299–314.

Brown, B., Walker, A., 1993. The dentition. In: Walker, A., Leakey, R. (Eds.), The Nariokotome *Homo erectus* Skeleton. Harvard University Press, Cambridge.

5006 Carbonell, E., Bermúdez de Castro, J. M., Arsuaga, J. L., Allue, E., Bastir, M., Benito,
5007 A., Cáceres, T., Canals, J., Díez, J. C., van der Made, J., Mosquera, M., Ollé, A.,
5008 Pérex-González, A., Rodríguez, J., Rodríguez, X. P., Rosas, A., Rosell, J., Sala,
5009 R., Vallverdú, J., Vergés, J. M., 2005. An Early Pleistocene hominin mandible
5010 from Atapuerca-TD6, Spain. Proceedings of the National Academy of Sciences
5011 USA 102, 5674–5678.
5012 Clarke, R.J., 1977a. The cranium of the Swartkrans hominid SK 847 and its relevance to
5013 human origins. Ph.D. Dissertation, University of the Witwatersrand.
5014 Clarke, R.J., 1977b. A juvenile cranium and some adult teeth of early *Homo* from
5015 Swartkrans, Transvaal. South African Journal of Science 73, 46–49.
5016 Clarke, R., 1985. Early Acheulean with *Homo habilis* at Sterkfontein. In: Tobias, P.V.
5017 (Ed.), Hominid Evolution: Past, Present and Future. Alan R. Liss, New York, pp.
5018 287–298.
5019 Clarke, R.J., 2012. A *Homo habilis* maxilla and other newly-discovered hominid fossils
5020 from Olduvai Gorge, Tanzania. Journal of Human Evolution 63, 418–428.
5021 Cofran, Z., Walker, C.S., 2017. Dental development in *Homo naledi*. Biology Letters 13,
5022 20170339.
5023 Curnoe, D., 2009. The mandible from Bed 3, Cave of Hearths. In: McNabb, J., Sinclair,
5024 A. (Eds.), The Cave of Hearths: Makapan Middle Pleistocene Research Project:
5025 Field research by Anthony Sinclair and Patrick Quinney, 1996–2001.
5026 Archaeopress, Oxford, pp. 138–149.
5027 Curnoe, D., Tobias, P.V., 2006. Description, new reconstruction, comparative anatomy,
5028 and classification of the Sterkfontein Stw 53 cranium, with discussions about the

taxonomy of other southern African early *Homo* remains. Journal of Human Evolution 50, 36–77.

Dart, R.A., 1925. *Australopithecus africanus*: The man-ape of South Africa. Nature 115, 195–199.

Davies, T.W., Delezene, L.K., Gunz, P., Hublin, J.-J., Berger, L.R., Gidna, A., Skinner, M.M., 2020. Distinct mandibular premolar crown morphology in *Homo naledi* and its implications for the evolution of *Homo* species in southern Africa. Scientific Reports 10, 13196.

Davies, T.W., Delezene, L.K., Gunz, P., Hublin, J.-J., Skinner, M.M., 2019a. Endostructural morphology in hominoid mandibular third premolars: Geometric morphometric analysis of dentine crown shape. Journal of Human Evolution 133, 198–213.

Davies, T.W., Delezene, L.K., Gunz, P., Hublin, J.-J., Skinner, M.M., 2019b. Endostructural morphology in hominoid mandibular third premolars: Discrete traits at the enamel-dentine junction. Journal of Human Evolution 136, 102670

Dembo, M., Radovčić, D., Garvin, H.M., Laird, M.F., Schroeder, L., Scott, J.E., Brophy, J., Ackermann, R.R., Musiba, C.M., de Ruiter, D.J., Mooers, A.Ø., 2016. The evolutionary relationships and age of *Homo naledi*: An assessment using dated Bayesian phylogenetic methods. Journal of Human Evolution 97, 17–26.

Dirks, P.H., Berger, L.R., Roberts, E.M., Kramers, J.D., Hawks, J., Randolph-Quinney, P.S., Elliott, M., Musiba, C.M., Churchill, S.E., de Ruiter, D.J., Schmid, P., 2015. Geological and taphonomic context for the new hominin species *Homo naledi* from the Dinaledi Chamber, South Africa. eLife 4, e09561.

5052 Dirks, P.H., Roberts, E.M., Hilbert-Wolf, H., Kramers, J.D., Hawks, J., Dosseto, A.,
5053 Duval, M., Elliott, M., Evans, M., Grün, R. and Hellstrom, J., 2017. The age of
5054 *Homo naledi* and associated sediments in the Rising Star Cave, South Africa.
5055 eLife 6, e24231.
5056 Dreyer, T.F., 1935. A human skull from Florisbad, Orange Free State, with a note on the
5057 endocranial cast by C. U. Ariens Kappers. Proc. K. Ned. Akad. Wet. 38, 119–128.
5058 Elliott, M.C., Peixotto, B., Morris, H., Feuerriegel, E.M., Tucker, S., Hunter, R.,
5059 Ramalepa, M., Tsikoane, M., Roberts, E.M., Spandler, C. Hawks, J., 2018.
5060 Hominin material recovered from the base of the Chute in the Hill Antechamber,
5061 in the Dinaledi Chamber System of the Rising Star Cave. American Journal of
5062 Physical Anthropology 165, 76.
5063 Feuerriegel, E.M., Green, D.J., Walker, C.S., Schmid, P., Hawks, J., Berger, L.R.
5064 Churchill, S.E., 2017. The upper limb of *Homo naledi*. Journal of Human
5065 Evolution 104, 155–173.
5066 Garvin, H.M., Elliott, M.C., Delezene, L.K., Hawks, J., Churchill, S.E., Berger, L.R.,
5067 Holliday, T.W., 2017. Body size, brain size, and sexual dimorphism in *Homo*
5068 *naledi* from the Dinaledi Chamber. Journal of Human Evolution 111, 119–138.
5069 Grine, F.E., 1989. New hominid fossils from the Swartkrans Formation (1979–1986):
5070 Craniodental specimens. American Journal of Physical Anthropology 79, 409–
5071 449.
5072 Grine, F.E., 2005. Early *Homo* at Swartkrans, South Africa: A review of the evidence and
5073 an evaluation of recently proposed morphs. South African Journal of Science 101,
5074 43–52.

Grine, F.E., 2016. The Late Quaternary hominins of Africa: The skeletal evidence from MIS 6–2. In: Jones, S.C., Stewart, B.A. (Eds.), Africa from MIS 6–2: Population Dynamics and Paleoenvironments. Springer, Dordecht, pp. 323–381.

Grine, F.E., Bailey, R.M., Harvati, K., Nathan, R.P., Morris, A.G., Henderson, G.M., Ribot, I., Pike, A.W.G., 2007. Late Pleistocene skull from Hofmeyr, South Africa, and modern human origins. Science 315, 226–229.

Grine, F.E., Gonzalvo, E., Rossouw, L., Holt, S., Black, W., Braga, J., 2021. Variation in Middle Stone Age mandibular molar enamel-dentine junction topography at Klasies River Main Site assessed by diffeomorphic surface matching. Journal of Human Evoltuion 161, 103079.

Grine F.E., Jungers, W.L., Schultz, J., 1996. Phenetic affinities among early *Homo* crania from East and South Africa. Journal of Human Evolution 30, 189–225.

Grine, F.E., Marean, C.W., Faith, J.T., Black, W., Mongle, C.S., Trinkaus, E., le Roux, S.G., du Plessis, A., 2017. Further human fossils from the Middle Stone Age deposits of Die Kelders Cave 1, Western Cape Province, South Africa. Journal of Human Evolution 109, 70–78.

Grine, F.E., Smith, H.F., Heesy, C.P., Smith, E.J., 2009. Phenetic affinities of Plio-Pleistocene *Homo* fossils from South Africa: Molar cusp proportions. In: Grine, F.E., Fleagle, J.G., Leakey, R.E. (Eds.), The First Humans—Origin and Early Evolution of the Genus *Homo*. Springer, Dordrecht, pp. 49–62.

Grine, F.E., Wurz, S., Marean, C.W., 2017. The Middle Stone Age human fossil record from Klasies River Main site. Journal of Human Evolution 103, 53–78.

Grün, R., Brink, J.S., Spooner, N.A., Taylor, L., Stringer, C.B., Franciscus, R.G., Murray, A.S., 1996. Direct dating of Florisbad hominid. Nature 382, 500–501.

Grün, R., Pike, A., McDermott, F., Eggins, S., Mortimer, G., Aubert, M., Kinsley, L., Joannes-Boyau, R., Rumsey, M., Denys, C., Brink, J., 2020. Dating the skull from Broken Hill, Zambia, and its position in human evolution. Nature 580, 372–375.

Guatelli-Steinberg, D., Irish, J. D., 2005. Brief Communication: Early hominin variability in first molar dental trait frequencies. American Journal of Physical Anthropology 128, 477–484.

Guatelli-Steinberg, D., O'Hara, M.C., Le Cabec, A., Delezene, L.K., Reid, D.J., Skinner, M.M., Berger, L.R., 2018. Patterns of lateral enamel growth in *Homo naledi* as assessed through perikymata distribution and number. Journal of Human Evolution 121, 40–54.

Harcourt-Smith, W.E.H., Throckmorton, Z., Congdon, K.A., Zipfel, B., Deane, A.S., Drapeau, M.S.M., Churchill, S.E., Berger, L.R., DeSilva, J.M., 2015. The foot of *Homo naledi*. Nature Communications 6, 8432.

Harvati, K., Bauer, C.C., Grine, F.E., Benazzi, S., Ackermann, R.R., van Niekerk, K.L., Henshilwood, C.S., 2015. A human deciduous molar from the Middle Stone Age (Howiesons Poort) of Klipdrift Shelter, South Africa. Journal of Human Evolution 82, 190–196.

Hawks, J., Elliott, M., Schmid, P., Churchill, S.E., de Ruiter, D.J., Roberts, E.M., Hilbert-Wolf, H., Garvin, H.M., Williams, S.A., Delezene, L.K., Feuerriegel, E.M., Randolph-Quinney, P., Kivell, T.L., Laird, M.F., Tawane, G., DeSilva, J.M., Bailey, S.E., Brophy, J.K., Meyer, M.R., Skinner, M.M., Tocheri, M.W.,

VanSickle, C., Walker, C.S., Campbell, T.L., Kuhn, B., Kruger, A., Tucker, S., Gurtov, A., Hlophe, N., Hunter, R., Morris, H., Peixotto, B., Ramalepa, M., van Rooyen, D., Tsikoane, M., Boshoff, P., Dirks, P.H.G.M., Berger, L.R., 2017. New fossil remains of *Homo naledi* from the Lesedi Chamber, South Africa. eLife 6, e24232.

Herries, A.I.R., Martin, J.M., Leece, A.B., Adams, J.W., Boschian, G., Joannes-Boyau, R., Edwards, T.R., Mallett, T., Massey, J., Murszewski, A., Neubauer, S., Pickering, R., Strait, D.S., Armstrong, B.J., Baker, S., Caruana, M.V., Denham, T., Hellstrom, J., Moggi-Cecchi, J., Mokobane, S., Penzo-Kajewski, P., Rovinsky, D.S., Schwartz, G.T., Stammers, R.C., Wilson, C., Woodhead, J., Menter, C., 2020. Contemporaneity of *Australopithecus*, *Paranthropus*, and early *Homo erectus* in South Africa. Science 368, eaaw7293.

Hlusko, L.J., 2004. Protostylid variation in *Australopithecus*. Journal of Human Evolution 46, 579–594.

Holloway, R.L., Hurst, S.D., Garvin, H.M., Schoenemann, P.T., Vanti, W.B., Berger, L.R., Hawks, J., 2018. Endocast morphology of *Homo naledi* from the Dinaledi Chamber, South Africa. Proceedings of the National Academy of Sciences USA 115, 5738–5743.

Hublin, J.J., Ben-Ncer, A., Bailey, S.E., Freidline, S.E., Neubauer, S., Skinner, M.M., Bergmann, I., Le Cabec, A., Benazzi, S., Harvati, K., Gunz, P., 2017. New fossils from Jebel Irhoud, Morocco and the pan-African origin of *Homo sapiens*. Nature 546, 289.

Hughes, A.R., Tobias, P.V., 1977. A fossil skull probably of the genus *Homo* from Sterkfontein, Transvaal. Nature 265, 310–312.

Irish, J.D., Bailey, S.B., Guatelli-Steinberg, D., Delezene, L.K., Berger, L.R., 2018. Ancient teeth, phenetic affinities, and African hominins: Another look at where *Homo naledi* fits in. Journal of Human Evolution 122, 108–123.

Irish, J.D., Grabowski, M., 2021. Relative tooth size, Bayesian inference, and *Homo naledi*. American Journal of Physical Anthropology 176, 262–282.

Irish, J.D., Guatelli-Steinberg, D., Legge, S.S., de Ruiter, D.J., Berger, L.R., 2013. Dental morphology and the phylogenetic "place" of *Australopithecus sediba*. Science 340, 1233062.

Johanson, D.C., White, T.D., Coppens, Y., 1978. A new species of the genus *Australopithecus* (Primates: Hominidae) from the Pliocene of eastern Africa. Kirtlandia 28, 1–14.

Kimbel, W.H., 2009. The origin of *Homo*. In: Grine, F.E., Fleagle, J.G., Leakey, R.E. (Eds.), The First Humans—Origin and early evolution of the genus *Homo*. Springer, Dordrecht. 31–37.

Kimbel, W.H., Delezene, L.K., 2009. "Lucy" redux: A review of research on *Australopithecus afarensis*. American Journal of Physical Anthropology 140, 2–48.

Kimbel, W.H., Johanson, D.C., Rak, Y., 1997. Systematic assessment of a maxilla of *Homo* from Hadar, Ethiopia. American Journal of Physical Anthropology 103, 235–262.

Kivell, T.L., Deane, A.S., Tocheri, M.W., Orr, C.M., Schmid, P., Hawks, J., Berger, L.R., Churchill, S.E., 2015. The hand of *Homo naledi*. Nature Communications 6, 8431.

Klein, R.G., Grine, F.E., 1993. Late Pleistocene human remains from the Sea Harvest site, Saldanha Bay, South Africa. South African Journal of Science 89, 145–152.

Kruger, A., Randolph-Quinney, P., Elliott, M., 2016. Multimodal spatial mapping and visualization of Dinaledi Chamber and Rising Star Cave. South African Journal of Science 112, 1–11.

Kuman, K., Clarke, R.J., 1986. Florisbad—New investigations at a Middle Stone Age hominid site in South Africa. Geoarchaeology 1, 103–125.

Kuman, K., Clarke, R.J., 2000. Stratigraphy, artifact industries and hominid associations from Sterkfontein Member 5. Journal of Human Evolution 38, 827–847.

Kupczik, K., Delezene, L.K., Skinner, M.M., 2019. Mandibular molar root and pulp cavity morphology in *Homo naledi* and other Plio-Pleistocene hominins. Journal of Human Evolution 130, 83–95.

Laird, M.F., Schroeder, L., Garvin, H.M., Scott, J.E., Dembo, M., Radovčić, D., Musiba, C.M., Ackermann, R.R., Schmid, P., Hawks, J., Berger, L.R., 2017. The skull of *Homo naledi*. Journal of Human Evolution 104, 100–123.

Leakey, L.S.B., 1959. A new fossil skull from Olduvai. Nature 184, 491–493.

Leakey, M.G., Feibel, C.S., McDougall, I., Ward, C., Walker, A., 1998. New specimens and confirmation of an early age for *Australopithecus anamensis.* Nature 393, 62–66.

Leakey, M.B., Spoor, F., Dean, M.C., Feibel, C.S., Anton, S.C., Kiarie, C., Leakey, L.N., 2012. New fossils from Koobi Fora in northern Kenya confirm taxonomic diversity in early *Homo*. Nature 488, 201–204.

Leakey, L.S.B., Tobias, P.V., Napier, J.R., 1964. A new species of the genus *Homo* from Olduvai Gorge. Nature 202, 7–9.

Lordkipanidze, D., Ponce de León, M.S., Margvelashvili, A., Rak, Y., Rightmire, G.P., Vekua, A., Zollikofer, C.P., 2013. A complete skull from Dmanisi, Georgia, and the evolutionary biology of early *Homo*. Science 342, 326–331.

Marchi, D., Walker, C.S., Wei, P., Holliday, T.W., Churchill, S.E., Berger, L.R., DeSilva, J.M., 2017. The thigh and leg of *Homo naledi*. Journal of Human Evolution 104, 174–204.

Marean, C.W., Nilssen, P.J., Brown, K., Jerardino, A. Stynder, D., 2004. Paleoanthropological investigations of Middle Stone Age sites at Pinnacle Point, Mossel Bay (South Africa): Archaeology and hominid remains from the 2000 field season. Paleoanthropology 2004, 14–83.

Martin, J.M., Leece, A.B., Neubauer, S., Baker, S.E., Mongle, C.S., Boschian, G., Schwartz, G.T., Smith, A.L., Ledogar, J.A., Strait, D.S., Herries, A.I.R., 2021. Drimolen cranium DNH 155 documents microevolution in an early hominin species. Nature Ecology and Evolution 5, 38–45.

Martinón-Torres, M., de Castro, J. M. B., Gómez-Robles, A., Margvelashvili, A., Prado, L., Lordkipanidze, D., Vekua A., 2008. Dental remains from Dmanisi (Republic of Georgia): Morphological analysis and comparative study. Journal of Human Evolution 55, 249–273.

Martinón-Torres, M., de Castro, J.M.B., Gómez-Robles, A., Prado-Simón, L., Arsuaga, J. L., 2012. Morphological description and comparison of the dental remains from Atapuerca-Sima de los Huesos site (Spain). Journal of Human Evolution 62, 7–58.

McNabb, J., 2009. The ESA stone tool assemblage from the Cave of Hearths, Beds 1–3. In: McNabb, J., Sinclair, A. (Eds.), The Cave of Hearths: Makapan Middle Pleistocene Research Project: Field research by Anthony Sinclair and Patrick Quinney, 1996–2001. Archaeopress, Oxford, pp. 76–104.

Menter, C.G., Kuykendall, K.L., Keyser, A.W., Conroy, G.C., 1999. First record of hominid teeth from the Plio-Pleistocene site of Gondolin, South Africa. Journal of Human Evolution 37, 299–307.

Moggi-Cecchi, J., Grine, F.E., Tobias, P.V., 2006. Early hominid dental remains from Members 4 and 5 of the Sterkfontein Formation (1966–1996 excavations): Catalogue, individual associations, morphological descriptions and initial metrical analysis. Journal of Human Evolution 50, 239–328.

Moggi-Cecchi, J., Menter, C., Boccone, S., Keyser, A., 2010. Early hominin dental remains from the Plio-Pleistocene site of Drimolen, South Africa. Journal of Human Evolution 58, 374–405.

Moggi-Cecchi, J., Tobias, P.V., Beynon, A.D., 1998. The mixed dentition and associated skull fragments of a juvenile fossil hominid from Sterkfontein, South Africa. American Journal of Physical Anthropology 106, 425–465.

Niespolo, E.M., Sharp, W.D., Avery, G., Dawson, T. E., 2021. Early, intensive marine resource exploitation by Middle Stone Age humans at Ysterfontein 1 rockshelter,

South Africa. Proceedings of the National Academy of Sciences USA 118, e2020042118.

Odes, E.J., Delezene, L.K., Randolph-Quinney, P.S., Smilg, J.S., Augustine, T.N., Jakata, K., Berger, L.R., 2018. A case of benign osteogenic tumour in *Homo naledi*: Evidence for peripheral osteoma in the UW 101-1142 mandible. International Journal of Paleopathology 21, 47–55.

Prabhat, A.M., Miller, C.M., Prang, T.C., Spear, J., Williams, S.A., DeSilva, J.M., 2021. Homoplasy in the evolution of modern human-like joint proportions in *Australopithecus afarensis*. eLife 10, e65897.

Rak, Y., Kimbel, W.H., Moggi-Cecchi, J., Lockwood, C.A., Menter, C., 2021. The DNH 7 skull of *Australopithecus robustus* from Drimolen (Main Quarry), South Africa. Journal of Human Evolution 151, 102913.

Reynolds, S.C., Clarke, R.J., Kuman, K.A., 2007. The view from the Lincoln Cave: Mid- to late Pleistocene fossil deposits from Sterkfontein hominid site, South Africa. Journal of Human Evolution 53, 260–271.

Riga, A., Oxilia, G., Panetta, D., Salvadori, P.A., Benazzi, S., Wadley, L., Moggi-Cecchi, J., 2018. Human deciduous teeth from the Middle Stone Age layers of Sibudu Cave (South Africa). Journal of Anthropological Sciences 96, 75–87.

Rightmire, G.P., 1978. Florisbad and human population succession in southern Africa. American Journal of Physical Anthropology 48, 475–486.

Rightmire, G.P., 2008. *Homo* in the Middle Pleistocene: Hypodigms, variation, and species recognition. Evolutionary Anthropology 17, 8–21.

5254 Robbins, J.L., Dirks, H.G.M., Roberts, E.M., Kramer, J.D., Makhubela, T.V., Hilbert-
5255 Wolf, H.L., Elliott, M., Wiersma, J.P., Placzek, C.J., Evans, M., Berger, L.R.,
5256 2021. Providing context to the *Homo naledi* fossils: Constraints from flowstones
5257 on the age of sediment deposits in Rising Star Cave, South Africa. Chemical
5258 Geology 567, 120108.
5259 Robinson, J.T., 1953. *Telanthropus* and its phylogenetic significance. American Journal
5260 of Physical Anthropology 11, 445–501.
5261 Robinson, J.T., 1954. Prehominid dentition and hominid evolution. Evolution 8, 324–
5262 334.
5263 Robinson J.T., 1956. The Dentition of the Australopithecinae. Transvaal Museum
5264 Memoir 9. Transvaal Museum, Pretoria.
5265 Scott, R.S, Irish, J. D., 2017. Human Tooth Crown and Root Morphology: The Arizona
5266 State University Dental Anthropology System. Cambridge University Press,
5267 Cambridge.
5268 Scott, G.R., Turner, C.G., 1997. Anthropology of Modern Human Teeth. Cambridge
5269 University Press, Cambridge.
5270 Skinner, M.M., Lockey, A.L., Gunz, P., Hawks, J., Delezene, L.K., 2016. Enamel-dentine
5271 junction morphology and enamel thickness of the Dinaledi dental collection.
5272 American Journal of Physical Anthropology 159, 293.
5273 Skinner, M.M., Wood, B.A., Hublin, J.-J., 2009. Protostylid expression at the outer
5274 enamel surface and at the enamel-dentine junction of mandibular molars of
5275 *Paranthropus robustus* and *Australopithecus africanus*. Journal of Human
5276 Evolution 56, 76–85.

Skinner, M.M., Wood, B.A., Boesch, C., Olejniczak, A.J., Rosas, A., Smith, T.S., Hublin, J.-J., 2008. Dental trait expression at the enamel-dentine junction of lower molars in extant and fossil hominoids. Journal of Human Evolution 54, 173–186.

Skinner, M.F., 2019. Developmental stress in South African hominins: Comparison of recurrent enamel hypoplasias in *Australopithecus africanus* and *Homo naledi*. South African Journal of Science 115, 1–10.

Smith, B.H., 1984. Patterns of molar wear in hunter-gatherers and agriculturalists. American Journal of Physical Anthropology 63, 39–56.

Smith, T.M., Olejniczak, A.J., Tafforeau, P., Reid, D.J., Grine, F.E., Hublin, J.-J., 2006. Molar crown thickness, volume, and development in South African Middle Stone Age humans. South African Journal of Science 102, 513–517.

Stynder, D.D., Moggi-Cecchi, J., Berger, L.R., Parkington, J.E., 2001. Human mandibular incisors from the late Middle Pleistocene locality of Hoedjiespunt 1, South Africa. Journal of Human Evolution 41, 369–383.

Suwa, G., White, T. D., Howell, F. C., 1996. Mandibular postcanine dentition from the Shungura Formation, Ethiopia: crown morphology, taxonomic allocations, and Plio-Pleistocene hominid evolution. American Journal of Physical Anthropology 101, 247–282.

Tobias, P.V., 1965. New discoveries in Tanganyika: Their bearing on hominid evolution. Current Anthropology 6, 391–399.

Tobias, P.V., 1971. Human skeletal remains from the Cave of Hearths, Makapansgat, Northern Transvaal. American Journal of Physical Anthropology 34, 335–367.

Towle, I., Irish, J.D., De Groote, I., 2017. Behavioral inferences from the high levels of dental chipping in *Homo naledi*. American Journal of Physical Anthropology 164, 184–192.

Towle, I., Irish, J. D., Groote, I. D., Fernée, C., Loch, C., 2021. Dental caries in South African fossil hominins. South African Journal of Science 117, 1–8.

Ungar, P.S., Berger, L.R., 2018. Brief communication: Dental microwear and diet of *Homo naledi*. American Journal of Physical Anthropology 166, 228–235.

Van Reenen, J. F., and Reid, C., 1995. The Carabelli trait in early South African hominids: a morphological study. In: Moggi-Cecchi, J. (Ed.), Aspects of Dental Biology: Palaeontology, Anthropology, and Evolution. International Institute for the Study of Man, Florence, pp 291–298.

VanSickle, C., Cofran, Z., García-Martinez, D., Williams, S.A., Churchill, S.E., Berger, L.R., Hawks, J., 2018. *Homo naledi* pelvic remains from the Dinaledi Chamber, South Africa. Journal of Human Evolution 125, 122–136.

Vandermeersch, B., 1981. Les Hommes Fossiles de Qafzeh (Israel). Cahiers de Paléontologie (Paléoanthropologie). Editions du CNRS, Paris.

Villmoare, B., Kimbel, W.H., Seyoum, C., Campisano, C.J., DiMaggio, E.N., Rowan, J., Braun, D.R., Arrowsmith, J.R., Reed, K.E., 2015. Early *Homo* at 2.8 Ma from Ledi-Geraru, Afar, Ethiopia. Science 347, 1352–1355.

Weidenreich, F., 1943. The skull of *Sinanthropus pekinensis*: A comparative study on a primitive hominid skull. Palaeontol. Sin. D 10, 1–484.

Weidenreich, F., 1937. The dentition of *Sinanthropus pekinensis*: A comparative odontography of the hominids. Palaeontol. Sin. D 1, 1–180.

Will, M., El-Zaatari, S., Harvati, K., Conard, N.J., 2019. Human teeth from securely stratified Middle Stone Age contexts at Sibudu, South Africa. Archaeological and Anthropological Sciences 11, 3491 – 3501.

Wood, B.A., 1991. Koobi Fora Research Project, Vol. 4. Hominid Cranial Remains. Clarendon Press, Oxford.

Wood, B.A., Abbott, S.A., Uytterschaut, H., 1988. Analysis of the dental morphology of Plio-Pleistocene hominids. IV. Mandibular postcanine root morphology. Journal of Anatomy 156, 107–139.

Wood, B.A., van Noten, F.L., 1986. Preliminary observations on the BK 8518 mandible from Baringo, Kenya. American Journal of Physical Anthropology 69, 117–127.

Zanolli, C., 2013. Additional evidence for morpho-dimensional tooth crown variation in a new Indonesian *H. erectus* sample from the Sangiran Dome (Central Java). PLoS One 8, e67233.

Zanolli, C., Davies, T.W., Joannes-Boyau, R., Beaudet, A., Bruxelles, L., de Beer, F., Hoffman, J.H., Hublin, J.-J., Jakata, K., Kgasi, L., Kullmer, O., Macchiarelli, R., Pan, L., Schrenk, F., Santos, F., Stratford, D., Tawane, M., Thackeray, F., Xing, S., Zipfel, B., Skinner, M.M., 2022. Dental data challenge the ubiquitous presence of *Homo* in the Cradle of Humankind. Proceedings of the National Academy of Sciences USA 119, e2111212119.

FIGURE LEGENDS

Figure 1. Maxillary deciduous central incisors. For all teeth, from left to right, lingual, labial, mesial, and distal views: A) U.W. 101-544C (right dI^1); B) U.W. 101-1331 (left dI^1). Scale bar is 10 mm.

Figure 2. Maxillary deciduous lateral incisor. From left to right, lingual, labial, mesial, and distal views of U.W. 101-1304 (left dI^2). Scale bar is 10 mm.

Figure 3. Maxillary deciduous canines. For all teeth, from left to right, lingual, labial, mesial, and distal views: A) U.W. 101-595 (left dC^1); B) U.W. 101-728 (right dC^1); C) U.W. 101-1287A (left dC^1). Scale bar is 10 mm.

Figure 4. Maxillary first deciduous molars. For all teeth, from left to right, occlusal, mesial, distal, buccal, and lingual views: A) U.W. 101-823 (right dP^3); B) U.W. 101-1377 (left dP^3). Scale bar is 10 mm.

Figure 5. Maxillary second deciduous molars. For all teeth, from left to right, occlusal, mesial, distal, buccal, and lingual views: A) U.W. 101-384 (right dP^4); B) U.W. 101-544A (right dP^4); C) U.W. 101-1376 (left dP^4); D) U.W. 101-1687 (right dP^4). Scale bar is 10 mm.

Figure 6. Mandibular deciduous lateral incisor. From left to right, lingual, labial, mesial, and distal views of U.W. 101-1612 (right dI_2). Scale bar is 10 mm.

Figure 7. Mandibular deciduous canines. For all teeth, from left to right, lingual, labial, mesial, and distal views: A) U.W. 101-824 (left dC_1); B) U.W. 101-1571 (left dC_1); C) U.W. 101-1611 (right dC_1). Scale bar is 10 mm.

Figure 8. Mandibular first deciduous molar. From left to right, occlusal, mesial, distal, buccal, and lingual views of U.W. 101-1685 (right dP_3). Scale bar is 10 mm.

Figure 9. Mandibular second deciduous molar. From left to right, occlusal, mesial, distal, buccal, and lingual views of U.W. 101-1686 (right dP_4). Scale bar is 10 mm.

Figure 10. Maxillary central incisors. For all teeth, from left to right, lingual, labial, mesial, and distal views: A) U.W. 101-038 (right I^1); B) U.W. 101-591 (left I^1); C) U.W. 101-931 (left I^1); D) U.W. 101-1012 (right I^1); E) U.W. 101-1558 (right I^1). Scale bar is 10 mm.

Figure 11. Maxillary lateral incisors. For all teeth, from left to right, lingual, labial, mesial, and distal views: A) U.W. 101-073 (right I^2); B) U.W. 101-417 (left I^2); C) U.W. 101-709 (right I^2); D) U.W. 101-932 (left I^2). Scale bar is 10 mm.

Figure 12. Maxillary lateral incisors. For all teeth, from left to right, lingual, labial, mesial, and distal views: A) U.W. 101-952 (left I^2); B) U.W. 101-1588 (left I^2); C) U.W. 101-1684 (left I^2). Scale bar is 10 mm.

Figure 13. Maxillary canines. For all teeth, from left to right, lingual, labial, mesial, and distal views: A) U.W. 101-337 (right C^1); B) U.W. 101-412 (left C^1); C) U.W. 101-501 (left C^1); D) U.W. 101-544B (lingual and labial views only; right C^1). Scale bar is 10 mm.

Figure 14. Maxillary canines. A) U.W. 101-706 (left C^1); B) U.W. 101-816 (right C^1); C) U.W. 101-908 (right C^1); D) U.W. 101-1403 (right C^1). Scale bar is 10 mm.

Figure 15. Maxillary canines. A) U.W. 101-1510 (right C^1); B) U.W. 101-1548 (lingual and labial views only; left C^1); C) U.W. 101-1556 (left C^1). Scale bar is 10 mm.

Figures 16. Maxillary third premolars. For all teeth, from left to right, occlusal, mesial, distal, buccal, and lingual views: A) U.W. 101-037 (right P^3); B) U.W. 101-182 (right P^3); C) U.W. 101-729 (right P^3); E) U.W. 101-786 (left P^3). Scale bar is 10 mm.

Figure 17. Maxillary third premolars. For all teeth, from left to right, occlusal, mesial, distal, buccal, and lingual views: A) U.W. 101-1004 (right P^3); B) U.W. 101-1107 (left P^3); C) U.W. 101-1402 (right P^3); D) U.W. 101-1560 (left P^3). Scale bar is 10 mm.

Figure 18. Maxillary fourth premolars. For all teeth, from left to right, occlusal, mesial, distal, buccal and lingual views: A) U.W. 101-277 (left P^4); B) U.W. 101-333 (left P^4 or

left P^3); C) U.W. 101-334 (right P^4); D) U.W. 101-455 (right P^4); E) U.W. 101-808 (left P^4). Scale bar is 10 mm.

Figure 19. Maxillary fourth premolars. For all teeth, from left to right, occlusal, mesial, distal, buccal, and lingual views: A) U.W. 101-1362 (left P^4); B) U.W. 101-1401 (right P^4); C) U.W. 101-1561 (left P^4). Scale bar is 10 mm.

Figure 20. Maxillary first molars. For all teeth, from left to right, occlusal, mesial, distal, buccal, and lingual views: A) U.W. 101-445 (left M^1); B) U.W. 101-525 (right M^1); C) U.W. 101-583 (right M^1); D) U.W. 101-708 (left M^1); E) U.W. 101-796 (left M^1). Scale bar is 10 mm.

Figure 21. Maxillary first molars. For all teeth, from left to right, occlusal, mesial, distal, buccal, and lingual views: A) U.W. 101-999 (right M^1); B) U.W. 101-1305 (left M^1); C) U.W. 101-1396 (right M^1); D) U.W. 101-1463 (right M^1); E) U.W. 101-1676 (left M^1); F) U.W. 101-1688 (right M^1). Scale bar is 10 mm.

Figure 22. Maxillary second molars. For all teeth, from left to right, occlusal, mesial, distal, buccal, and lingual views: A) U.W. 101-005 (right M^2); B) U.W. 101-505 (left M^2); C) U.W. 101-528 (left M^2); D) U.W. 101-593 (right M^2); E) U.W. 101-867 (right M^2). Scale bar is 10 mm.

Figure 23. Maxillary second molars. For all teeth, from left to right, occlusal, mesial, distal, buccal, and lingual views: A) U.W. 101-1006 (right M^2); B) U.W. 101-1015 (left M^2); C) U.W. 101-1063 (left M^2?); D) U.W. 101-1135 (right M^2); E) U.W. 101-1522 (left M^2). Scale bar is 10 mm.

Figure 24. Maxillary third molars. For all teeth, from left to right, occlusal, mesial, distal, buccal, and lingual views: A) U.W. 101-418C (left M^3); B) U.W. 101-527 (left M^3); C) U.W. 101-594 (right M^3); D) U.W. 101-1269 (left M^3); E) U.W. 101-1398A (right M^3); F) U.W. 101-1471 (left M^3). Scale bar is 10 mm.

Figure 25. Mandibular central incisors. For all teeth, from left to right, lingual, labial, mesial, and distal views: A) U.W. 101-039 (right I_1); B) U.W. 101-601 (left I_1); C) U.W. 101-1005A (left I_1); D) U.W. 101-1005B (right I_1); E) U.W. 101-1132 (left I_1); F) U.W. 101-1133 (right I_1). Scale bar is 10 mm.

Figure 26. Mandibular lateral incisors. For all teeth, from left to right, lingual, labial, mesial, and distal views: A) U.W. 101-335 (right I_2); B) U.W. 101-998 (left I_2); C) U.W. 101-1005C (right I_2). Scale bar is 10 mm.

Figure 27. Mandibular lateral incisors. For all teeth, from left to right, lingual, labial, mesial, and distal views: A) U.W. 101-1075 (right I_2); B) U.W. 101-1131 (left I_2); C) U.W. 101-1400 (left I_2). Scale bar is 10 mm.

Figure 28. Mandibular canines. For all teeth, from left to right, lingual, labial, mesial, and distal views: A) U.W. 101-245 (right C_1); B) U.W. 101-339 (right C_1); C) U.W. 101-359 (left C_1); D) U.W. 101-886 (right C_1). Scale bar is 10 mm.

Figure 29. Mandibular canines. For all teeth, from left to right, lingual, labial, mesial, and distal views: A) U.W. 101-985 (left C_1); B) U.W. 101-1076 (left C_1); C) U.W. 101-1126 (left C_1); D) U.W. 101-1610 (right C_1). Scale bar is 10 mm.

Figure 30. Mandibular third premolars. For all teeth, from left to right, occlusal, mesial, distal, buccal, and lingual views: A) U.W. 101-144 (left P_3); B) U.W. 101-298 (right P_3); C) U.W. 101-358 (left P_3); D) U.W. 101-506 (right P_3). Scale bar is 10 mm.

Figure 31. Mandibular third premolars. For all teeth, from left to right, occlusal, mesial, distal, buccal, and lingual views: A) U.W. 101-800 (right P_3); B) U.W. 101-889 (left P_3); C) U.W. 101-1565 (left P_3). Scale bar is 10 mm.

Figure 32. Mandibular fourth premolars. For all teeth, from left to right, occlusal, mesial, distal, buccal, and lingual views: A) U.W. 101-184 (left P_4); B) U.W. 101-383 (right P_4); C) U.W. 101-887 (left P_4). Scale bar is 10 mm.

Figure 33. Mandibular first molars. For all teeth, from left to right, occlusal, mesial, distal, buccal, and lingual views: A) U.W. 101-285 (right M_1); B) U.W. 101-297 (right

M_1); C) U.W. 101-582 (left M_1); D) U.W. 101-809 (left M_1); E) U.W. 101-814 (left M_1). Scale bar is 10 mm.

Figure 34. Mandibular first molars. For all teeth, from left to right, occlusal, mesial, distal, buccal, and lingual views: A) U.W. 101-905 (left M_1); B) U.W. 101-1287B (right M_1); C) U.W. 101-1400 (left M_1); D) U.W. 101-1689 (right M_1). Scale bar is 10 mm.

Figure 35. Mandibular second molars. For all teeth, from left to right, occlusal, mesial, distal, buccal and lingual views: A) U.W. 101-145 (left M_2); B) U.W. 101-284 (left M_2); C) U.W. 101-507 (right M_2); D) U.W. 101-655 (right M_2); E) U.W. 101-789 (left M_2); F) U.W. 101-1002 (right M_2). Scale bar is 10 mm.

Figure 36. Mandibular third molars. For all teeth, from left to right, occlusal, mesial, distal, buccal, and lingual views: A) U.W. 101-006 (right M_3); B) U.W. 101-516 (left M_3). Scale bar is 10 mm.

Figure 37. Root fragments. A) U.W. 101-293; B) U.W. 101-388; C) U.W. 101-589; D) U.W. 101-602. Scale bar is 10 mm.

Figure 38. Occlusal view of U.W. 101-652, cusp germ of postcanine tooth. Scale bar is 10 mm.

Figure 39. Root fragments. A) U.W. 101-653; B) U.W. 101-654; C); U.W. 101-686; D) U.W. 101-864. Scale bar is 10 mm.

Figure 40. From left to right, lateral, anterior, and occlusal views of the U.W. 101-1277 maxilla with dentition. Scale bar is 10 mm.

Figure 41. Clockwise from top left, buccal, lingual, and occlusal views of U.W. 101-001 (right mandible fragment with P_4–M_3) and U.W. 101-850 (right P_3 with surrounding alveolar bone), which are refitted together. Scale bar is 10 mm.

Figure 42. Clockwise from top left, buccal, lingual, and occlusal views of U.W. 101-010 (right mandible fragment with C_1–P_3). Scale bar is 10 mm.

Figure 43. From top to bottom: buccal, lingual, and occlusal views of U.W. 101-361 (left mandible fragment with M_2 and M_3). Scale bar is 10 mm.

Figure 44. Clockwise from top left: buccal, lingual, and occlusal views of U.W. 101-377 (right mandible fragment with P_3–M_2) and U.W. 101-1014 (right C_1), which are refitted together. Scale bar is 10 mm.

Figure 45. Clockwise from top left, buccal, lingual, occlusal, and occlusal view of U.W. 101-1142 (right mandible fragment with M_2 and M_3), with the U.W. 101-1287B M_1 placed in its alveolus and without U.W. 101-1287B M_1. Scale bar is 10 mm.

Figure 46. Occlusal view of the U.W. 101-1261 complete mandibule with dentition. Scale bar is 10 mm.

Figure 47. From left to right, buccal, lingual, and occlusal views of U.W. 101-1400 (mandible fragment with dC_1–dP_4). Scale bar is 10 mm.

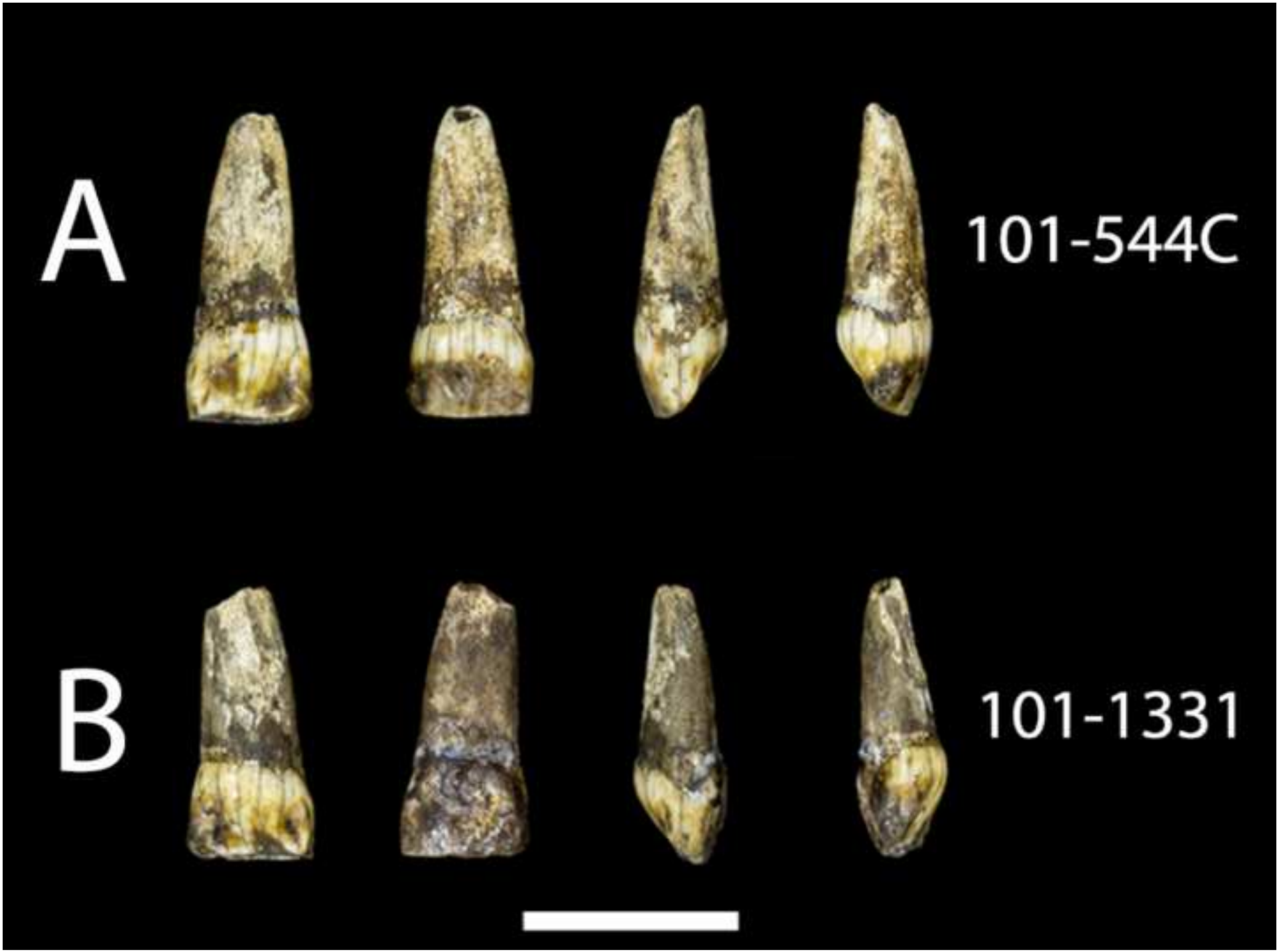

Figure 2_upper deciduous lateral incisor_color.tif

Figure 3_deciduous maxillary canines.tif

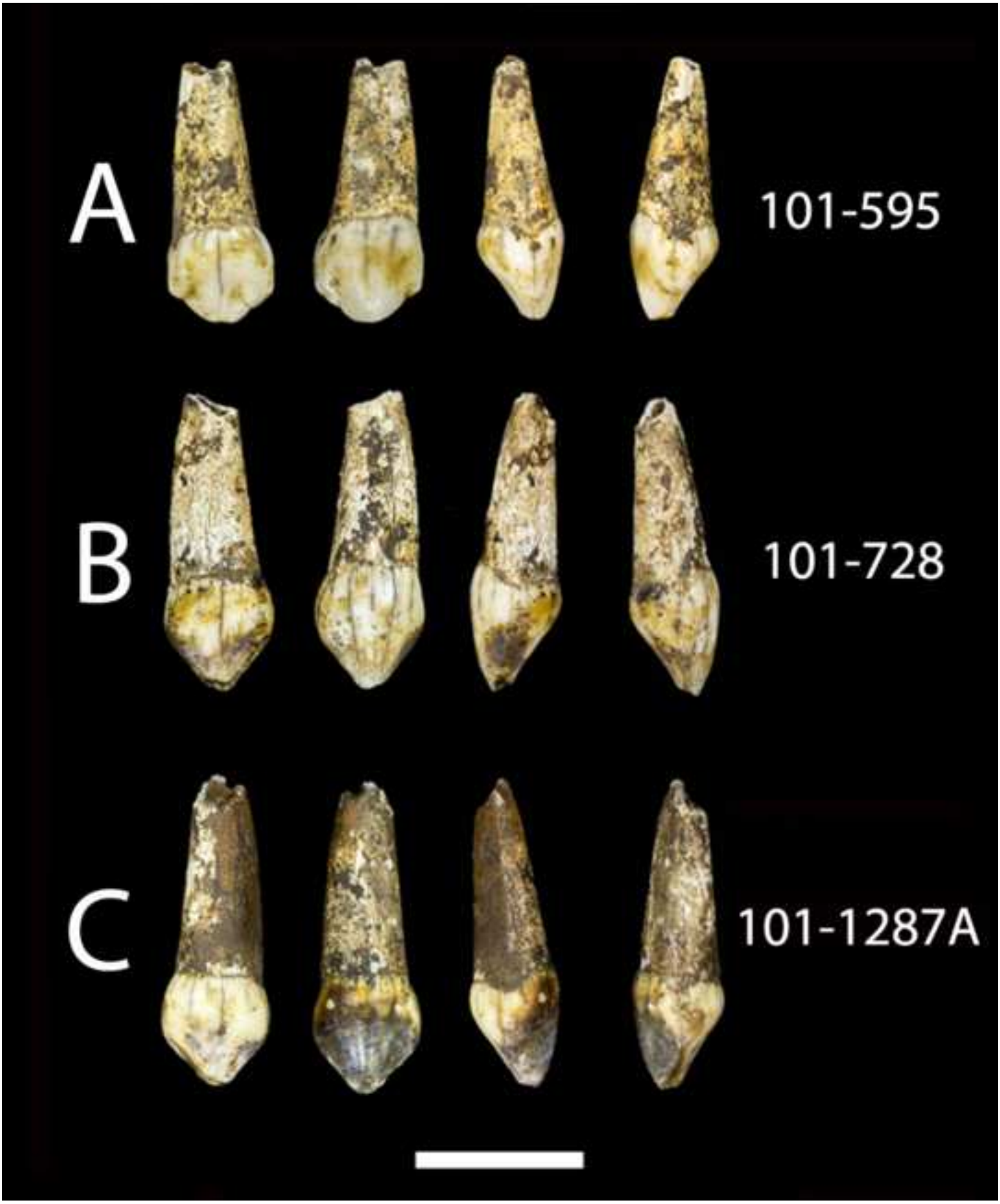

Figure 4_Upper dm1_color.tif

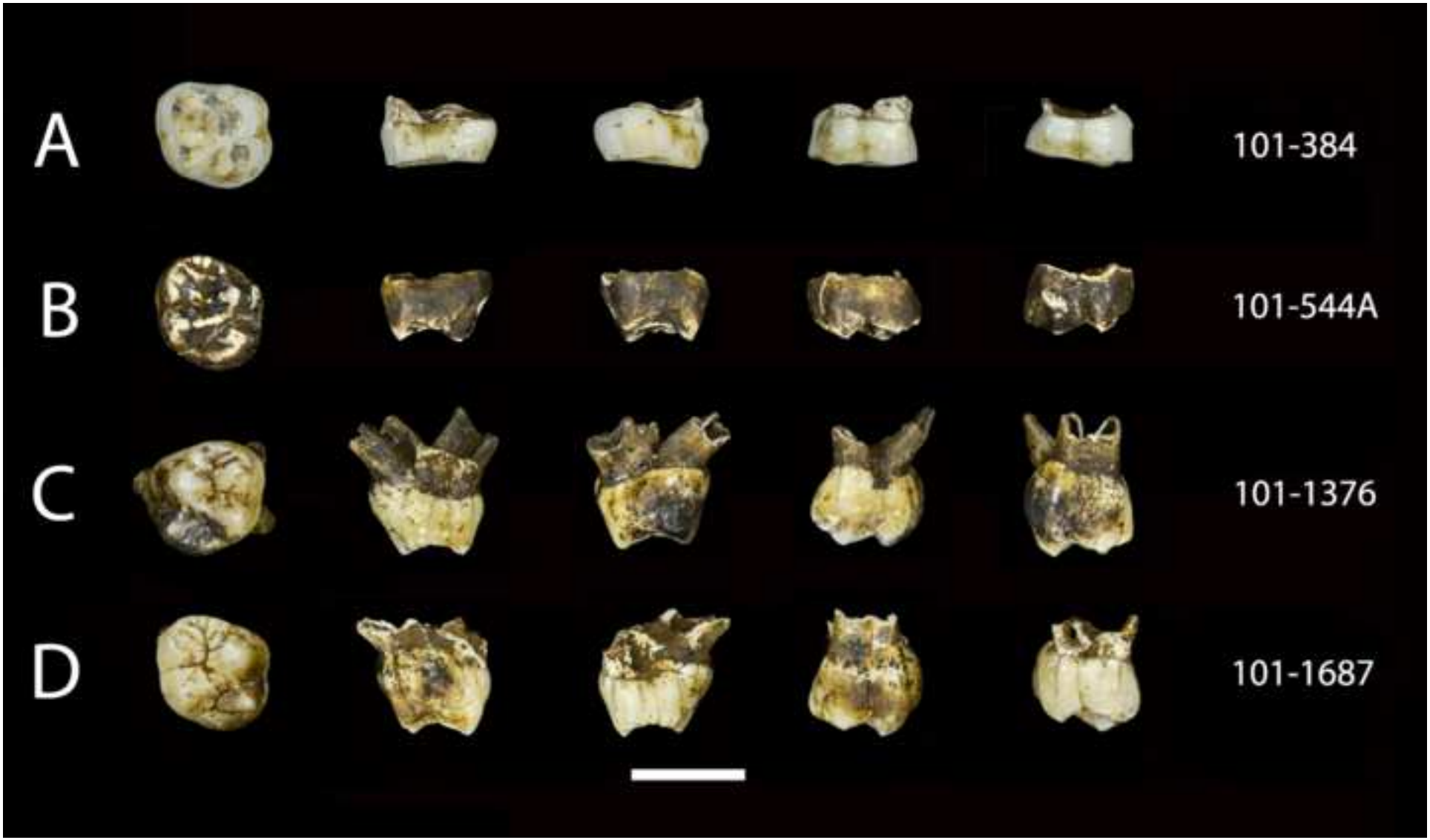

Figure 5_upper dm2s_color.tif

Figure 6_deciduous mandibular second incisors_color.tif

Figure 7_lower deciduous canines_color.tif

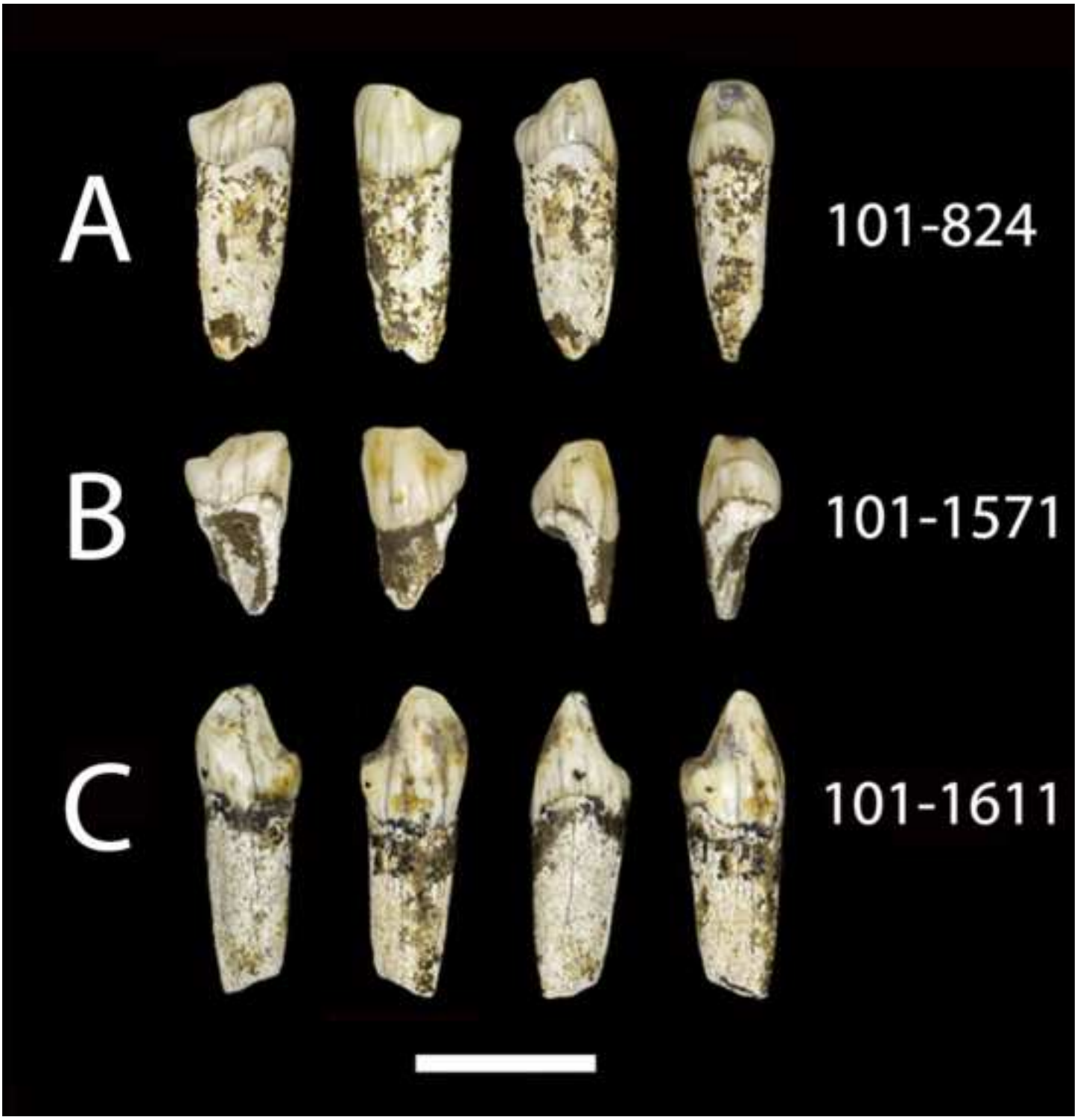

Figure 8_deciduous mandibular first molar_color.tif

Figure 9_deciduous mandibular second molars_color.tif

Figure 10_upper left and right I1_color.tif

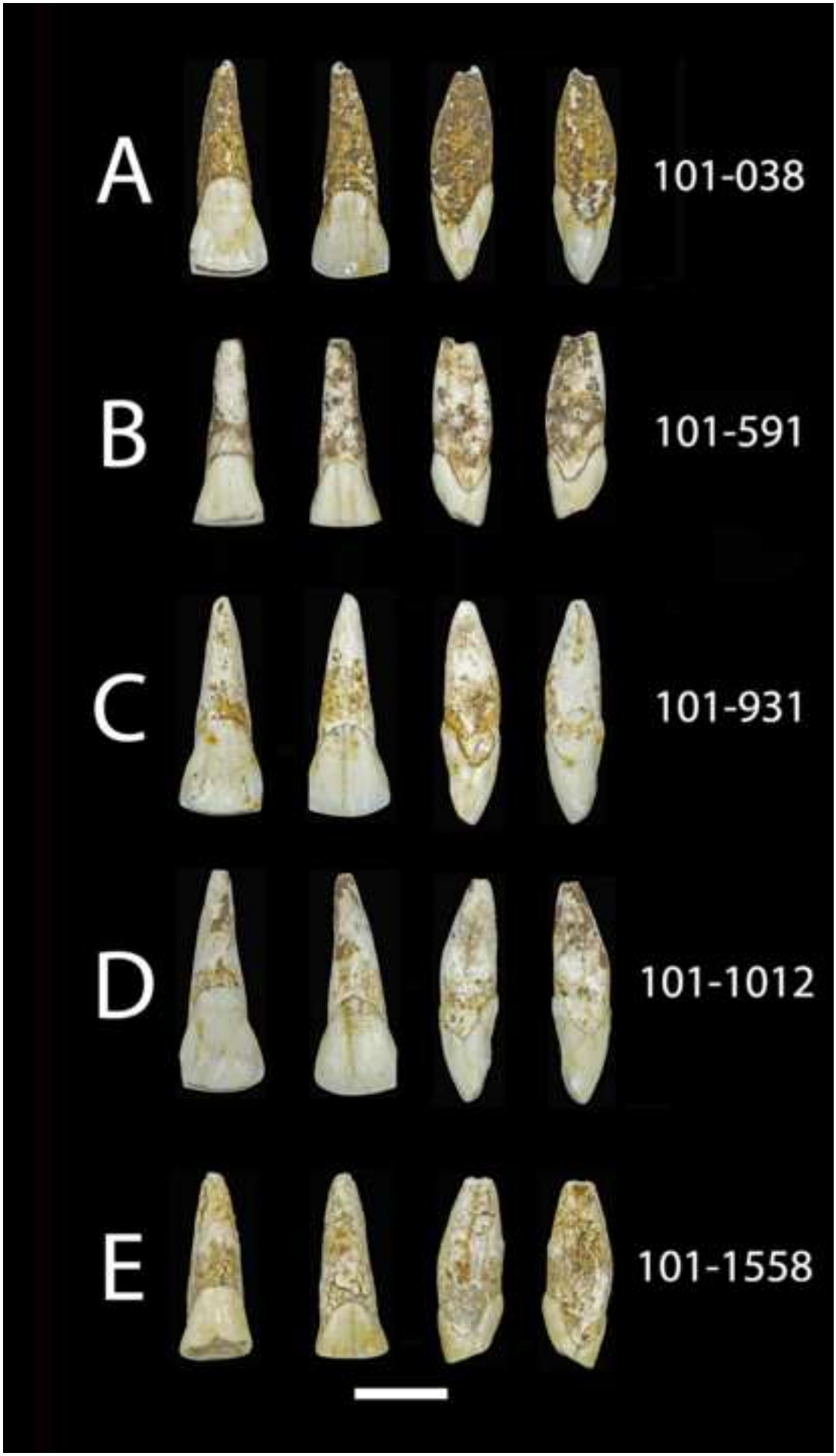

Figure 11_upper I2_color.tif

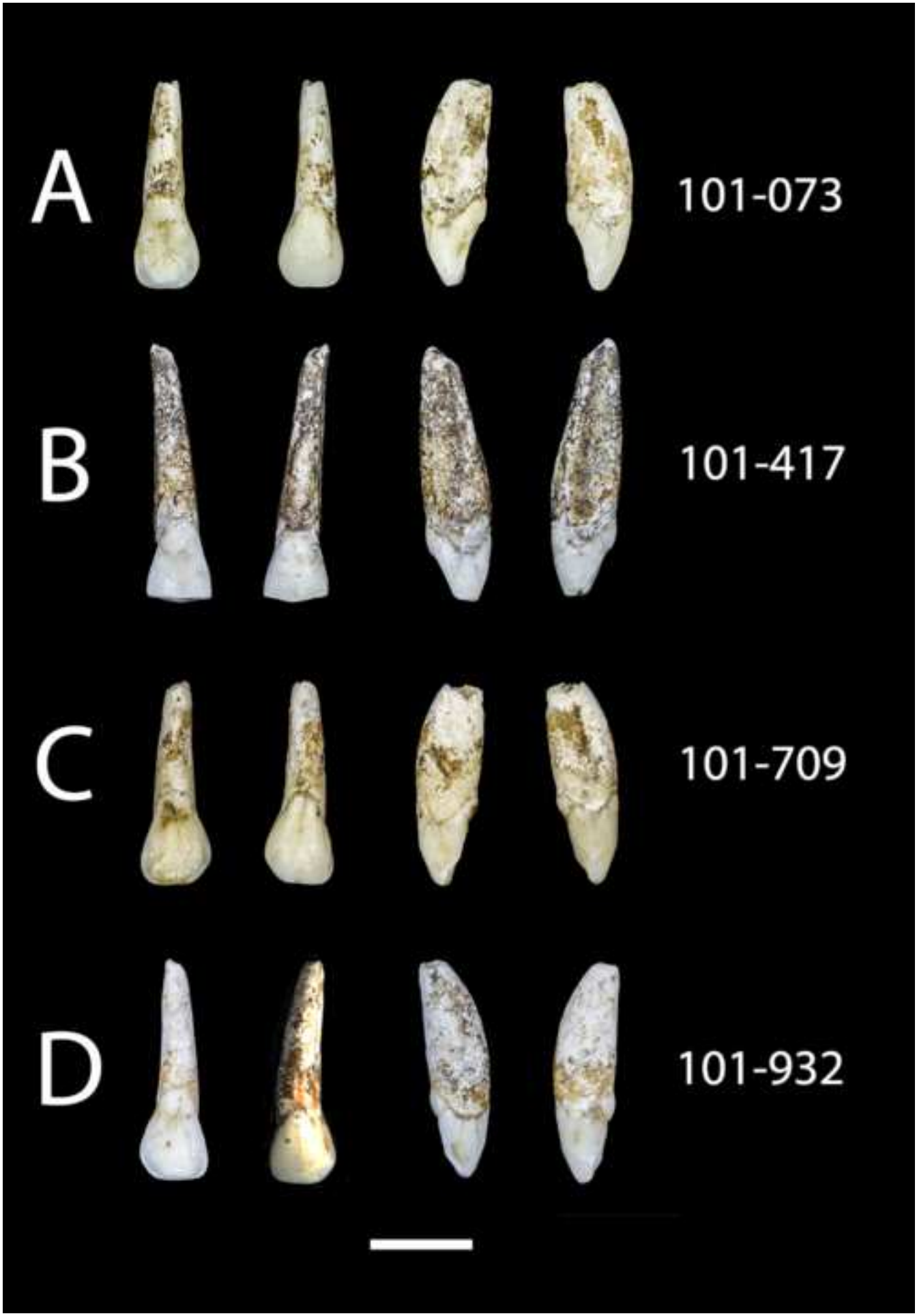

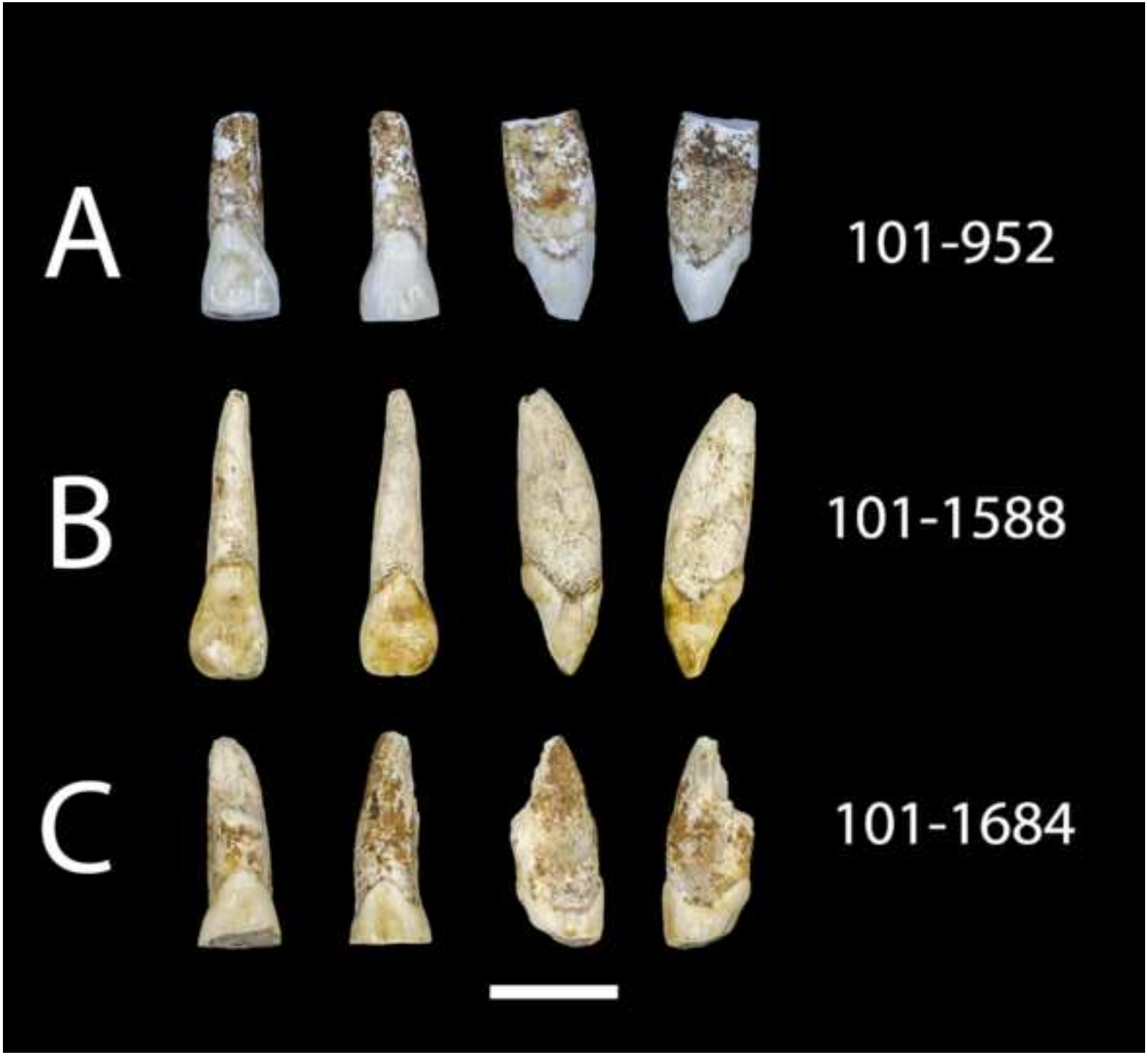

Figure 12_upper I2_cont_color.tif

Figure 13_upper canines_color.tif

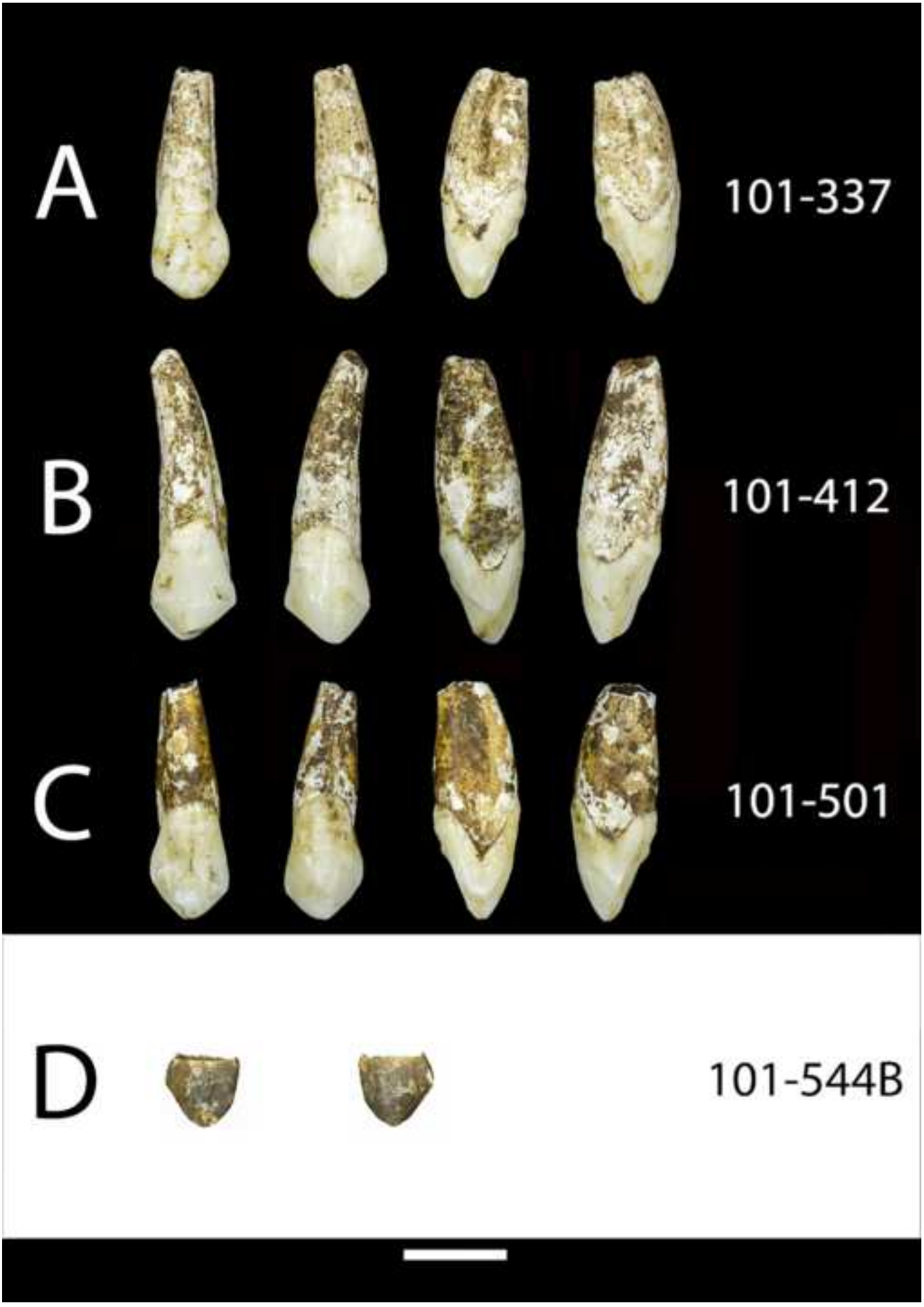

Figure 14 _upper canines_part 2_color.tif

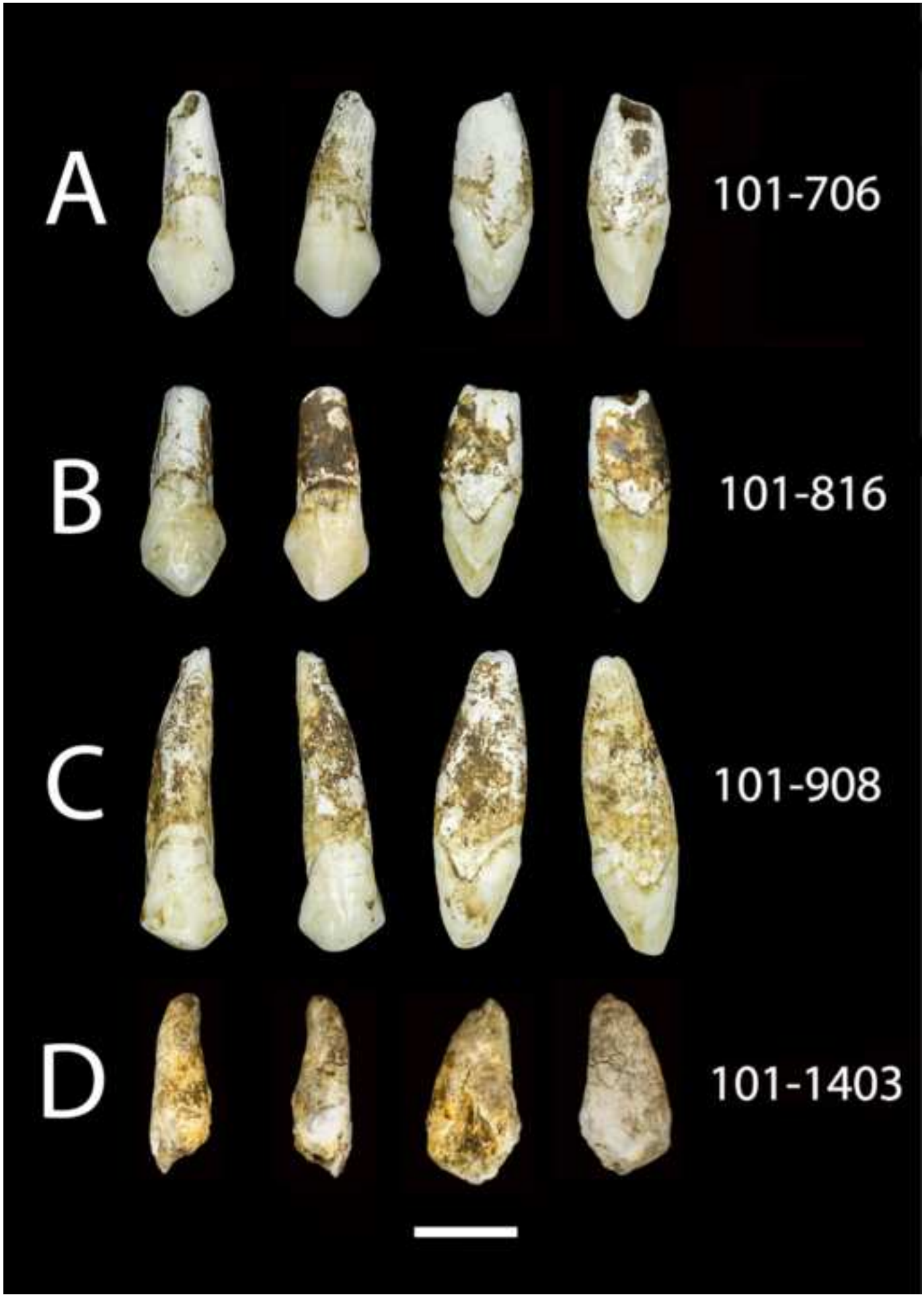

Figure 15 _upper canines_part 3_color.tif

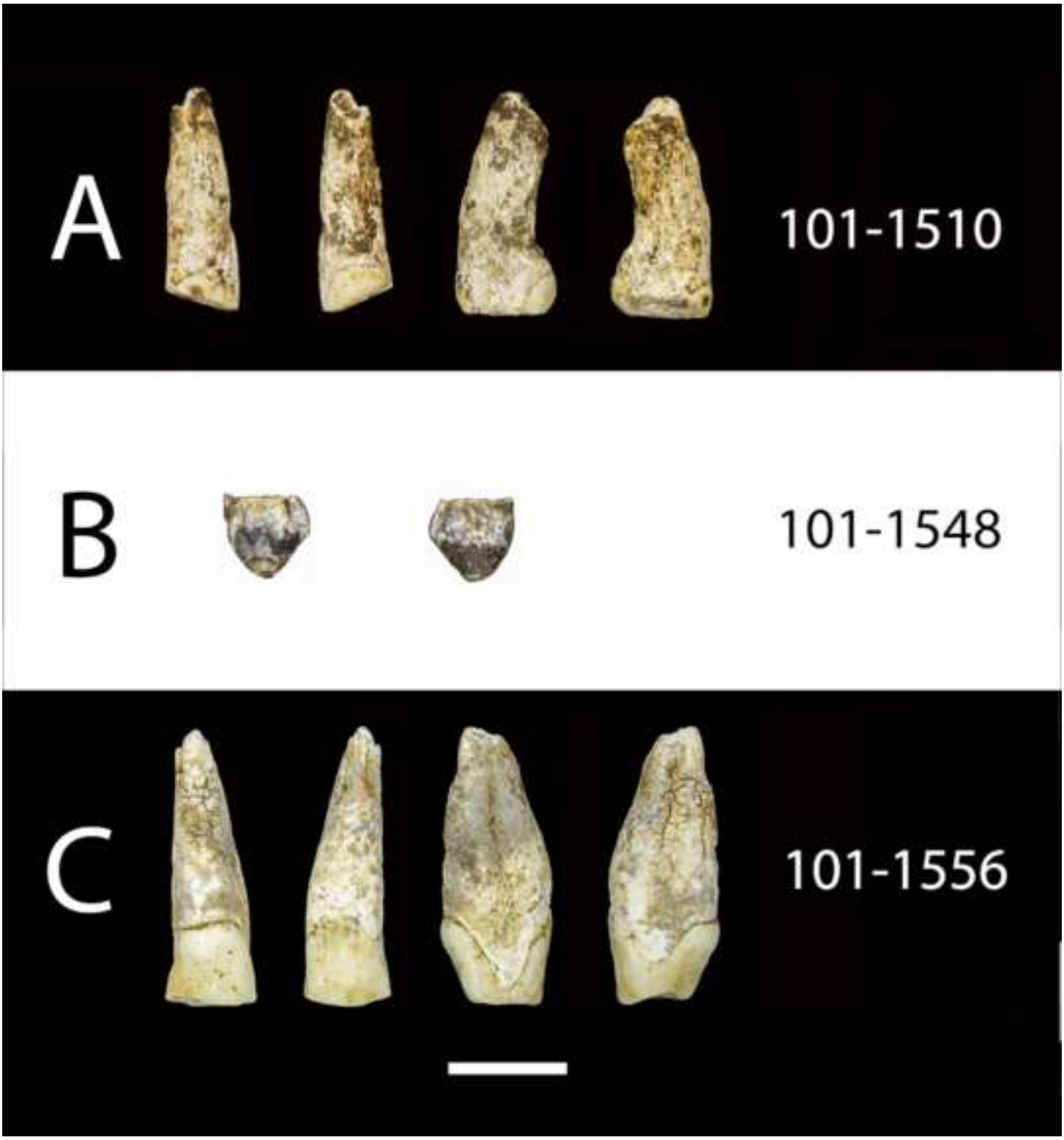

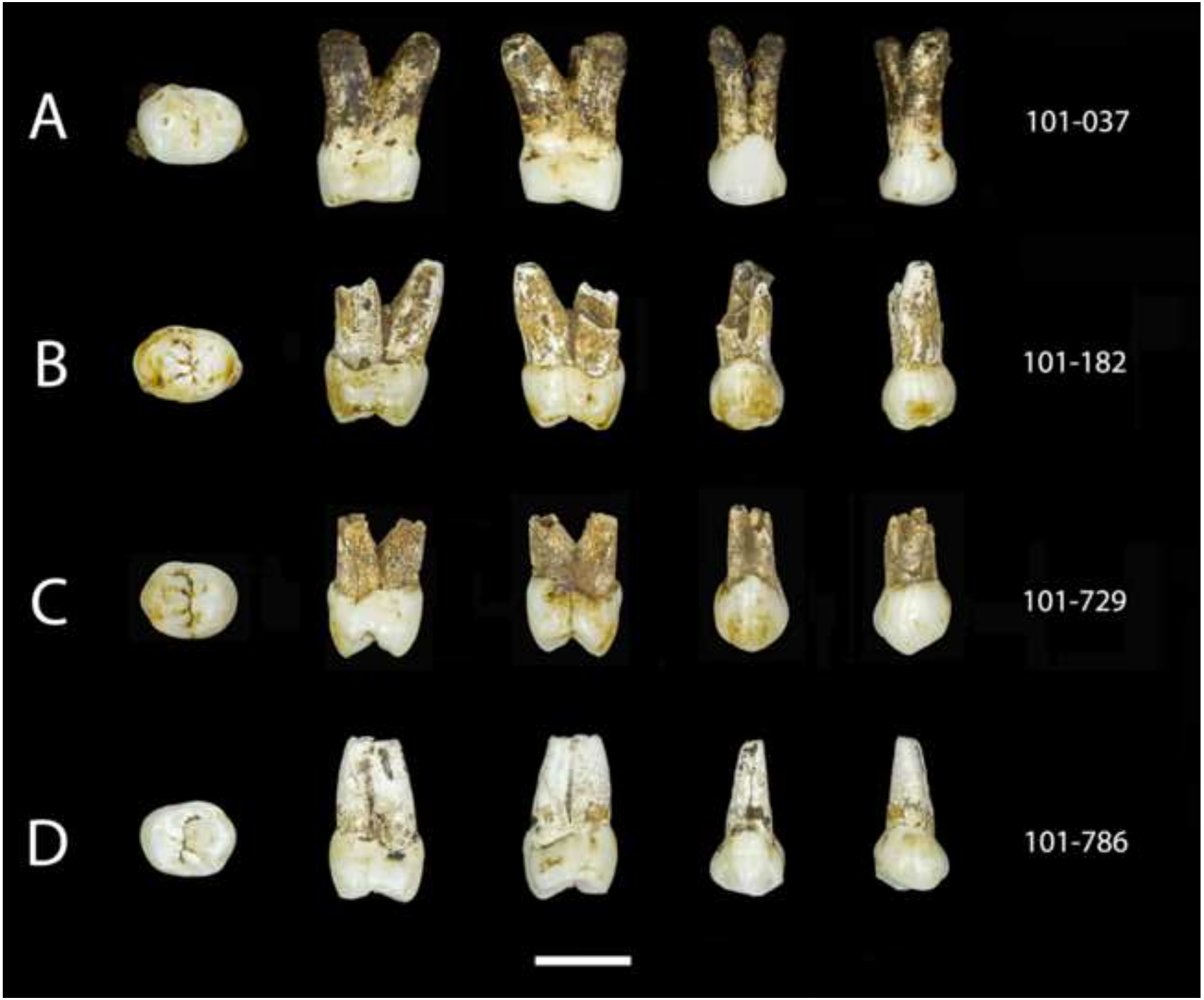

Figure 16_Upper p3_color.tif

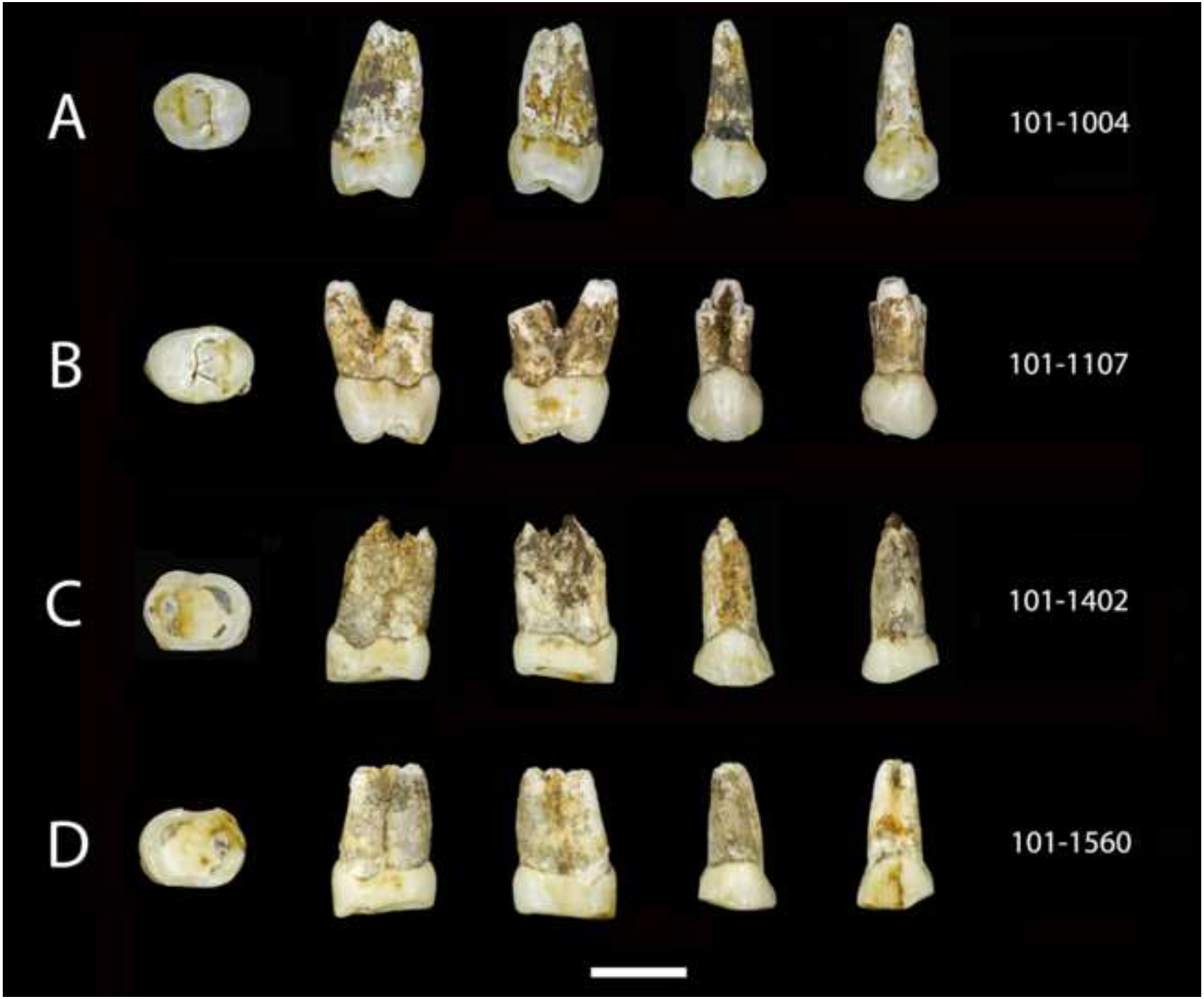

Figure 17_Upper p3_cont_color.tif

Figure 18_Upper p4s_color.tif

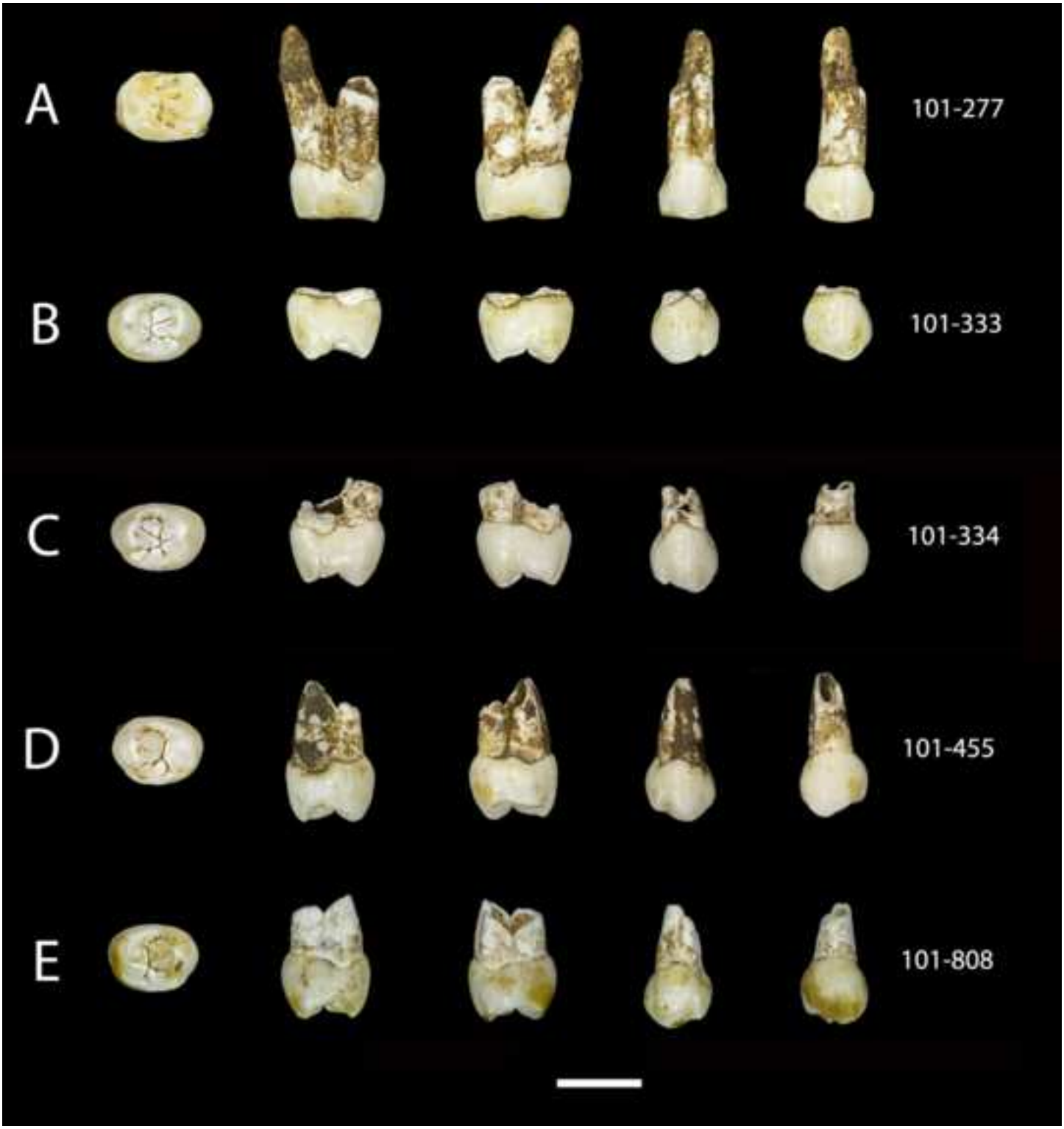

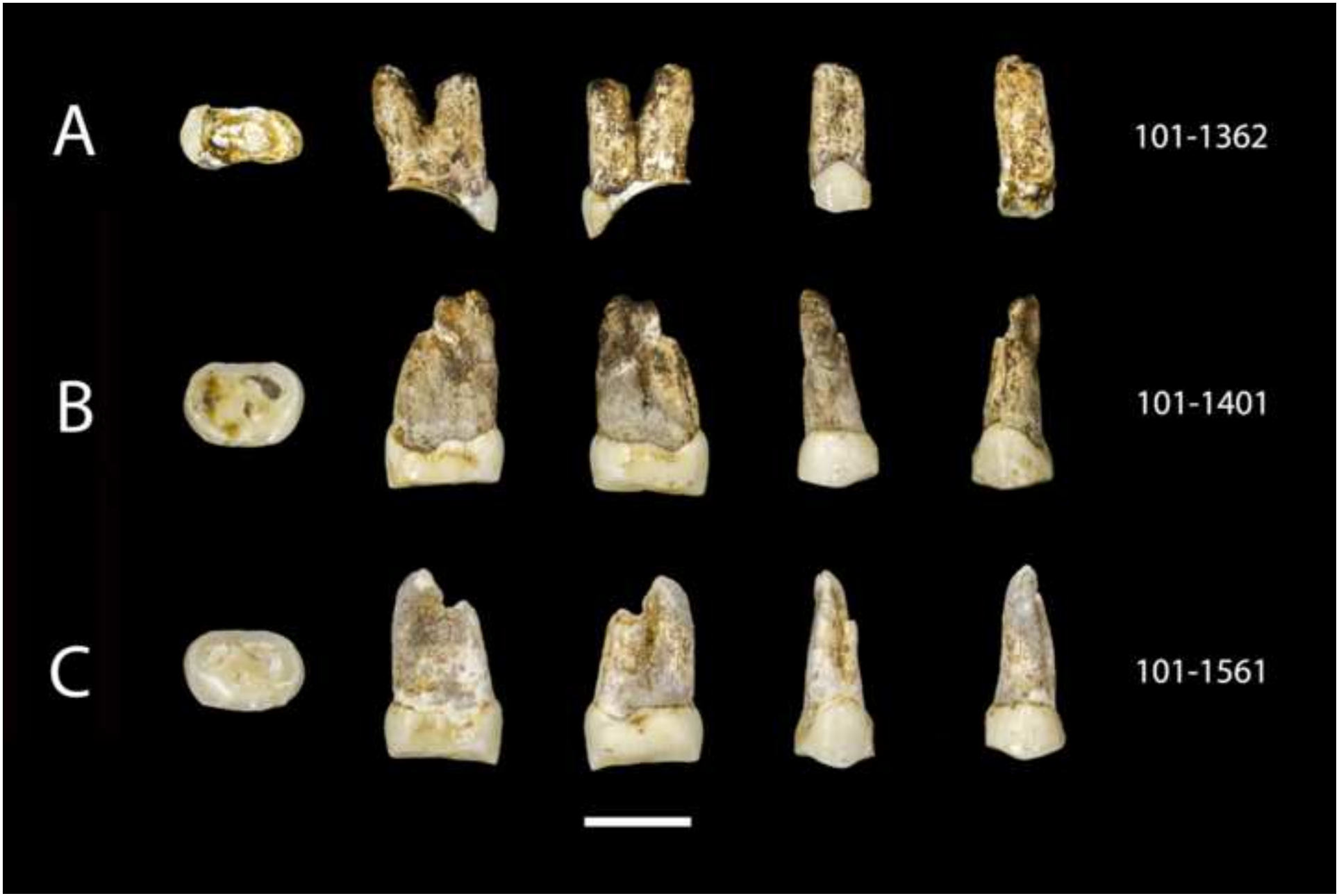

Figure 19_Upper p4s_continued_color.tif

Figure 20_upper M1_color.tif

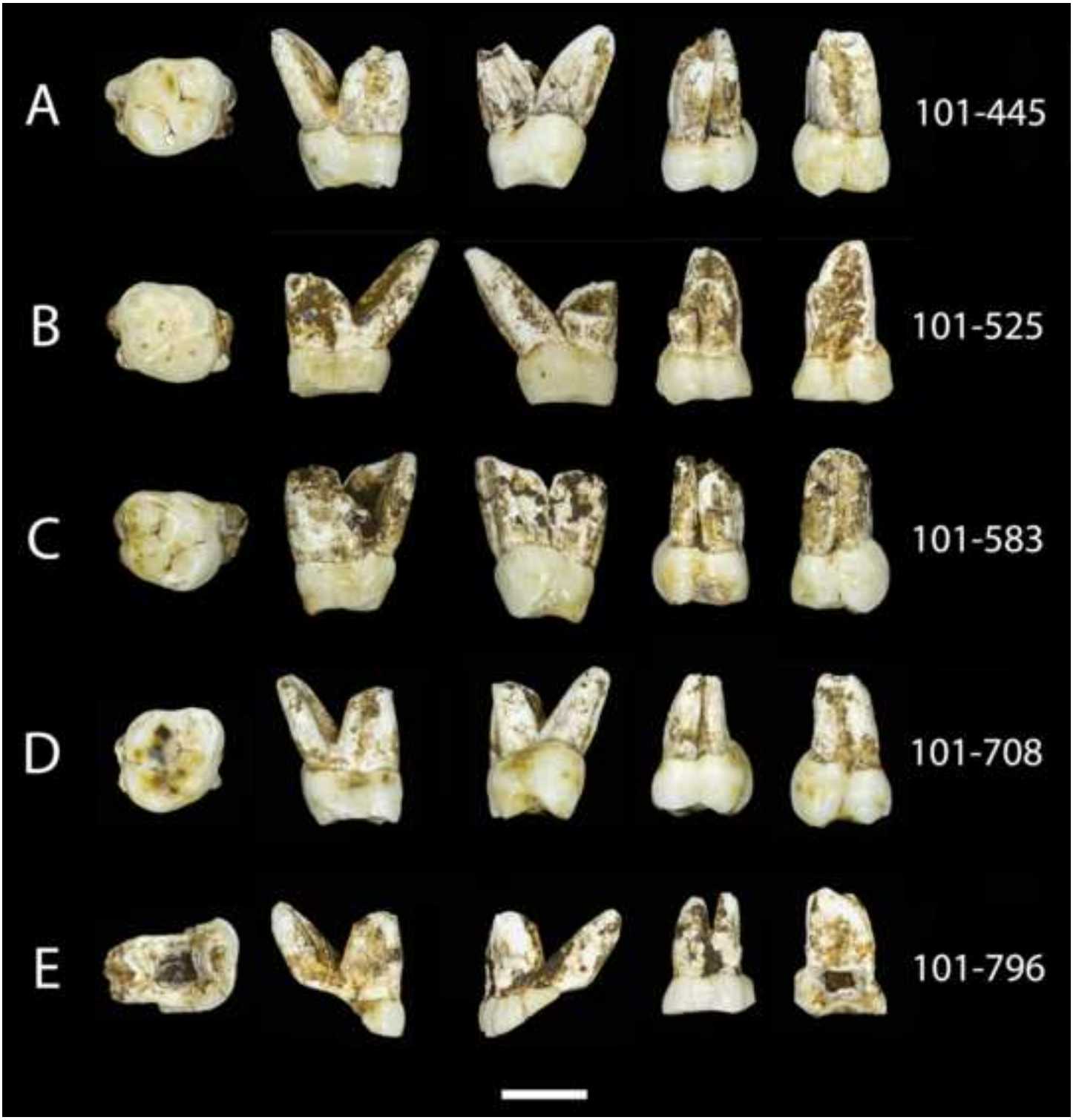

Figure 21 _upper M1_cont_color.tif

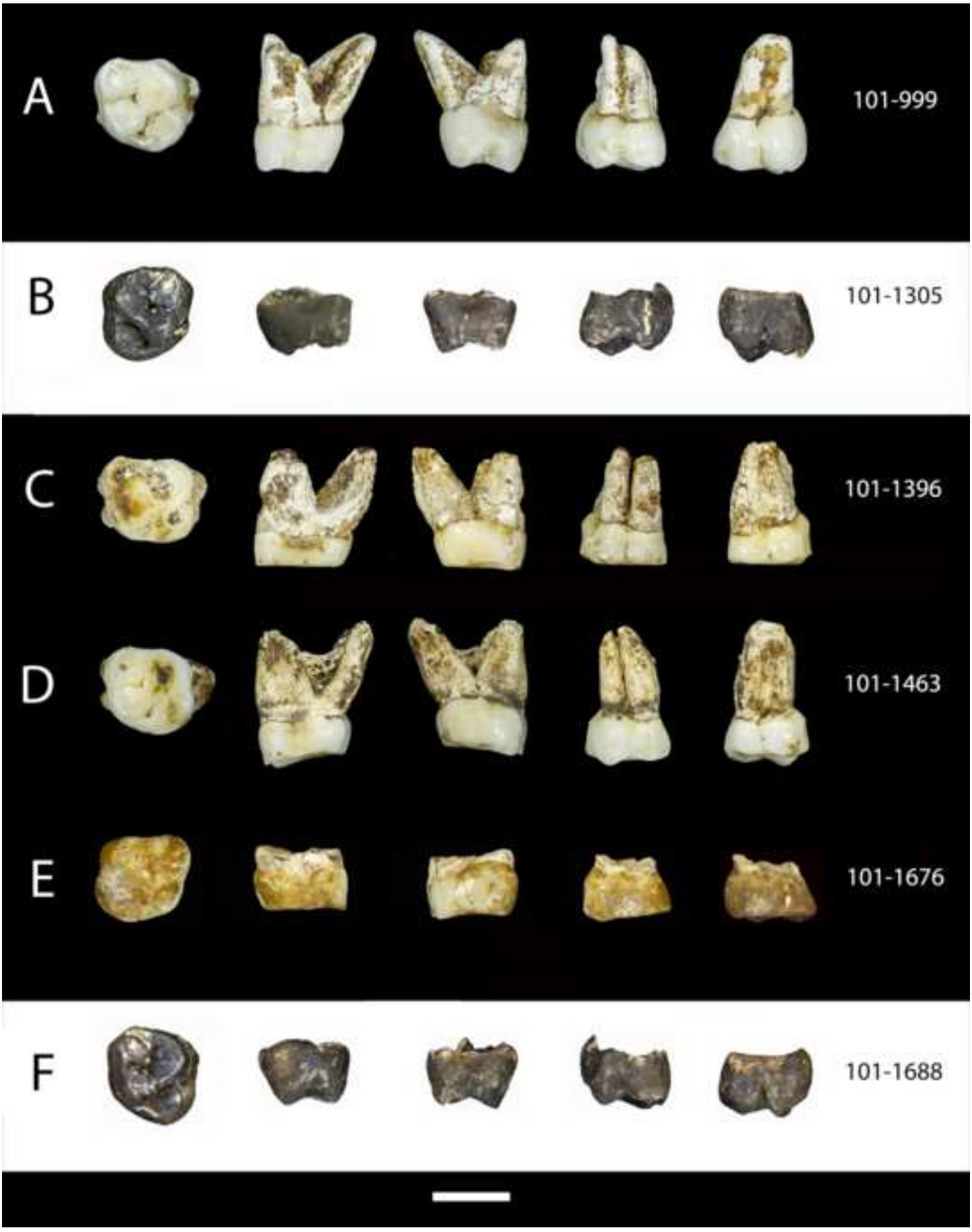

Figure 22_Maxillary M2_color.tif

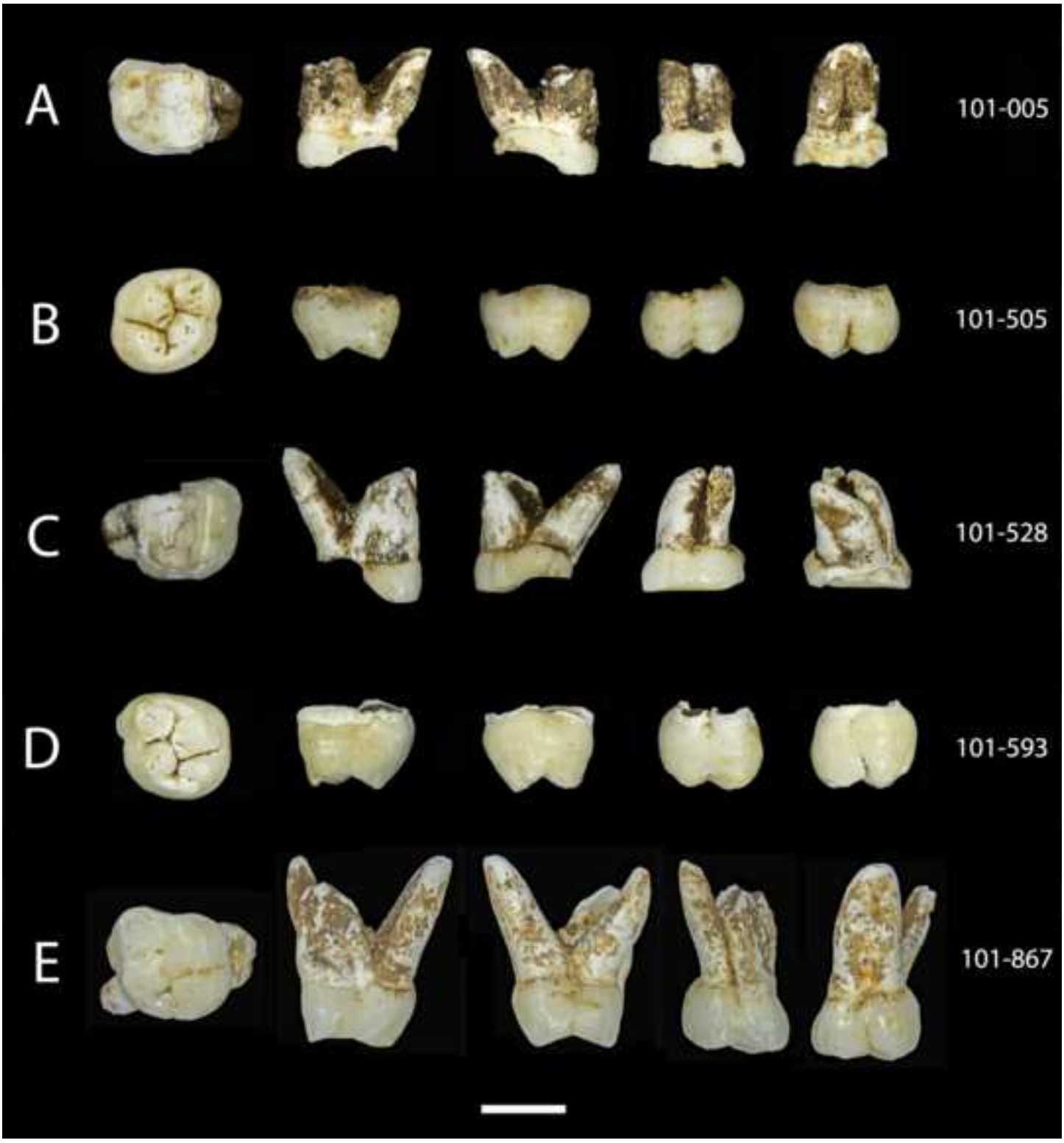

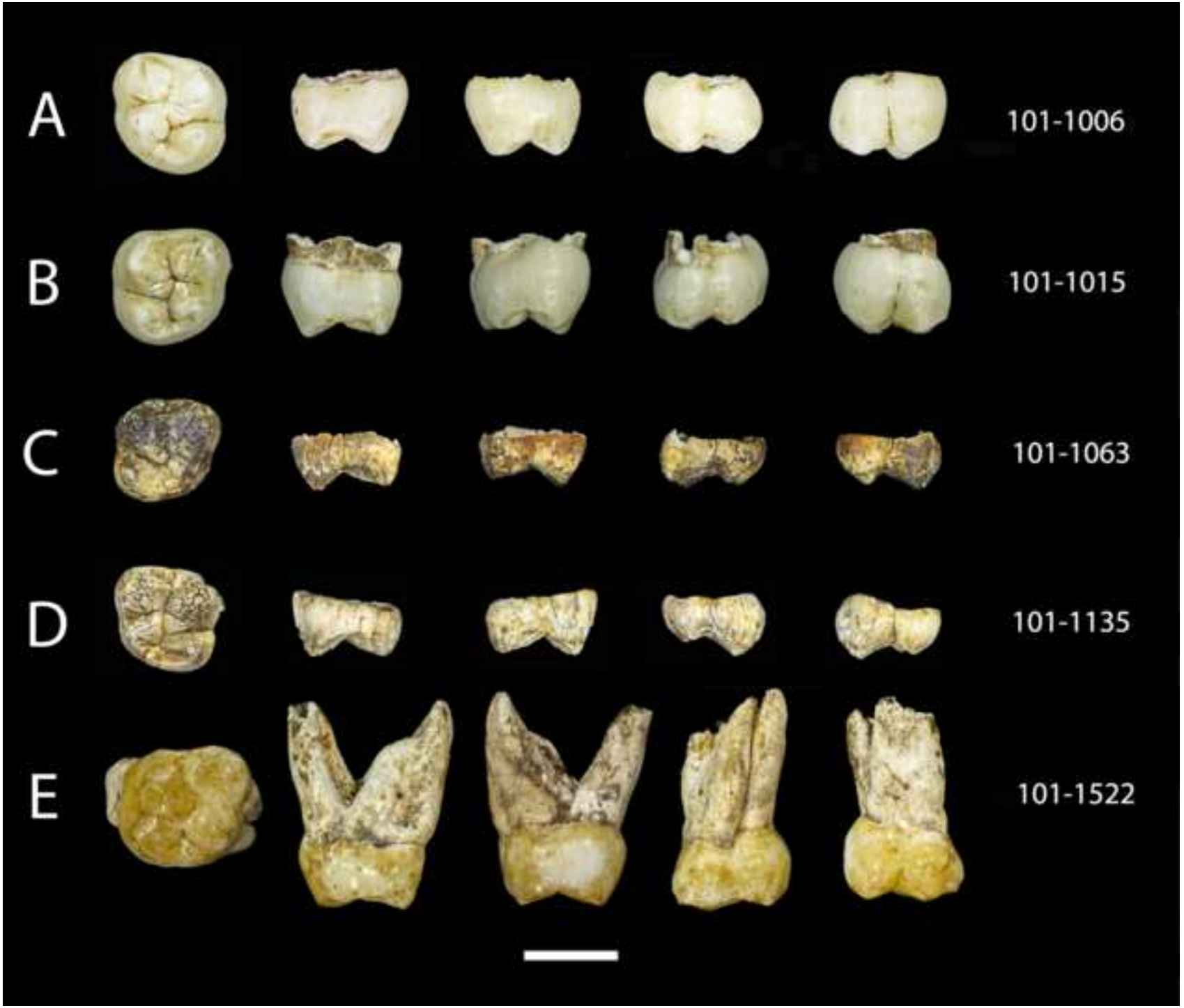

Figure 23 _Maxillary M2_continued_color.tif

Figure 24_upper M3s_color.tif

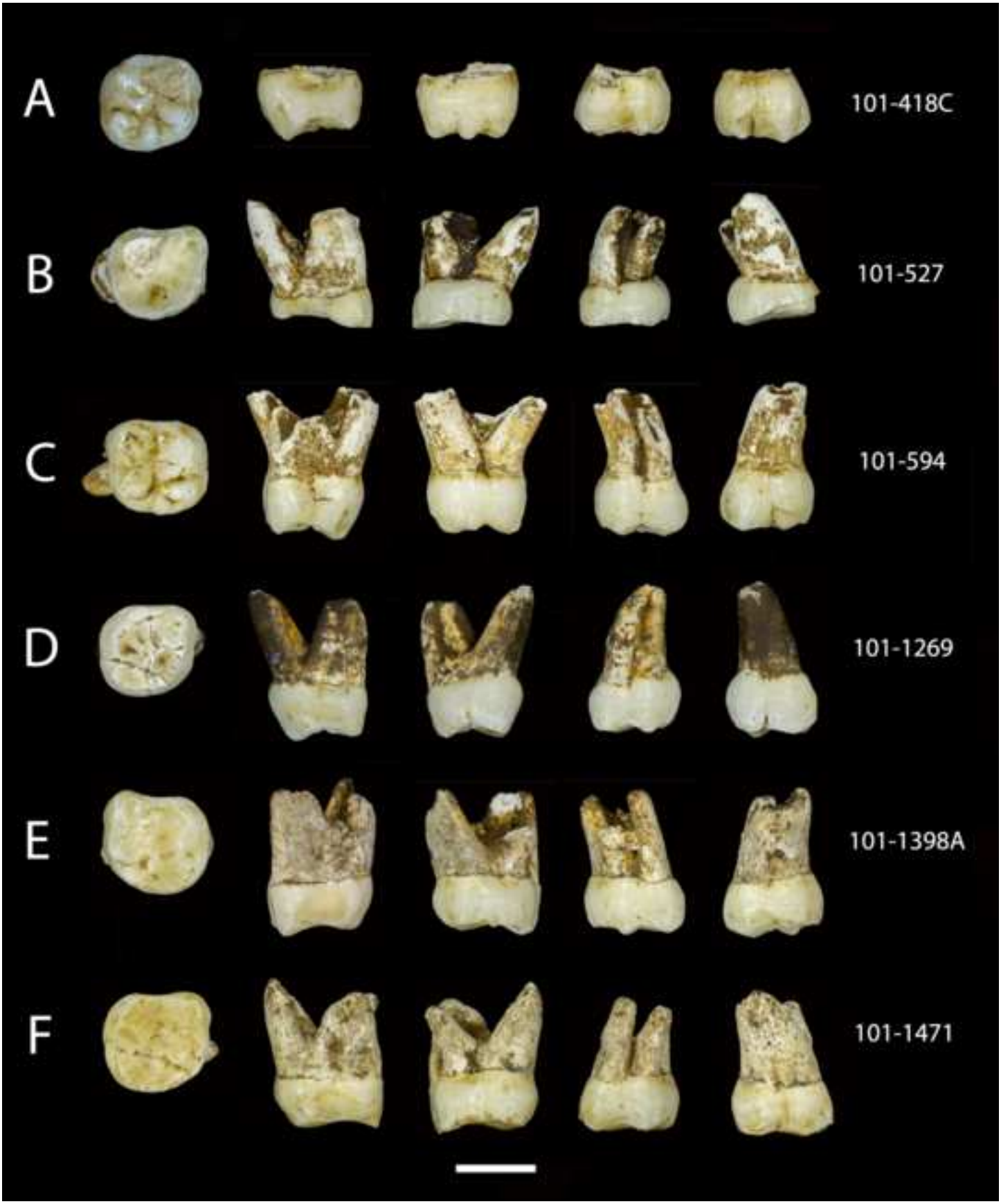

Figure 25_lower I1_color.tif

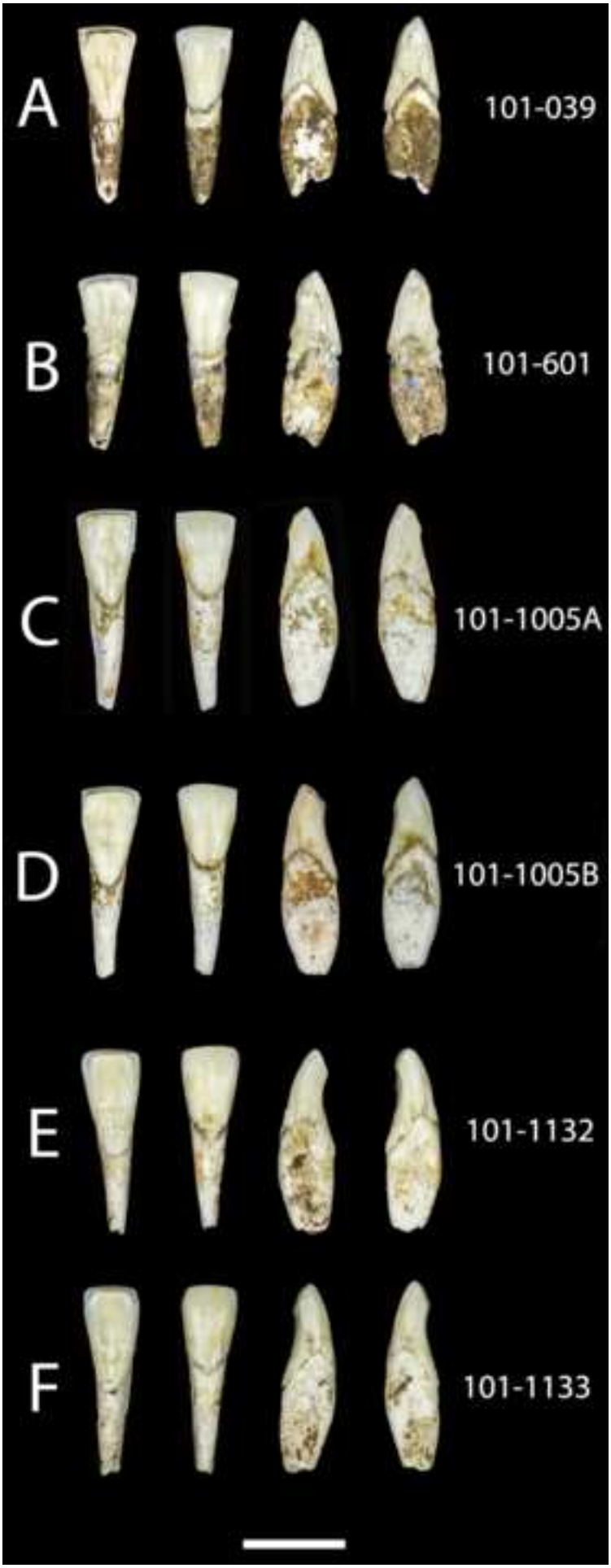

Figure 26_lower I2_color.tif

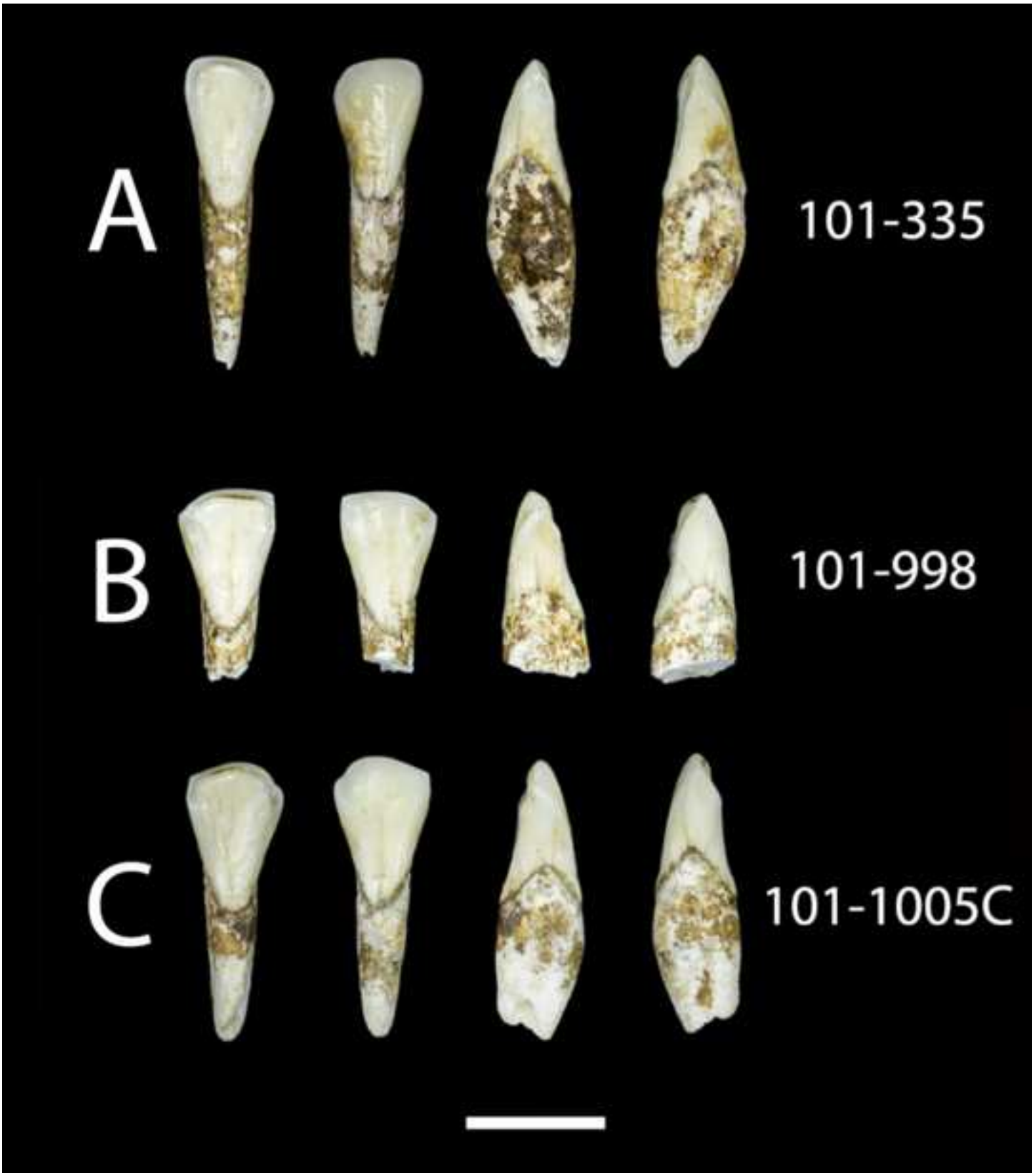

Figure 27_lower I2_cont_color.tif

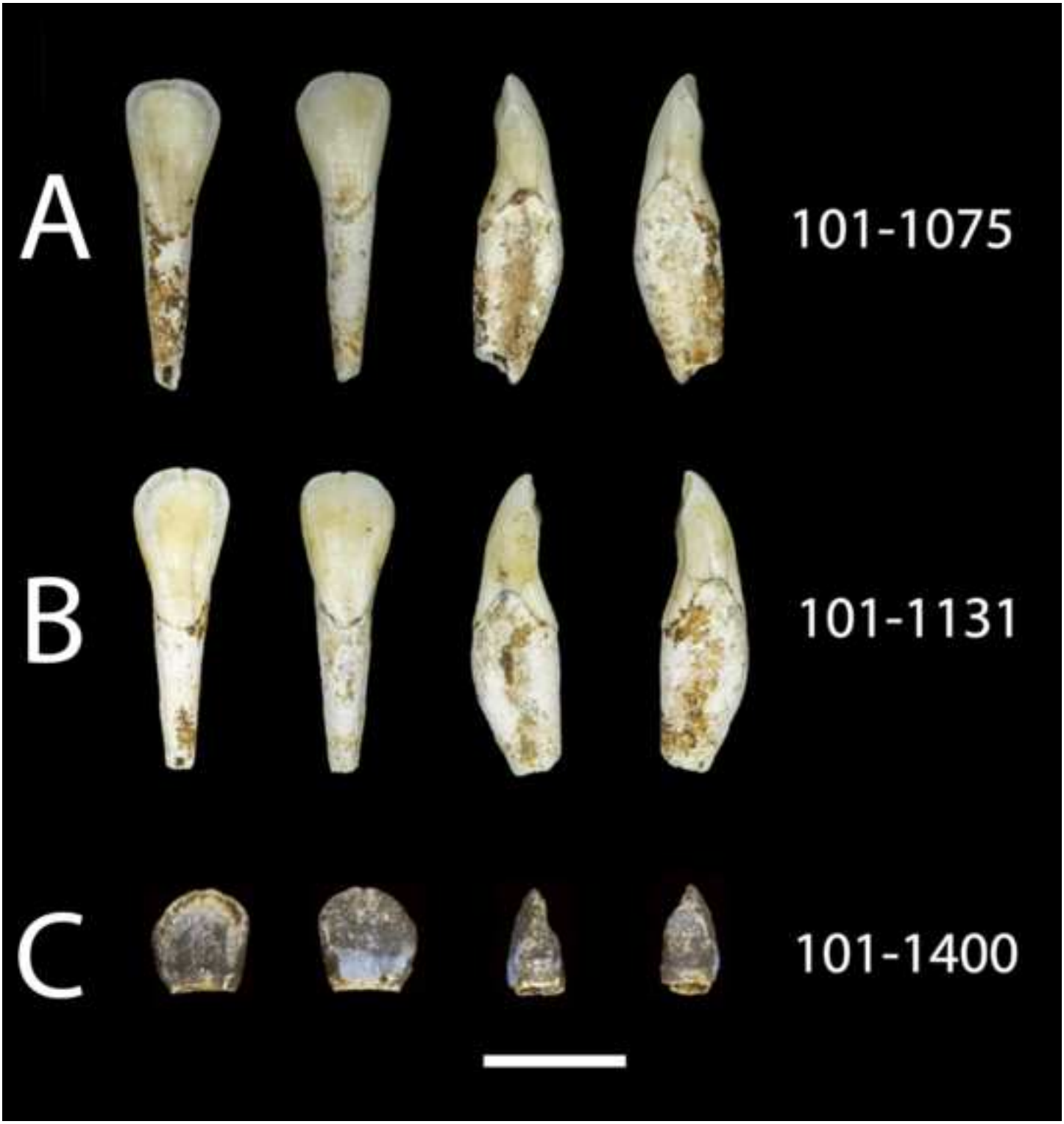

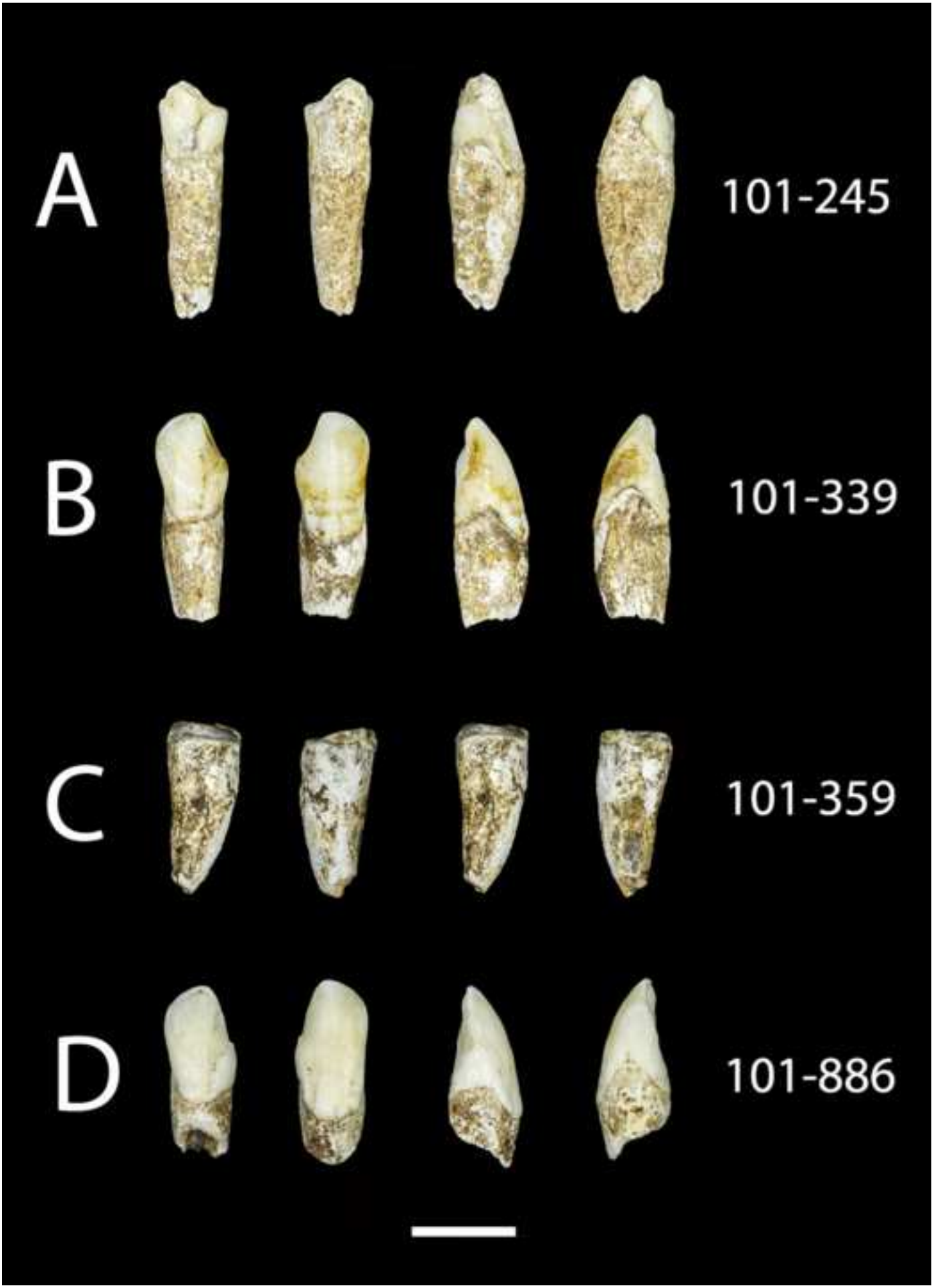

Figure 29_lower canines_cont_color.tif

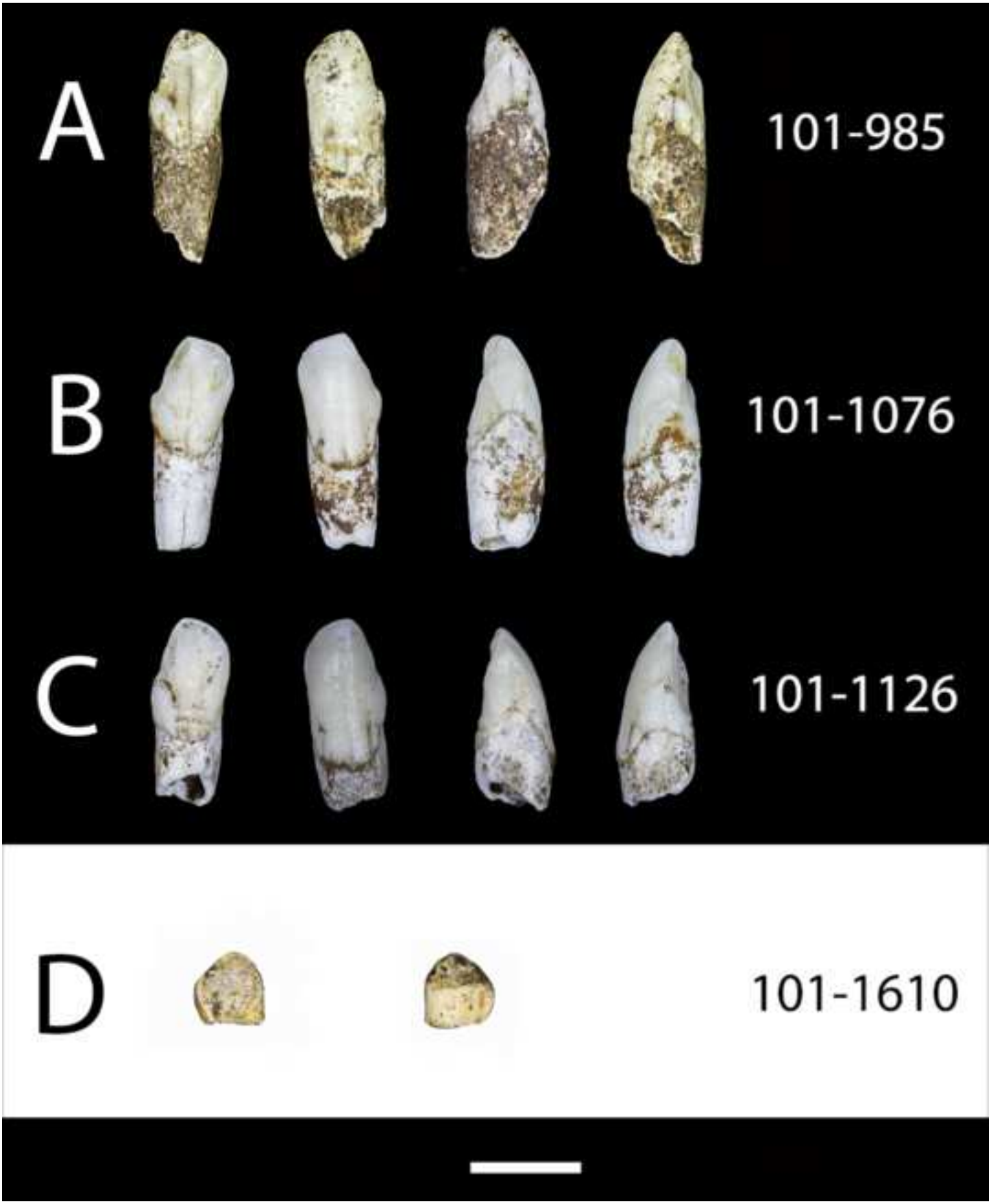

Figure 30_lower P3_color.tif

Figure 31_lower P3_cont_color.tif

Figure 32_lower P4s_color.tif

Figure 33_lower m1s_color.tif

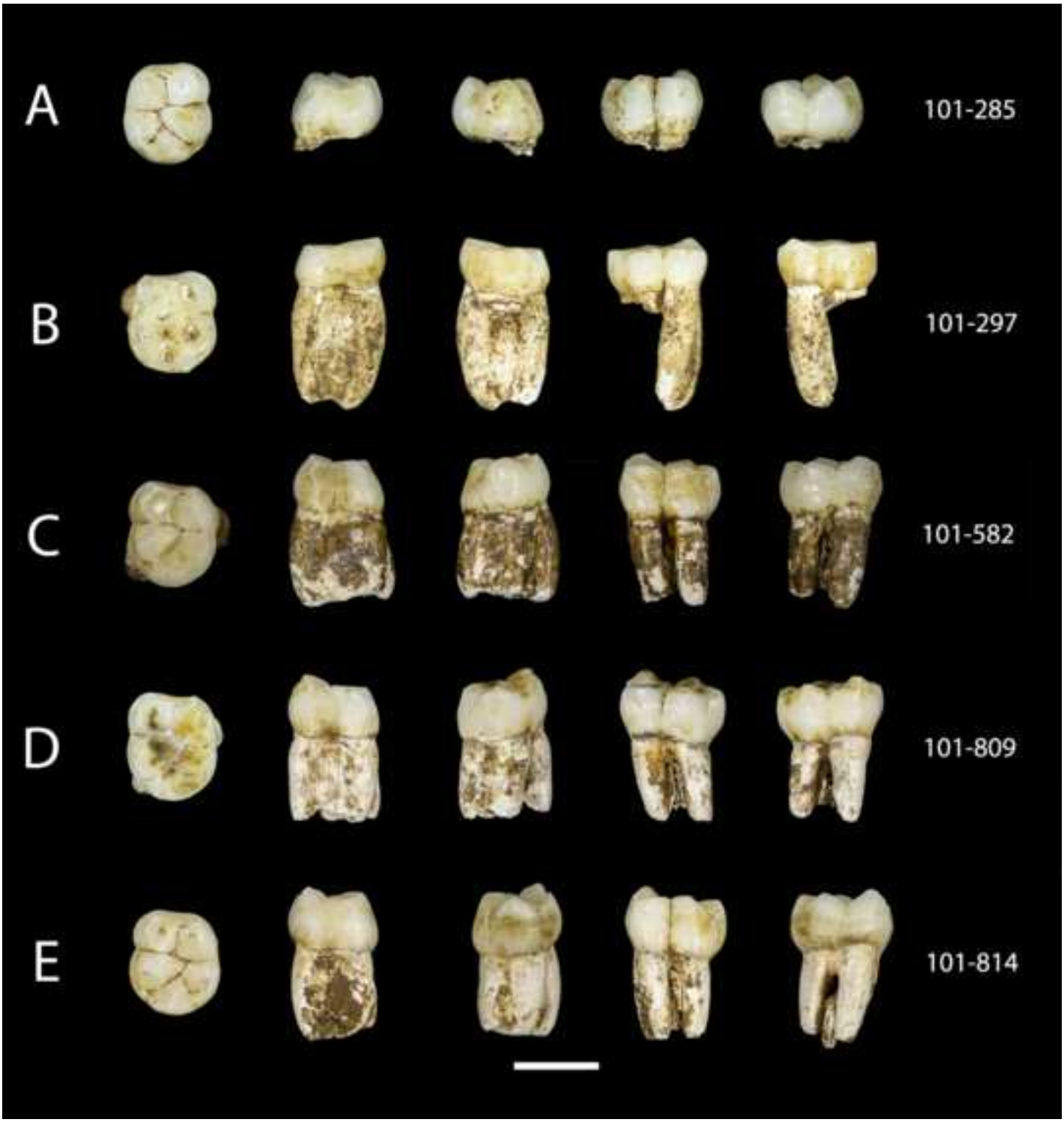

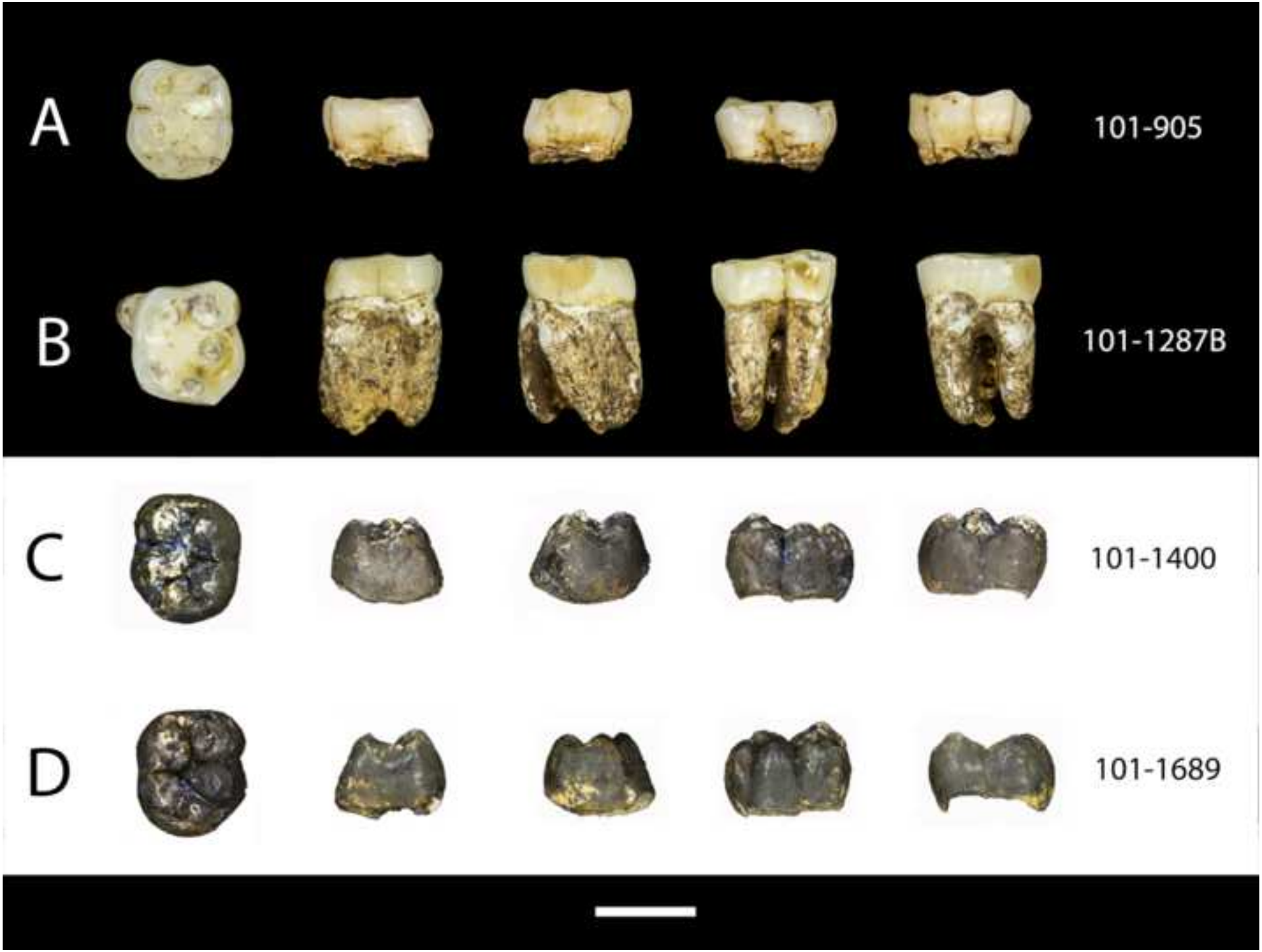

Figure 34_lower m1s_cont_color.tif

Figure 35_lower M2s_color.tif

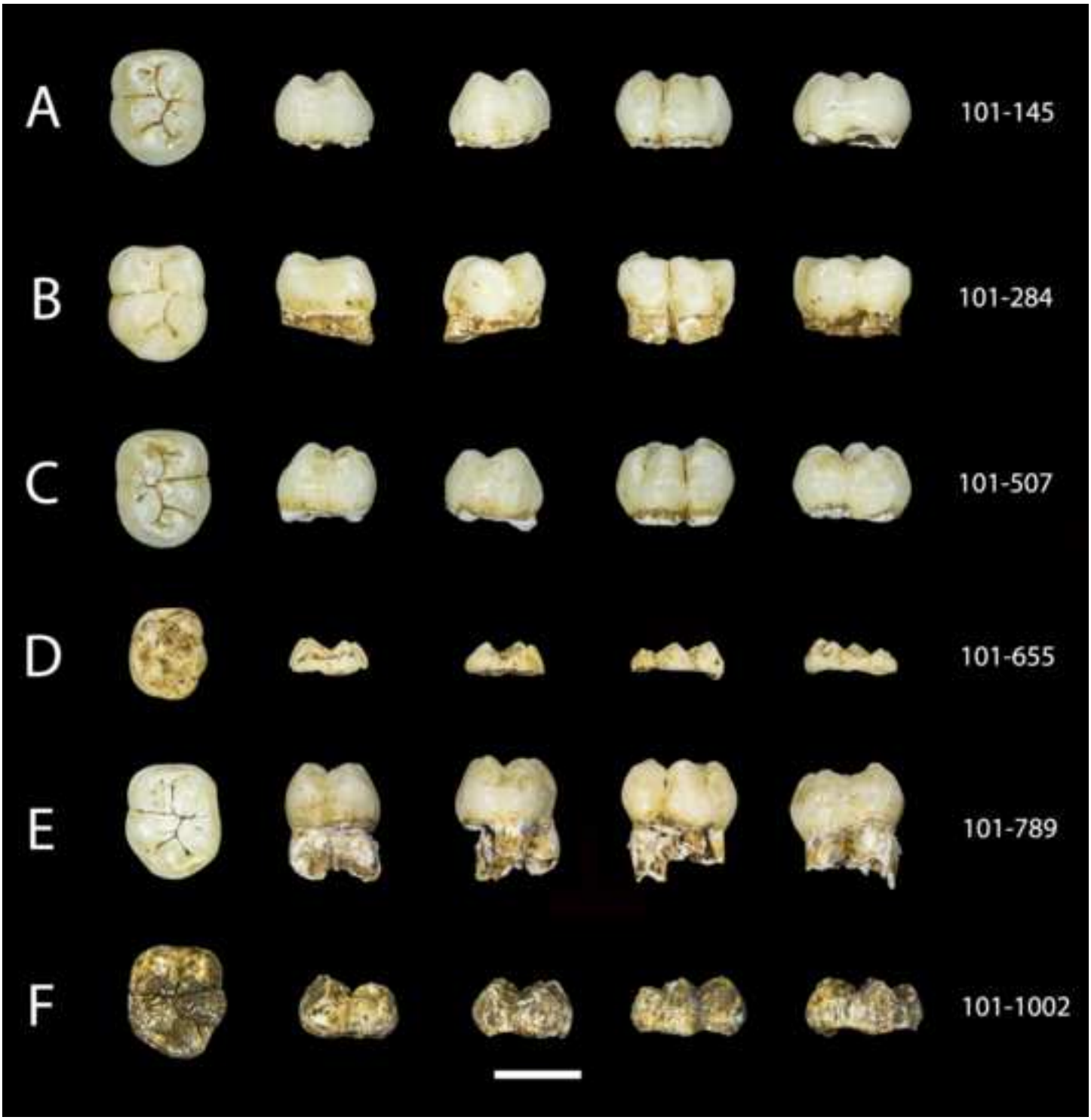

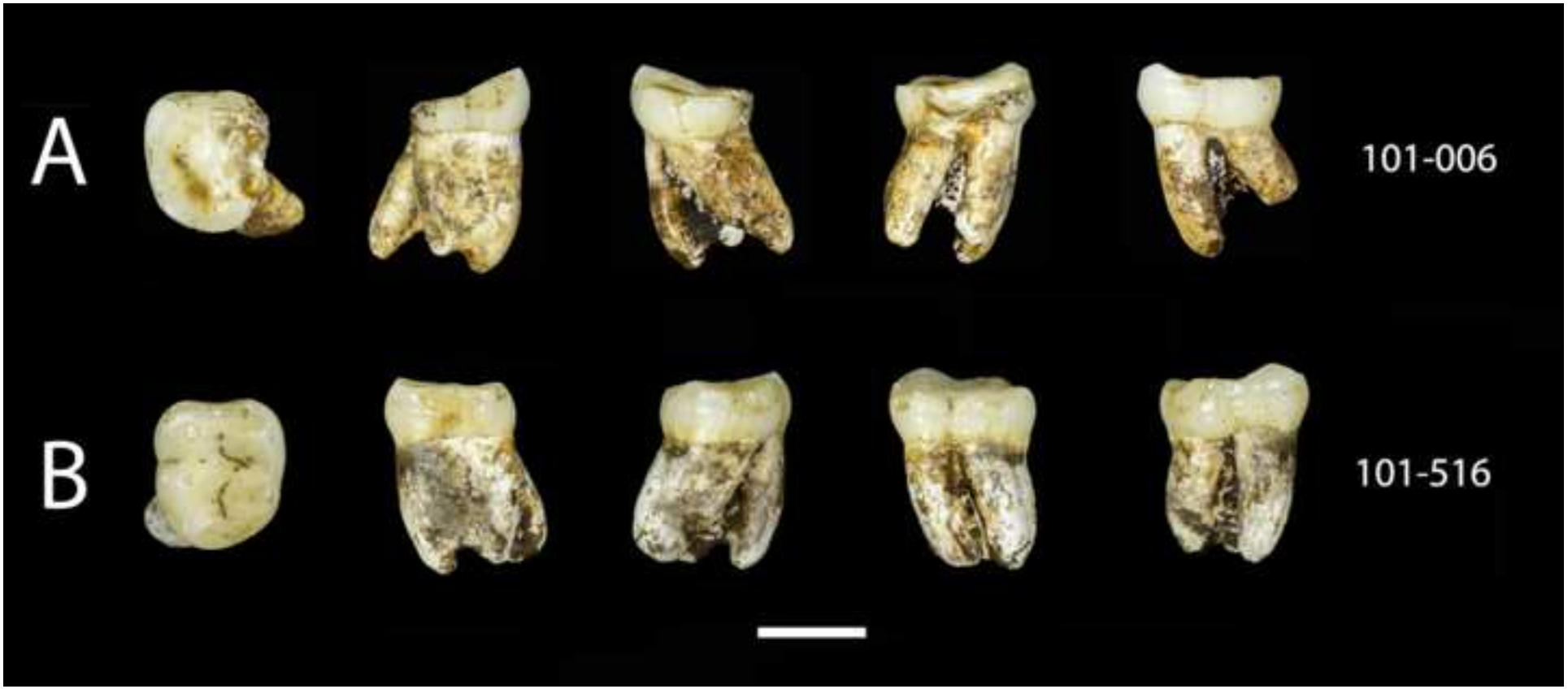

Figure 36_lower M3s_color.tif

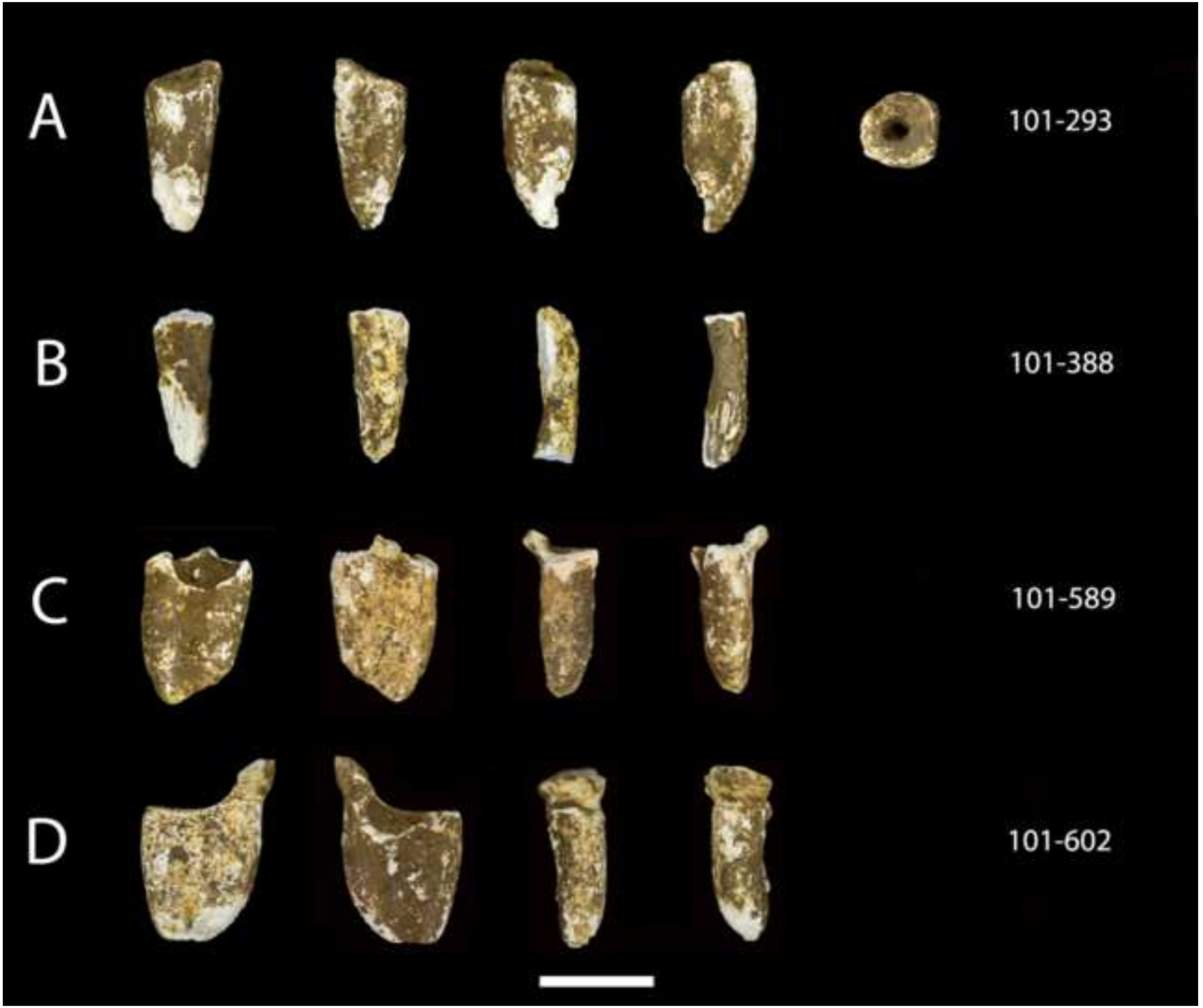

Figure 37_unknown.tif

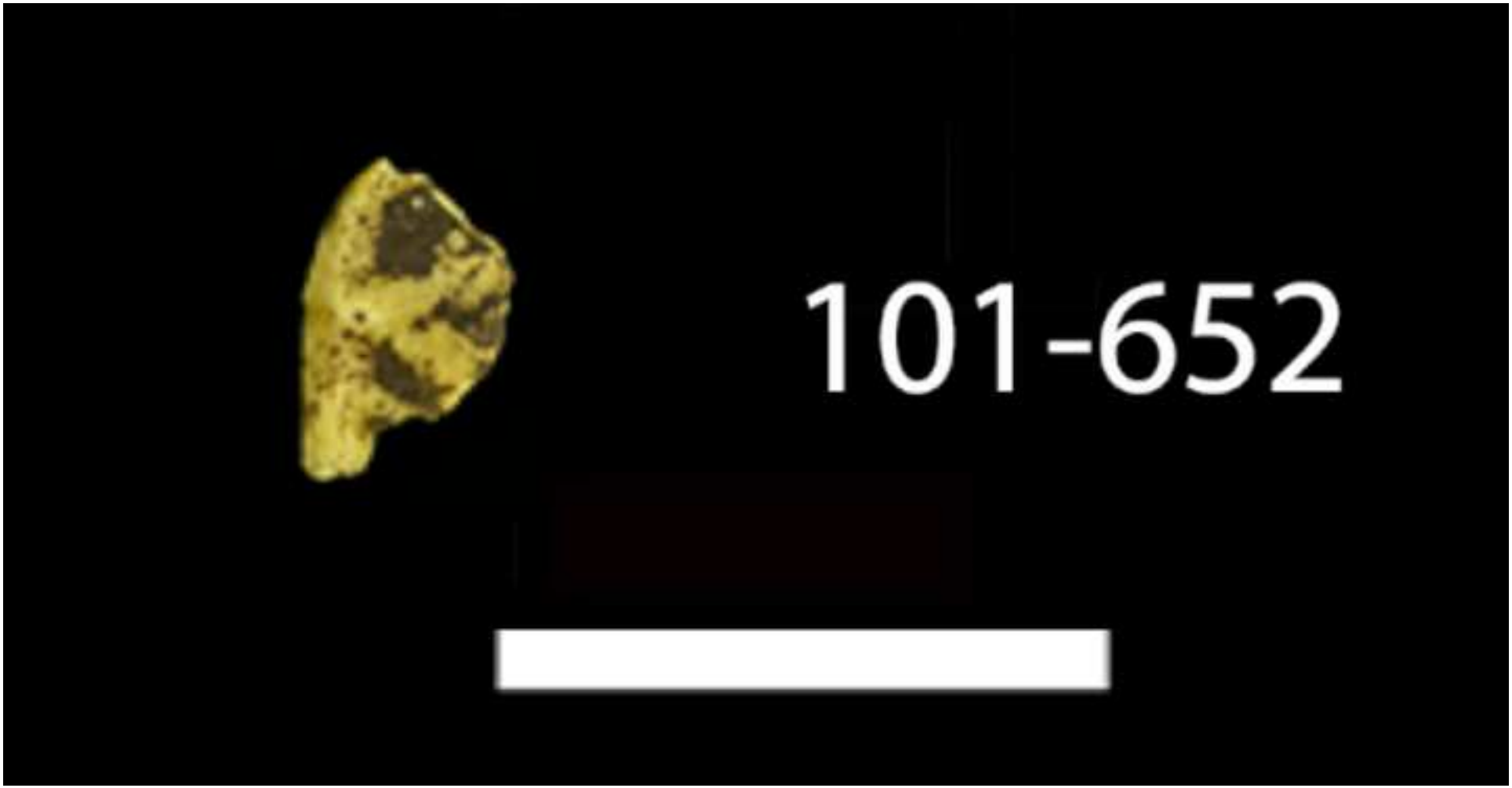

Figure 38_developing cusp_color.tif

Figure 39 _unknown_cont.tif

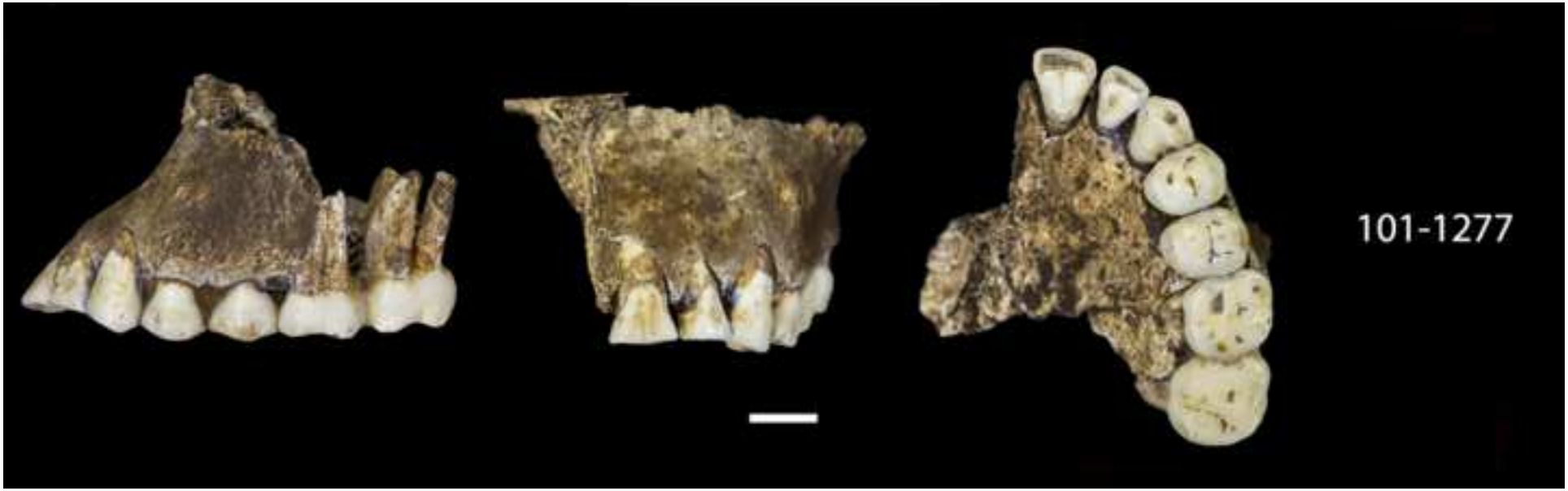

Figure 40_1277 maxilla_color.tif

Figure 41_UW 101_001_color.tif

Figure 42_010_mandible_color.tif

Figure 43_361 mandible_color.tif

Figure 44_377 mandible_color.tif

Figure 45_1142 mandible_color.tif

Figure 46_1261 mandible_color.tif

Figure 47_1400 mandible_color.tif

Table 1

Dental elements from the 2013–2015 excavations of the Dinaledi chamber. Mesiodistal (MD), buccolingual (BL), and labiolingual (LaL) measurements are reported in millimeters.

Specimen No.	Element	Figure	Basis for ID[a]	Wear stage[b]	MD (mm)	BL/LaL (mm)	Notes
U.W. 101-001	RP_4 crown and roots	41	1	5	8.7	10.2	
	RM_1 crown and roots	41	1	5	11.8		
	RM_2 crown and roots	41	1	4	13.3	11.7	
	RM_3 crown and roots	41	1	2	13.8	12.1	
U.W. 101-005	RM^2 crown and roots	22A	3	6	(11.0)[c]	(12.2)[c]	Measurements not corrected for heavy interproximal and occlusal wear
U.W. 101-006	RM_3 crown and roots	36A	3	5	13.4		
U.W. 101-010	RC_1 crown and root	42	1	7			

	RP_3 crown and roots	42	1	6–7		9.7
U.W. 101-037	RP^3 crown and roots	16A	3	2	8.3	10.8
U.W. 101-038	RI^1 crown and root	10A	3	3–4	8.8	6.6
U.W. 101-039	RI_1 crown and root	25A	3	4	5.9	5.5
U.W. 101-073	RI^2 crown and root	11A	3	1	6.3	6.3
U.W. 101-144	LP_3 crown and roots	30A	3	1	8.7	8.5
U.W. 101-145	LM_2 crown	35A	3	1	13.3	10.8
U.W. 101-182	RP^3 crown and roots	16B	3	1–2	7.8	10.9
U.W. 101-184	LP_4 crown and root	32A	3	1	9.0	8.5
U.W. 101-245	RC_1 partial crown and root	28A	3	4		
U.W. 101-277	LP^4 crown and roots	18A	3	1–2	8.4	11.3
U.W. 101-284	LM_2 crown and partial root	35B	3	1	13.8	11.4
U.W. 101-285	RM_1 crown and partial root	33A	3	3	12.0	10.6
U.W. 101-293	C^1? root	37A	3	8		

U.W. 101-294	LM_1 mesial root	No figure	3	4			Described with U.W. 101-905
U.W. 101-297	RM_1 crown and mesial root	33B	3	4	12.4		
U.W. 101-298	RP_3 crown	30B	3	1	9.2	8.5	
U.W. 101-333	LP^4 crown	18B	3	1	8.0	11.1	
U.W. 101-334	RP^4 crown and roots	18C	3	1	8.0	11.1	
U.W. 101-335	RI_2 crown and root	26A	3	2	6.7	5.9	
U.W. 101-337	RC^1 crown and root	13A	3	1	7.7	8.3	
U.W. 101-339	RC_1 crown and root	28B	3	1	7.0	7.4	
U.W. 101-357	mesial root of LM_1?	No figure	3				
U.W. 101-358	LP_3 crown and roots	30C	3	6+	(7.2)[c]	(9.6)[c]	Measurements not corrected for heavy interproximal and occlusal wear
U.W. 101-359	LC_1 root	28C	3	7			

U.W. 101-361	LP_4 root?	No figure	3				
	LM_2	43	1	8			
	LM_3	43	1	5	13.2	11.8	
U.W. 101-377	RP_3 crown and roots	44	1	1	9.0	8.6	
	RP_4 crown	44	1	1	8.8	9.0	
	RM_1 crown and roots	44	1	2	12.1	10.9	
	RM_2 crown and roots	44	1	1	12.9	11.2	
U.W. 101-383	RP_4 crown and partial root	32B	3	1	9.1	8.9	
U.W. 101-384	RdP^4 crown and partial roots	5A	3	4	9.3	10.3	
U.W. 101-388	Root fragment	37B	3				
U.W. 101-412	LC^1 crown and root	13B	3	3–4	8.5	8.3	
U.W. 101-417	LI^2 crown and root	11B	3	3	(6.3)[c]	6.4	MD length not corrected for incisal and interproximal wear

U.W. 101-418C	LM^3 crown	24A	3	1	12.0	12.8	
U.W. 101-445	LM^1 crown and partial roots	20A	3	1	12.2	11.6	
U.W. 101-455	RP^4 crown and root	18D	3	1	8.1	10.7	
U.W. 101-501	LC^1 crown and root	13C	3	1	7.7	8.4	
U.W. 101-505	LM^2 germ	22B	3	1	12.3	12.6	
U.W. 101-506	RP_3 crown and roots	30D	3	1	8.9	8.5	
U.W. 101-507	RM_2 crown	35C	3	1	13.6	11.1	
U.W. 101-516	LM_3 crown and roots	36B	3	3	13.6	11.9	
U.W. 101-525	RM^1 crown and partial roots	20B	3	3	11.7	11.8	Refits to U.W. 101-1574
U.W. 101-527	LM^3 crown and roots	24B	3	3	11.5	12.4	
U.W. 101-528	LM^2 crown and roots	22C	3	5	(11.8)[c]	(12.9)[c]	Measurements not corrected for heavy interproximal and occlusal wear

U.W. 101-544A	RdP^4 germ	5B	3	1	9.7	9.5	
U.W. 101-544B	RC^1 germ	13D	3	1	(7.3)[c]	(4.7)[c]	Measurements reflect current size of germ
U.W. 101-544C	RdI^1 crown and root	1A	3	3	4.3	6.2	
U.W. 101-582	LM_1 crown and roots	33C	3	2	12.3	10.6	
U.W. 101-583	RM^1 crown and roots	20C	3	2	11.7	12.2	
U.W. 101-589	$M_?$ root	37C	3				
U.W. 101-591	LI^1 crown and root	10B	3	4	(7.6)[c]	6.4	
U.W. 101-593	RM^2 crown	22D	3	1	12.4	13.0	
U.W. 101-594	RM^3 crown and roots	24C	3	1	11.9	12.6	
U.W. 101-595	LdC^1 crown and roots	3A	3	2	5.2	6.5	
U.W. 101-601	LI_1 crown and roots	25B	3	3	6.0	(5.4)[c]	LaL breadth approximated given cervical damage
U.W. 101-602	$RM_?$?	37D	3	7–8			

U.W. 101-652	Developing cusp	38	3			
U.W. 101-653	Incisor root?	39A	3	7		
U.W. 101-654	$LM_?$ root	39B		8		
U.W. 101-655	$RM_?$ germ (likely RM_2)	35D	3	1		
U.W. 101-680	$M^?$ lingual root?	No figure	3			
U.W. 101-686	anterior tooth root	39C	3			
U.W. 101-706	LC^1 crown and root	14A	3	1	8.5	8.2
U.W. 101-708	LM^1 crown and roots	20D	3	1	11.6	11.6
U.W. 101-709	RI^2 crown and root	11C	3	1	6.7	5.8
U.W. 101-728	RdC^1 crown and root	3B	3	1	5.3	6.4
U.W. 101-729	RP^3 crown and roots	16C	3	1	7.9	9.9
U.W. 101-786	LP^3 crown and root	16D	3	1	7.9	10.0
U.W. 101-789	LM_2 crown and partial roots	35E	3	1	13.3	10.8
U.W. 101-796	LM^1 crown and roots	20E	3	7–8		
U.W. 101-800	RP_3 crown and roots	31A	3	4–5	9.4	8.9

U.W. 101-808	LP^4 crown and root	18E	3	1	8.0	10.6	
U.W. 101-809	LM_1 crown and roots	33D	3	2	12.5	10.6	
U.W. 101-814	LM_1 crown and roots	33E	3	2	12.1	10.5	
U.W. 101-816	RC^1 crown and root	14B	3	1	8.5	8.2	
U.W. 101-823	RdP^3 crown and roots	4A	3	2	9.4	9.0	
U.W. 101-824	LdC_1 crown and root	7A	3	3–4	4.8	6.0	
U.W. 101-850	RP_3 crown and roots	41	3	4	8.0	9.6	refit to U.W. 101-001
U.W. 101-864	Crown and root fragment	39D	3				
U.W. 101-867	RM^2 crown and roots	22E	3	1	12.7	13.3	
U.W. 101-886	RC_1 crown and root	28D	3	1	7.1	7.1	
U.W. 101-887	LP_4 crown and root	32C	3	1	8.7	8.9	
U.W. 101-889	LP_3 crown and root	31B	3	1	9.1	8.5	
U.W. 101-905	LM_1 crown	34A	3	4	(11.9)[c]	10.8	MD length not corrected for interproximal wear

U.W. 101-908	RC^1 crown and root	14C	3	2	8.8	8.7	
U.W. 101-931	LI^1 crown and root	10C	3	3–4	9.3	6.4	
U.W. 101-932	LI^2 crown and root	11D	3	1	6.8	5.9	
U.W. 101-952	LI^2 crown and root	12A	3	3	(6.1)[c]	6.4	MD length not corrected for interproximal wear
U.W. 101-985	LC_1 crown and root	29A	3	1	7.3	7.2	
U.W. 101-998	LI_2 crown and root	26B	3	2	7.3	6.0	
U.W. 101-999	RM^1 crown and roots	21A	3	1	12.2	11.8	
U.W. 101-1002	RM_2? germ	35F	3		(13.0)[c]	(11.3)[c]	Measurements reflect observed size of germ
U.W. 101-1004	RP^3 crown and root	17A	3	1	7.9	9.9	
U.W. 101-1005A	LI_1 crown and root	25C	3	2	6.0	5.4	
U.W. 101-1005B	RI_1 crown and root	25D	3	2	6.3	5.5	

U.W. 101-1005C	RI_2 crown and root	26C	3	2	7.1	6.0	
U.W. 101-1006	RM^2 crown	23A	3	1	12.5	12.4	
U.W. 101-1012	RI^1 crown and root	10D	3	2	9.3	6.3	
U.W. 101-1014	RC_1 crown and root	44	1,2,3	1	6.6	7.0	Refit to U.W. 101-377
U.W. 101-1015	LM^2 crown and partial root	23B	3	1	12.6	12.4	
U.W. 101-1063	LM^2 germ?	23C	3		(11.2)[c]	(11.4)[c]	Measurements reflect size of crown incomplete germ
U.W. 101-1075	RI_2 crown and root	27A	3	1	6.6	6.0	
U.W. 101-1076	LC_1 crown and root	29B	3	1	7.4	6.9	
U.W. 101-1107	LP^3 crown and roots	17B	3	1	8.0	10.9	
U.W. 101-1126	LC_1 crown and root	20C	3	1	7.1	7.2	
U.W. 101-1131	LI_2 crown and root	27B	3	1	6.5	6.2	
U.W. 101-1132	LI_1 crown and root	25E	3	1	5.7	5.4	

U.W. 101-1133	RI_1 crown and root	25F	3	1	5.7	5.3	
U.W. 101-1135	RM^2 germ?	23D	3		(11.0)[c]	(11.9)[c]	Measurements reflect size of crown incomplete germ
U.W. 101-1142	RM_2 crown and roots	45	1	2	13.6	12.1	
	RM_3 crown and roots	45	1	1	13.9	12.7	
	LI_1 crown and root	46	1	4–5	(4.9)[c]	6.0	MD length not corrected for interproximal wear.
	RI_1 crown and root	46	1	4–5	(4.8)[c]	5.9	MD length not corrected for interproximal wear.
	LI_2 crown and root	46	1	4–5	(5.8)[c]	6.1	MD length not corrected for interproximal wear.
U.W. 101-1261							

RI_2 crown and root	46	1	4–5	(6.1)[c]	6.0	MD length not corrected for interproximal wear.
LC_1 crown and root	46	1	4	7.1	7.0	
RC_1 crown and root	46	1	4	7.2	7.0	
LP_3 crown and roots	46	1	2	8.7	8.4	
RP_3 crown and roots	46	1	2	8.6	8.6	
LP_4 crown and roots	46	1	3	8.7	9.0	
RP_4 crown and roots	46	1	3	8.3	8.9	
LM_1 crown and roots	46	1	4	11.3	10.8	
RM_1 crown and roots	46	1	4	11.2	10.7	
LM_2 crown and roots	46	1	2	12.2	11.1	
RM_2 crown and roots	46	1	2	12.4	11.0	
LM_3 crown and roots	46	1	1	13.1	12.3	
RM_3 crown and roots	46	1	1	13.0	11.6	

U. W. 101-1269	LM^3 crown and roots	24D	2,3	1	11.5	12.2	
U.W. 101-1277	LI^1 crown and root	40	1	4–5	(8.1)[c]	6.4	MD length not corrected for interproximal wear
	LI^2 crown and root	40	1	4	(6.2)[c]	6.0	MD length not corrected for interproximal wear
	L^C crown and root	40	1	3	7.9	8.2	
	LP^3 crown and roots	40	1	2–3	8.0	10.2	
	LP^4 crown and roots	40	1	2	8.6	11.2	
	LM^1 crown and roots	40	1	3–4	11.0	11.3	
	LM^2 crown and roots	40	1	1	12.1	12.5	
U.W. 101-1287A	LdC^1 crown and root	3C	3	2	6.5	5.4	

U.W. 101-1287B	RM_1 crown and roots	34B	3	4	(12.3)[c]	11.4	MD length not corrected for interproximal wear
U.W. 101-1304	LdI^2	2	3	1	4.9	4.1	
U.W. 101-1305	LM^1 germ	21B	3		12.3	11.8	
U.W. 101-1331	LdI^1 crown and root	1B	3	3	6.1	4.2	
U.W. 101-1362	LP^4 crown and roots	19A	3	7			
U.W. 101-1376	LdP^4 crown and roots	5C	3	1	10.3	10.1	
U.W. 101-1377	LdP^3 crown and roots	4B	3	2	9.3	8.7	
U.W. 101-1396	RM^1 crown and roots	21C	3	5	(11.3)[c]	12.4	MD length not corrected for interproximal wear
U.W. 101-1398A	RM^3 crown and roots	24E	3	1–2	12.7	13.1	
U.W. 101-1398B	I^2 root?	No Figure	3				
U.W. 101-1400	LdC_1 crown and root	47	1	1	5.7	5.0	

	LdP_3 crown and roots	47	1	2	9.5	7.1	
	LdP_4 crown and roots	47	1	1	11.4	9.0	
	LI_2 germ	27C	1				
	LC_1 germ	No figure	1				
	LM_1 germ	34C	1		12.7	10.9	
U.W. 101-1401	RP^4 crown and roots	19B	3	5	(7.5)[c]	11.1	MD length not corrected for interproximal wear
U.W. 101-1402	RP^3 crown and roots	17C	3	4–5	8.3	10.9	
U.W. 101-1403	RC^1 root	114D	3				
U.W. 101-1463	RM^1 crown and roots	21D	3	3	11.1	11.7	
U.W. 101-1471	LM^3 crown and roots	24F	3	2	12.7	13.1	
U.W. 101-1510	RC^1 crown and root?	15A	3	7			
U.W. 101-1522	LM^2 crown and roots	23E	3	2	12.9	13.6	

U.W. 101-1548	LC[1] germ	15B	3		(7.3)[c]	(4.6)	Measurements reflect size of crown incomplete germ
U.W. 101-1556	LC[1] crown and root	15C	3	5	(7.5)[c]	9.4	MD length not corrected for interproximal wear
U.W. 101-1558	RI[1] crown and root	10E	3	5	(7.9)[c]	7.1	MD length not corrected for interproximal wear
U.W. 101-1560	LP[3] crown and roots	17D	3	4–5	8.4	10.8	
U.W. 101-1561	LP[4] crown and roots	19C	3	5	(7.4)[c]	11.0	MD length not corrected for interproximal wear
U.W. 101-1565	LP_3 crown and partial root	31C	3	1	9.1	8.6	
U.W. 101-1571	LdC_1 crown and partial root	7B	3	4	6.0	4.6	

U.W. 101-1574	RM^1 distobuccal root	No figure	3				Refits to U.W. 101-525
U.W. 101-1588	LI^2 crown and root	12B	3	1	6.2	6.3	
U.W. 101-1605	$LM_?$ germ?	No figure	3				
U.W. 101-1610	RC_1 germ	29D	3				
U.W. 101-1611	RdC_1 crown and root	7C	3	1	5.8	5.0	
U.W. 101-1612	RdI_2 crown and root	6	3	1	4.7	4.2	
U.W. 101-1676	LM^1 crown	21E	3	3–4	11.7	11.9	
U.W. 101-1684	LI^2 crown and root	12C	3	5	(6.5)[c]	6.8	
U.W. 101-1685	RdP_3 crown and roots	8	1	2	9.3	7.0	
U.W. 101-1686	RdP_4 crown and root	9	3	1	11.4	9.0	
U.W. 101-1687	RdP^4 crown and roots	5D	3	1	10.4	10.1	
U.W. 101-1688	RM^1 germ	21F	3		12.1	12.0	
U.W. 101-1689	RM_1 germ	34D	3		12.6	11.2	

Abbreviations: ID = identification to class and side; L = left; R = right; $M^?$ = maxillary molar (unknown position); $M_?$ = mandibular molar (unknown position).

[a] Basis for ID codes are as follows: (1) in situ; (2) associated based on interproximal contact facets; (3) based on morphology.

[b] Wear stages are based on Smith (1984).

[c] Values in parentheses are uncorrected for wear, are observed measurements for incompletely formed crowns or broken crowns or are estimated values; please see accompanying Notes for each specimen for further details. Measurements reported in parentheses are not intended to be included in comparative analyses of tooth size.

Table 2

Proposed associations among the Dinaledi teeth. Specimens for each proposed association are arranged by specimen number.

Association	Associated teeth
1	U.W. 101-544B (RC^1 germ), U.W. 101-544C (dI^1), U.W. 101-728 (RdC^1), U.W. 101-1287A (LdC^1), U.W. 101-1305 (LM^1), U.W. 101-1376 (LdP^4), U.W. 101-1377 (LdP^3), U.W. 101-1331 (dI^1), U.W. 101-1400 (LdC_1, LdP_3, LdP_4, LI_2 germ, and LM_1 germ in situ), U.W. 101-1548 (LC^1 germ), U.W. 101-1610 (RC_1 germ), U.W. 101-1611 (RdC_1), U.W. 101-1612 (RdI_2), U.W. 101-1685 (RdP_3), U.W. 101-1686 (RdP_4), U.W. 101-1687 (RdP^4), U.W. 101-1688 (RM^1 germ), U.W. 101-1689 (RM_1 germ)
2	U.W. 101-377 (RP_3–RM_2), U.W. 101-789 (LM_2), U.W. 101-809 (LM_1), U.W. 101-887 (LP_4), U.W. 101-889 (LP_3), U.W. 101-998 (RI_2), U.W. 101-1005A (LI_1), U.W. 101-1005B (RI_1), U.W. 101-1005C (RI_2), U.W. 101-1014 (R_C), U.W. 101-1076 (L_C),
3	U.W. 101-706 (LC^1), U.W. 101-709 (RI^2), U.W. 101-816 (RC^1), U.W. 101-931 (LI^1), U.W. 101-932 (LI^2), U.W. 101-1012 (RI^1)

4	U.W. 101-886 (RC_1), U.W. 101-1075 (RI_2), U.W. 101-1126 (LC_1), U.W. 101-1131 (LI_2), U.W. 101-1132 (LI_1), U.W. 101-1133 (RI_1)
5	U.W. 101-277 (LP^4), U.W. 101-418C (LM^3), U.W. 101-1522 (LM^2), U.W. 101-1676 (LM^1), and possibly U.W. 101-525 (RM^1) and U.W. 101-594 (RM^3)
6	U.W. 101-1396 (RM^1), U.W. 101-1401 (RP^4), U.W. 101-1402 (RP^3), U.W. 101-1403 (RC^1), U.W. 101-1556 (LC^1), U.W. 101-1560 (LP^3), U.W. 101-1561 (LP^4), and possibly U.W. 101-1684 (LI^2)
7 (DH1)	U.W. 101-1261 (complete mandibular dentition), U.W. 101-1269 (LM^3), U.W. 101-1277 (LI^1–LM^2 in situ), and U.W. 101-1463 (RM^1)
8 (DH3)	U.W. 101-357 (mesial root of LM_1), U.W. 101-358 (LP_3), U.W. 101-359 (LC_1), and U.W. 101-361 (LP_4–LM_3 in situ)
9	U.W. 101-527 (LM^3), U.W. 101-528 (LM^2), U.W. 101-796 (LM^1), U.W. 101-1362 (LP^4), and possibly U.W. 101-005 (RM^2)

Abbreviations: L = left; R = right.